

JOTCS

JOURNAL of the TURKISH CHEMICAL SOCIETY
Section: A

A

Volume 1, Issue 1

June 2018



An Open-Access-Based Scholarly Chemical Journal
www.dergipark.ulakbim.gov.tr/Jotcsa



TURKISH
CHEMICAL SOCIETY

jotcsa@turchemsoc.org

Published, in English, Biannually
(every June and December)

Turkish Translations of Titles and Abstracts are Available.

Correspondance to:
Dr. Barbaros AKKURT, PHD, Managing Editor

Turkish Chemical Society
Halikuzgah Str. Ucuq. Apt. No:15 068, Haliççe-Saklı-İstanbul/Turkey

Journal of the Turkish Chemical Society, Section A: Chemistry (JOTCSA)

e-ISSN: 2149-0120

A triannual, open-access chemical journal, hosted by Dergipark

(Published, in English, in every February, June, and October)

Editorial Board (sorted by the lastnames)

Prof. Dr. Göktürk, Sinem (Physical Chemistry, Marmara University, Turkey)

Prof. Dr. Karagözler, A. Alev (Biochemistry, Adnan Menderes University, Turkey)

Prof. Dr. Karagözler, A. Ersin (Electrochemistry, Adnan Menderes University, Turkey)

Assoc. Prof. Dr. Köse, Dursun Ali (Inorganic Chemistry, Hitit University, Turkey)

Assoc. Prof. Dr. Küçükbay, F. Zehra (Analytical Chemistry, İnönü University, Turkey)

Prof. Dr. Küçükbay, Hasan (Organic Chemistry, İnönü University, Turkey) Editor-in-Chief

Assoc. Prof. Dr. Taşdelen, M. Atilla (Polymer Chemistry, Yalova University, Turkey)

Prof. Dr. Yalçın, Esin A. (Computational Chemistry, Ankara University, Turkey)

Address: Halaskargazi Str. Uzay Apt. No: 15/8, 34373 Harbiye, Istanbul/Turkey.

Fax: +90 212 231 70 37

E-mail: jotcsa@turchemsoc.org

Website: <http://turchemsoc.dergipark.gov.tr/jotcsa>.

(*)JOTCSA is a peer-reviewed publication of the Turkish Chemical Society. Peer-reviewing process is performed with the Ulakbim Journal System (UDS).

(*)The ideas outlined by the authors cannot be attributed to the journal management nor the editorial board.

Aim and Scope of the Journal

The journal will publish, after a peer-reviewing process, the following:

- a)** Research articles,
- b)** Review articles,
- c)** Letters to the editor.

If requested, the journal will also publish the following, without committing a peer-review:

- d)** Book reviews,
- e)** Thesis abstracts.

The journal's scope will include, but not limited to, the following disciplines of chemistry:

- i)** Analytical chemistry,
- ii)** Biochemistry,
- iii)** Computational chemistry,
- iv)** Electrochemistry,
- v)** Inorganic chemistry,
- vi)** Organic chemistry
- vii)** Physical chemistry,
- viii)** Polymer chemistry.

ETHICAL GUIDELINES

Guidelines for the Editors

An editor (editors, associate editors, etc.) should provide impartial consideration to all manuscripts offered for publication, judging each on its particular feature without regard to race, religion, nationality, sex, seniority, or institutional affiliation of the author(s). An editor should review and treat a manuscript submitted for publication with all reasonable speed. An editor takes the sole responsibility for accepting or rejecting a manuscript for publication. An editor may seek assistance on a manuscript from specialists chosen for their expertise and fair judgment. An editor should not reveal any information about the manuscript under consideration to anyone other than the author and designated reviewers until after the evaluation process is complete. An editor should respect the intellectual independence of authors.

Authors

Our journal considers a person as an author who is responsible at least for a part of the work. Authors should be able to explain the problem in study in a deep manner. For our journal, all authors are responsible for the content they submitted. The corresponding author is responsible for the agreement of all the authors and to keep them informed about the submission process since first submission of their manuscript. He/she is responsible for providing the license to publish, in case of acceptance, on behalf of all the authors. Our journal assumes that submitting the paper implies in total agreement from all the authors. For manuscripts with more than 8 authors, all the authors should provide a declaration specifying what was their contribution to the manuscript. It is not acceptable for JOTCSA to consider for publication anything that was previously published, neither entirely nor partly in other journals. Anything sent to our journal must not be under analysis by anywhere else. Simultaneous submissions to JOTCSA and any other journal, is considered a major conduct flaw, and all the authors will be definitely banned, and all their previous publications in JOTCSA will be publicly retracted. Plagiarism and self-plagiarism will be treated in the same way. Multiple manuscripts, dealing with closely related subjects and/or variables are discouraged as long as they could figure in a single paper.

Reviewers

JOTCSA invites peers to review its submissions, relying on their expertise, curricula, and their will to review them as volunteers. By accepting to review a manuscript, the reviewer commits himself to do so in due time. Delays are extremely negative to the review process and makes it last much longer than it should. When a reviewer is requested, he/she is gently asked to answer the invitation e-mail, informing if he/she is willing or not willing to review the manuscript. It is a gesture of politeness, and it avoids delays too. By accepting to review a manuscript, the reviewer declares that no conflicts of interests do exist, and he/she is doing his/her revision for the wealth and progress of Science. Those reviewers who answer our requests, agreeing or not, and those who respect the deadlines, are scored positively, and eventual submissions they could send to JOTCSA will be treated with priority.

The online version of this declaration can be viewed on http://dergipark.ulakbim.gov.tr/public/journals/5106/ethical_guidelines.pdf.

Editorial Advisory Board Members

(sorted alphabetically by the last names)

Abo-dya, Nader Elmaghwry (Zagazig University, Egypt)

do Amaral, Marcos Serrou (Federal University of Mato Grosso do Sul, Brazil)

Beatriz, Adilson (Federal University of Mato Grosso do Sul, Brazil)

Carta, Fabrizio (Università degli Studi di Firenze, Italy)

El-Khatib, Mirna (University of Pennsylvania, USA)

Florio, Saverio (CINMPIS, Italy)

Jisikriani, Davit (University of Pennsylvania, USA)

Külcü, Nevzat (Mersin University, Turkey)

Lebedeva, Iryna (Augusta University, USA)

Nájera, Carmen (Royal Spanish Academy of Sciences, Spain)

Orhan, Ersin (Düzce University, Turkey)

Panda, Siva S. (Augusta University, USA)

Panmand, Deepak S. (India)

Pillai, Girinath G. (University of Tartu, Estonia)

Souizi, Abdelaziz (University of Ibn Tofail, Morocco)

Seçen, Hasan (Atatürk University, Turkey)

Stanovnik, Branko (University of Ljubljana, Slovenia)

Supuran, Claudiu T. (University of Florence, Italy)

Tural, Bilsen (Dicle University, Turkey)

Tüfekçi, Mehmet (Karadeniz Technical University, Turkey)

Yaman, Mehmet (Firat University, Turkey)

Yılmaz, İsmet (İnönü University, Turkey)

Yılmaz, Ülkü (İnönü University, Turkey)

Yus, Miguel (Universidad de Alicante, Spain)

Table of Contents, Volume 4, issue 2

Title of the Manuscript	Pages
1. SYNTHESIS OF NOVEL SCHIFF BASES DERIVED FROM FERROCENE AS A CHIRAL SENSOR (Erratum-Asuman UÇAR)	viii-x
2. EASY SYNTHESIS OF 3,4-DIHYDROPYRIMIDIN-2-(1H)-ONE DERIVATIVES USING PHOSPHATE FERTILIZERS MAP, DAP, AND TSP AS EFFICIENT CATALYSTS (Sarrah SIBOUS, Said BOUKHRIS, Rachida GHAILANE, Nouzha HABBADI, Amina HASSIKOU, and Abdelaziz SOUIZI)	477-488
3. BORON AND MOLYBDENUM CONTENTS OF VERBASCUM OLYMPICUM BOISS. GROWING AROUND AN ABANDONED TUNGSTEN MINE: A CASE STUDY FOR ECOLOGICAL PROBLEM SOLVING (Ümran SEVEN ERDEMİR)	489-500
4. Synthesis of Novel Diarylethenes Bearing Naphthalimide Moiety and Photochromic Fluorescence Behaviors (Ersin ORHAN)	501-516
5. An Efficient Catalyst for Aldol Condensation Reactions (Yusuf HASSAN, Rosa KLEIN, Perry T KAYE)	517-524
6. Using Natural Stone Pumice in Van Region on Adsorption of Some Textile Dyes (Ali Rıza KUL, Veysel BENEK, Ahmet SELÇUK, and Nilgün ONURSAL)	525-536
7. Determination of Cd(II) Ions by using Cyclodextrin-Based Polymeric Fluorescence Sensor (Soner ÇUBUK, Özge YILMAZ, Ece KÖK YETİMOĞLU, and Memet Vezir KAHRAMAN)	537-548
8. Development of UV-cured Polymeric Fluorescence Sensor for Boron Determination (Soner ÇUBUK, Mirgöl KOSİF, Ece KÖK YETİMOĞLU, and Memet Vezir KAHRAMAN)	549-562
9. Chemical investigation and antioxidant activity of fractions of <i>Lannea humilis</i> (Oliv.) Engl. (ACHIKA Jonathan Ilemona, AYO Racheal Gbekele-Oluwa, OYEWALE Adebayo Ojo, and JAMES Dama Habila)	563-572
10. Theoretical Investigation of Corrosion Inhibition of Iron Metal by Some Benzothiazole Derivatives: A Monte Carlo Study (Savaş KAYA and Nail ALTUNAY)	573-578
11. A versatile water soluble ball-type phthalocyanine as potential antiproliferative drug: the interaction with G-quadruplex formed from Tel 21 and cMYC (Efkan BAĞDA, Esra BAĞDA, and Ebru YABAŞ)	579-596
12. Novel Straight-Chained Sulfanyl Members of Arylamino-1,4-naphthoquinones: Synthesis and Characterization (Nilüfer BAYRAK)	597-606
13. Determination of Bisphenol A in Beverage Samples Using Ultrasonic- Extraction and Atomic Absorption Spectrometry (Emre YILDIRIM, Nail ALTUNAY, and Ramazan GÜRKAN)	607-630
14. CSA-Catalyzed Three-component Synthesis of Fused Polycyclic Pyrazolo[4,3-e]pyridines Under Ultrasonic Irradiation and Their Antioxidant Activity (Emel PELİT)	631-648
15. Synthesis and Characterization of Novel Aromatic Substituted γ - and δ -Ketoxime Esters (Belma HASDEMİR)	649-660



TURKISH CHEMICAL SOCIETY

**Editorial, Vol. 4, issue 2 (2017): Submissions between
February-June, 2017**

We are very happy to present the volume 4, issue 2 of "**Journal of the Turkish Chemical Society, Section A: Chemistry (JOTCSA)**" which has already been indexed in **TR-Dizin** of TÜBİTAK (The Scientific and Technological Research Council of Turkey)

(<http://cabim.ulakbim.gov.tr/?s=Journal+of+Turkish+chemical+society+section+a+chemistry>) and **Chemical Abstracts**

(http://cassi.cas.org/publication.jsp?P=eCQtRPJo9AQyz133K_Il3zLPXfcr-WXf-1IG1_aXCEAyz133K_Il3zLPXfcr-WXf-9sRQmIixJMyz133K_Il3zLPXfcr-WXfm62XYhyRweqA4Krr_z8o_Q).

This issue includes 15 papers, 3 by authors of various nationalities and 12 by Turkish authors.

We wish to thank all the authors and reviewers of the manuscripts, and to the editorial team of Journal of the Turkish Chemical Society, Section A: Chemistry for your contributions over the last three years to making a success of **JOTCSA**.

Please visit to the website of our journal at <http://turchemsoc.dergipark.gov.tr/jotcsa> and send your research papers/articles using our website. In case of any queries please do not hesitate to contact our managing editor, Mr. Barbaros AKKURT, at jotcsa@turchemsoc.org or myself at hasan.kucukbay@inonu.edu.tr.

There is no any publication, processing or subscription charge for our open-access journal.

Best regards,

Prof. Dr. Hasan KÜÇÜKBAY, PhD

Editor-in-chief, JOTCSA

JOTCSA, 2(3), 2015

Synthesis of Novel Schiff Bases Derived From Ferrocene as a Chiral Sensor (Erratum)

Kiral Sensör Olarak Ferrosen Türevli Yeni Schiff Bazının Sentezi (Hata bildirimi)

Asuman UÇAR*^a, Mükerrerem FINDIK^a, Haluk BİNGÖL^b, Ersin GÜLER^a, Emine ÖZCAN^a

^aDepartment of Chemistry, Faculty of Science, Selcuk University, 42075 Konya, Turkey

^bChemistry Department, Ahmet Kelesoglu Education Faculty, Necmettin Erbakan University, 42099 Konya, Turkey

asucar340@gmail.com.

ABSTRACT

Ferrocene and ferrocenyl compounds are widely used in fluorescence studies due to the realizing of energy and electron transfer [1]. In addition to the high selectivity, because of their potential applications in the fields of analytical, biological, clinical and biochemistry, enantioselective fluorescence sensor studies are listed in the literature [2]. Amino acids are important to obtain chiral receptor due to the being natural chiral molecule and excellent hydrogen bond made by amide bonds [3].

In this study the chiral compound **3** was synthesized and fluorescence properties of **3** was studied. When we investigated the fluorescence changes after the interaction of this compound with various chiral amino acids (D-Methionine L-Methionine, D-Alanine, L-Alanine, D-Valine, L-Valine, D-Serine, L-Serine, D-Histidine, L-Histidine, D- Cysteine, L- Cysteine and D-Threonine, L-Threonine), it was seen that there is a visible change observed against the D-methionine unlike other aminoacids.

Keywords

Ferrocene, Schiff base, Amino acids methylester , Fluorescence sensors, Chiral recognition

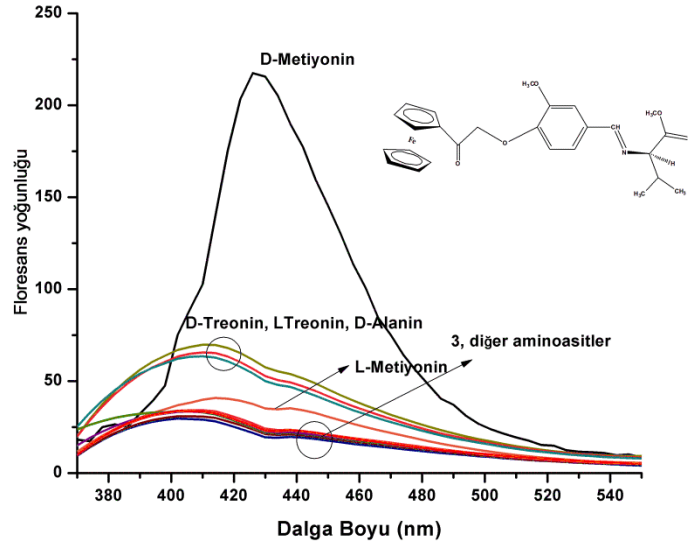


Figure 1: The structure of the synthesized compounds and the fluorescence spectra of **3** upon the titration of various amino acids.

Şekil 1: Sentezlenen bileşiğin yapısı ve incelenen amino asitlere karşı değişen floresans yoğunluk grafiği.

ÖZET

Ferrosen ve ferrosenil bileşikleri enerji ve elektron transferi gerçekleştirebilmesinden dolayı floresans çalışmalarında yaygın olarak kullanılmıştır (1). Yüksek seçiciliğin yanında analitik, biyolojik, klinik ve biyokimya alanlarında potansiyel uygulamaları nedeniyle enantioselektif floresans sensör çalışmaları literatürlerde yer almaktadır (2). Aminoasitler hem doğal kiral moleküller olduğu için hem de amid bağları mükemmel hidrojen bağı yaptıkları için kiral reseptör eldesinde önem taşımaktadırlar (3).

Bu çalışmada kiral yapıda olan **3** bileşiği sentezlenmiş ve floresans özellikleri çalışılmıştır. Bu bileşiğin çeşitli kiral aminoasitlerle (D- Metiyonine, L- Metiyonine, D-Alanin, L-Alanin, D-Valin, L-Valin, L-Serin, D-Serin, D-Histidin, L-Histidin, D-Sistein, L- Sistein D- Treonin, L- Treonin) etkileşimi sonucu floresans değişimleri incelendiğinde D-metiyonine karşı gözle görülür bir değişim söz konusuysen incelenen diğer amino asitlere karşı bu artışın mevcut olmadığı görülmüştür. Bu sonuçlar sentezlenen bileşiğin D-metiyonin enantioselektif tanınması için kullanışlı bir sensör olduğunu göstermektedir.

Anahtar Kelimeler: : Ferrosen, Schiff bazı, Aminoasit metilester, Floresans sensör, Kiral tanınma

REFERENCES/KAYNAKLAR

- [1] Qing G.Y, Sun T. L, He Y. B, Wang F, Chen Z. H. HIGHLY SELECTIVE FLUORESCENT RECOGNITION OF PHENYL AMINO ALCOHOL BASED ON FERROCENYL MACROCYCLIC DERIVATIVES. *Tetrahedron: Asymmetry*, 2009 Feb;20: 575-583.
- [2] Meng J, Wei G, Huang X, Dong Y, Cheng Y, Zhu C. A FLUORESCENCE SENSOR BASED ON CHIRAL POLYMER FOR HIGHLY ENANTIOSELECTIVE RECOGNITION OF PHENYLALANINOL. *Polymer*, 2011 Dec;52: 363-367.
- [3] Zhang X, Yin J, Yoon J. RECENT ADVANCES IN DEVELOPMENT OF CHIRAL FLUORESCENT AND COLORIMETRIC SENSORS. *Chem. Rev.* 2014 Feb;114:4918-4959.



EASY SYNTHESIS OF 3,4-DIHYDROPYRIMIDIN-2-(1H)-ONE DERIVATIVES USING PHOSPHATE FERTILIZERS MAP, DAP, AND TSP AS EFFICIENT CATALYSTS

Sarra Sibous, Said Boukhris, Rachida Ghailane, Nouzha Habbadi, Amina Hassikou and Abdelaziz Souizi *

Laboratory of Organic, Organometallic and Theoretical Chemistry, University of IbnTofail, Faculty of Science, B.P. 133, 14000 Kenitra, Morocco

Abstract: A simple, efficient, and green procedure has been developed for the synthesis of dihydropyrimidinones (Products of Biginelli) using phosphate fertilizers (mono-ammonium phosphate (MAP), di-ammonium phosphate (DAP) and triple super phosphate (TSP)) as catalyst. The one-step reaction involved the three compounds, which are registered aromatic aldehydes, dicarbonyl compounds and the urea/thiourea. This new method provides some advantages such as obtaining excellent yields (98%), as well as the short duration of the reaction, which may attain 2 minutes. These catalytic heterogeneous systems present also the advantage of being easily recycled.

Keywords: Heterogeneous catalysts; MAP; DAP; TSP; 3,4-dihydropyrimidin-2(1H)-ones; phosphate fertilizers.

Submitted: January 21, 2017. **Revised:** February 13, 2017. **Accepted:** March 06, 2017.

Cite this: Sibous S, Boukhris S, Ghailane R, Habbadi N, Hassikou A, Souizi A. EASY SYNTHESIS OF 3,4-DIHYDROPYRIMIDIN-2-(1H)-ONE DERIVATIVES USING PHOSPHATE FERTILIZERS MAP, DAP, AND TSP AS EFFICIENT CATALYSTS. JOTCSA. 2017;4(2):1-12.

DOI: 10.18596/jotcsa.286900.

*Corresponding author. E-mail: contact@medjchem.com.

INTRODUCTION

The dihydropyrimidinone derivatives constitute a major family usually with therapeutic and pharmacological properties such as antiviral agents, antimitotic, anticarcinogenic, antihypertensive medications and especially, as modulators of calcium channels (1–4). The Biginelli reaction was described for the first time by the Italian chemist Pietro Biginelli 1893(5), where the reaction was carried out in one-step, putting together an aromatic aldehyde and urea with the ethyl acetoacetate in a strongly acidified ethanolic reflux. However, this method has some disadvantages, such as the severe conditions in which the reaction takes place and attains low yields. The use of catalysts in the condensation of Biginelli became necessary to improve the yields and the time of reaction. We note in recent years, significant efforts made in order to find new procedures to produce 3,4-dihydropyrimidin-2(1H)-one derivatives with good yields. The use of catalysts in the condensation of Biginelli became necessary to improve the yields and the time of reaction. We note in recent years, significant efforts which have been made to find new procedures to produce 3,4-dihydropyrimidin-2(1H)-one derivatives. These protocols use either Brønsted acids (6) metal catalysts such as sulfonic acid nanomagnetic (7) and the iron (III) tosylate (8), bis[(L)-prolinato-N,O]Zn-water (9), the 1-glycyl-3-methyl copper chloride imidazolium (II) (10), but the use of transition metals is toxic and dangerous. The aim of this work is to use a simple synthetic, green, and effective protocol for the synthesis of dihydropyrimidin-2(1H)-one and dihydropyrimidin-2(1H)-thione derivatives using three phosphate compounds as catalysts, in addition to traditional reagents of Biginelli reaction: urea or thiourea, ester β -ketones and aldehyde in ethanol. This method gave the expected products with good yields accompanied by a reduction in reaction time, compared to conventional conditions.

MATERIALS AND METHODS

All chemicals were purchased from Merck or Fluka Chemical Companies. The known products were identified by comparison of their melting points and spectral data with those reported in the literature. TLC using silica gel SIL G/UV 254 plates monitored the progress of the reactions. Melting points were recorded on a Kofler hot stage apparatus and are uncorrected.

General procedure of synthetic 3,4-dihydropyrimidin-2(1H)-one or thione derivatives

4. A mixture of aromatic aldehyde (1 mmol), 1,3-dicarbonyl compounds (1 mmol), urea or thiourea (1.5 mmol) was prepared. After that we added MAP (3 mol %) or DAP or TSP (1 mol %) as catalyst. The mixture was dissolved in 1 mL of absolute ethanol. The mixture was refluxed for appropriate time and the progress of the reaction was monitored by TLC. After

completion of the reaction the catalyst was recovered by filtration, the filtrate was evaporated and treated with acetonitrile and the solid was then washed with water. The product was purified by recrystallization with ethanol to give the pure 3,4-dihydropyrimidin-2(1H)-one derivatives **4a-k** and 3,4-dihydropyrimidin-2(1H)-thione derivatives **4l-o**.

All spectral data of synthesized products are described below and compare favorably to those reported in the literature. Melting points are reported in Table 4.

5-Acetyl-6-methyl-4-phenyl-3,4-dihydropyrimidin-2(1H)-one **4a**: ^1H NMR (300 MHz, DMSO- d_6 , δ ppm): 9.16 (s, 1H, NH), 7.78 (s, 1H, NH), 6.84-7.18 (m, 5H, ArH), 5.21 (s, 1H, CH), 2.35 (s, 3H, CH₃), 2.16 (s, 3H, CH₃). Anal. Calcd for C₁₃H₁₄N₂O₂: C, 67.81; H, 6.13; N, 12.17%. Found C, 67.80; H, 6.15; N, 12.15%.

5-Acetyl-4-(4-chlorophenyl)-3,4-dihydro-6-methylpyrimidin-2(1H)-one **4b**: ^1H NMR (300 MHz, DMSO- d_6 , δ ppm): 9.17 (s, 1H, NH), 7.69 (s, 1H, NH), 7.17 (d, J = 8.2 Hz, 2H, ArH), 6.86 (d, J = 8.2 Hz, 2H, ArH), 5.10 (s, 1H, CH), 2.32 (s, 3H, CH₃), 2.10 (s, 3H, CH₃). Anal. Calcd for C₁₃H₁₃ClN₂O₂: C, 58.98; H, 4.95; N, 10.57; Cl, 13.38%. Found C, 58.97; H, 4.67; N, 10.55; Cl, 13.36%.

5-Acetyl-6-methyl-4-(4-nitrophenyl)-3,4-dihydropyrimidin-2(1H)-one **4c**: ^1H NMR (300 MHz, DMSO- d_6 , δ ppm): 9.18 (s, 1H, NH), 8.20 (d, J = 8.4 Hz, 2H, ArH), 7.92 (s, 1H, NH), 7.50 (d, J = 8.4 Hz, 2H, ArH), 5.18 (s, 1H, CH), 2.31 (s, 3H, CH₃), 2.18 (s, 3H, CH₃). Anal. Calcd for C₁₃H₁₃N₃O₄: C, 56.72; H, 4.76; N, 15.27%. Found C, 56.70; H, 4.74; N, 15.28%.

5-Acetyl-4-(4-methoxyphenyl)-6-methyl-3,4-dihydropyrimidin-2(1H)-one **4d**: ^1H NMR (300 MHz, DMSO- d_6 , δ ppm): 9.35 (s, 1H, NH), 8.26 (d, J = 8.2 Hz, 2H, ArH), 7.99 (s, 1H, NH), 7.46 (d, J = 8.2 Hz, 2H, ArH), 5.31 (s, 1H, CH), 3.43 (s, 3H, OCH₃), 2.32 (s, 3H, CH₃), 2.09 (s, 3H, CH₃). Anal. Calcd for C₁₄H₁₆N₂O₃: C, 64.61; H, 6.20; N, 10.75%. Found C, 64.63; H, 6.22; N, 10.74%.

5-Ethoxycarbonyl-4-(4-methoxyphenyl)-6-methyl-3,4-dihydropyrimidin-2(1H)-one **4e**: ^1H NMR (300 MHz, DMSO- d_6 , δ ppm): 9.19 (s, 1H, NH), 8.16 (d, J = 8.1 Hz, 2H, ArH), 7.92 (s, 1H, NH), 7.58 (d, J = 8.1 Hz, 2H, ArH), 5.20 (s, 1H, CH), 3.97 (q, J = 7.0 Hz, 2H, OCH₂CH₃), 3.34

(s, 3H, OCH₃), 2.19 (s, 3H, CH₃), 1.07 (t, *J* = 7.0 Hz, 3H, OCH₂CH₃). Anal. Calcd for C₁₅H₁₈N₂O₄: C, 62.05; H, 6.25; N, 9.65%. Found C, 62.07; H, 6.23; N, 9.68%.

5-Ethoxycarbonyl-6-methyl-4-(4-nitrophenyl)-3,4-dihydropyrimidin-2(1H)-one **4f**: ¹H NMR (300 MHz, DMSO-d₆, δ ppm): 9.31 (s, 1H, NH), 7.87 (s, 1H, NH), 7.40 (d, *J* = 8.2 Hz, 2H, ArH), 7.21 (d, *J* = 8.2 Hz, 2H, ArH), 5.25 (s, 1H, CH), 3.92 (q, *J* = 7.0 Hz, 2H, OCH₂CH₃), 2.26 (s, 3H, CH₃), 1.06 (t, *J* = 7.0 Hz, 3H, OCH₂CH₃). Anal. Calcd for C₁₄H₁₅N₃O₅: C, 55.08; H, 4.92; N, 13.77%. Found: C, 55.14; H, 4.95; N, 13.69%.

5-Ethoxycarbonyl-4-(4-chlorophenyl)-6-methyl-3,4-dihydropyrimidin-2(1H)-one **4g**: ¹H NMR (300 MHz, DMSO-d₆, δ ppm): 9.25 (s, 1H, NH), 7.78 (s, 1H, NH), 7.37 (d, *J* = 8.3 Hz, 2H, ArH), 7.23 (d, *J* = 8.3 Hz, 2H, ArH), 5.26 (s, 1H, CH), 3.95 (q, *J* = 7.0 Hz, 2H, OCH₂CH₃), 2.24 (s, 3H, CH₃), 1.10 (t, *J* = 7.0 Hz, 3H, OCH₂CH₃). Anal. Calcd for C₁₄H₁₅ClN₂O₃: C, 57.05; H, 5.13; N, 9.50, Cl, 12.03%. Found: C, 57.13; H, 5.09; N, 9.44, Cl, 12.04%.

5-Ethoxycarbonyl-6-methyl-4-phenyl-3,4-dihydropyrimidin-2(1H)-one **4h**: ¹H NMR (300 MHz, DMSO-d₆, δ ppm): 9.18 (s, 1H, NH), 7.85 (s, 1H, NH), 7.20-7.30 (m, 5H, ArH), 5.20 (s, 1H, CH), 3.98 (q, *J* = 7.2 Hz, 2H, OCH₂CH₃), 2.22 (s, 3H, CH₃), 1.08 (t, *J* = 7.2 Hz, 3H, OCH₂CH₃). Anal. Calcd for C₁₄H₁₆N₂O₃: C, 64.61; H, 6.20; N, 10.77%. Found: C, 64.63; H, 6.18; N, 10.80%.

5-Ethoxycarbonyl-6-methyl-4-(p-tolyl)-3,4-dihydropyrimidin-2(1H)-one **4i**: ¹H NMR (300 MHz, DMSO-d₆, δ ppm): 8.98 (s, 1H, NH), 7.94 (s, 1H, NH), 7.21 (d, *J* = 8.1 Hz, 2H, ArH), 7.09 (d, *J* = 8. Hz, 2H, ArH), 5.17 (s, 1H, CH), 4.01 (q, *J* = 7.2 Hz, 2H, OCH₂CH₃), 2.35 (s, 3H, CH₃), 2.27 (s, 3H, CH₃), 1.10 (t, *J* = 7.2 Hz, 3H, OCH₂CH₃). Anal. Calcd for C₁₅H₁₈N₂O₃: C, 65.68; H, 6.62; N, 10.21%. Found: C, 65.65; H, 6.60; N, 10.17%.

5-Ethoxycarbonyl-6-methyl-4-(4-N,N-dimethylaminophenyl)-3,4-dihydropyrimidin-2(1H)-one **4j**: ¹H NMR (300 MHz, DMSO-d₆, δ ppm): 9.21 (s, 1H, NH), 7.78 (s, 1H, NH), 7.21-7.32 (m, 4H, ArH), 5.23 (s, 1H, CH), 3.94 (q, *J* = 7.3 Hz, 2H, OCH₂CH₃), 1.11 (t, *J* = 7.3 Hz, 3H, OCH₂CH₃), 2.60 (s, 6H, N(CH₃)₂), 2.24 (s, 3H, CH₃). Anal. Calcd for C₁₆H₂₁N₃O₃: C, 63.35; H, 6.99; N, 13.85%. Found C, 63.33; H, 6.96; N, 13.86%.

5-Ethoxycarbonyl-4-(2,4-dichlorophenyl)-6-methyl-3,4-dihydropyrimidin-2(1H)-one **4k**: ^1H NMR (300 MHz, DMSO- d_6 , δ ppm): 10.34 (s, 1H, NH), 9.66 (s, 1H, NH), 7.20-7.63 (m, 3H, ArH), 5.18 (s, 1H, CH), 4.09 (q, 2H, $J= 7.2$ Hz, OCH_2CH_3), 2.29 (s, 3H, CH_3), 1.12 (t, 3H, $J= 7.2$ Hz, OCH_2CH_3). Anal. Calcd for $\text{C}_{14}\text{H}_{14}\text{Cl}_2\text{N}_2\text{O}_3$: C, 51.08; H, 4.29; N, 8.51; Cl, 21.54%. Found C, 51.10; H, 4.32; N, 8.53; Cl, 21.52%.

5-Ethoxycarbonyl-6-methyl-4-(4-methoxyphenyl)-3,4-dihydropyrimidin-2(1H)-thione **4l**: ^1H NMR (300 MHz, DMSO- d_6 , δ ppm): 9.16 (s, 1H, NH), 8.01 (s, 1H, NH), 7.46 (d, $J= 8.1$ Hz, 2H, ArH), 7.11 (d, $J= 8.1$ Hz, 2H, ArH), 5.10 (s, 1H, CH), 3.98 (q, $J= 7.1$ Hz, 2H, OCH_2CH_3), 3.35 (s, 3H, OCH_3), 2.25 (s, 3H, CH_3), 1.12 (t, $J= 7.2$ Hz, 3H, OCH_2CH_3). Anal. Calcd for $\text{C}_{15}\text{H}_{18}\text{N}_2\text{O}_3\text{S}$: C, 58.80; H, 5.92; N, 9.14, S, 10.47%. Found C, 58.82; H, 5.90; N, 9.16, S, 10.49%.

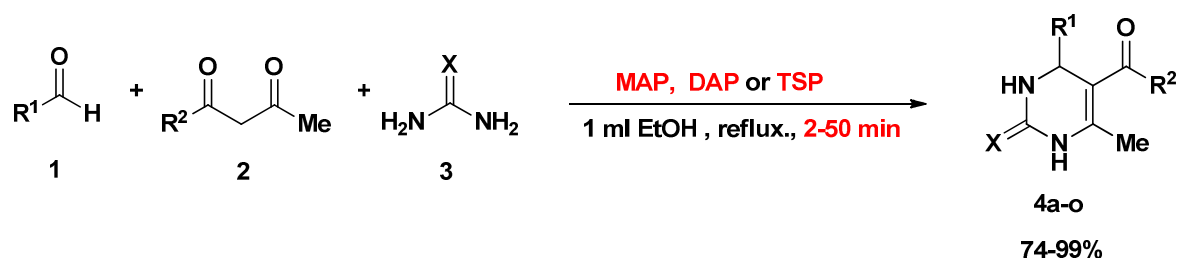
5-Ethoxycarbonyl-6-methyl-4-(4-chlorophenyl)-3,4-dihydropyrimidin-2(1H)-thione **4m**: ^1H NMR (300 MHz, DMSO- d_6 , δ ppm): 9.25 (s, 1H, NH), 8.01 (s, 1H, NH), 7.37 (d, $J= 8.3$ Hz, 2H, ArH), 7.23 (d, $J= 8.3$ Hz, 2H, ArH), 5.18 (s, 1H, CH), 4.08 (q, $J= 7.1$ Hz, 2H, OCH_2CH_3), 2.26 (s, 3H, CH_3), 1.15 (t, $J= 7.1$ Hz, 3H, OCH_2CH_3). Anal. Calcd for $\text{C}_{14}\text{H}_{15}\text{ClN}_2\text{O}_2\text{S}$: C, 51.10; H, 8.87; N, 9.01, Cl, 11.41, S, 10.32%. Found: C, 51.08; H, 8.86; N, 9.04, Cl, 11.40, S, 10.30%.

5-Ethoxycarbonyl-6-methyl-4-phenyl-3,4-dihydropyrimidin-2(1H)-thione **4n**: ^1H NMR (300 MHz, DMSO- d_6 , δ ppm): 9.41 (s, 1H, NH), 8.28 (s, 1H, NH), 7.14-7.31 (m, 5H, ArH), 5.16 (s, 1H, CH), 4.12 (q, 2H, $J= 7.2$ Hz, OCH_2CH_3), 2.29 (s, 3H, CH_3), 1.11 (t, 3H, $J= 7.2$ Hz, OCH_2CH_3). Anal. Calcd for $\text{C}_{14}\text{H}_{16}\text{N}_2\text{O}_2\text{S}$: C, 60.85; H, 5.84; N, 10.14, S, 11.61%. Found: C, 60.84; H, 5.82; N, 10.15, S, 11.60%.

5-Ethoxycarbonyl-6-methyl-4-(p-tolyl)-3,4-dihydropyrimidin-2(1H)-thione **4o**: ^1H NMR (300 MHz, DMSO- d_6 , δ ppm): 9.32 (s, 1H, NH), 8.10 (s, 1H, NH), 7.30 (d, $J= 8.1$ Hz, 2H, ArH), 7.10 (d, $J= 8.3$ Hz, 2H, ArH), 5.20 (s, 1H, CH), 3.98 (q, $J= 7.2$ Hz, 2H, OCH_2CH_3), 2.35 (s, 3H, CH_3), 2.26 (s, 3H, CH_3), 1.10 (t, $J= 7.2$ Hz, 3H, OCH_2CH_3). Anal. Calcd for $\text{C}_{15}\text{H}_{18}\text{N}_2\text{O}_2\text{S}$: C, 62.04; H, 6.25; N, 9.65, S, 11.04%. Found: C, 62.01; H, 6.23; N, 9.61, S, 11.09%.

RESULTS AND DISCUSSION

The synthesis of 3,4-dihydropyrimidin-2(1H)-one and 3,4-dihydropyrimidin-2(1H)-thione derivatives is carried out according to the overall reaction below in the presence of catalysts phosphates (11) (MAP or DAP or TSP) (Figure 1).



$\text{R}_1 = \text{C}_6\text{H}_5, 4\text{-MeOC}_6\text{H}_4, 4\text{-NO}_2\text{C}_6\text{H}_4, 4\text{-ClC}_6\text{H}_4, 4\text{-MeC}_6\text{H}_4, 4\text{-N(Me)}_2\text{C}_6\text{H}_4, 2,4\text{-(Cl)}_2\text{C}_6\text{H}_3$.
 $\text{R}_2 = \text{OEt, Me}$.
 $\text{X} = \text{O, S}$.

Figure 1. Synthesis of the 3,4 -dihydropyrimidin-2-one derivatives in the presence of catalysts MAP or DAP or TSP.

To find the optimum conditions for the Biginelli reaction, we chose a reaction model on which we will study the influence of certain parameters that control the reaction, namely the solvent of the reaction, the volume of the solvent and the catalyst amount used. The condensation between benzaldehyde, ethyl acetoacetate and urea has been selected as a model of the reaction.

The 5-acetyl-6-methyl-4-phenyl-3,4-dihydropyrimidine-2-(1H)-one **4a** ($\text{R}^1 = \text{C}_6\text{H}_5, \text{R}^2 = \text{Me}, \text{X} = \text{O}$) has been prepared according to the reaction described in figure 1, in the presence of 5 mol% of MAP or DAP or TSP in 1 mL EtOH reflux, the yields and time of the reactions are shown in Table 1.

Table 1. Comparison between a few catalysts described in the literature and our catalysts.

Entry	Catalyst	Time	Yield %
1	nano- $\gamma\text{-Fe}_2\text{O}_3\text{-SO}_3\text{H}$	2 h	80 (7)
2	ASANPs	5.3 h	60 (12)
3	SBNPSA	3-4 h	90-95 (13)
4	MAP	7 min	87
5	DAP	17 min	98
6	TSP	7 min	92

According to the observed results, we note that the effectiveness of our three catalysts are higher than those of some catalysts described in the literature with respect to time and reaction yields. It should be noted that it is in heterogeneous catalysis in solid/liquid phase, the effect of the solvent is an essential factor. It can play a role as activating or inhibitor of the reaction. We studied the effect of the solvent on the reaction model chosen previously with different solvents, always in the presence of 5 mol% of the catalyst placed at reflux. The results are shown in Table 2 where the efficiency of the reaction in ethanol was higher compared to other solvents. Therefore, ethanol is the ideal solvent for this reaction.

Table 2. Influence of the solvent on the reaction of Biginelli^a.

Entry	Solvent (1 ml)	Time (min)			Yield% ^b		
		MAP	DAP	TAP	MAP	DAP	TSP
1	Ethanol	7	7	7	87	98	92
2	Methanol	11	7	7	57	97.7	88
3	Butanol	8	3	3	46	95	81
4	Isopropanol	23	4	4	53	86	80
5	DMF	8	4	4	48	89	89
6	Acetonitrile	14	11	11	54	78,7	86

^a Reaction conditions: acetoacetate (**2a**) (1 mmol), benzaldehyde (**1a**) (1 mmol) and urea (**3a**) (1.5 mmol), catalyzed MAP or DAP or TSP under conditions at reflux.

^b Isolated yield.

We have studied another factor, which is the volume of the solvent. To study the influence of this parameter we used ethanol; previously found to be the ideal solvent for this reaction (Table 2) by changing just the volume of the latter. The results summarized in Table 3 showed that the reaction yield does not exceed 58% in the absence of ethanol. Good yields were obtained when we used 1 mL of ethanol, but when the volume of ethanol is greater than 1 mL, it was noted that there is a lowering in the reaction yield. It may be explained by the formation of a film (layer) of ethanol into the surface of the catalyst disabling the interaction between the reactants and the catalyst, in addition to the dispersion of the substrates. Therefore, the optimal volume for carrying out this reaction is 1 mL.

Table 3. Influence of the solvent volume ^a

Entry	Volume of Ethanol	Time (min)			Yield % ^b		
		MAP	DAP	TSP	MAP	DAP	TSP
1	Solvent-free	3	2	4	58	74	89
2	1mL	7	7	7	87	98	92
3	2mL	30	50	21	86,3	90	90
4	3mL	55	110	40	85	60	85

^a Reaction conditions: acetoacetate (**2a**) (1 mmol), benzaldehyde (**1a**) (1 mmol) and urea (**3a**) (1.5 mmol), catalyzed MAP or DAP or TSP under conditions at reflux.

^b Isolated yield.

The effect of the amount of the catalysts was studied on the reaction of the synthesis of 3,4-dihydropyrimidin-2(1H)-one derivatives. To study the influence of this parameter on the

reaction, we have changed the amount of catalysts from 1 up to 10 mol%, the results are presented in Table 4. The good yields were obtained when we used the optimal weights (1 mol %) for the catalysts DAP or TSP, (3 mol %) for the catalyst MAP, we noted that when the amount of catalysts exceeds 4 mol%, the yields of reaction decreases.

One of the most significant features of the present article is the recyclability and reuse of the catalyst. The reuse of the catalyst was studied after the completion of the reaction performed under the optimized conditions. After the completion of the reaction, the catalyst was filtered hot and washed several times with ethyl acetate, then dried in the oven at 40°C. After these steps the catalyst was reused in other reactions. The experiment shows that our catalysts can be recycled five times without significant loss of catalytic activity (Figure 2).

Table 4. Optimization of amount of catalyst^a.

Entry	Amount of catalyst (mol %)	Time (min)			Yield % ^b		
		MAP	DAP	TSP	MAP	DAP	TSP
1	1	58	7	4	72	98	97
2	2	43	30	2	88	98	96
3	3	23	33	3	95	98	95
4	4	20	25	5	90	98	94
5	5	7	17	7	87	98	92
6	6	10	16	6	68	95	91
7	7	17	5	12	67	90	87
8	8	20	21	13	66	88	85
9	9	25	6	3	61	82	82
10	10	32	36	21	61	79	79

^a Reaction conditions: acetoacetate (**2a**) (1 mmol), benzaldehyde (**1a**) (1 mmol) and urea (**3a**) (1.5 mmol), catalyzed MAP or DAP or TSP under conditions at reflux.

^b Isolated yield.

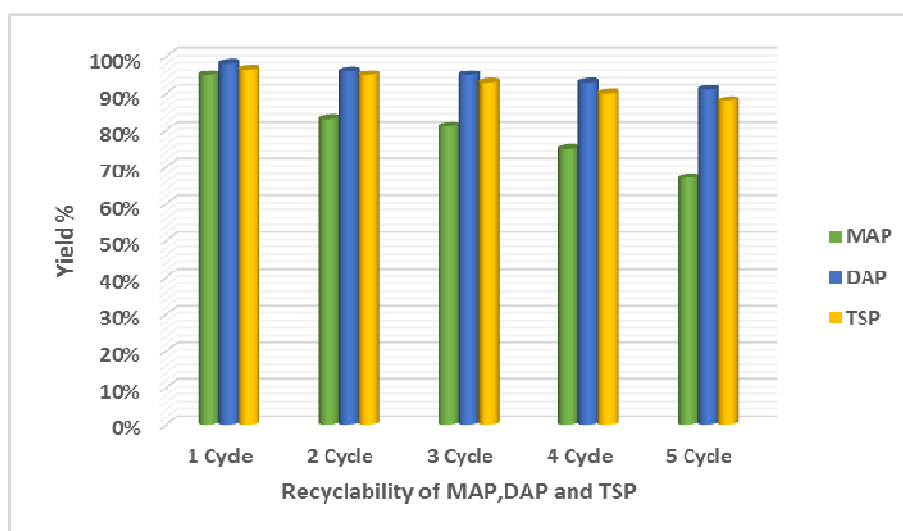


Figure 2. Recyclability of catalyst MAP, DAP and TSP in synthesis of 3,4-dihydropyrimidin-2(1H)-one.

After the optimization of the reaction conditions, we next thought to study the generality for the series of 3,4-dihydropyrimidin-2(1H)-one and 3,4-dihydropyrimidin-2(1H)-thione derivatives, using a wide range of various aryl-substituted aldehydes with different substituted β -ketoester (acetyl acetone or ethyl acetoacetate) and (urea or thiourea) under the optimal conditions. The results are presented in Table 5. As shown in this latter, the reaction of variety of substituted aromatic aldehydes with acetyl acetone and urea afforded the 3,4-dihydropyrimidin-2-one derivatives (entries **4a-4d**) at short time (2-25 min) in high yields (83-98%) and high purities. When using ethyl acetoacetate instead of acetyl acetone, the desired compounds were also obtained at significantly shortened times (2-50 min) and excellent yields (86-99%) (entries 4e-4k). Furthermore, the use of thiourea instead of urea the reaction provides the corresponding 3,4-dihydropyrimidin-2-thiones (**4l-4o**) with remarkable time-saving (2-9 min) and high-yielding process (74-98%).

CONCLUSION

In this work, we investigated a methodology for the synthesis of 3,4-dihydropyrimidin-2(1H)-one derivatives using phosphate fertilizers (MAP or DAP or TSP) as heterogeneous catalysts. We synthesized 3,4-dihydropyrimidin-2(1H)-one derivatives through a one step reaction using ethanol as a green solvent in short reaction times with high yields.

Table 5. Generalization of the synthesis of 3,4-dihydropyrimidin-2(1H)-one/thione **4** derivatives.

Compound no	R ¹	R ²	X	Time (min)			Yield % ^b			Mp °C	
				MAP	DAP	TSP	MAP	DAP	TSP	Found	Reported
4a	C ₆ H ₅	Me	O	7	7	4	98	95	96.5	210-212	208-219 (14)
4b	4-ClC ₆ H ₄	Me	O	6	10	3	98	88	88	224-226	226-227 (14)
4c	4-NO ₂ C ₆ H ₄	Me	O	3	2	2	91	90	89	236-238	238-240 (14)
4d	4-MeOC ₆ H ₄	Me	O	20	25	10	84	83	97	190-191	191-193 (19)
4e	4-MeOC ₆ H ₄	OEt	O	11	15	5	92	93	86	201-203	200-201 (13)
4f	4-NO ₂ C ₆ H ₄	OEt	O	2	2	2	99	98	97	209-210	209-210 (13)
4g	4-ClC ₆ H ₄	OEt	O	17	20	10	94	93	90	212-214	214-215 (13)
4h	C ₆ H ₅	OEt	O	7	12	3	98	90	93	201-202	201-203 (13)
4i	4-MeC ₆ H ₄	OEt	O	4	7	3	98	86	90	212-213	213-215 (16)
4j	4-N(Me) ₂ C ₆ H ₄	OEt	O	35	50	20	92	91	92	231-233	228-230 (17)
4k	2,4-(Cl) ₂ C ₆ H ₃	OEt	O	17	20	5	91	90	90	248-250	248-250 (13)
4l	4-MeOC ₆ H ₄	OEt	S	7	5	3	97	98	92	138-140	140-141 (15)
4m	4-ClC ₆ H ₄	OEt	S	3	5	2	98	96	97	192-194	193-195 (18)
4n	C ₆ H ₅	OEt	S	4	9	5	74	94	91	208-209	209-210 (13)
4o	4-MeC ₆ H ₄	OEt	S	3	3	2	90	88	93	214-215	214-215 (20)

^b Isolated yield.

REFERENCES

1. Lal J, Gupta SK, Thavaselvam D, Agarwal DD. Design, synthesis, synergistic antimicrobial activity and cytotoxicity of 4-aryl substituted 3, 4-dihydropyrimidinones of curcumin. *Bioorg Med Chem Lett.* 2012;22(8):2872–2876.
2. Wan J-P, Pan Y. Recent advance in the pharmacology of dihydropyrimidinone. *Mini Rev Med Chem.* 2012;12(4):337–349.
3. Wan J-P, Liu Y. Synthesis of dihydropyrimidinones and thiones by multicomponent reactions: strategies beyond the classical Biginelli reaction. *Synthesis.* 2010; 2010(23):3943–3953.
4. Narahari SR, Reguri BR, Gudaparthi O, Mukkanti K. Synthesis of dihydropyrimidinones via Biginelli multi-component reaction. *Tetrahedron Lett.* 2012; 53(13):1543–1545.
5. Japp FR, Klingemann F. I.—Ethylic phenanthroxylylene-acetoacetate. *J Chem Soc Trans.* 1891;59(0):1–26.
6. Zhang Y, Wang B, Zhang X, Huang J, Liu C. An efficient synthesis of 3, 4-dihydropyrimidin-2 (1H)-ones and thiones catalyzed by a novel Brønsted acidic ionic liquid under solvent-free conditions. *Molecules.* 2015;20(3):3811–3820.
7. Kolvari E, Koukabi N, Armandpour O. A simple and efficient synthesis of 3, 4-dihydropyrimidin-2-(1H)-ones via Biginelli reaction catalyzed by nanomagnetic-supported sulfonic acid. *Tetrahedron.* 2014;70(6):1383–1386.
8. Starcevich JT, Laughlin TJ, Mohan RS. Iron(III) tosylate catalyzed synthesis of 3,4-dihydropyrimidin-2(1H)-ones/thiones via the Biginelli reaction. *Tetrahedron Lett.* 2013 Feb;54(8):983–5.
9. Siddiqui ZN. Bis [(L) prolinato-N, O] Zn–water: A green catalytic system for the synthesis of 3, 4-dihydropyrimidin-2 (1H)-ones via the Biginelli reaction. *Comptes Rendus Chim.* 2013;16(2):183–188.
10. Karthikeyan P, Aswar SA, Muskawar PN, Bhagat PR, Kumar SS. Development and efficient 1-glycyl-3-methyl imidazolium chloride–copper (II) complex catalyzed highly enantioselective synthesis of 3, 4-dihydropyrimidin-2 (1H)-ones. *J Organomet Chem.* 2013; 723:154–162.
11. Bahammou I, Esaady A, Boukhris S, Ghailane R, Habbadi N, Hassikou A, et al. Direct use of mineral fertilizers MAP, DAP, and TSP as heterogeneous catalysts in organic reactions. *Mediterr J Chem.* 2016;5(6):615–623.
12. Nasr-Esfahani M, Taei M. Aluminatesulfonic acid nanoparticles: synthesis, characterization and application as a new and recyclable nanocatalyst for the Biginelli and Biginelli-like condensations. *RSC Adv.* 2015;5(56):44978–44989.
13. Jetti SR, Bhatewara A, Kadre T, Jain S. Silica-bonded N-propyl sulfamic acid as an efficient recyclable catalyst for the synthesis of 3, 4-dihydropyrimidin-2-(1H)-ones/thiones under heterogeneous conditions. *Chin Chem Lett.* 2014;25(3):469–473.
14. Zhao Y, Zhao Y, Zhang J, Liu H, Liang L. Polyphosphoric acid catalyst for the one-pot synthesis of 3, 4-dihydropyrimidin-2 (1H)-ones by grinding under solvent-free conditions. *Indian J Chem.* 2015; 54:139–141.
15. 1883 - AASR-2012-4-2-988-993.pdf [Internet]. [cited 2017 Jan 19]. Available from: <http://s3.amazonaws.com/academia.edu.documents/31197657/AASR-2012-4-2-988-993.pdf?AWSAccessKeyId=AKIAJ56TQJRTWSMTNPEA&Expires=1484852299&Signature=p9ui5dB>

BpphVSBZpuS6vv4csihc%3D&response-content-disposition=inline%3B%20filename%3DGreen_protocol_for_the_synthesis_of_3_4-.pdf

16. Elhamifar D, Nazari E. Preparation of Iron-Containing Schiff Base and Ionic Liquid Based Bifunctional Periodic Mesoporous Organosilica and Its Application in the Synthesis of 3,4-Dihydropyrimidinones. *ChemPlusChem*. 2015 May;80(5):820–6.
17. Wang J, Li N, Qiu R, Zhang X, Xu X, Yin S-F. Air-stable zirconocene bis (perfluorobutanesulfonate) as a highly efficient catalyst for synthesis of N-heterocyclic compounds. *J Organomet Chem*. 2015;785:61–67.
18. Sarrafi Y, Pazokie F, Azizi SN, Alimohammadi K, Mehrasbi E, Chiani E. Mesoporous SBA-15 nanoparticles: An efficient and eco-friendly Catalyst for one-pot synthesis of 3, 4-dihydropyrimidin-2(1H)-ones under solvent-free conditions. *Curr Chem Lett*. 2014;3(2):97–102.
19. 1883 - zotero://attachment/100/ [Internet]. [cited 2017 Jan 19]. Available from: zotero://attachment/100/
20. Su W, Li J, Zheng Z, Shen Y. One-pot synthesis of dihydropyrimidiones catalyzed by strontium (II) triflate under solvent-free conditions. *Tetrahedron Lett*. 2005; 46(36):6037–6040.



Boron and Molybdenum Contents of *Verbascum olympicum* boiss. Growing Around an Abandoned Tungsten Mine: A Case Study for Ecological Problem Solving

Ümran SEVEN ERDEMİR

Uludağ University, Faculty of Art and Sciences, Department of Chemistry, 16059, Bursa-Turkey

Abstract: Interactions among micro-elements can affect their uptake by plants. Thus, it is important to evaluate nutrient interactions when designing phytoremediation strategies. In this study, the competitive or complementary effects between B and Cd, Cu, Fe, Mn, Mo, Pb, Zn, and W elements in leaf tissues of *Verbascum olympicum* Boiss. (Scrophulariaceae) were evaluated. This species is one of the main endemic species growing around the abandoned Etibank tungsten mine at Uludağ Mountain (Bursa, Turkey). Leaf and soil samples were collected from unpolluted and polluted areas around the mine. Inductively coupled plasma-mass spectrometry was used to determine the levels of selected elements in soil samples and in leaves of *V. olympicum*. Classical open wet and Kjeldahl digestion methods were used to process the samples. The analytical accuracy was guaranteed using two kinds of certified reference materials. Complementary behaviors of B and Mo were observed in leaves of *V. olympicum*, but not in the soil. This result provides information on the adaptation properties of this species in a polluted area.

Keywords: Boron; molybdenum; *Verbascum olympicum*; Tungsten mine; ICP-MS.

Submitted: December 29, 2016. **Revised:** February 13, 2017. **Accepted:** March 10, 2017.

Cite this: Seven Erdemir Ü. Boron and Molybdenum Contents of *Verbascum olympicum* boiss. Growing Around an Abandoned Tungsten Mine: A Case Study for Ecological Problem Solving. JOTCSA. 2017;4(2):13–24.

DOI: 10.18596/jotcsa.282219.

Corresponding author. E-mail: useven@uludag.edu.tr, Tel:+90 224 2941739

INTRODUCTION

In plants, mineral nutrition is important for physiological and biochemical processes (1). Boron (B) is one of the mineral nutrients required for plant growth, and it is essential for cell structures (1, 2). The importance of B as an essential element for higher plant growth has been demonstrated (1). It is involved in many important processes in plants, including cell wall strength, cell wall synthesis and development, cell wall structural integrity, lignification, respiration, cell division, carbohydrate metabolism, fruit and seed formation and development, petal and leaf bud formation, vascular tissue repair, sugar transport, hormone development, metabolism of ribose nucleic acids, indoleacetic acid, and phenol, membrane stability, cytokinin production and transfer, pollen budding, and stimulation or inhibition of specific metabolic pathways (1–3). Elevated B levels may affect the metabolism of higher plants via its effects on enzyme activities (4). It has been suggested that B may generate oxidative stress in higher plants via the production of reactive oxygen species as a result of changes in the photosynthetic system (5). Total B levels in soils have been reported to range from 20 to 200 mg B kg⁻¹ with less than 5%–10% in a form available to plants (2). Nutrient availability mainly depends on soil texture, organic matter content, and especially pH (6). The availability of B is also affected by interrelationships with other elements and environmental factors. For example, moderate to heavy rainfall, dry weather, and high light intensity are important factors for B availability to plants (2).

In plants, B interacts with macro-elements including nitrogen, phosphorus, potassium, and calcium (1). Compared with other elements, B reaches a toxic concentration at a lower level (4). Also, its mobility in plants differs from that of other elements, and this affects its function (7). Molybdenum (Mo) and B have complementary functions in the biological processes of soybean, which has higher Mo requirements than other plants. It is considered that Mo is an essential micro-nutrient for plants, while B is an essential micro-element for higher plants. The functions of B, the mechanisms of Mo uptake in plants, and the combined effects of B and Mo have been studied (8). While Mo is actively absorbed into the cell from the soil by roots mainly in the forms of MoO₄²⁻ and HMoO₄⁻, B is passively absorbed in the form of H₃BO₃ (8), and there is a co-supplementary interaction between Mo and B (8, 9). On the other hand, tungsten (W) inhibits molybdoenzymes in plants (10); therefore, the interactions among B, Mo, and W elements in contaminated soils are significant in terms of their uptake and function.

The aim of this study was to evaluate the interactions between B and other elements in a plant growing around a polluted site. *Verbascum olympicum* Boiss. (Scrophulariaceae) was

selected as the plant material in this study, since it is one of the dominant endemic species growing around an abandoned tungsten mine on Uludağ Mountain (Bursa, Turkey), and its restoration and/or remediation properties in this area have been studied previously (11, 12). The main objective of this study was to investigate the influence of the mine and its residual wastes on *V. olympicum* growing at the mine site, and to collect data on its uptake of B and other related elements in this environment. Analyses of the contents of many elements in this plant can reveal competitive or complementary effects. Understanding the mutual, antagonistic, or synergistic interactions among elements is important for designing fertilization and/or phytoremediation strategies. Inductively coupled plasma-mass spectrometry (ICP-MS) was used to detect and quantify elements in soil and plant samples because of its multi elemental determination capability, low detection limits, and wide linear ranges.

MATERIALS AND METHODS

Sampling site and sample preparation

Verbascum olympicum Boiss. (Scrophulariaceae), one of the main species growing around the abandoned Etibank tungsten mine on Uludağ Mountain in Turkey (Figure 1), was selected for analysis in this study. The mine is located at an altitude between 2100 and 2487 m and lies at the intersection of 40°N latitude and 29°E longitude. It was active for approximately 20 years from 1969 to 1989. The ore generated tungsten oxide (40%), concentrated magnetite, pyrite, and by-products. The substratum of the waste removal pools and waste canals is granite at lower altitudes, and a calcareous substrate at upper altitudes (13). Samples were collected around the waste removal pools of this abandoned mine. The canals (on the right side) and waste-removal pools (on the left side) in the area are shown in Figure 2. Five soil samples were collected from each of three sites (sites I, II, and III) at 0- to 15-cm depth. Sites I and II were unpolluted, and site III was a polluted site at the waste removal pools. Soil samples were sieved (0.5 mm mesh) and air-dried under laboratory conditions. Plant materials collected at the same sites were washed and then dried to constant weight in an oven at 80°C. The dried plant materials were ground with a mortar and pestle, and the ground plant material and soil samples were stored in clear paper bags until element analyses. Leaf samples (100–500 mg) were subjected to open wet digestion in a borosilicate glass vessel with HNO₃ (5 mL) and H₂O₂ (3 mL). Soil samples (0.5 g) were digested by phosphoric acid, nitric acid, and hydrogen peroxide as described by Bednar *et al.* (14) using a DK 20 Kjeldahl digestion unit (VELP Scientifica, Milan, Italy).

Certified reference materials and blank samples were prepared in the same way as samples ($n=3$).



Figure 1. *Verbascum olympicum* Boiss. (Scrophulariaceae) (Photo by G. Güteryüz).



Figure 2. Sample collection area in the abandoned tungsten mine on Uludağ Mountain (Photo by G. Güteryüz).

Chemicals and Apparatus

A single-element standard solution of W at a concentration of $1000 \mu\text{g mL}^{-1}$ (Perkin Elmer, Shelton, CT, USA) and a multi-element standard solution containing 100 mg L^{-1} B and 10 mg L^{-1} Mo in a mixture of 30 elements (Merck 110580; Darmstadt, Germany) were used to prepare calibration standards. Nitric acid (65%) was of "suprapur" quality and was obtained

from Merck, as were the other reagents. The calibration curves for all elements were constructed from 0.5 to 1000 $\mu\text{g L}^{-1}$. The ^{11}B , ^{98}Mo , and ^{184}W isotope levels together with the concentrations of ^{111}Cd , ^{63}Cu , ^{57}Fe , ^{55}Mn , ^{208}Pb , and ^{64}Zn isotopes were determined in soil and plant samples by inductively coupled plasma-mass spectrometry (ICP-MS) using an Elan 9000 (Perkin Elmer SCIEX) instrument. The ICP-MS system comprised a Ryton cross-flow nebulizer, a Scott-type double-pass spray chamber, a standard glass torch, and a nickel sampler and skimmer cones (1.1 and 0.9 mm i.d., respectively). The conditions for ICP-MS were as follows: RF power, 1000 W; plasma argon flow rate, 17.0 L min^{-1} ; nebulizer gas flow rate, 0.85 L min^{-1} ; sample uptake rate, 1.5 mL min^{-1} ; dwell time, 50 ms; scanning mode, peak hopping; and detector mode, dual. Soil samples were digested using the DK 20 model Kjeldahl digestion unit (VELP Scientifica). Digests were filtered through PVDF (polyvinylidene fluoride) hydrophilic syringe filters (0.45- μm pore size, Millex-HV, Millipore Corp., Bedford, MA, USA) and analyzed after appropriate dilution. The water used was ultrapure grade (18.3 $\text{M}\Omega\cdot\text{cm}^{-1}$, Zeneer Power I, Human Corporation, Seoul, South Korea). Argon (99.999% purity) was purchased from Asalgaz (Bursa, Turkey). The method was validated by analyses of GBW07605 tea leaves (National Research Center for Certified Reference Materials, Beijing, China) and NIST 1570 spinach leaves (National Institute of Standards and Technology, Gaithersburg, MD, USA). Data were analyzed by one-way ANOVA and Tukey's HSD test using Statistica 5.0 software. Differences were considered significant at $p \leq 0.05$.

RESULTS AND DISCUSSION

The contents of elements at mg kg^{-1} levels were determined in above-ground parts (leaves) of *V. olympicum* and in soils at sampling sites I and II (unpolluted) and site III (polluted) (Table 1). The measured levels of all elements were in good agreement with the certified values of mentioned reference materials at the 95% confidence level, indicating that the total element determinations were accurate. For all elements, the limits of quantitation were below the measured values.

Table 1. Mean contents ($\text{mg kg}_{\text{dw}}^{-1}$) of elements in soil and plant parts of *Verbascum olympicum* at sites (non-polluted, sites I and II; polluted, within the waste removal pool, site III) of the abandoned tungsten mine on Uludağ Mountain, Bursa Turkey.

<i>Elements</i>	<i>Element Levels* in sites</i>					
	Site I		Site II		Site III	
	Soil	Leaf	Soil	Leaf	Soil	Leaf
B	78.7 ^a ± 19.9	40.2 ^a ± 7.7	9.2 ^a ± 17.2	22.8 ^{ab} ± 10.7	63.1 ^a ± 12.6	17.1 ^b ± 6.5
W	20.6 ^b ± 2.4	1.3 ^b ± 0.4	26.7 ^b ± 0.8	0.4 ^b ± 0.1	1868.8 ^a ± 215.3	44.2 ^a ± 25.7
Fe	39486 ^b ± 20580	48.2 ^a ± 23.9	25425 ^b ± 799	8.5 ^b ± 5.7	184346 ^a ± 26822	35.2 ^{ab} ± 4.3
Mo	14.0 ^a ± 6.8	0.6 ^a ± 0.2	7.2 ^a ± 0.4	0.5 ^a ± 0.3	5.7 ^a ± 1.4	0.3 ^a ± 0.1
Zn	169.9 ^b ± 17.1	34.3 ^b ± 5.1	220.6 ^b ± 11.8	19.3 ^b ± 4.6	3224.5 ^a ± 368.5	116.4 ^a ± 35.8
Cu	211.1 ^a ± 4.3	11.8 ^{ab} ± 2.4	242.0 ^a ± 5.5	5.4 ^b ± 1.7	595.4 ^a ± 386.3	20.6 ^a ± 7.1
Cd	0.22 ^b ± 0.02	0.02 ^b ± 0.00	0.62 ^b ± 0.09	0.04 ^b ± 0.03	12.94 ^a ± 1.86	0.22 ^a ± 0.09
Mn	970 ^b ± 388	538 ^a ± 207	1721 ^b ± 169	1237 ^a ± 458	8689 ^a ± 1565	1289 ^a ± 718
Pb	27.97 ^b ± 1.90	0.75 ^b ± 0.16	48.81 ^a ± 3.07	0.66 ^b ± 0.19	49.34 ^a ± 0.84	1.39 ^a ± 0.29

Mean values are shown ($n = 3$) ± standard deviation. Different letters indicate significant differences between sampling sites (Tukey's HSD test; $p < 0.05$).

The B levels in leaf and soil samples from sites I and II ranged widely. Unlike other elements, B shows a wide range of concentrations in soil (2). The B concentrations in soils from site III (polluted) were higher than those in samples from site II, but lower than those in soil samples from site I. Therefore, the mean value of B at unpolluted sites was compared with the B content at the polluted site. The B levels in leaf samples were lower at polluted sites than at the unpolluted site. There is competition between W and Mo, as reported earlier (15), and a positive correlation between B and Mo has also been reported (10). Thus, there is some competition or completion for transport between B and W and between B and Mo, respectively. As a result, low B and Mo levels in leaves were associated with higher W levels. This is consistent with the results shown in Table 1; that is, leaf samples with higher W levels had lower Mo and B levels. There also appeared to be some competition between B and Mo in soil samples; that is, soil samples with higher levels of B had lower levels of Mo, and vice versa. Thus, B and Mo also showed complementary behaviors in leaves of this species, as outlined by Liu *et al.* (10). This may indicate that they are interchangeable in some physiological functions of the plant. The association between B and Mo may have some significance in terms of the adaptation of this plant to the polluted area.

When W levels were present at excessive levels in soils at the polluted site, this appeared to interfere with the functions of B and Mo as they became competitive elements. Thus, any mutual effects of elements also depends on the other elements present, their concentrations, and how they interfere with other elements in the soil. As shown in Table 1, all of the other studied elements, especially W, were present at higher concentrations in soil at the polluted site than in soil at the unpolluted sites. However, the transportation ratios (element concentration in leaves divided by element concentration in soil) of B, Fe, Zn, and Mn were lower at the polluted site than at the unpolluted site. These three elements (Fe, Zn, and Mn) may be associated with B. The only element present at lower concentrations at the polluted site than at the unpolluted site was Mo.

Apart from other micro-elements, macro-elements and their quantity in the area, together with soil pH, are important factors that can enhance or inhibit the uptake of the studied elements from soil into plants. Phosphate was one of the main macro-elements, since water removal pools are known to be rich in phosphate (13). Thus, the high levels of the selected elements in leaf samples from the polluted (waste removal pools) site may be due to water-soluble phosphate complexes that are readily taken up by plants, depending on the pH (16).

Although it might be expected that large amounts of an element in the soil will lead to high transportation, and thus accumulation in plants, the opposite effect was observed for B. This may have been due to direct interference from W and Mo with the indirect interference from Mo to B. Higher W levels in leaves were associated with lower Mo and B levels. However, when the soil B levels were high, the B levels in leaves were low. This illustrates the importance of transportation in determining which elements will be present at high levels in leaves. Different transportation behaviors were observed for Mo. Therefore, interactions among elements may also inhibit B transport in plants.

As shown in Table 1, the other effected elements with their transportation ratios were Zn and Cd. Table 2 summarizes correlations between pairs of elements in plant parts. There was a significant correlation ($r^2 = 0.849$) between B content and Mo content in leaf tissues of *V. olympicum*, confirming the complementary effects between these elements for translocation. This led to the conclusion that B and Mo function similarly in this species. There was no significant correlation between B and other elements, even W. Thus the adaptation capability of *V. olympicum* depends on the complementary effects of B and Mo directly, and also B and W indirectly depending on the W–Mo interaction. There was no significant correlation between leaf and soil B levels in this species ($r^2 = 0.011$, $P = 0.789$, regression equation = $21.706 + 0.06233 \times \text{Soil B}$). This result highlighted that high B levels in leaves were not associated with high B levels in soils, but depended on competition with other elements for uptake in the natural adaptation processes of this plant.

Table 2. Simple correlation coefficients (r^2), significance levels (P) and linear regression equations ($Y = a + bx$) between contents of various elements and boron in *Verbascum olympicum* ($n = 9$, $P < 0.05$ considered as significant correlation).

	r^2	P	$Y = a + bx$
Leaf-B	0.294	0.131	Leaf-B = $30.922 - 0.2747 \times \text{Leaf-W}$
Leaf-B	0.262	0.159	Leaf-B = $17.402 + 0.30398 \times \text{Leaf-Fe}$
Leaf-B	0.849	0.000	Leaf-B = $8.0080 + 41.361 \times \text{Leaf-Mo}$
Leaf-B	0.143	0.315	Leaf-B = $32.319 - 0.0990 \times \text{Leaf-Zn}$
Leaf-B	0.048	0.571	Leaf-B = $31.339 - 0.3669 \times \text{Leaf-Cu}$
Leaf-B	0.319	0.113	Leaf-B = $33.179 - 68.47 \times \text{Leaf-Cd}$
Leaf-B	0.187	0.245	Leaf-B = $39.696 - 13.93 \times \text{Leaf-Pb}$
Leaf-B	0.101	0.406	Leaf-B = $33.979 - 0.0071 \times \text{Leaf-Mn}$

CONCLUSION

Determining soil composition through elemental analyses is important for evaluating the synergism and antagonism between elements in terms of uptake by plants. Apart from environmental factors, the competition between B and other elements for uptake by *V. olympicum* plants affected its final concentration in plant tissues. This information provides a realistic picture about the uptake of elements under natural conditions. These results will be useful for optimizing the formulation of fertilizers containing B, especially those intended for use in areas with high concentrations of particular elements. As excess uptake of certain elements from fertilizers can lead to stress responses in plants, it is important to understand the synergistic or antagonistic relationships among elements. These data will also be useful for designing management strategies for the area around the abandoned mine. Although the data suggested that there is a relationship between B and Mo, this may not be the case in other plant species or under different environmental conditions. For this reason, many elements should be taken into account in environmental risk assessments. There is still much to learn about the roles of various micro-elements, including B, in the synthesis and function of molecular and macromolecular structures. This research on the relationships among micro-elements in plants growing under stress conditions can provide a useful baseline for further laboratory-based research on the role of B in higher plants. Further research at the organelle and molecular levels is necessary to clarify the role of B. The knowledge gained from such studies will be useful for producing environmentally friendly materials.

ACKNOWLEDGEMENTS

The sampling was conducted with the permission of the General Directorate of Nature Protection and National Parks of Republic of Turkey Ministry of Forestry and Water Affairs. The author thanks Prof. Dr. Şeref Güçer for valuable discussions, Prof. Dr. Gürcan Gülerüz and Prof. Dr. Hülya Arslan for providing samples, photos, and comments on the mining area and for statistical analysis. The author also thanks Gözde Dede and Ayça Çiçek for help with sample preparation. The Commission of Scientific Research Projects of Uludağ University (project no: F-2008/25, and KUAP(F)-2015/64) are gratefully acknowledged for providing ICP-MS facilities and soil materials, respectively.

CONFLICT OF INTEREST

The author declares no conflict of interest.

REFERENCES

1. Ahmad W, Niaz A, Kanwal S, Rasheed MK. Role of boron in plant growth: a review. *Journal of Agricultural Research*. 2009;47(3).
2. Ahmad W, Niaz A, Zia MH, Saifullah, Malhi SS. Boron Deficiency in soils and crops: a review. INTECH Open Access Publisher; 2012.
3. Aref F, others. Influence of zinc and boron interaction on residual available iron and manganese in the soil after corn harvest. *Am Euras J Agric Environ Sci*. 2010;8(6):767-772.
4. Rajaie M, Ejraie AK, Owliaie HR, Tavakoli AR. Effect of zinc and boron interaction on growth and mineral composition of lemon seedlings in a calcareous soil. *International Journal of Plant Production [Internet]*. 2009 Jan [cited 2017 Mar 15];(1). Available from: http://ijpp.gau.ac.ir/article_630.html
5. Giansoldati V, Tassi E, Morelli E, Gabellieri E, Pedron F, Barbafieri M. Nitrogen fertilizer improves boron phytoextraction by *Brassica juncea* grown in contaminated sediments and alleviates plant stress. *Chemosphere*. 2012 Jun;87(10):1119-25.
6. Valenciano J, Boto J, Marcelo V. Chickpea (*Cicer arietinum* L.) response to zinc, boron and molybdenum application under field conditions. *New Zealand Journal of Crop and Horticultural Science*. 2011 Dec;39(4):217-29.
7. Brown PH, Shelp BJ. Boron mobility in plants. *Plant and Soil*. 1997 Jun 1;193(1-2):85-101.
8. Sun T, Wang YP, Wang ZY, Liu P, Xu GD. The effects of molybdenum and boron on the rhizosphere microorganisms and soil enzyme activities of soybean. *Acta Physiologiae Plantarum*. 2013 Mar;35(3):763-70.
9. Liu P, Yang Y, Xu G, Fang Y, Yang Y. The response of antioxidant enzymes of three soybean varieties to molybdenum and boron in soil with a connection to plant quality. *PLANT SOIL AND ENVIRONMENT*. 2005;51(8):351-9.
10. Adamakis I-D, Panteris E, Eleftheriou E. Tungsten Toxicity in Plants. *Plants*. 2012 Nov 16;1(2):82-99.
11. Arslan H, Güteryüz G, Akpınar A, Kırmızı S, Erdemir ÜS, Güçer Ş. Responses of *Ruderal Verbascum olympicum* Boiss. (Scrophulariaceae) Growing under Cadmium Stress: Responses of *Verbascum olympicum* to Cadmium Stress. *CLEAN - Soil, Air, Water*. 2014 Jun;42(6):824-35.

12. Akpınar A, Arslan H, Güteryüz G, Kırmızı S, Erdemir ÜS, Güçer Ş. Ni-induced Changes in Nitrate Assimilation and Antioxidant Metabolism of *Verbascum olympicum* Boiss.: Could the Plant be Useful for Phytoremediation or/and Restoration Purposes? *International Journal of Phytoremediation*. 2015 Jun 3;17(6):546–55.
13. Güteryüz G, Arslan H, Kırmızı S, Güçer S. Investigation of influence of tungsten mine wastes on the elemental composition of some alpine and subalpine plants on Mount Uludağ, Bursa, Turkey. *Environmental Pollution*. 2002 Dec;120(3):707–16.
14. Bednar AJ, Jones WT, Chappell MA, Johnson DR, Ringelberg DB. A modified acid digestion procedure for extraction of tungsten from soil. *Talanta*. 2010 Jan;80(3):1257–63.
15. Güteryüz G, Erdemir ÜS, Arslan H, Güçer Ş. Elemental composition of *Marrubium astracanicum* Jacq. growing in tungsten-contaminated sites. *Environmental Science and Pollution Research*. 2016 Sep;23(18):18332–42.
16. Gürmen S, Timur S, Arslan C, Duman I. Acidic leaching of scheelite concentrate and production of hetero-poly-tungstate salt. *Hydrometallurgy*. 1999 Feb;51(2):227–38.



Synthesis of Novel Diarylethenes Bearing Naphthalimide Moiety and Photochromic Fluorescence Behaviors

Ersin Orhan^{1*}

¹Department of Chemistry, Faculty of Arts and Science, Düzce University, 81620 Düzce, Turkey

Abstract: The objective of the research was to synthesize new photo-switchable photochromic fluorescence compounds. Starting from N-butyl-4-bromo-3-iodo-1,8-naphthalimide, new compounds, namely 3,4-bis(2-phenyl-5-methyl-4-thiazolyl)-N-butyl-1,8-naphthalimide **10** and 3,4-bis(3,5-dimethyl-4-isoxazolyl)-N-butyl-1,8-naphthalimide **20** were prepared via two-step Suzuki coupling reaction of aryl boronic acid and esters, and their photochromic fluorescence properties were investigated. Although all prepared bisaryl naphthylimides fluoresce due to the naphthylimide moiety, among them photochrome **10** displayed photochromism. On exposure to ultraviolet light, the photochrome **10** showed a pale yellow to blue-green color change due to the formation of ring closed form **1C**, which reversed to the ring opened form **10** on exposure to visible light. Conversion ratio and quantum efficiency (from O to C form) for **10** were also determined. Additionally, a solvent effect on the fluorescence properties of **10** and **20** was investigated. Increase of solvent polarity results in a red shift (to longer wavelengths) of the fluorescence emissions.

Keywords: Photochromism; fluorescence; diarylethene; naphthalimide; solvent effect.

Cite this: Orhan E. Synthesis of Novel Diarylethenes Bearing Naphthalimide Moiety and Photochromic Fluorescence Behaviors. JOTCSA. 2017;4(2):25-40.

Submitted: March 05, 2017. **Revised:** March 14, 2017. **Accepted:** March 18, 2017.

DOI: 10.18596/jotcsa.296370.

*Corresponding author. E-mail: ersinorhan@duzce.edu.tr Tel.: +90 380 5412404 (internal 3959); Fax: +90 3805412403.

INTRODUCTION

Photochromism is defined as a reversible change of the chemical on irradiation with the relevant light wavelength. Color change is caused by a two sided isomerization of the molecule (1). Photochromic organic molecules have attracted considerable interest due to their potential applications in optical memory and molecular systems; diarylethers are one of the most promising organic photochromic molecules because of their fatigue resistance and high thermal stability. Photochromic compounds have attracted to these applications because of their significant fatigue resistance and high reactivity in the solid state due to the thermal stability of the respective isomers. The photochromic compounds change not only the absorption spectrum but also the geometric and electronic structures in a reversible manner. Changes in molecular structure cause changes in physical properties of molecules such as fluorescence, electrical conductivity, magnetism, refractive index, and polarizability. In particular, the fluorescence modulation associated with the isomerization of diarylethylenes is seen as a promising means of obtaining non-destructive reading and safety records (2-8, 22).

Recently, a lot of research on photochromism has focused on the synthesis of new photochromic devices with modified central ethenes of diarylethylenes. Some examples of recently published novel photochromic compounds synthesized by this approach are as follows: bisarylthiazoles, bisarylthiophenes, naphthalimide derivatives, bisarylindenone derivatives, bisarylbenzindenone derivatives, bisaryl cyclopentenones, bisarylnaphthoquinones and the like (9-14).

Photochromic diarylethines have received great interest both in terms of both basic and practical perspectives. Although photochromic diaryl ethers have been extensively investigated for their application as optoelectronic devices based on changes in magnetic properties, electrochemical behavior, and chemical reaction, the main applications of photochromic diarylethenes are based on two methods: Producing transitions between two isomers different from their natural abilities; and the other is to perform a fluorescent diarylethene with a UV-Vis light source, showing the on/off fluorescent transition between the two isomers. External effect stimuli are usually sound, light, electrical, and mechanical power, and the light control mode among them is the easiest compared to other stimuli. Photochromic fluorescence diarylethers can be used to fabricate many light-sensitive materials. The diarylethenes can be considered promising because of their advantages such as two alternating photochromism, rapid reaction, high quantum yield, fatigue resistance, large variations in the absorption wavelength between the two isomers (15-19).

Multifunctional fluorescent molecules that combine diarylethene units have been examined for their intended applications in optical memory. If the chromophore's fluorescence matches the absorption of the near isomer of diarylethene, ultra-high density storage may be achieved by combining solid state fluorescence of solid emitters and photochromism of diarylethene. Some other chromophores, such as tetrafluoroethylene, naphthalimide, can be converted to diarylethene-like derivatives to obtain high contrast fluorescent keys (20-23).

Recent developments in the design of diarylethene derivatives have allowed the central bridge unit to be flexibly selected. In this context, a heteroaryl ring is provided as the central bridging unit of diarylethenes to form photochromic naphthalimide derivatives (11, 19, 24-25).

So, our aim in this study is to synthesize a number of new diarylethene type photochromic fluorescence compounds that contains bisaryl naphthalimide moieties utilizing the Suzuki coupling reaction.

EXPERIMENTAL

Materials and methods

Materials

4-Bromo-1,8-naphthalic anhydride, 3,5-Dimethylisoxazole-4-boronic acid pinacol ester and other starting chemical compounds were purchased from the company Merck, Sigma-Aldrich, Acros Organics, and ABCR. 4-Bromo-N-butyl-3-iodo-1,8-naphthalimide (**1**) (11) and (5-methyl-2-phenylthiazole-4-yl)boronic acid (**2**) were prepared according to the procedures in the literature [26].

Methods

Some parts of solvent were of analytical grade and purified by distillation before use. Other reagents were used as received without further purification. Some part of studies of naphthalimide derivatives were performed under argon using standard schlenk techniques and dry solvents. All chemicals were purchased from Merck, Acros Organics, ABCR and Aldrich Chemical Company. ^1H and ^{13}C NMR spectra were recorded on Bruker 400 MHz spectrometers for samples in $(\text{CD}_3)_2\text{SO}$ or CDCl_3 . The signals are expressed as parts per million downfield from tetramethylsilane, used as an internal standard (δ value). Splitting patterns are indicated as s, singlet; d, doublet; t, triplet; q, quartet; m, multiplet. Mass spectra were recorded with an AB Sciex 4000 QTRAP LC-MS/MS. FT-IR spectra were measured using a SHIMADZU FT-IR spectrometer. Luminescence spectra were measured

on a SHIMADZU RF-5301PC fluorescence spectrophotometer. UV-Vis spectra were recorded on a T80+ UV-VIS spectrophotometer. Photochemical reactions in organic solvents were carried out in a 10 mm path length quartz cell using an 8W Three-Way UV lamp (Cole-Parmer) (for 365 nm) and an Obelux CR9 Forensic Lights Green (for 530 nm). During the photoreaction, solutions in the cell were stirred. Melting points were measured in open capillary tubes with a Thermo Scientific 9200 melting point apparatus and are not corrected. Solvents were dried over anhydrous sodium sulfate. Flash column chromatographic separation was carried out on Merck Kieselgel 60 (230-400 mesh) using ethyl acetate and hexane as the eluent. Analytical thin-layer chromatography was performed on Merck pre-coated silica gel 60 F-254, 0.25-mm thick TLC plates.

Synthesis

3,4-Bis(2-phenyl-5-methylthiazole-4-yl)- N-butyl-1,8-naphthalimide (**10**)

3-(2-phenyl-5-methyl-4-thiazole-4-yl)-4-bromo-N-butyl-1,8-naphthalimide (0.08 g, 0.15 mmol), 2-phenyl-5-methyl-4-thiazolyl boronic acid (0.10 g, 0.46 mmol) (2), potassium carbonate (0.20 g, 1.5 mmol), tetrakis(triphenylphosphine)palladium(0) (0.017 g, 0.015 mmol), and a catalytic quantity of tris(dibenzylideneacetone) dipalladium(0) in tetrahydrofuran (15 mL) and water (3 mL) were stirred for 2 h at 45–50 °C, and then mixture of solution was boiled for 3 h. The reaction was followed by TLC. The reaction mixture was quenched with aqueous %10 NaHCO₃ solution and extracted with ethyl acetate. The organic phase was washed with saturated NaCl solution, dried with anhydrous MgSO₄, and the desiccant agent was filtered. Then the solvent was evaporated on a rotary evaporator. Raw product was purified by column chromatography over silica gel with ethyl acetate/n-hexane. **10** yellowish solid. Yield 0.04 g (41%) m.p.: 212-214 °C. ¹H NMR (400 MHz, CDCl₃, ppm): δ 0.85 (t, 3H, -CH₂CH₃), 1.27-1.41 (m, 2H, -CH₂CH₃), 1.58-1.70 (m, 2H, -NCH₂CH₂-), 2.34 (s, 3H, -CH₃, thiazole), 2.38 (s, 3H, -CH₃, thiazole), 4.12 (t, 2H, -NCH₂-), 7.73 (t, 1H, naphthalene-H), 7.60 (s, 1H, naphthalene-H), 7.20-7.69 (m, 3H, phenyl-H), 7.80 (d, 2H, ³J_{H-H}=6.8 Hz, phenyl-H), 8.55-8.65 (m, 2H, naphthalene-H). ¹³C NMR (100 MHz, CDCl₃, ppm): δ= 11.10 (CH₃), 12.91 (CH₃), 19.22 (CH₃), 28.64 (CH₂), 29.33 (CH₂), 39.15 (N-CH₂), 119.83 (C_{Ph}), 121.43 (C_{Ph}), 124.09 (C_{Ph}), 124.72 (C_{Ph}), 125.65 (C_{Ph}), 126.14 (C_{Ph}), 126.58 (C_{Ph}), 126.91 (C_{Ph}), 127.36 (C_{Ph}), 127.62 (C_{Ph}), 128.27 (C_{Ph}), 128.52 (C_{Ph}), 128.87 (C_{thiazole}), 129.11 (C_{thiazole}), 129.48 (C_{thiazole}), 129.92 (C_{thiazole}), 130.16 (C_{thiazole}), 130.49 (C_{thiazole}), 131.21 (C_{naphthalene}), 131.63 (C_{naphthalene}), 131.89 (C_{naphthalene}), 132.34 (C_{naphthalene}), 132.57 (C_{naphthalene}), 132.90 (C_{naphthalene}), 133.66 (C_{naphthalene}), 136.12 (C_{naphthalene}), 140.02 (C_{naphthalene}), 147.45 (C_{naphthalene}), 164.20 (C=O), 166.35 (C=O). MS (ESI (+) positive ion mode [M+]⁺ C₃₆H₂₉N₃O₂S₂ Found: 599,7644; Calculated: 600,2996. IR (ATR) V_{max}(cm⁻¹) 2954, 2924, 2862, 1695 (C=O), 1656 (C=O), 1633, 1614, 1595, 1579,

1519, 1456, 1435, 1394, 1348, 1315, 1228, 1257, 1192, 1118, 1072, 1029, 972, 781, 761, 717.

3-(3,5-dimethyl-4-isoxazolyl)-N-butyl-4-bromo-1,8-naphthalimide(**4**)

N-butyl-3-iodo-4-bromo-1,8-naphthalimide (0.2 g, 0.43 mmol) (**1**), 3,5-dimethyl-isoxazole-4-boronic acid pinacol ester (0.28 g, 1.29 mmol) (**3**), potassium carbonate (0.59 g, 4.3 mmol), tetrakis(triphenylphosphine)palladium(0) (0.049 g, 0.043 mmol), and a catalytic quantity of tris(dibenzylideneacetone)dipalladium(0) in tetrahydrofuran (20 mL) and water (4 mL) were stirred for 4 h at room temperature, and then this mixture was stirred for 2 h at 45–50 °C. The mixture of solution was quenched with aqueous %10 NaHCO₃ solution and extraction was carried out with ethyl acetate. The organic phase was washed with saturated NaCl solution, dried with anhydrous MgSO₄ and the desiccant agent filtered. Then the solvent was evaporated on a rotary evaporator. Raw product was purified by column chromatography over silica gel with ethyl acetate/n-hexane. **4** yellow solid. Yield 0.014 g (76%) m.p.:113-116 °C. ¹H NMR (400 MHz, CDCl₃, ppm): δ 0.90 (t, 3H, -CH₂CH₃), 1.30-1.42 (m, 2H, -CH₂CH₃), 1.59-1.71 (m, 2H, -NCH₂CH₂-), 2.11 (s, 3H, -CH₃, isoxazole), 2.32 (s, 3H, -CH₃, isoxazole), 4.09 (t, 2H, -NCH₂-), 7.84 (t, 1H, naphthalene-H), 8.32 (s, 1H, naphthalene-H), 8.62 (d, 2H, ³J_{H-H}=6.1 Hz, naphthalene-H). ¹³C NMR (100 MHz, CDCl₃, ppm): δ= 10.74 (CH₃), 11.91 (CH₃), 13.61 (CH₃), 20.40 (CH₂), 30.18 (CH₂), 40.50 (CH₂), 114.15 (C_{isoxazole}), 121.72 (C_{isoxazole}), 123.20 (C_{isoxazole}), 128.40 (C_{naphthalene}), 128.46 (C_{naphthalene}), 128.53 (C_{naphthalene}), 128.59 (C_{naphthalene}), 128.65 (C_{naphthalene}), 130.00 (C_{naphthalene}), 131.11 (C_{naphthalene}), 132.18 (C_{naphthalene}), 133.28 (C_{naphthalene}), 138.96 (C_{naphthalene}), 159.01 (C=O), 163.23 (C=O). MS (ESI (+) positive ion mode [M+]) C₂₁H₁₉BrN₂O₃ Found: 426,0579; Calculated: 426,8548. IR (ATR) V_{max}(cm⁻¹) 2927, 2862, 1697 (C=O), 1649 (C=O), 1600, 1498, 1431, 1377, 1342, 1307, 1261, 1220, 1155, 1076, 1045, 972, 854, 821, 785, 665, 632.

3,4-Bis(3,5-dimethyl-4-isoxazolyl)-N-butyl-1,8-naphthalimide(**20**)

3-(3,5-dimethyl-4-isoxazolyl)-N-butyl-4-bromo-1,8-naphthalimide (**4**) (0.14 g, 0.32 mmol), 3,5-dimethyl-isoxazole-4-boronic acid pinacol ester (0.14 g, 0.65 mmol) (**3**), potassium carbonate (0.44 g, 3.2 mmol), tetrakis (triphenylphosphine)palladium(0) (0.036 g, 0.032 mmol), and a catalytic quantity of tris(dibenzylideneacetone) dipalladium(0) in tetrahydrofuran (20 mL) and water (4 mL) were stirred for 2 h at 45–50 °C, and then mixture of solution was boiled for 4 h. The reaction was followed by TLC. Mixture of solution was quenched with aqueous %10 NaHCO₃ solution and extracted with ethyl acetate. The organic phase was washed with saturated NaCl solution, dried with anhydrous MgSO₄ and the desiccant agent filtered. Then the solvent was removed on a rotary evaporator. Raw product was purified by column chromatography over silica gel with ethyl acetate/hexane. **20** yellow solid. Yield 0.08 g (54%) m.p.: 128-130 °C. ¹H NMR (400 MHz, CDCl₃, ppm): δ

0.91 (t, 3H, -CH₂CH₃), 1.32-1.40 (m, 2H, -CH₂CH₃), 1.60-1.68 (m, 2H, -NCH₂CH₂-), 2.19 (s, 6H, -CH₃, isoxazole), 2.30 (s, 3H, -CH₃, isoxazole), 4.12 (t, 2H, -NCH₂-), 7.85 (t, 1H, naphthalene-H), 8.33 (s, 1H, naphthalene-H), 8.63 (d, 2H, ³J_{H-H}=6.2 Hz, naphthalene-H). ¹³C NMR (100 MHz, CDCl₃, ppm): δ= 11.71 (CH₃), 11.91 (CH₃), 13.95 (CH₃), 20.27 (CH₃), 20.47 (CH₃), 24.96 (CH₂), 30.06 (CH₂), 40.46 (CH₂), 114.07 (C_{isoxazole}), 114.27 (C_{isoxazole}), 121.62 (C_{isoxazole}), 121.82 (C_{isoxazole}), 123.25 (C_{isoxazole}), 128.34 (C_{isoxazole}), 128.55 (C_{naphthalene}), 129.98 (C_{naphthalene}), 131.00 (C_{naphthalene}), 131.20 (C_{naphthalene}), 132.02 (C_{naphthalene}), 132.19 (C_{naphthalene}), 132.22 (C_{naphthalene}), 133.24 (C_{naphthalene}), 138.95 (C_{naphthalene}), 158.93 (C_{naphthalene}), 163.57 (C=O), 166.98 (C=O). MS (ESI (+) positive ion mode [M⁺] C₂₆H₂₅N₃O₄ Found: 443.4944; Calculated: 444.1030. IR (ATR) V_{max}(cm⁻¹) 3084, 3051, 2929, 2862, 1697 (C=O), 1647 (C=O), 1589, 1500, 1435, 1382, 1348, 1305, 1261, 1224, 1161, 1078, 1043, 1002, 945, 856, 821, 783, 742, 665, 632.

RESULTS AND DISCUSSION

The Suzuki cross-linking reaction is an organohalide with organoborane reaction to give the coupling product using a palladium catalyst and base. The result is a new C-C bond.

C-C bond formation reactions are crucial in the development of bioactive molecules as well as in the development of organic and inorganic materials with new electrical-electronic, mechanical and optical properties (28).

In this study, N-butyl-3-iodo-4-bromo-1,8-naphthalimide and thiazole group containing arylboronic acid were prepared via a multi-stage reaction with method published by the author's group (11).

3,4-Bisaryl-N-butyl-1,8-naphthalimides were synthesized from the two-step Suzuki coupling reaction of N-butyl-3-iodo-4-bromo-1,8-naphthalimide and arylboronic acid or pinacol ester of arylboronic acid in a medium yield (Figure 1).

10 was conveniently synthesized in moderate yield via one-step Suzuki coupling reaction between 1 equivalent of N-butyl-3-iodo-4-bromo-1,8-naphthalimide **1** and average 3 equivalent of arylboronic acid **2**. On similar terms, the reaction between N-butyl-3-iodo-4-bromo-1,8-naphthalimide **1** and pinacol ester of arylboronic acid **3** to give compound **20** failed.

Instead, the intermediate product **4** was obtained as a yellow solid. Despite the fact that the one-step reaction was repeated with an extreme amount of arylboronic acid ester **3** as

well as more effective reaction conditions, the desired product **20** was not isolated and some non-isolable by-products on TLC were observed. However, when the pure intermediate product **4** was treated with an extreme quantity of boronic acid ester **3**, the expected product **20** was achieved in 54% yield as a yellow solid.

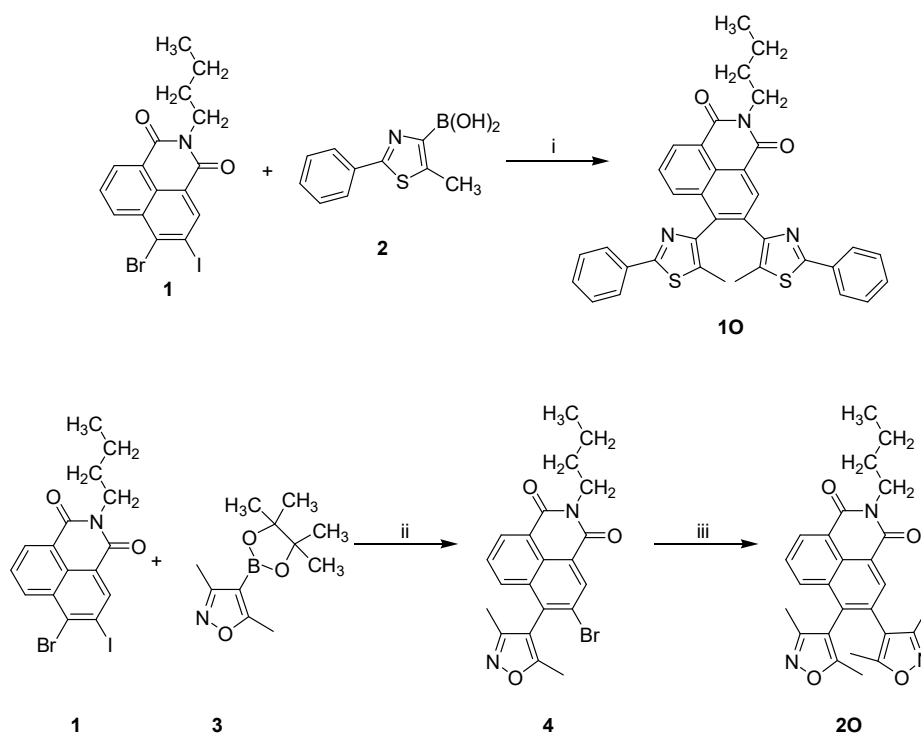


Figure 1. Synthesis of **10** and **20**.

Reaction conditions: i) $\text{K}_2\text{CO}_3/\text{Pd}(\text{PPh}_3)_4$, H_2O , THF, 60°C , 5h; ii) $\text{K}_2\text{CO}_3/\text{Pd}(\text{PPh}_3)_4$, H_2O , THF, r.t., 24 h; iii) Extreme reagent **3**/ $\text{K}_2\text{CO}_3/\text{Pd}(\text{PPh}_3)_4$, THF 60°C , 5 h.

Irradiation of thiazole group containing N-butyl-1,8-naphthalimide **10** in ethyl acetate with 365 nm light caused a little yellow to blue-green color change, due to the formation of close form. The colored form (at pss) turned back to the first pale yellow solution of **10** upon exposure to visible light (530 nm). The close form with appropriate wavelength light and opening to the ring manifested itself as a common behavior of organic photochromic devices (Figure 2). Also, this compound **10** showed a good level fluorescence property.

Irradiation of **10** in ethyl acetate with 365 nm light caused a pale yellow to blue-green color change, because of the formation of **1C**. The colored form **1C** (at pss) turned back to the first light yellow solution of **10** upon exposure to visible light (Figure 4).

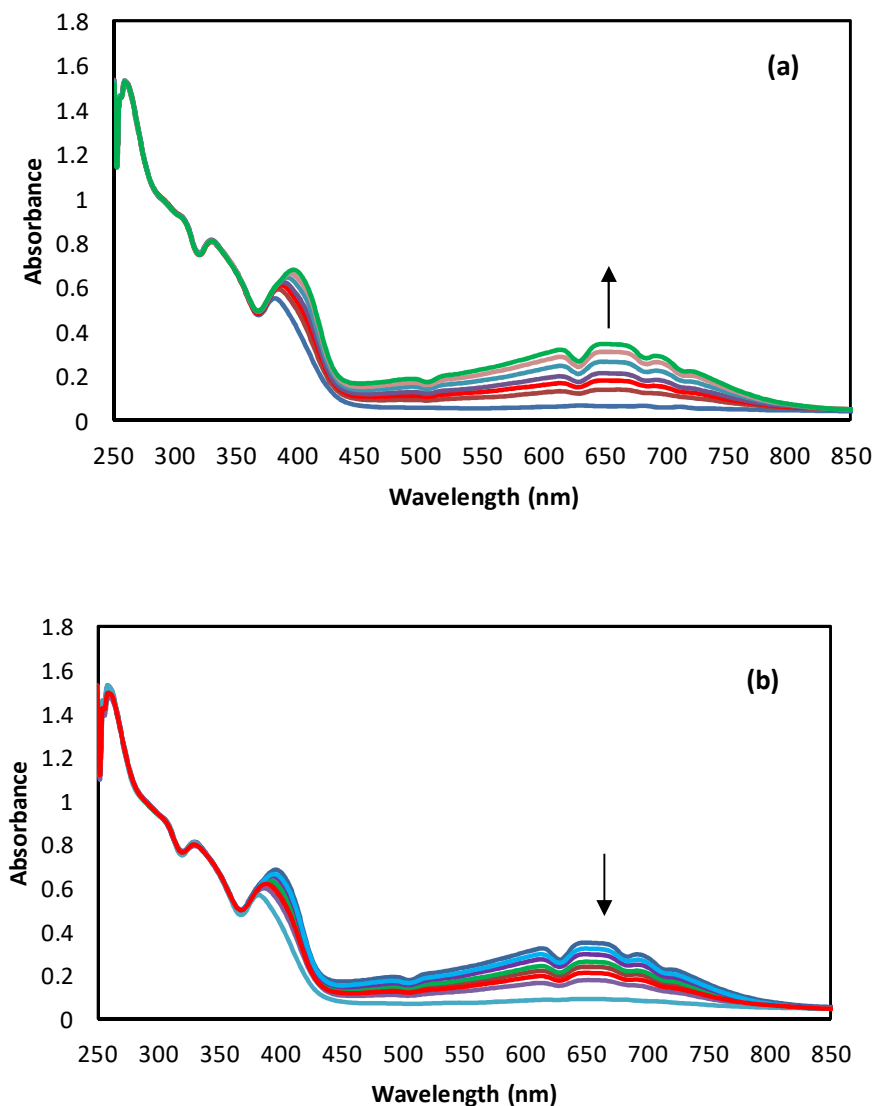


Figure 2. Absorption changes in acetonitrile (1×10^{-5} M). (a) **10** to **1C** (Ultraviolet-PSS). Irradiated with 365 nm ultraviolet light; (b) **1C** (Ultraviolet-PSS) to **10**. Irradiated with 530 nm visible light.

Other synthesized bis(3,5-dimethyl-4-isoxazolyl)-N-butyl-1,8-naphthalimide **20** was not photochromic. On the other hand, this prepared bis(3,5-dimethyl-4-isoxazolyl)-N-butyl-1,8-naphthalimide **20** displayed certain amount of fluorescence properties.

During the irradiation with 365 nm light, neither a color nor a spectral change was seen. The reason why **20** does not show any photochromism is not certain clear at this step. However, this can be said by paying attention to the steric clogging of the methyl groups on carbon atom at 3 position on the isoxazoles with hydrogen atoms of naphthalimide moiety. If cyclic during photoreaction, the methyl group is thought to coincide with the

hydrogen of the naphthalimide ring in Figure 3. Although **20** is not a photochromic compound, **20** showed fluorescence. in Fig.

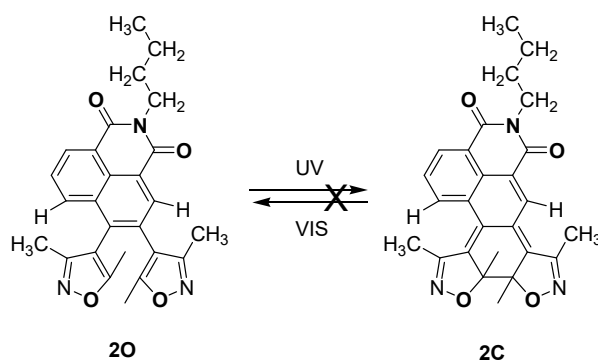


Figure 3. Possible photoreaction of non-photochromic **20**.

Photochromism, Quantum yield, and conversion rate

There was no absorption band in the visible range of **10** and the solutions seen colorless. Upon irradiation with Ultraviolet light, the solution **10** turned greenish with an increase in novel peaks in the visible region. This shows an extended π system on the photochromic reaction, as shown in Figure 4.

Forward and backward photoreaction of 3,4-bisaryl-N-butyl-1,8-naphthalimides in solutions was carried out with different light wavelengths. Upon irradiation of **10** and **20** in solutions with ultraviolet light (365 nm), the color changes from near colorless to blue-green was appeared due to the formation of their closed form **C**-form, which turned back to the colorless states upon exposure to visible light (530 nm). Figure 4 shows the photochromic structure changes of 3,4-bis(2-phenyl-5-methyl-4-thiazolyl)-N-butyl-1,8-naphthalimide **10**. The absorption spectral variations of **10** to its photostationary state (pss) incorporating **1c** in acetonitrile upon ultraviolet and visible beam irradiation are shown in Figure 2.

Ultraviolet-visible absorptivity and extinction coefficients of open-form **10** and this ring closure form **1c** are summarized in Table 1 before and after irradiation in different solvents. Generally, for photochromic compound **10**, the two thiazolyl groups are not in the same plane due to their steric congestion, but are every time in parallel and antiparallel form. Whereby the observed characteristic absorption peaks of the naphthalimide units indicate poor conjugation between the open thiazolyl groups and the naphthalimide moiety.

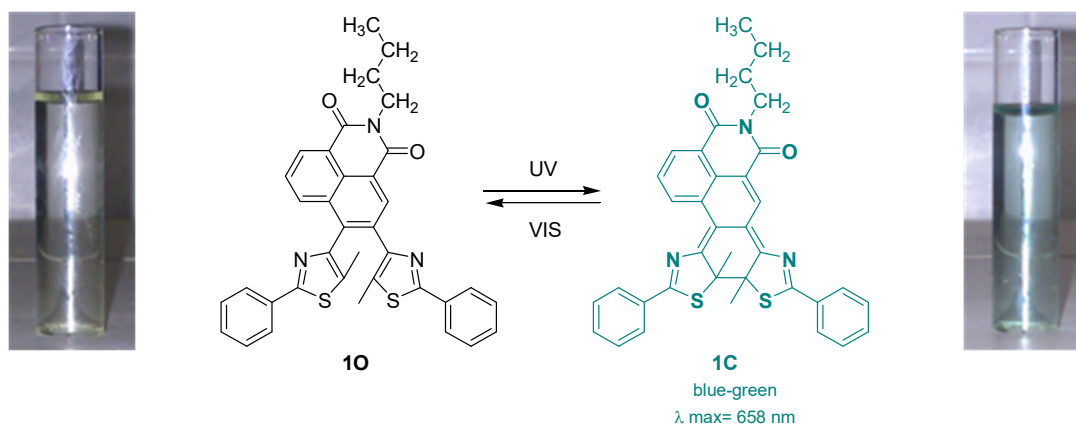


Figure 4. Photochromic structure changes of **10**.

The colored blue-green photochromic compound **1C** has maximum absorption approximately at 750 nm with an absorption trough to the near infrared region. The diode in 780 λ <math><840</math> nm region can react to laser radiation. It is essential for these optical memory devices.

Solvent effects on the open-form **10** and its closure isomer **1C** were studied in four various solvents and the data are given in Table 1. The polarity of the solvent showed a bathochromic shift in both colored and uncolored forms. The quantum efficiency of coloring (ϕ_c) at 365 nm and open-form **10** bleaching (ϕ_b) at 530 nm of its colored form **1C** were calculated with reference to the chemical actinometer Aberchrome 540 as developed by Heller (27).

Table 1. Ultraviolet-Visible maximum absorption and extinction coefficients of open-form **10** and its closed isomer **1C** in several solvents.

Solvent	O-Form (10)		C-Form (1C)	
	λ_{\max} (nm)	ϵ_{\max} ($\text{mol}^{-1} \text{dm}^3 \text{cm}^{-1}$)	λ_{\max} (nm)	Absorbance (at Pss)
Hexane	328	36800	651	0.276
Toluene	336	37500	657	0.266
Ethyl acetate	342	29900	658	0.283
Acetonitrile	361	32000	672	0.598

The quantum yields of the ring closure isomer ($\Phi_{O \rightarrow C}$) of O-form **10** with 365 nm beam irradiation and the ring open isomer ($\Phi_{C \rightarrow O}$) of **1C** form with 530 nm beam irradiation were calculated with reference to Langan R. and Heller HG. Aberchrome 540[27]. The quantum efficiency for coloring (ϕ_c) and bleaching (ϕ_b) were calculated to be $\Phi_{O \rightarrow C} = 0.44$ and $\Phi_{C \rightarrow O} = 0.09$. Reference the actinometer is known as $\Phi_{O \rightarrow C} = 0.20$ at 366 nm

and $\Phi_{C \rightarrow O} = 0.04$ 4.69% at 546 nm in toluene. The quantum yield of **10** and **1C** are quite good from the reference compound.

HPLC followed the closed form of the photocyclization. The conversion ratio from **10** to **1C** (at the pss) of 365 nm light irradiation was detected by HPLC and was calculated to be 71%. Conversion rate was found by calculation of HPLC peak areas. The HPLC chromatogram of **10**, before and after irradiation (365 nm) to pss are given in Figure 5.

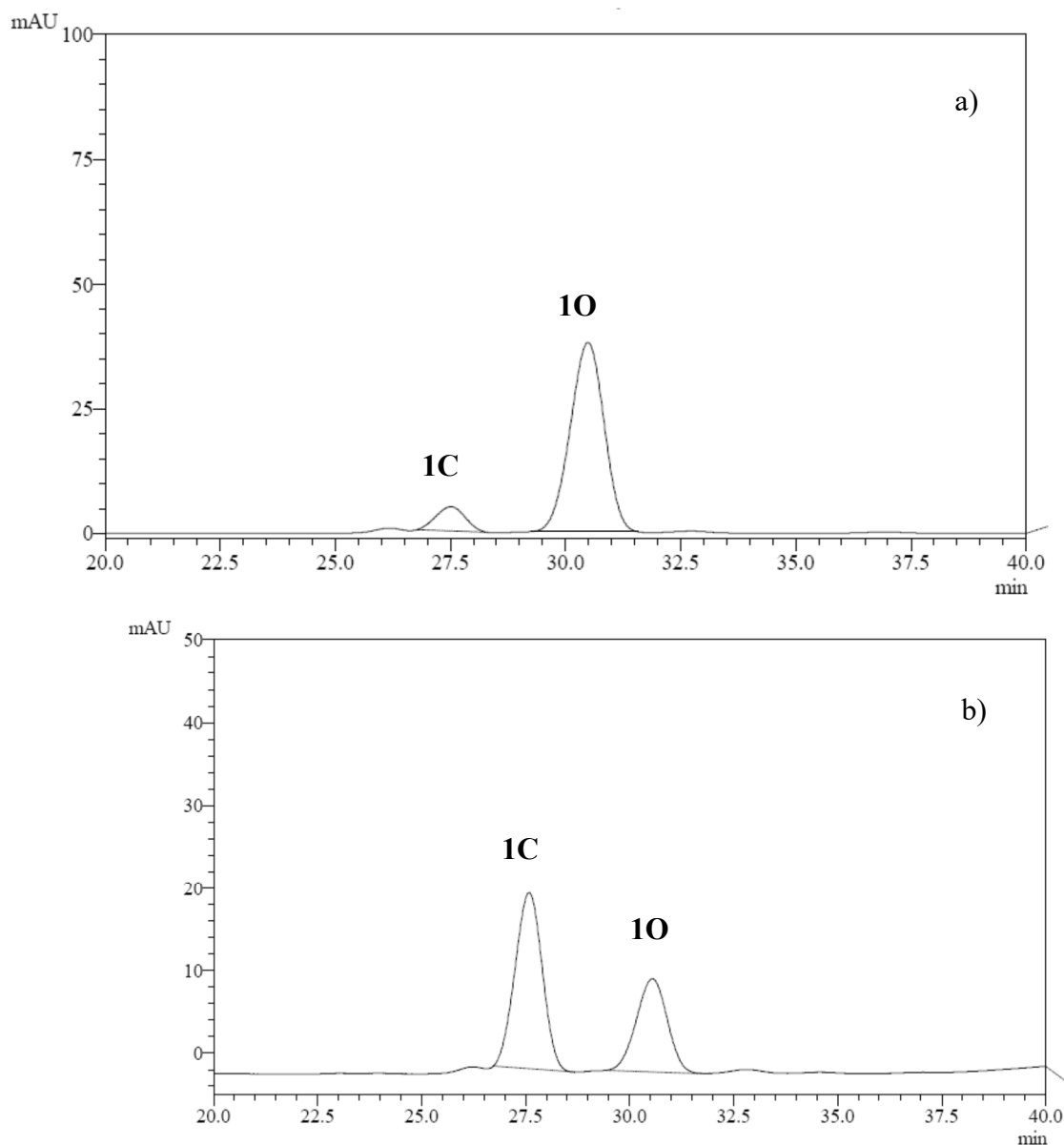


Figure 5. HPLC chromatogram of **10**. a) Before 365 nm irradiation; b) After 365 nm irradiation to pss. HPLC conditions: Column (C8-3); Eluent: H₂O/CH₃CN (50% / 50%, v/v); Current: 0.7 mL/minute; Injection: 20 μ L; detection wavelength: 320 nm (isobestic point in CH₃CN).

Fluorescent behavior

Photochromic compounds can potentially be applied in the recording medium, where the two states can be read with properties prepared by photochromic reactions such as electrochemical states, fluorescence, and absorbance. Fluorescence emission between these outputs is considered one of the interesting due to the simply of detection. The naphthalimide unit as the fluorophore was included in the direct centering bridge for the fluorescence unit target. Upon irradiation at 365 nm, the polar and nonpolar solution of **10** showed a fluorescence quenching, a significant fluorescence quenching that markedly decreased when it reached the photodenase state in Figure 6. The reason for this is the closed form isomer as a fluorescence extinguisher in the possible resonance energy transfer channel.

2-phenylthiazole group with naphthalimide exhibits a fluorescence photo-transfer property. By irradiation with 350 nm light, open structure isomer **10** showed maximum fluorescence emission at 460 nm, but closed structure isomer **1C** showed lower intensity fluorescence in Figure 6.

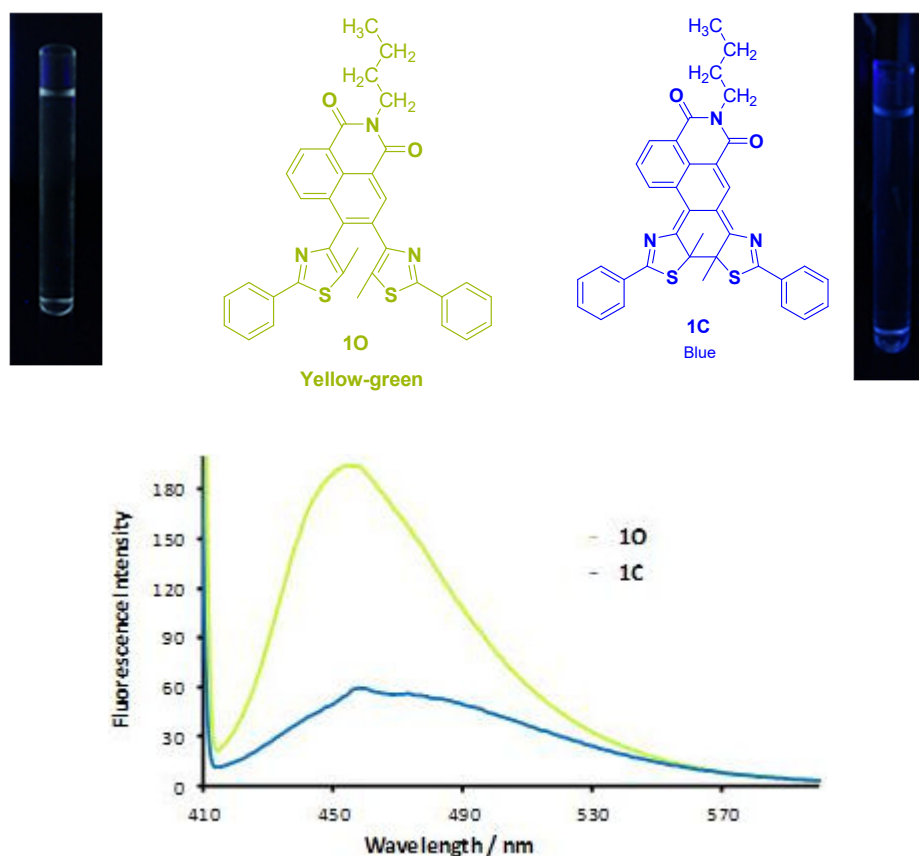


Figure 6. Fluorescence intensity spectra of **10** and **1C** before and after upon irradiation with UV light in ethyl acetate (1×10^{-5} M).

Similarly, the open form **20** compound containing the isoxazole group gave fluorescence intensity at longer wavelengths in the polar solvent (Figure 7).

Compound **20** gave an emission intensity around 460 nm in the non-polar hexane solution. Compound **20** showed an emission intensity around 520 nm in polar acetone in Figure 7. In the polar solvent, a longer wavelength of fluorescence intensity was seen.

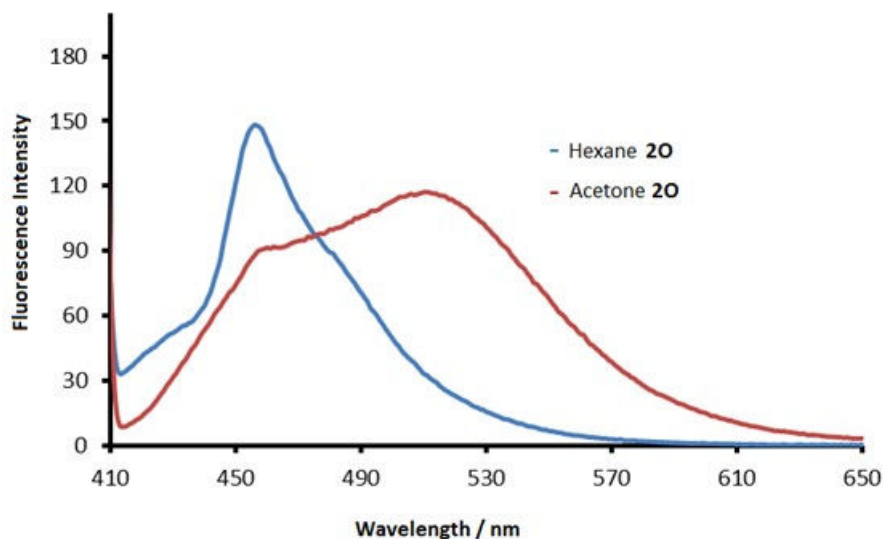


Figure 7. Fluorescence emission spectral changes of compound **20** in hexane and acetone (1×10^{-5}), (λ_{ex} 380 nm).

We can say that solvent polarity is an important factor in the red shift between nonpolar hexane and polar acetonitrile at the luminescence wavelength of **10**. In general, as the solvent polarity increases, the emission intensity shifts to a longer wavelength.

The fluorescence color of **10** can be well modulated by adjusting the solvent polarity ratio with 20% increase in the acetone volume ratio of 0-100%, which can be seen directly by the naked eye in Figure 8.

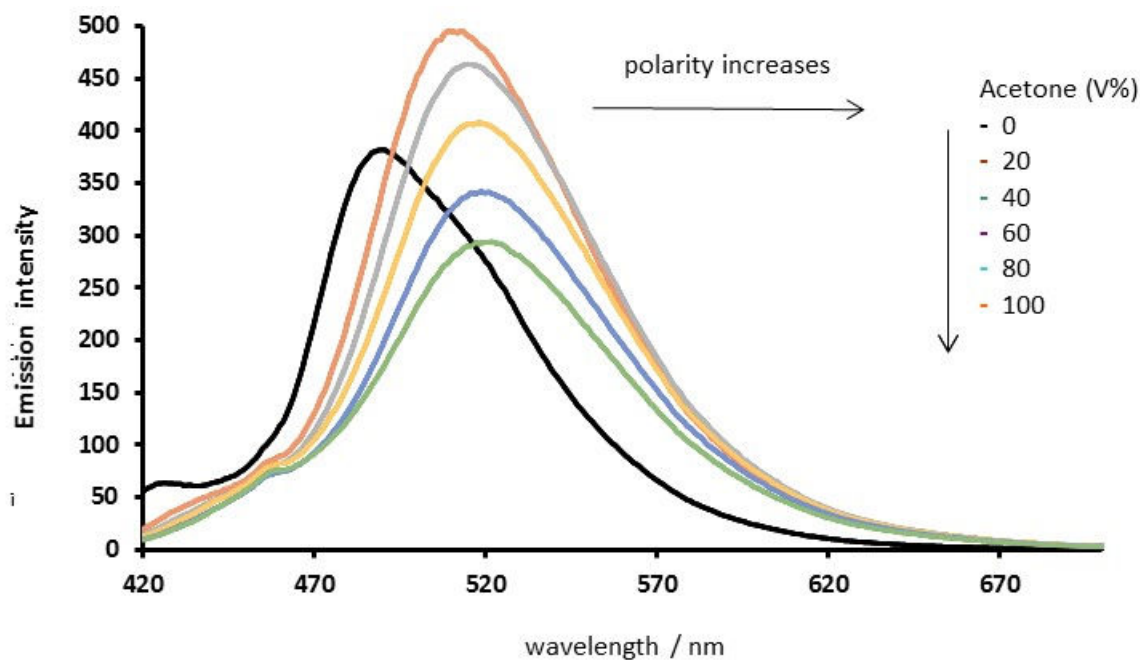


Figure 8. Solvent effect on the fluorescence of **10** with an increase of acetone proportion in n-hexane.

CONCLUSIONS

Starting compound "N-butyl-4-bromo-3-iodo-1,8-naphthalimide" was prepared from 4-bromo-1,8-naphthalic anhydride with multiple-step reactions. Bisaryl naphthalimide derivatives were synthesized from the Suzuki coupling reaction of N-butyl-3-iodo-4-bromo-1,8-naphthalimide and heteroaryl boronic acid or heteroaryl boronic acid pinacol ester. From N-butyl-3-iodo-4-bromo-1,8-naphthalimide symmetrical isoxazole and thiazole group containing N-butyl-1,8-naphthalimides were prepared by Suzuki coupling reaction. Among them, only thiazole group containing N-butyl-1,8-naphthalimides **10** displayed photochromism. Detailed photochromic and fluorescence property of **10** and **1C** was investigated. As well as the fluorescence behavior of **20**.

Solvent factor on the fluorescence properties of **10** and **20** was studied. Increase of solvent polarity results in a red shift (to longer wavelengths) of the fluorescence emissions. Conversion ratios were also calculated from HPLC chromatograms.

ACKNOWLEDGEMENTS

The author thanks to TÜBİTAK (Scientific and Technical Research Council of Turkey) (Grant No.: 111T490) and Duzce University Research Fund (Grant No.: BAP-2012.05.03.097) for the financial contribution of this work.

REFERENCES

1. Tsujioka T, Irie M. Electrical functions of photochromic molecules. *Journal of Photochemistry and Photobiology C: Photochemistry Reviews*. 2010 Mar;11(1):1-14.
2. Rau H, Durr H. Photochromism: molecules and systems. *Photochromism, Molecules and Systems*. 1990;165-192.
3. Irie M. Diarylethenes for Memories and Switches. *Chemical Reviews*. 2000 May;100(5):1685-716.
4. Köse M, Orhan E. Comparison of photochromic properties and thermal stabilities of fulgide, fulgimide, and benzimidazole[1,2-a]pyrrolidine-2-one derivatives. *Turk J Chem*. 2009;33:579-88.
5. Kose M, Orhan E, Büyükgüngör O. Synthesis of novel photochromic methyl cyanoacetate-condensed fulgide derivatives. *Journal of Photochemistry and Photobiology A: Chemistry*. 2007 May;188(2-3):358-63.
6. Kose M, Orhan E. Studies on photochromic benzimidazol[1,2a]pyrrolidin-2-ones from the condensation of 2-methyl-3-benzothienylethylidene-(isopropylidene)succinic anhydride with 1,2-diaminobenzenes. *Journal of Photochemistry and Photobiology A: Chemistry*. 2006 Jan;177(2-3):170-6.
7. Matsuda K, Irie M. Diarylethene as a photoswitching unit. *Journal of Photochemistry and Photobiology C: Photochemistry Reviews*. 2004 Oct;5(2):169-82.
8. Krayushkin M, Ivanov S, Martynkin AY, Lichitsky B, Dudinov A, Uzhinov B. Photochromic dihetarylethenes. 7. Synthesis of bis (thienylazoles), photochromic analogs of diarylethenes. *Russian Chemical Bulletin*. 2001;50(1):116-121.
9. Nakashima T, Atsumi K, Kawai S, Nakagawa T, Hasegawa Y, Kawai T. Photochromism of Thiazole-Containing Triangle Terarylenes. *European Journal of Organic Chemistry*. 2007 Jul;2007(19):3212-8.
10. Orhan E, Gundogdu L, Kose M, Yokoyama Y. Synthesis and photochromic properties of 4,5-bisaryl-3(2H)-pyridazinones. *Journal of Photochemistry and Photobiology A: Chemistry*. 2016 Jan;314:164-70.
11. Meng X, Zhu W, Zhang Q, Feng Y, Tan W, Tian H. Novel Bisthienylethenes Containing Naphthalimide as the Center Ethene Bridge: Photochromism and Solvatochromism for Combined NOR and INHIBIT Logic Gates. *The Journal of Physical Chemistry B*. 2008 Dec 11;112(49):15636-45.
12. Tian H, Wang S. Photochromic bisthienylethene as multi-function switches. *Chem Commun*. 2007;(8):781-92.
13. Kanazawa R, Nakashima T, Kawai T. Photophysical Properties of a Terarylene Photoswitch with a Donor-Acceptor Conjugated Bridging Unit. *The Journal of Physical Chemistry A*. 2017 Mar 2;121(8):1638-46.
14. Cheng H-B, Tan X, Pang M-L. Near-Infrared Photochromic Diarylethenes Based on the Changes in the π -Conjugated System and the Electronic Properties of the Heteroaryl Moieties: Near-IR Photochromic Diarylethenes. *European Journal of Organic Chemistry*. 2013 Dec;2013(35):7933-40.
15. Nakashima T, Goto M, Kawai S, Kawai T. Photomodulation of Ionic Interaction and Reactivity: Reversible Photoconversion between Imidazolium and Imidazolinium. *Journal of the American Chemical Society*. 2008 Nov 5;130(44):14570-5.
16. Liu H-H, Chen Y. Modulation of absorption and fluorescence of photochromic diarylethene by intramolecular hydrogen bond. *Journal of Physical Organic Chemistry*. 2012 Feb;25(2):142-6.

17. Lin Q, Xiao S, Li R, Tan R, Wang S, Zhang R. Intermolecular hydrogen bonding-assisted high contrast fluorescent switch in the solid state. *Dyes and Pigments*. 2015 Mar;114:33–9.
18. Fukaminato T. Single-molecule fluorescence photoswitching: Design and synthesis of photoswitchable fluorescent molecules. *Journal of Photochemistry and Photobiology C: Photochemistry Reviews*. 2011 Nov;12(3):177–208.
19. Jiang G, Wang S, Yuan W, Zhao Z, Duan A, Xu C, et al. Photo- and Proton-Dual-Responsive Fluorescence Switch Based on a Bisthiénylene-Bridged Naphthalimide Dimer and Its Application in Security Data Storage. *European Journal of Organic Chemistry*. 2007 May;2007(13):2064–7.
20. Kose M, Orhan E, Suzuki K, Tutar A, Ünlü CS, Yokoyama Y. Preparation and photochromic properties of 2,3-bisarylbenz[f]indenones. *Journal of Photochemistry and Photobiology A: Chemistry*. 2013 Apr;257:50–3.
21. Berberich M, Natali M, Spent P, Chiorboli C, Scandola F, Würthner F. Nondestructive Photoluminescence Read-Out by Intramolecular Electron Transfer in a Perylene Bisimide-Diarylethene Dyad. *Chemistry - A European Journal*. 2012 Oct 22;18(43):13651–64.
22. Pu S, Li H, Liu G, Liu W, Cui S, Fan C. Synthesis and the effects of substitution upon photochromic diarylethenes bearing an isoxazole moiety. *Tetrahedron*. 2011 Feb;67(7):1438–47.
23. Kawai S, Nakashima T, Kutsunugi Y, Nakagawa H, Nakano H, Kawai T. Photochromic amorphous molecular materials based on dibenzothienylthiazole structure. *Journal of Materials Chemistry*. 2009;19(22):3606-3611.
24. Shirinian VZ, Lonshakov DV, Kachala VV, Zavarzin IV, Shimkin AA, Lvov AG, et al. Regio- and Chemoselective Bromination of 2,3-Diarylcyclopent-2-en-1-ones. *The Journal of Organic Chemistry*. 2012 Sep 21;77(18):8112–23.
25. Morinaka K, Ubukata T, Yokoyama Y. Structurally Versatile Novel Photochromic Bisarylindenone and Its Acetal: Achievement of Large Cyclization Quantum Yield. *Organic Letters*. 2009 Sep 3;11(17):3890–3.
26. Kose M, Şekerci ÇY, Suzuki K, Yokoyama Y. Synthesis of photochromic 2,3-bis(5-methyl-2-phenyl-4-thiazolyl)-1,4-naphthoquinone derivatives. *Journal of Photochemistry and Photobiology A: Chemistry*. 2011 Mar;219(1):58–61.
27. Heller HG, Langan JR. Photochromic heterocyclic fulgides. Part 3. The use of (E)- α -(2,5-dimethyl-3-furylethylidene)(isopropylidene)succinic anhydride as a simple convenient chemical actinometer. *J Chem Soc, Perkin Trans 2*. 1981;(2):341–3.
28. Miyaura N, Yamada K, Suzuki A. A new stereospecific cross-coupling by the palladium-catalyzed reaction of 1-alkenylboranes with 1-alkenyl or 1-alkynyl halides. *Tetrahedron Letters*. 1979 Jan;20(36):3437–40.



An Efficient Catalyst for Aldol Condensation Reactions

Yusuf Hassan^{1*} Rosa Klein² Perry T. Kaye²

¹Department of Chemistry, Umaru Musa Yar'adua University, Katsina, Nigeria

²Department of Chemistry, Rhodes University, Grahamstown, South Africa

Abstract: A New manganese complex was synthesised around *S,S*-1,2-diaminocyclohexane linked ketopinic acid scaffold, and successfully utilised as a catalyst in the aldol condensation reactions of benzaldehyde with various aliphatic ketones to obtain products with excellent yield of >99%.

Keywords: Lewis acid; ketopinic acid; catalysis; aldol condensation.

Cite this: Hassan Y, Klein R, Kaye P. An Efficient Catalyst for Aldol Condensation Reactions. JOTCSA. 2017;4(2):41–48.

Submitted: February 22, 2017. **Revised:** March 10, 2017. **Accepted:** March 24, 2017.

DOI: 10.18596/jotcsa.293058.

*Corresponding author. E-mail: yusuf.hassan@umyu.edu.ng

INTRODUCTION

Aldol condensation reaction as a C-C bond formation reaction continued to provide opportunity for the synthesis of valuable intermediates, natural products, as well as other biologically important compounds (1-3). The major concern with some of the reported methodologies has always been the issue of atom economy (4, 5). Although a number of catalytic methods were developed to improve the condition, it however often incorporates the use of harsh temperatures. For instance, Climent and co-workers have utilised solid base catalysts derived from hydrotalcites to achieve high yields and selectivities in the preparation of chalcones and flavanones of pharmacological interest, such as Vesidryl (6). Similarly Kottapali *et al.* have investigated the aldol condensation of benzaldehyde and acetone in the liquid phase on hydrotalcites transformed into basic solid with good yield (7). Corma and Martin-Aranda have modified sepiolites by substituting a part of the Mg ²⁺ located at the borders of its channels with alkaline ions to afford strong base catalyst for the aldol condensation (8). Also Corma *et al.* have carried out the condensation of benzaldehyde with various active methylene compounds in the presence of zeolites as a basic catalyst (9). In an effort to improve the catalytic activity of their earlier reported method on the use of hydrotalcites, Climent and co-workers successfully increased the surface area of the catalyst by sonication, and employed it in the aldol condensation reactions (10). In this work, a new organic-metal complex based on ketopinic acid scaffold and manganese was constructed and tested as catalyst in the aldol condensation of various aliphatic substrates at a mild temperature.

MATERIALS AND METHODS

Reagent-grade ethanol was used as received from commercial source, tetrahydrofuran was distilled from benzophenone/ketyl solutions and chloroform was passed through a column of basic alumina. Analytical thin-layer chromatography was performed on ALUGRAM XTRA silica gel 0.2 mm (containing a fluorescent indicator at 254 nm). Flash chromatography was carried out on MN Kieselgel 60 0.063-0.2 mm/ 70-230 mesh. All other reagents were purchased from Aldrich and used as received. NMR spectra were recorded on Bruker Avance III HD spectrometer (400 and 600 MHz). All signals were expressed as ppm down field from TMS, referenced to the residual protonated solvent signals in ¹H NMR (7.26 ppm) and to the deuterated carbon signals in ¹³C NMR (77.36 ppm). FTIR spectral measurements were carried out on a Perkin Elmer spectrum 400 FT-IR spectrometer (ATR). Elemental analyses were conducted using an Elementar Vario

micro cube. Melting points were determined by means of a Reichert apparatus and are uncorrected.

2,2'-(1S,2S)-cyclohexane-1,2-diylbis(azan-1-yl-1-ylidene)bis(7,7-dimethylbicyclo[2.2.1]heptane-1-carboxylic acid) 3

Ketopinic acid (382 mg, 2.096 mmol) was dissolved in CHCl_3 (5 mL) and *S,S*-1,2-diaminocyclohexane (126 μL , 1.05 mmol) acetic acid (0.1 mL) were added successively at room temperature. The mixture was refluxed for 36 h and then the reaction was quenched with H_2O (5 mL). The biphasic solution was extracted with CH_2Cl_2 (10 mL), and then separated. The subsequent organic layer was washed with brine (5 mL), dried over anhydrous MgSO_4 , and concentrated. Purification of the crude product was effected by column chromatography on silica gel using 4/1 EtOAc/ CH_2Cl_2 as eluent and the product were obtained as a white solid (0.35g, 29%); m.p. 161-164 °C; δ_{H} (400 MHz; CDCl_3) 0.86 (s, 6H), 1.22 (s, 6H), 1.24-1.60 (m, 6H), 1.67-1.81 (m, 4H), 1.98-2.11 (m, 6H), 2.36 (m, 2H), 2.52 (m, 2H), 3.45 (m, 2H); δ_{C} (100 MHz; CDCl_3) 20.2, 20.5, 27.2, 28.2, 31.7, 32.7, 35.3, 43.8, 50.0, 60.8, 64.7, 173.3, 183.6 FTIR (neat, cm^{-1}) 2988, 2543, 1726, 1580

2,2'-(1S,2S)-cyclohexane-1,2-diylbis(azan-1-yl-1-ylidene)bis(7,7-dimethylbicyclo[2.2.1]heptane-1-carboxylato) manganese (III) chloride 4

Solutions of ligand **3** (119 mg, 0.268 mmol) and KOH (0.5M, 8 mL) in ethanol were allowed to reflux with $\text{Mn}(\text{OAc})_2 \cdot 4\text{H}_2\text{O}$ (138 mg, 0.563 mmol) under nitrogen atmosphere for 12 h. The reaction mixture was then cooled to room temperature and then brine (8 mL) was added to give a biphasic solution which was later filtered and concentrated *in vacuo*. The residue obtained was redissolved in dichloromethane and the aqueous layer was removed using a separating funnel. After concentrating the organic layer, the resulting complex was recrystallized from acetonitrile to furnish a brown amorphous powder (66.8 mg, 47% yield). Anal. Calcd for $\text{C}_{26}\text{H}_{36}\text{ClMnN}_2\text{O}_4$ %: C, 60.75; H, 8.50; N, 4.72. Found: C, 60.75; H, 8.52; N, 4.73. FTIR (neat, cm^{-1}): 1738 (C=O), 1687 (C=N).

Typical procedure for the aldol condensation reactions

Potassium hexamethyldisilazide (KHMDs, 43.2 μL , 0.0216 mmol, 0.5 M in toluene) and a solution of water (48 μL , 0.048 mmol, 1 M in THF) were vigorously stirred for 20 min. This was followed with the addition of ketone (15 mmol) and further stirring for additional 10 min. To the resulting solution, catalyst **S,S-4** (66 mg, 10 mole %) and aldehyde (1.5 mmol) in THF (0.5 mL) were added. The mixture was continuously stirred with regular monitoring by ^1H NMR.

(Z)-2-benzylidenecyclohexanone 7

Yellow oil; >99% yield, δ_{H} (600 MHz; CDCl_3) 1.50 (q, $J = 2.0$ Hz, CH_2), 1.55 (q, $J = 2.3$ Hz, CH_2), 1.57 (t, $J = 3.1$ Hz, CH_2), 1.63 (t, $J = 3.1$ Hz, CH_2), 6.88 (s, 2H), 7.32-7.33 (m, 2H), 7.40 (s, 1H), 7.61 (s, 1H), δ_{C} (100 MHz; CDCl_3) 22.2, 24.3, 35.0, 128.2, 128.3, 128.4, 133.1, 134.0, 139.5, 198.3. FTIR (neat, cm^{-1}) 3038, 1671, 1638, 1450.

(E)-2-benzylidene-6-methylcyclohexanone 9a

Yellow oil; >99% yield; δ_{H} (600 MHz; CDCl_3) 1.22 (d, $J = 1.2$ Hz, CH_3), 1.23-1.24 (m, 2H), 1.32-1.36 (m, 2H), 2.10-2.12 (m, 2H), 2.22-2.32 (m, 2H), 6.89 (s, 2H), 7.41-7.43 (m, 2H), 7.54 (s, 1H), 7.81 (s, 1H). δ_{C} (100 MHz; CDCl_3) 16.2, 26.3, 29.2, 30.6, 40.6, 133.2, 136.3, 136.7, 134.2, 134.8, 140.1, 199.3. FTIR (neat, cm^{-1}) 3045, 1674, 1632, 1447.

(E)-2-benzylidene-4-methylcyclohexanone 9b

Yellow oil; >99% yield, δ_{H} (600 MHz; CDCl_3) 0.99 (d, $J = 0.5$ Hz, CH_3), 1.62-1.68 (m, 2H), 1.85-1.93 (m, 2H), 2.33-2.80 (m, 2H), 2.86-2.93 (m, 1H), 3.20-3.52 (m, 1H), 3.62-3.72 (m, 1H), 7.02 (s, CH), 7.61-7.68 (m, 2H), 7.72 (s, 1H), 7.84 (s, 1H). δ_{C} (100 MHz; CDCl_3) 16.2, 26.3, 29.2, 30.6, 40.3, 133.2, 136.3, 136.7, 134.2, 134.8, 140.1, 199.5. FTIR (neat, cm^{-1}) 3044, 1675, 1632, 1447.

Trans-1-phenylhept-1-en-3-one 9c

Yellow oil; >99% yield, δ_{H} (600 MHz; CDCl_3) 0.96 (t, $J = 0.9$ Hz, 3H), 1.52-1.59 (m, 4H), 3.20 (t, $J = 3.1$ Hz, 2H), 6.53 (d, $J = 12.0$ Hz, 1H), 6.66 (d, $J = 12.0$ Hz, 1H), 6.83 (d, $J = 6.5$, 2H), 7.66-7.68 (m, 3H). δ_{C} (100 MHz; CDCl_3) 12.3, 23.4, 28.6, 40.2, 128.3, 129.0, 131.1, 135.1, 140.1, 147.2, 199.5. FTIR (neat, cm^{-1}) 3051, 1668, 1646, 1510.

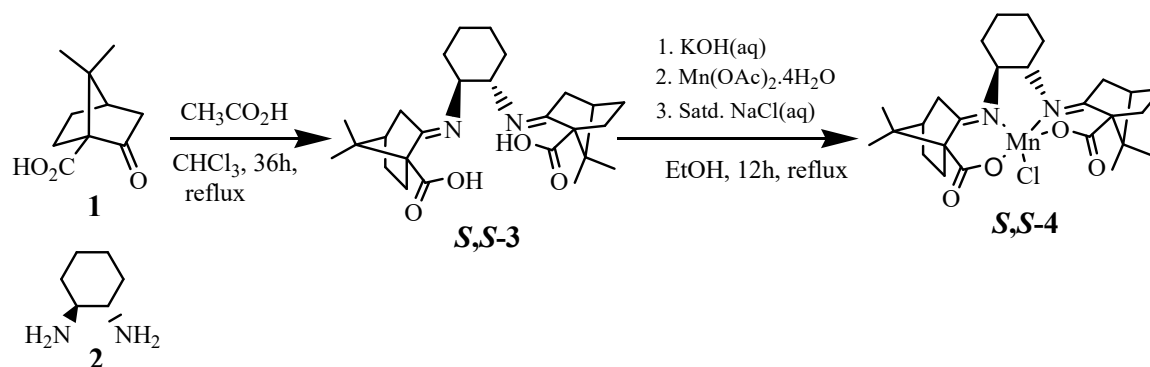
Cis-4,4-dimethyl-1-phenylpent-1-en-3-one 9d

Yellow oil ; >99% yield, δ_{H} (600 MHz; CDCl_3) 1.51 (s, 9H), 6.93 (d, $J = 6.0$ Hz, 1H), 7.43 (d, $J = 6.0$ Hz, 1H), 7.66-7.68 (m, 2H), 7.72-7.75 (m, 3H). δ_{C} (100 MHz; CDCl_3) 33.2, 43.1, 127.3, 129.1, 129.8, 133.10, 138.0, 140.2, 198.5. FTIR (neat, cm^{-1}) 3055, 1671, 1644, 1525.

RESULTS AND DISCUSSION

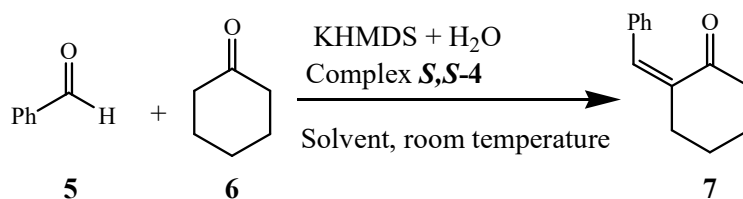
The ligand **3** reported by Yang et al. (11) was synthesised using the standard procedure, followed by the complexation step (Scheme 1) to obtain the new Mn(III) complex **S,S-4** (12). Hence, the synthesis was carried out by refluxing ketopinic acid **1** with the *S,S*-1,2-diaminocyclohexane **2** and a catalytic amount of glacial acetic acid, using chloroform as solvent (Scheme 1). Condensation of ketopinic acid (2 equiv.), with the *S,S*-1,2-

diaminocyclohexane as a linker enabled the generation of the C-2 symmetry and expand the space occupied by the ligand on each face of the final complex. It was hoped that the position of the manganese atom tightly situated at the centre of the ketopinic acid moieties would enhance the coordination of the electrophilic centres of the substrates during reaction.



Scheme 1. Synthesis of ketopinic acid-derived complex

The catalytic activity of complex **S,S-4** was investigated following the procedure reported by Yoshikawa *et al.* (13) with modification. Hence benzaldehyde was reacted with cyclohexanone in different ethereal solvents and at three catalyst loadings (Table 1). The results shows that THF is the most efficient solvent as it allows the formation of the aldol product in >99% yield at relatively shorter time. Attempt to reduce the catalyst loading result in longer duration of the reaction. Although not captured in Table 1, but the method development reveals that any attempt to reduce the cyclohexanone equivalent furnish the corresponding aldol in negligible amount. In fact it could only be detected in the ^1H NMR spectroscopic analysis of the crude mixture.

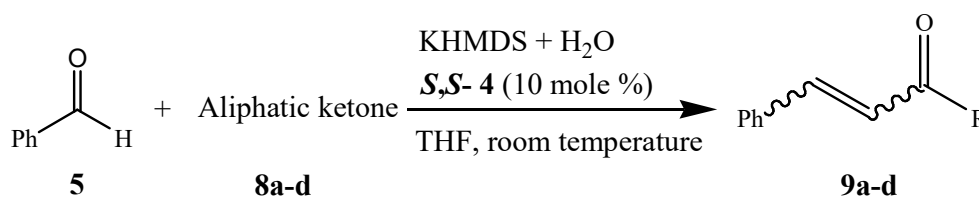
Table 1. Aldol condensation of benzaldehyde with cyclohexanone in three different solvents in the presence of complex **S,S-4**¹

Solvent	4 (mole %)	Time (h)	Yield (%) ²
THF	1	18	>99
	5	15	>99
	10	4.5	>99
EtOAc	1	24	>99
	5	21	>99
	10	24	>99
Dioxane	1	24	trace
	5	21	trace
	10	24	trace

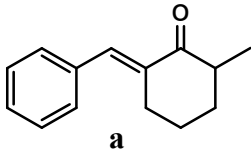
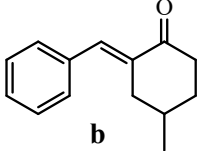
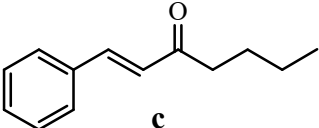
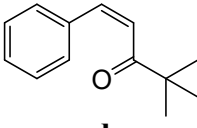
¹Benzaldehyde (1.5 mmol), cyclohexanone (15 mmol). *Cis* assignment for **7** was determined using DFT calculation of the lowest energy isomer.

²Determined by the analysis of the reaction mixture using ¹H NMR spectroscopy

Based on the catalyst performance, other substrates were explored to further ascertain its efficacy. The results (Table 2) demonstrate that the catalyst has relatively wide spectrum of activity.

Table 2. Aldol condensation of various aliphatic substrates in the presence of **S,S-4** (10 mole %)¹

	Aliphatic ketone
a	2-Methylcyclohexanone
b	4-Methylcyclohexanone
c	2-Hexanone
d	Pinacolone

Aldol product, 9 ²	Time (h)	Yield (%) ³
 a	5	>99
 b	5.2	>99
 c	5.1	>99
 d	5.8	>99

¹Benzaldehyde (1.5 mmol), Ketone (15 mmol)

² Geometrical assignment was determined using DFT calculation of the lowest energy isomers

³Determined by the analysis of the reaction mixture using ¹H NMR spectroscopy

CONCLUSIONS

Ketopinic acid was successfully employed as a scaffold in the synthesis of a manganese (III) complex. The catalytic efficiency of the obtained complex was investigated in the aldol condensation of benzaldehyde with cyclohexanone to obtain product with excellent yield at a short duration. Subsequently other aliphatic ketones were reacted with the benzaldehyde at the optimized reaction condition to furnish the corresponding aldol products with an impressive yield. Interestingly, it was found that irrespective of the structure of the aliphatic ketone, the yield of the products was always excellent within a short duration. This suggest that the catalytic system developed in this work possess strong Lewis acidity which help in the activation of the carbonyl groups in the reacting species.

ACKNOWLEDGMENTS

The financial support of the National Research Foundation and the Tertiary Education Trust Fund, Nigeria for granting fellowship to Yusuf Hassan is gratefully acknowledged.

REFERENCES

1. Heathcock CH, Ellis JE, McMurry JE, Coppolino A. Acid-catalyzed Robinson Annulations. *Tetrahedron Letters*. January 1971;12(52):4995–6.
2. Vashchenko V, Kutulya L, Krivoshey A. Simple and Effective Protocol for Claisen—Schmidt Condensation of Hindered Cyclic Ketones with Aromatic Aldehydes. *ChemInform* [Internet]. November 20, 2007 [source 03 April 2017];38(47). Available at: <http://doi.wiley.com/10.1002/chin.200747094>
3. Badía C, Castro JM, Linares-Palomino PJ, Salido S, Altarejos J, Nogueras M, vd. (E)-6-(2,2,3-Trimethyl-cyclopent-3-enyl)-hex-4-en-3-one. *Molbank*. March 29, 2004;2004(1):M388.
4. Sugiura M, Ashikari Y, Nakajima M. One-Pot Synthesis of β,β -Disubstituted α,β -Unsaturated Carbonyl Compounds. *The Journal of Organic Chemistry*. September 04, 2015;80(17):8830–5.
5. Wang Z, Yin G, Qin J, Gao M, Cao L, Wu A. An Efficient Method for the Selective Iodination of α,β -Unsaturated Ketones. *Synthesis*. November 2008;2008(22):3675–81.
6. Climent MJ, Corma A, Iborra S, Primo J. Base Catalysis for Fine Chemicals Production: Claisen-Schmidt Condensation on Zeolites and Hydrotalcites for the Production of Chalcones and Flavanones of Pharmaceutical Interest. *Journal of Catalysis*. January 1995;151(1):60–6.
7. Rao KK, Gravelle M, Valente JS, Figueras F. Activation of Mg–Al Hydrotalcite Catalysts for Aldol Condensation Reactions. *Journal of Catalysis*. January 1998;173(1):115–21.
8. Corma A. Alkaline-substituted sepiolites as a new type of strong base catalyst. *Journal of Catalysis*. July 1991;130(1):130–7.
9. Corma A, Fornés V, Martín-Aranda RM, García H, Primo J. Zeolites as base catalysts: Condensation of aldehydes with derivatives of malonic esters. *Applied Catalysis*. March 1990;59(1):237–48.
10. Climent M. Increasing the basicity and catalytic activity of hydrotalcites by different synthesis procedures. *Journal of Catalysis*. July 2004;225(2):316–26.
11. Yang K-S, Lee W-D, Pan J-F, Chen K. Chiral Lewis Acid-Catalyzed Asymmetric Baylis–Hillman Reactions. *The Journal of Organic Chemistry*. February 2003;68(3):915–9.
12. Kureshy RI, Khan NH, Abdi SHR, Iyer P, Bhatt AK. Enantioselective catalytic epoxidation of nonfunctionalized prochiral olefins by dissymmetric chiral Schiff base complexes of Mn(III) and Ru(III) metal ions II. *Journal of Molecular Catalysis A: Chemical*. June 1997;120(1–3):101–8.
13. Yoshikawa N, Yamada YMA, Das J, Sasai H, Shibasaki M. Direct Catalytic Asymmetric Aldol Reaction. *Journal of the American Chemical Society*. May 1999;121(17):4168–78.



Using Natural Stone Pumice in Van Region on Adsorption of Some Textile Dyes

Ali Rıza KUL^{1*}, Veysel BENEK¹, Ahmet SELÇUK², Nilgün ONURSAL³

¹Science Faculty of Yuzuncu Yil University, 65300, Van, Turkey

²Faculty of Education Yuzuncu Yil University, 65300, Van, Turkey

³Faculty of Education of Siirt University, 56100, Siirt, Turkey

Abstract: Toxic effect of textile dyes their increasing quantities in air, soil and water environments, because of growing of industrial activities, they must be taken into consideration since they give harm to the environment. We come across textile dyes in natural wetlands as result of uncontrolled industrial wastes. Textile dyes that can accumulate easily in their environments may show toxic effects. Pumice, accruing as a result of volcanic events and durable against chemical factors, is a rock that has porous structure. Pumices have a porous structure because of sudden cooling of the rock and sudden leaving of gases a result of volcanic events. Thanks to these pores, pumices' heat and sound insulation are quite high. The most distinctive feature of pumice from other rocks is that it has different colors and there is not crystal water in its porous structure. Adsorption studies are applied with Van Pumice at pH = 6, the adsorption mechanism and changing dye concentration. As result of these researches, it has been found out that there are different adsorption movements at pH 6 between Neutral Red and Van Pumice. The result of this study shows that the Pumice found in Lake Van gives a better fit for the Langmuir Isotherm (model) and the amount of adsorption increases with the temperature. We thereby conclude that the Pumice located in Lake Van is a recommended adsorbent for filtering the used textile dye in aqueous medium.

Keywords: Textile dyes; adsorption; isotherm; Van pumice; thermodynamics.

Cite this: Kul A, Benek V, Selcuk A, Onursal N. Using Natural Stone Pumice in Van Region on Adsorption of Some Textile Dyes. JOTCSA. 2017;4(2):49-60.

Submitted: February 17, 2017. **Revised:** February 28, 2017. **Accepted:** April 04, 2017.

DOI: 10.18596/jotcsa.292662.

Corresponding author. E-mail: alirizakul@yyu.edu.tr.

INTRODUCTION

Pumice is a glassy, porous, and volcanic rock which occurs with the result of hollow, spongy, volcanic rocks and is resistant against the physical and chemical effects (22). The name "Ponza" or "Pomza" comes from Italian. There are different names in different languages. In French it is called as "Ponce", in English, the middle ones are "Pumice", naturally the tiny ones are "Pumicite", In German, the big ones are called as "Bimstein", and tiny ones are called as "Bims". In Turkish, it is known as "Sünger taşı", "Köpük taşı", "Topuktaşı" (6).

Because pumice is mostly porous, its heat and sound insulation is quite high. According to Mohs scale, its hardness is 5-6. It does not contain crystal water. Its chemical component; 60%-70% SiO₂, 13%-15% Al₂O₃, 1%-4% Fe₂O₃, 1%-2% CaO, 1%-2% MgO, 2%-5% Na₂O, 3%-4% K₂O and it contains TiO₂, SO₃ and Cl (13, 24).

During formation, because of sudden cooling and the gases inside the pumice's leaving, it contains countless pores from macro scale to micro scale. Between pores are generally (especially micro ones) disconnected hollows. Pores on pumice are mostly not connected to each other. Each pore is isolated from each other with a glassy membrane. Because of this feature, pumice is a good adsorbent (24, 3).

Pores on pumice are smaller than 1 mm. Pores are irregular, spherical, round and like elongated pipes (11, 2).

The more pumice's piece size increases the more porous percent increases. Pumice's excess of porous percent and low specific weight ensure it to be used as a pouring material for insulation areas. Also, thanks to the same features, it is highly porous; Pumice pieces are not too much resistant. However, its durability is suitable for rock durability which was used in carrier wall construction. (To 6 floors). Pumice is a good heat insulator. This feature is increased with the event, which is called as "stack Porousness", in pumice block manufacture that is especially struggled to reach. For the stack porousness, concrete is prepared with a quite thin mortar and is ensured to cover only surround of pumice pieces in a thin manner. The Pumice pores are not only helpful for insulation but also pumice structure elements are highly adsorbent because it has features of removing capillary. Pumice is grinded easily because of being a volcanic glass. Granulated Pumice was used for similar goals both for the purpose of polishing and stoning and in match factories as an ignition material and filling material, soap and cosmetic industry (21, 26).

Because of porous being disconnected and having spaces, pumice is light, it can swim for a long time and its permeability is low and its insulation (heat – sound insulation) is quite high. Chemically, it contains about 75% silica. The amount of SiO₂ that rock contains, provides an abrasive feature to the rock, therefore, it reveals a chemical status that can easily erode steel. The compound of Al₂O₃ provides a high resistant to fire and heat. Na₂O and K₂O are known as minerals which give reactions in textile industry (9).

Economically functioned reserves are generally after tertiary reserves. World's pumice reserves are more than 16 billion tonnes. USA has the biggest reserves while Turkey is the second in terms of total pumice reserves. Important reserves of Turkey are in Tatvan and Ahlat, Niğde-Nevşehir, Iğdır and Kars, Mollakasım (Van), Erciş (Van), Gündül (Ankara), Doğubeyazıt (Ağrı) and Cumaovası' (İzmir).

Main manufacturers are Italy, Greece, Spain, Turkey, France, and Germany (26, 8).

Pumice rocks have recently gained updating as a popular industrial raw material parallel to various industries' establishment and development. Pumice was used in a large area mainly as a light structure material, cement production, and filter material, acoustic and polishing in industry. However, in our country, it is mostly used in bleaching jeans and in production of briquette as a light structural material (24, 16).

Coloring of objects is expressed as "dyeing". Dye was used to protect the surface of objects from external influences and to give a nice view. In speech, dye and dye material words are used in the place of each other. These two words are not synonyms. Dyes are generally inorganic. They are mixtures, which are mixed with a connector but dissolved in the medium. They can be removed by scoping in large forms.

The materials which are used to color fabric and fiber are called as "dyeing material" However, all colorful materials or color giving materials are not dye materials. Coloring, applied by dye materials are not similar to coloring, applied by dye. Coloring is generally applied with various dye methods in the form of solution or suspension.

All dye materials are organic compounds. The material to be dyed changes its structure by chemical interaction with the dye. For this reason, the applicant cannot bring the material back to the original by washing or cleaning. For that reason, the first dyes that are used are mixture of metal–oxide, clay and some plant's sap (19).

Fe_2O_3 , Cr_2O_3 , Pb_3O_4 , HgS , graphite can be given as examples for the natural inorganic dyes. Some of the dye materials are from natural sources, and some of them are synthetic. Natural dye materials can be obtained generally from skin of animals and glands, root, shell, seed, and fruit of plants and from microorganisms like yeast bacteria in the result of simple chemical applications (4).

In the textile industry, one of the main problems is the removal of dyes and pigments from the wastewater. It is known that most dyes are toxic, carcinogenic, and mutagenic to aquatic organisms, so they have to be removed. Several methods, such as filtration, coagulation, chemical oxidation, adsorption, etc., are used in order to remove dyes from wastewater (18, 23, 9).

One of our aims is to evaluate pumice of the local resource, Van (Turkey), the original material for production of adsorbent. Besides, it is known that pumice has pores. The second purpose of this study is to investigate the adsorption isotherm, kinetics and the thermodynamic parameters adsorption onto pumice derived from the Van region.

MATERIALS AND METHODS

Chemical Materials: Experimental data are obtained from pH=6 solution. Different concentrations of dye material's solution (50 ppm, 60 ppm, 70 ppm) are prepared for the experiment.

Adsorbents: Van Pumice was used as an adsorbent during experiment. Chemical component of this pumice given in Table 1.

Table 1. Chemical components of Van pumice.

Van Pumice	SiO_2	Al_2O_3	Fe_2O_3	CaO	MgO	K_2O	Na_2O	SO_3	Loss of Combustion
	69.00	14.65	2.51	1.11	0.55	3.520	2.48	0.40	4.76

Method: In this study, Van Pumice was used whose chemical analysis results are given. Adsorption studies were applied with Van Pumice.

Pumices were applied the following operations detailed below:

a) Washing stage: Van Pumice which was grinded in the mill and which was filtered from 230 mesh sieve, was dried for 5.5 hours in the oven. 100 grams of Van Pumice was mixed 12 hours with 1.7 liter of pure water in the mixer. After mixing stage was finished, the material was kept idle for 12 hours. It was observed that aqueous phase and solid phase

were separated. Solid phase was separated by filtering. Solid phase was kept at ambient conditions for 168 hours to dry. Dried Van pumice was filtered again with 230 mesh sieve. It was placed in a desiccator until the time of experiment. Van Pumice was grinded in the mill. After that, the size of the piece was minimized by filtrating 230 mesh sieves.

In the studies of adsorption balance, 1 gram of Pumice was treated 500 mL of dye material solution. Dyeing material solutions were prepared in 50, 60, and 70 ppm concentrations, were shaken with Van Pumice at different times (2, 5, 10, 15, 20, 25, 30, 40, 50, 60, 70, 80, 90, 100, 120, 150, and 180 minutes) in 25 °C, 35 °C, 45 °C temperatures.

Dyeing material adsorption was examined depending on heat and time in the example of Van Pumice. All of the adsorption measurement was applied with a spectrophotometer (T80+ UV/VIS).

RESULTS AND DISCUSSION

Freundlich Isotherm

The Freundlich isotherm assumes an empirical equation based on the heterogeneous surface of adsorbent. The linear form of the Freundlich isotherm is expressed as (15):

$$\log q_e = \log K_f + n \log C_e \quad (1)$$

where K_f is the Freundlich coefficient related to adsorption capacity, and n relates to adsorption intensity. The values of the Freundlich constants were obtained from the linear correlations between the values of $\log q_e$ and $\log C_e$. In the Freundlich adsorption constant, n should be greater than 1.

Langmuir Isotherm

In the solid/liquid adsorption process, adsorption of the solute is usually characterized by either mass transfer (boundary layer diffusion) or intraparticle diffusion or even both (12). The adsorption data of dye removal from pumice was analyzed by the Freundlich and Langmuir isotherm models. The Langmuir isotherm model is valid for monolayer adsorption. The linear equation of the Langmuir isotherm is (10):

$$\frac{C_e}{q_e} = \frac{1}{b \times q_m} + \frac{1}{q_m} C_e \quad (2)$$

where, C_e is the equilibrium concentration of dye in the solution, q_e amount of dye adsorbed at equilibrium, q_m Langmuir adsorption capacity, and b Langmuir constant.

The values of the Langmuir constants and coefficient determination R^2 are given in Table 2. The Langmuir adsorption capacity (q_m) was found to be 27.3393, 26.5741 and 23.8115 mg/g at different temperatures (298, 308 and 318 K).

Table 2. Equal values of Neutral Red adsorption on Langmuir and Freundlich equals from different temperature.

T (K)	Langmuir			Freundlich		
	b (L/mg)	q _m (mg/g)	R ²	n	K _f (mg/g)	R ²
298	1,2921	27,3393	0,9997	3,7312	2,5977	0,9997
308	1,0537	26,5741	0,9971	10,0387	3,5430	0,9299
318	1,0209	23,8115	0,9990	34,4567	3,7676	0,7050

When R² values of both two adsorption isotherm models are taken into consideration, it shows that the adsorption process has better compliance with the Langmuir adsorption model than the Freundlich model. The Langmuir isotherm model is mostly valid for one layer adsorption over specific number of similar surfaces. If the molecular interaction is neglected, then it can be defined as adsorption behavior of a completely homogeneous surface area. Despite the heterogeneity of the surface, Freundlich-type adsorption isotherm displays the homogeneity of a Langmuir-type adsorption surface. The adsorption of Langmuir isotherm increases linearly together with initial concentration of the adsorbate. At maximum saturation point, the surface is coated with one layer and the amount of adsorbate on the surface remains constant. Also, in this isotherm, the adsorption energy is uniform. The speed of adsorption is directly proportional to the adsorbate concentration and the active places over the surface. The speed of desorption is directly proportionate to the amount of adsorbate adsorbed on the surface.

Thermodynamic Parameters

The thermodynamic parameters such as standard Gibbs free energy (ΔG), entropy change (ΔS) and enthalpy (ΔH) were calculated using following equations (17, 5):

$$K_d = \frac{C_0 - C_e}{C_e} \times \frac{V}{m} \quad (3)$$

$$\ln K_d = \frac{\Delta S}{R} - \frac{\Delta H}{RT} \quad (4)$$

$$\Delta G = \Delta H - T\Delta S \quad (5)$$

where K_d is the equilibrium constant, C_0 initial concentration (mg/dm³), C_e equilibrium concentration, V volume (cm³), m of the pumice (g), T (Kelvin), and R gas constant (8.314 J/mol). The changes in enthalpy (ΔH) and entropy (ΔS) were determined from the slope and intercept of the plots of $\ln K_d$ versus $1/T$. The Gibbs free energy (ΔG) was calculated using Eq (5).

Table 3. Thermodynamic parameters of Neutral Red adsorption on Van Pumice.

Temp (K)	K _c	ΔG, kJ/mol	ΔH, kJ/mol	ΔS, kJmol ⁻¹ K ⁻¹
298	2,6502	-2414,6987		
308	7,5660	-5182,0370	0,0013	0,0292
318	8,4715	-5649,1358		

Concerning the adsorption of Neutral Red solutions onto the Pumice found in Lake Van, thermodynamic parameters such as ΔG, ΔS and ΔH were determined at temperatures of 298, 308, and 318 K.

The negative value of Gibbs free energy (ΔG) shows that the adsorption process of Neutral Red onto the Pumice located in Lake Van is spontaneous. The (ΔG) value tends to decrease at increasing temperatures and thus demonstrates that this process can be carried out much easier at high temperatures. The positive value of ΔS shows that, at the interface between Neutral Red solution and the Pumice found in Lake Van, the sorption process tends toward increasing disorder. The positive value of ΔH points out that the sorption process is endothermic.

Adsorption Kinetics

The experimental data relating to adsorption of dye onto pumice was investigated using the Lagergren pseudo-first and pseudo-second order equation (1, 7):

$$\log(Q_e - Q_t) = \log(Q_e) - \frac{k_1 t}{2.303} \quad (6)$$

$$\frac{t}{q_t} = \frac{1}{k_2 q_e} + \frac{1}{q_e} t \quad (7)$$

where, q_e is the amount of dye adsorbed at equilibrium (mg/g), q_t amount of dye adsorbed at various times, t time of adsorption duration, and k_1 is a rate constant of the equation (min^{-1}).

The k_1 and q_e were calculated from the slope and intercept of the plots of $\log(q_e - q_t)$ versus t according to the pseudo-first-order model (Fig. 1) and t/q_t versus t according to the pseudo-second-order model (Fig. 2) as well as q_e and k_2 from the slope and intercept were calculated.

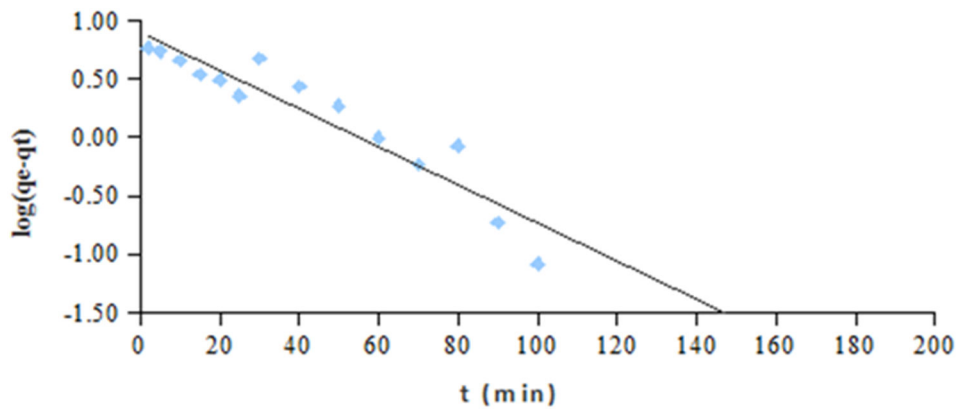


Figure 1: Pseudo first order graph of Dye Adsorption on Van Pumice.

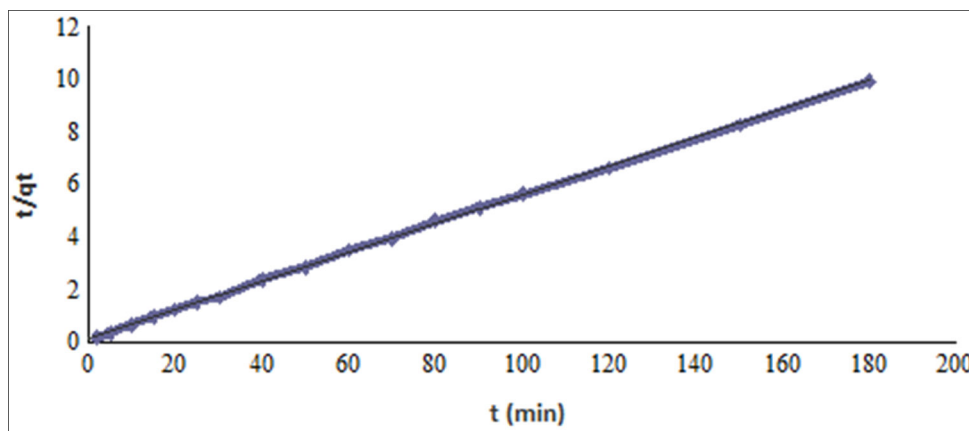


Figure 2: Pseudo second order graph of Dye Adsorption on Van Pumice

Table 4. Pseudo first order parameters of the dye.

T (K)	k_1	q_e (calc.)	q_e (exp.)	R^2
298	0,0215	2,7455	18,1510	0,7089
308	0,0374	7,8126	22,0815	0,8870
318	0,0357	3,0300	22,3605	0,7560

Table 5. Pseudo second order parameters of the dye.

T (K)	k_2	q_e (calc.)	q_e (exp.)	R^2
298	0,0250	18,2929	18,1510	0,9995
308	0,0115	22,5745	22,0815	0,9987
318	0,0388	22,5004	22,3605	0,9998

Regarding all the initial pumice amounts and temperature values of pumice, we concluded that the kinetics of sorption onto the pumice has indicated a good compliance with the quadratic form of the kinetic model. The correlation factor R^2 was found above 0,99.

CONCLUSION

Considering all these results, we have concluded that the Pumice found in Lake Van is a recommended adsorbent for the used dyestuff. We consider that the Pumice found in Lake Van which is currently used in many fields of application, can also be used as an adsorbent.

In his Master of science thesis, "BIOSORPTION OF VICTORIA BLUE R (VBR) ONTO IMMOBILIZED BIOMASS OF BONE CHAR AND SUNFLOWER HUSK", Ozdemir has applied his experimental data to the Langmuir isotherm model and obtained the resulting R² values at different temperatures, varying between 0,974 and 0,989. He later found out that these high regression coefficients and its biosorption have indicated good compliance with the Langmuir isotherm. Compliance with Langmuir isotherm showed out that the biosorption occurred on homogenous surfaces and the dye material VMR has coated the KIKU, forming only one layer (20).

In his master of science thesis "Removal of Dye Materials from Aqueous solutions by Adsorption on Coals and Cokes", Kayacan has observed that both types of cokes comply with the Freundlich isotherm and also with the Langmuir isotherms at the same time. Besides, the MKP cokes rather comply with the Langmuir isotherm and the DB cokes comply with Freundlich isotherm. It is thereby concluded that the MKP cokes have relatively homogenous surfaces, but on the other hand, the DB cokes have relatively heterogeneous surface. He found out that the b values of Langmuir's isotherm of MKP cokes were relatively high, thus he concluded that this is a clear proof of why these cokes are good adsorbents (14). It is clear that both studies support our study.

In their studies, Turkmenoglu and her friends have used acidic Pumice found in Lake Van in sizes of 0-2 mm, 2-4 mm and 4-8 mm respectively. They have found the physical features of Pumice found in Lake Van as follows (25):

Van Pumice	0-2 mm	2-4 mm	4-8 mm
Specific Weight Factor	1,72	1,32	1,06
Water Absorption Rate (%)	-	36,71	38,83
Bulk Density (kg/m ³)	636	495	413

The chemical and physical features of Pumice are some of those determining factors to find out if it is a good adsorbent or not.

REFERENCES

1. Aivalioti M, Papoulias P, Kousaiti A, Gidarakos E. Adsorption of BTEX, MTBE and TAME on natural and modified diatomite. *Journal of hazardous materials*. 2012;207:117–127.
2. Aksay E. Investigation of the Technological Properties of the Izmir-Menderes Pumice Ore. [İzmir]: Dokuz Eylül University; 2005.
3. Bardakci B, Cicek E. Use of Isparta Pumice for the Removal Radioactive Waste by Adsorption. In Isparta; 2005.
4. Başer İ, İnanıcı Y. Boyarmadde kimyası. Marmara Üniversitesi; 1990.
5. Caliskan N, Kul AR, Alkan S, Sogut EG, Alacabey I. Adsorption of Zinc (II) on diatomite and manganese-oxide-modified diatomite: A kinetic and equilibrium study. *Journal of hazardous materials*. 2011;193:27–36.
6. Cevikbas A, Ilgun F. Geology and Economics of Turkey Pumice. In: *Geology and Economics of Turkey Pumice*. Isparta; 1997. p. 13–8.
7. Chen M, Shang T, Fang W, Diao G. Study on adsorption and desorption properties of the starch grafted p-tert-butyl-calix [n] arene for butyl Rhodamine B solution. *Journal of hazardous materials*. 2011;185(2):914–921.
8. Çiftçi E. Yerbilimleri teknik terimler sözlüğü. (Earth Science Technical Words dictionary) NİĞDE, Hamle Yayıncılık. 2003;580.
9. Depci T, Kul AR, Onal Y, Disli E, Alkan S, Turkmenoglu ZF. Adsorption of crystal violet from aqueous solution on activated carbon derived from Gölbaşı lignite. *Physicochemical Problems of Mineral Processing*. 2012;48(1):253–270.
10. Doğan M, Alkan M, Demirbaş Ö, Özdemir Y, Özmetin C. Adsorption kinetics of maxilon blue GRL onto sepiolite from aqueous solutions. *Chemical Engineering Journal*. 2006 Nov;124(1–3):89–101.
11. Barker, J.M. and Austin, G.S. (1994): *Stone, Decorative*; in Carr, D.D., Senior Editor *Industrial Minerals and Rocks, Society for Mining, Metallurgy and Exploration*, Littleton, Colorado, 367–378.
12. Ghosh D, Bhattacharyya KG. Adsorption of methylene blue on kaolinite. *Applied Clay Science*. 2002 Feb;20(6):295–300.
13. Ilhan S, Nurbas M, Ekmekci S, Ozdag H. Use of Pumice as Adsorbent in Biotechnology. In Isparta; 1997. p. 39–46.

14. Kayacan S. Removal Of Dye Materials From Aqueous Solutions By Adsorption On Coals And Cokes [Master's thesis]. [Ankara]: Ankara University; 2007.
15. Khan T, Sharma T, Ali I. Adsorption of Rhodamine B dye from aqueous solution onto acid activated mango (*Mangifera indica*) leaf powder: Equilibrium, kinetic and thermodynamic studies. *J Toxicol Environ Health Sci.* 2011;3(10):286–97.
16. Kuscu M, Gedikoglu A. Geological Position of Regional Pumices of Isparta-Golcuk. *Engineering Geology Journal.* 1990;37:69–78.
17. Laidler K, Meiser J. In: *Physical Chemistry.* Houghton Mifflin, New York; p. 852.
18. Mohan D, Singh KP, Singh G, Kumar K. Removal of dyes from wastewater using flyash, a low-cost adsorbent. *Ind Eng Chem Res.* 2002;41(15):3688–3695.
19. Özcan Y, Ulusoy E. *Tekstil Elyaf ve Boyama Tekniği.* İstanbul: İstanbul Üniversitesi; 1978.
20. Özdemir N. Biosorption of Victoria Blue R (VBR) Onto Immobilized Biomass Of Bone Char And Sunflower Husk [Master's thesis]. [Çorum]: Hitit University; 2015.
21. Reyhanoğlu M. Pumice and its uses [Master's thesis]. [Adana]: Çukurova University; 1988.
22. Sariisik A, Tozacan B, Davraz M, Ugur I, Cankiran O. *Pumice technology.* Isparta: Süleyman Demirel University; 1998.
23. Senthilkumaar S, Kalaamani P, Subburaam C. Liquid phase adsorption of Crystal violet onto activated carbons derived from male flowers of coconut tree. *Journal of Hazardous Materials.* 2006 Aug 25;136(3):800–8.
24. Tozum S. Removal of pollutants from Olive Wastewater (Karasu) with Pumice by Adsorption [Master's thesis]. [Isparta]: Süleyman Demirel University; 2009.
25. Turkmenoglu Z, Kilic A, Depci T. Determination of Mechanical Properties of Self Compacting Lightweight Concrete Manufactured with Pumice in Van Region. *Çukurova Üniversitesi Mühendislik Mimarlık Fakültesi Dergisi.* 2015;30(1):105–116.
26. Yanik S. The usability of basic pumice as a concrete aggregate [Master's thesis]. [Adana]: Çukurova University; 2007.



Determination of Cd(II) Ions by using Cyclodextrin-Based Polymeric Fluorescence Sensor

Soner Çubuk*, Özge Yılmaz, Ece Kök Yetimoğlu, Memet Vezir Kahraman

Marmara University, Faculty of Arts and Sciences, Chemistry Department, 34722
Istanbul, Turkey

Abstract: In this study, Cd(II) ion was determined using a cyclodextrin-based polymeric fluorescence sensor prepared by UV-curing technique. The effects of several parameters such as pH, time, and coexisting ions on the fluorescence intensity were also examined. The excitation and emission wavelengths were found to be 374 nm and 422 nm, respectively. The measurement range was in the range of 4.45×10^{-9} mol L⁻¹ to 4.45×10^{-8} mol L⁻¹ for Cd(II) ions and the detection limit was calculated as 6.23×10^{-10} mol L⁻¹. In addition, sensor membrane was selective which was not influenced by common coexisting metal ions. The concentrations of the foreign ions such as Pb(II), Co(III), Ag(I), Zn(II), Cu(II), Cr(III) are 1000-fold higher than Cd(II) ions. Besides the prepared polymeric fluorescence sensor was successfully implemented to the determination of Cd(II) ions in biscuit and tap water samples.

Keywords: Fluorescence sensor; photopolymerization; Cd(II) ions.

Cite this: Cubuk S, Yilmaz O, Kok Yetimoglu E, Kahraman M. Determination of Cd(II) Ions by using Cyclodextrin-Based Polymeric Fluorescence Sensor. JOTCSA. 2017;4(2):61–72.

Submitted: February 13, 2017. **Accepted:** March 23, 2017.

DOI: 10.18596/jotcsa.292001.

Corresponding author: Soner Çubuk; sonercubuk@marmara.edu.tr

INTRODUCTION

The rapid spread of industrialization in the world, the emergence of new technologies, urbanization that has been continuously distorted due to the growing population around cities and villages and the attempt is made to provide all the requirements attached to them and the consumption of excessive quantities of chemical substances, including heavy metals, are closely related. Cadmium is among the heavy metals that cause environmental pollution today and it affects human life with ways such as cigarette smoke, refined foodstuff, water pipes, coffee, tea, shellfish, coal burning, and fertilizers. In addition, cadmium is used in coating industry, solar batteries, plastic stabilizers, and dye and pigment industries. Cadmium compounds can be released to the atmosphere through the metallurgical process or when the metal is removed by heating from its ore. Cadmium passes through the ground through the rain and accumulates at the same time. It moves through the layers of soil and enters the food chain, primarily through grains and vegetables. Cadmium enters the human body through contaminated food and water. It is quite poisonous, even at low concentrations, and causes damage to organs such as the liver, lungs, and kidneys with vital importance in the human body through bioaccumulation and it also increases the risk of getting some types of cancer, such as prostate and breast, as a result of toxic effects. Moreover, exposure to cadmium significantly affects the basic systems of our body such as digestion, respiration, lymph and blood circulatory, and urinary. Therefore, the level of cadmium in various matrices, such as food and water, especially in drinking water sources, must be constantly monitored and analyzed (1-3).

The determination of cadmium, which has such great effects on human health and environment, has become very important nowadays. For this reason, many methods including differential pulse anodic stripping voltammetry (DPASV) (4, 5), flame atomic absorption spectrometry (FAAS) (6), inductively coupled plasma optical emission spectrometry (ICP-OES) (7), potentiometry (8-9), spectrofluorimetry (10, 11), spectrophotometry (12, 13) and inductively coupled plasma atomic emission spectroscopy (ICP-AES) (14) have been developed. These methods can provide wide linear range values and good detection limits, but they need to use very expensive devices in the laboratory and a qualified staff for the application. However, spectrofluorometric methods have many advantages over sophisticated methods such as cost, fast response time, high precision. Considering the disadvantages of conventional methods, there is no doubt that alternative methods of cadmium ions detection will be needed instead of these methods and fluorescence methods will be important for cadmium ions determination.

In our study, reusable β -cyclodextrin (β -CD) based polymeric fluorescent sensor has been developed that provides sensitive, precise, fast and reproducible results for the determination of Cd(II) ions. Once the characterization of the sensor has been made, optimal conditions have been determined so that the analysis can be performed.

MATERIALS AND METHODS

Chemicals

In this study, all of the monomers and other chemical substances used in the preparation of the polymeric membrane were obtained from Sigma and all these were of analytical purity. All stock single metal solutions with a concentration of 1000 ppm were purchased from Merck Millipore. The working solutions of the metals used in the experiments were also prepared by diluting these stock solutions with distilled water to reach the desired concentrations.

Instrumentation

A Varian Cary Eclipse spectrofluorometer was used to record excitation and emission spectra. The Cd(II) ion concentration in real samples was analyzed by FAAS so that the results could be compared with the developed method. A Perkin Elmer Spectrum 100 spectrophotometer was used and ATR-FTIR spectrum of membrane and identify the surface of membrane was carried out by a Philips XL30 ESEM-FEG/EDAX scanning electron microscope. The results obtained from the Perkin Elmer AAnalyst 700 graphite furnace atomic absorption spectrophotometer (GF-AAS) were used to compare the Cd(II) concentrations of the real samples with those obtained by the developed method.

Method

Synthesis of the β -cyclodextrin acrylate (β -CD-A) monomer

The β -CD-A were synthesized following reported procedure by Constantin et. al (15). For the synthesis of the functional β -CD-A monomer, 11.38 g of β -CD was weighed in a three-neck round-bottom flask. Then 30 mL of dimethyl formamide (DMF) was added and dissolved at 50 °C and 12 g of trimethylamine (TEA) was added. Then 50 mL of DMF solution containing 10.8 g of acryloyl chloride (AC) was added dropwise to the reaction flask over 2 hours. At the end of the time, the reaction was stopped and flask content was filtered through the filter paper. All the filtrate was then poured dropwise onto cold acetone to obtain white precipitates. The precipitate was left to dry overnight in the lyophilizer.

Preparation of polymeric sensor

Polymeric sensor was prepared by UV-curing technique. The β -CD-A and 2-hydroxy-2-methylpropiophenone (HMPP) were used as a reactive monomer and as a photoinitiator, respectively. For preparation of the membrane, 1% β -CD-A, 25% 2-hydroxyethyl methacrylate (HEMA), 74% hexanedioldiacrylate (HDDA) and 3% of total formulation HMPP were placed in a beaker and then homogenized by mixing. The resulting mixture was transferred to a mold having dimensions of 12 mm x 40 mm x 2 mm and UV light (OSRAM 300 W, $\lambda_{\max} = 365$ nm) was applied for 3 minutes. The membranes obtained at the end of the period were removed from the matrix and allowed to stand in distilled water for 24 hours to remove the excess of unreacted monomers and initiator. Then the membranes were dried in a lyophilizer.

Preparation of real samples

In order to validate the developed method, two different real sample analyzes were performed for Cd(II) ions. One of them was biscuit as a food sample and the other was tap water. Biscuit samples were purchased from public market and tap water samples were collected from the consumer's tap. Microwave assisted acid digestion method was used for digestion of biscuit samples. These samples were prepared for analysis according to BS EN 13804:2013 method (16). The concentrations of Cd(II) ions in the solutions were measured by a developed sensor and GF-AAS method.

RESULTS AND DISCUSSION

Characterization

The ATR-FTIR spectrum of polymeric membrane obtained by scanning at a wavenumber between 400-4000 cm^{-1} is shown in Figure 1. Typical O-H vibrations in β -CD and HEMA structures seen in the spectrum are observed at 3384 cm^{-1} . The peaks corresponding to the C-O stretching vibration appear at 1023 cm^{-1} , 1072 cm^{-1} , 1151 cm^{-1} , 1245 cm^{-1} and 2166 cm^{-1} , respectively. In addition, the peak of the asymmetric $-\text{CH}_2-$ vibration is at 2918 cm^{-1} . The vibration of the C = O bonds is observed at 1719 cm^{-1} . The peaks at 2918 cm^{-1} and 1450 cm^{-1} represent the C-H bond. (15, 17).

The SEM image of the prepared membrane is shown in Figure 2. The SEM image demonstrates that the prepared membrane has a non-porous, crack-free and homogeneous structure as expected.

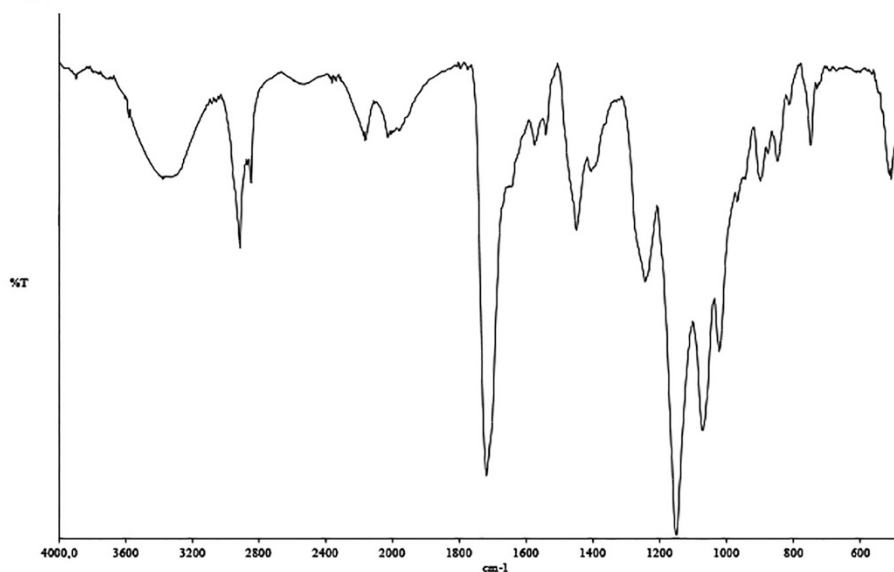


Figure 1. FTIR spectrum of polymeric membrane.

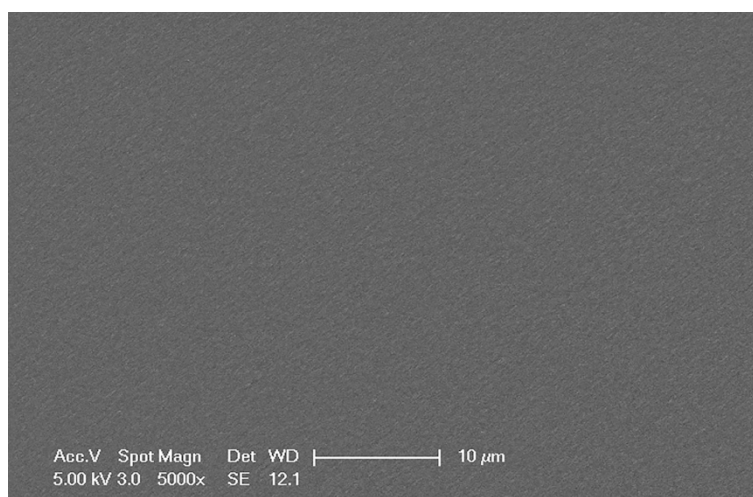


Figure 2. SEM micrograph of polymeric membrane at 5000x magnification.

Spectral characterization studies

In order to determine whether the polymeric membrane has a change in fluorescence intensity with Cd(II) ions, excitation and emission wavelength scans were performed in the absence and presence of 8.90×10^{-9} mol L⁻¹ Cd(II) ions. Excitation was at 374 nm and the emission spectra were scanned in the range of 400-600 nm at slit width 5 nm (Figure 3). The emission maximum wavelength was found to be 422 nm. Figure 3 shows the increase in fluorescence intensity in the presence of cadmium ions.

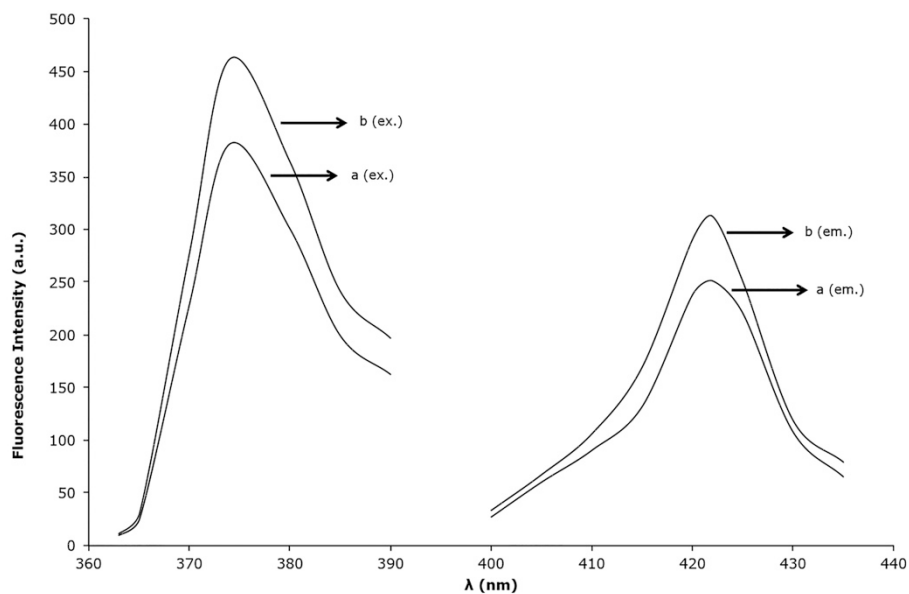


Figure 3. Excitation and emission spectra of polymeric membrane. (a) absence (line) and the (b) presence of $8.90 \times 10^{-9} \text{ mol L}^{-1} \text{ Cd(II)}$ (dotted line).

Optimization of the parameters for Cd(II) Determination

In order to optimize the parameters required for the determination of cadmium ions using the developed sensor, firstly the pH effect was examined between the pH ranges of 1.0 and 11.0 in the presence of $8.90 \times 10^{-9} \text{ mol L}^{-1}$ concentration of Cd(II). According to the results shown in Figure 4, the fluorescent intensity increased with increasing value of pH 1.0 to 5.0, and it started to decrease at values higher than pH 5. The highest fluorescence intensity has been reached at pH 5.0, therefore this pH value was chosen for further studies.

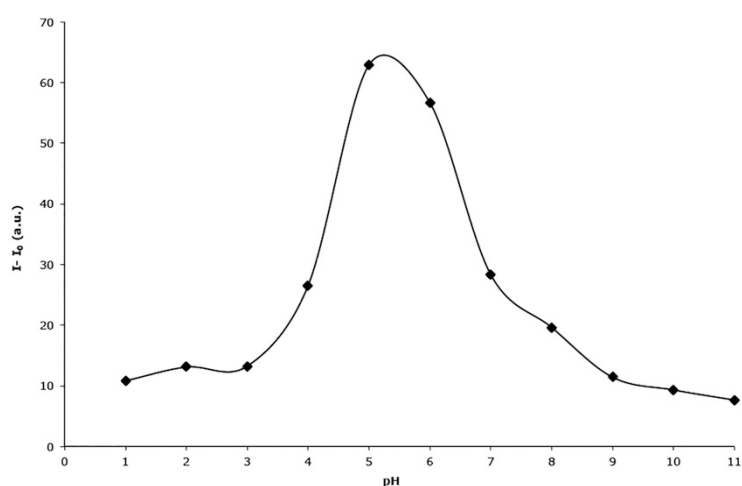


Figure 4. Fluorescence intensity change as a function of pH (I_0 and I are the fluorescence intensities before and after Cd(II) was added, respectively).

Secondly, the effect of the response time on the fluorescence intensity was examined for 300 seconds. Figure 5 depicts the time-dependent changes in the fluorescence intensity of the sensor in the presence of 8.90×10^{-9} mol L⁻¹ Cd(II) ions at pH 5.0. As it can be seen from the Figure 5, the fluorescence intensity of the sensor did not change between 15 and 90 seconds and then it started to decrease with the increase of time. Thus, for further experiments 30 s was selected as analysis time.

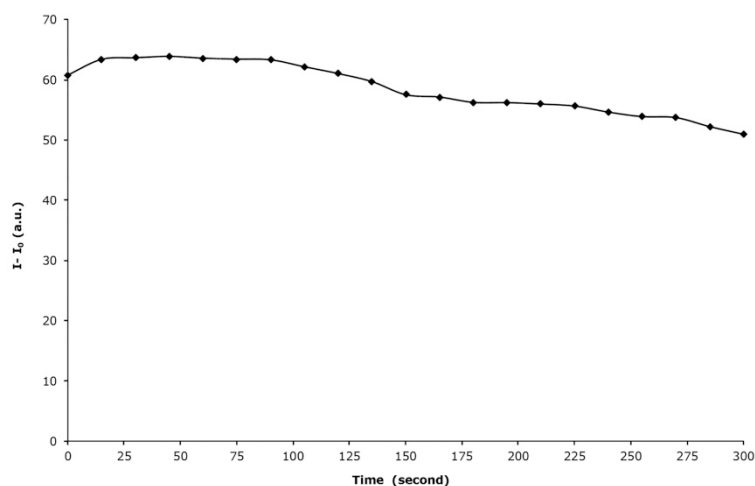


Figure 5. Time-dependent change in fluorescence intensity of the polymeric membrane ($\lambda_{ex/em}=374$ nm/422 nm; I and I₀ respectively indicate the states in which Cd(II) ions are present and absent in the solution medium).

Third, the regeneration, reversibility and reproducibility experiments of the sensor were made. After contacting the sensor membrane with the 8.90×10^{-9} mol L⁻¹ Cd (II) solution, the initial fluorescence intensity was only achieved by washing for less than one minute using distilled water. For this reason, distilled water was used for the regeneration of the sensor. These results indicated that the polymeric membrane is fully reversible. A single sensor was used approximately 160 times and reproducible results were obtained with a very low standard deviation of about 2.1% (95% confidence levels, n = 6). In addition, found that the same polymeric sensor was stable for at least 250 days.

Measuring range, limit of detection (LOD)

A graphical representation of the fluorescence intensities versus the logarithm of the different Cd(II) concentrations of the developed sensor was shown in Figure 6 where I₀ and I are the fluorescence intensities of the membrane in the absence and presence of Cd(II) ions. The graph shows linearity between the concentrations of 4.45×10^{-9} mol L⁻¹ and 4.45×10^{-8} mol L⁻¹ Cd(II) and was used as the calibration curve. Since this graph deviates from the linearity except for this concentration range, its values are not shown. LOD was

found to be 6.23×10^{-10} mol L⁻¹ by calculating three times the standard deviation of the blank solution intensity (n=6).

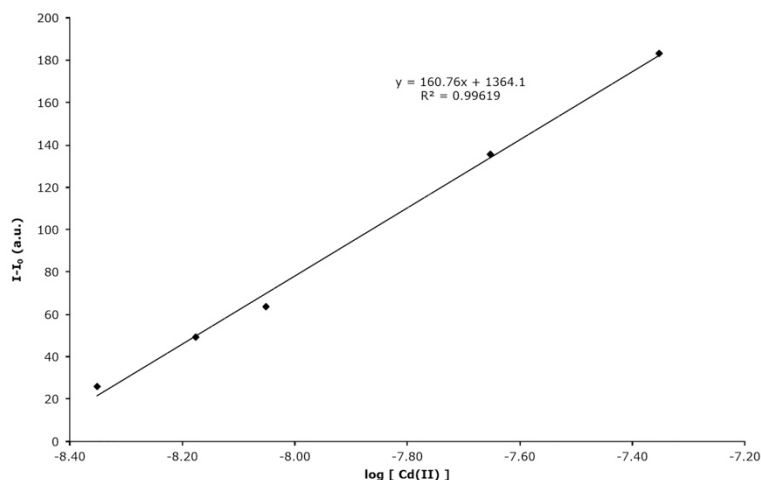


Figure 6. Calibration curve of polymeric fluorescence sensor ($\lambda_{\text{ex/em}}=374/422$, pH:5.0).

Effect of coexisting ions

The effect of foreign ions on the fluorescence intensity was investigated in the presence of 8.90×10^{-9} mol L⁻¹ cadmium ions at pH 5.0, with the experiment performed under the decided conditions, and the obtained results are shown in Table 1. From these results, it has been observed that even at about 1000 times of the cadmium ions, there was no effect of foreign ions on the prepared sensor intensity.

Table 1. Effect of coexisting ions on fluorescence intensity of sensor.

Species	Tolerable Limit ^a (mol L ⁻¹)
Au(III)	5.07×10^{-6}
Fe(III)	1.78×10^{-5}
Cr(III)	1.92×10^{-5}
Pb(II)	4.82×10^{-6}
Ag(I)	9.25×10^{-6}
Co(III)	1.70×10^{-5}
Mn(II)	1.80×10^{-5}
Zn(II)	1.54×10^{-5}
Cu(II)	1.56×10^{-5}
Mg(II)	4.16×10^{-5}
Hg(II)	2.49×10^{-6}
Ni(II)	8.53×10^{-6}
Ca(II)	1.25×10^{-5}

^a Less than $\pm 5\%$ relative error

Real sample applications and recovery studies of developed sensor

The Cd(II) concentrations in tap water and biscuits samples was calculated using the calibration graph. All experiments were conducted under optimum conditions. The results obtained from real sample applications of the prepared polymeric fluorescence sensor and the results of its recovery studies are summarized in Table 1. In addition, these results were compared with the results of analyzes carried out with GF-AAS of the same samples. The comparison showed that the developed sensor and GF-AAS results are in very good agreement with each other and the sensor can be used successfully in the determination of cadmium ions in real samples.

Table 1. Real samples applications and recovery studies of developed polymeric sensor (n=6).

Sample	Cd(II) added (mol L ⁻¹)	This work (mol L ⁻¹)	GF-AAS	RSD	Recovery (%)
Tap water	-	(1.47±0.08) ×10 ⁻⁸	(1.44±0.06) ×10 ⁻⁸	1.81	-
Tap water	2.31×10 ⁻⁸	(2.40±0.05) ×10 ⁻⁸	(2.34±0.04) ×10 ⁻⁸	2.23	103.8
Tap water	4.09×10 ⁻⁸	(4.21±0.13) ×10 ⁻⁸	(4.13±0.07) ×10 ⁻⁸	1.92	102.9
Biscuit Samples	-	(1.02±0.06) ×10 ⁻⁹	(1.01±0.04) ×10 ⁻⁹	0.79	-
Distillated water	-	<Detection Limit	<Detection Limit	-	-
Distillated water	2.67×10 ⁻⁸	(2.79±0.09) ×10 ⁻⁸	(2.70±0.10) ×10 ⁻⁸	3.26	104.3
Distillated water	8.90×10 ⁻⁸	(9.10±0.17) ×10 ⁻⁹	(8.96±0.07) ×10 ⁻⁹	1.51	102.2

Comparison of the developed sensor with the other spectroscopic techniques

Many methods have been developed for Cd(II) ions analysis and comparison of some of these methods with the developed method is shown in Table 2. As it can be seen from this table, the proposed sensor surpasses the other methods in terms of linear range and LOD value. The LOD value of the ICP-OES, ICP-AES and FAAS methods seems to be sufficient. But this value is higher than that of the developed sensor and these methods require expensive instruments. Although the analysis time of potentiometric methods seems to be the same as the method in this article, the detection limits are higher than this method. In addition, the analysis time of the spectrophotometric and spectrofluorometric methods given in the table ranges from 5 minutes to 25 minutes, which is considerably higher than the recommended sensor response time. It is also seen that it has superior performance compared to the literature methods given in Table 2.

Table 2. Comparison of some Cd(II) analysis methods reported in the literature with the developed method.

System	Method	pH or Medium	Linear Range (mol L ⁻¹)	LOD (mol L ⁻¹)	Response time	Ref.
CB-18-crown-6-GEC	DPASV	4.5	1.7x10 ⁻⁶ - 7.03x10 ⁻⁸	2.14x10 ⁻⁸	300 sec.	4
Nafion-coated bismuth film electrode	DPASV	4.5	3.56x10 ⁻⁸ - 3.20x10 ⁻⁷	1.51x10 ⁻⁹	180 sec.	5
Dowex Marathon C resin	FAAS	3.5	8.90x10 ⁻⁹ - 8.90x10 ⁻⁷	1.16x10 ⁻⁹	60 sec.	6
2,2-bipyridyl and erythrosine	ICP-OES	4.5	1.78x10 ⁻⁷ - 3.56x10 ⁻⁶	3.56x10 ⁻⁸	N.M.	7
1,13- bis (8quinolyl)-1,4,7,10,13- pentaotridecane	Potentiometric ion selective membrane	1.0-6.0	1x10 ⁻⁵ - 1x10 ⁻¹	8.4x10 ⁻⁶	15 sec.	8
2-nitrophenyloctyl ether	Potentiometric sensor	4.0-7.0	2.0x 10 ⁻⁷ - 1.0 x 10 ⁻²	1.0x10 ⁻⁷	15 sec.	9
Tetrakis (4-nitrophenyl) porphyrin	Spectrofluorometric	in ethanol	1.0x10 ⁻⁶ - 1.0x10 ⁻⁵	2.46x10 ⁻⁹	25 min.	10
Glyoxal-bis-(2-hydroxyanil)	Spectrofluorometric	12.0-13.0	8.90x10 ⁻⁹ - 8.90x10 ⁻⁸	5.78x10 ⁻⁹	10 min.	11
Alizarin Red S	Spectrophotometric	0.05M sulfuric acid	8.90x10 ⁻⁷ - 3.60x10 ⁻⁴	2.67x10 ⁻⁷	N.M.	12
p,p'-Dinitro-SYM-Diphenylcarbazid	Spectrophotometric	11.8 - 12.0	4.45x10 ⁻⁶ - 5.34x10 ⁻⁵	1.16x10 ⁻⁶	5 min.	13
1,5-bis(di-2-pyridyl) methylene thiocarbohydrazide (DPTH-gel)	ICP-AES	9.0	4.45x10 ⁻⁸ - 8.90x10 ⁻⁷	9.79x10 ⁻⁹	60 sec.	14
β- CD based polymeric sensor	Spectrofluorometric	5.0 546	4.45x10 ⁻⁹ - 4.45x 10 ⁻⁸	6.23x10 ⁻⁷ 10	15-90 sec.	OM

NM: Not Mentioned. OM: Our Method.

CONCLUSION

In this study, a reusable polymeric fluorescence sensor for the analysis of cadmium ions in water and food samples, has been developed. Parameters required for determination such as pH, measurement range, selectivity, precision, response time, and reproducibility were also systematically examined. Fluorescence spectra showed that the excitation/emission maxima of the sensor were at 374/422 nm, respectively. Cd(II) ions with developed sensor can be determined in a short period of about 30 seconds. The prepared sensor shows a linear response for Cd(II) ions at a measurement range of 4.45×10^{-9} to 4.45×10^{-8} mol L⁻¹ with a detection limit of 6.23×10^{-10} mol L⁻¹ at pH 5. The results show that the developed sensor can be successfully used to the detection of Cd(II) ions in various matrices.

ACKNOWLEDGMENTS

This work was supported by Marmara University, Commission of Scientific Research Project (M.Ü. BAPKO) under grant FEN-D-090217-0068.

REFERENCES

1. Robards K, Worsfold P. Cadmium: toxicology and analysis. A review. *The Analyst*. 1991;116(6):549.
2. Sherlock JC. Cadmium in foods and the diet. *Experientia*. 1984 Feb;40(2):152–6.
3. Parker SP, McGraw-Hill, inc, editors. McGraw-Hill encyclopedia of engineering. 2nd ed. New York: McGraw-Hill; 1993. 1414 p.
4. Serrano N, González-Calabuig A, del Valle M. Crown ether-modified electrodes for the simultaneous stripping voltammetric determination of Cd(II), Pb(II) and Cu(II). *Talanta*. 2015 Jun;138:130–7.
5. Xu H, Zeng L, Huang D, Xian Y, Jin L. A Nafion-coated bismuth film electrode for the determination of heavy metals in vegetable using differential pulse anodic stripping voltammetry: An alternative to mercury-based electrodes. *Food Chemistry*. 2008 Aug;109(4):834–9.
6. Daşbaşı T, Saçmacı Ş, Ülgen A, Kartal Ş. A solid phase extraction procedure for the determination of Cd(II) and Pb(II) ions in food and water samples by flame atomic absorption spectrometry. *Food Chemistry*. 2015 May;174:591–6.
7. Feist B, Mikula B, Pytlakowska K, Puzio B, Buhl F. Determination of heavy metals by ICP-OES and F-AAS after preconcentration with 2,2'-bipyridyl and erythrosine. *Journal of Hazardous Materials*. 2008 Apr;152(3):1122–9.
8. Ghaemi A, Tavakkoli H, Mombeni T. Fabrication of a highly selective cadmium (II) sensor based on 1,13-bis(8-quinolyl)-1,4,7,10,13-pentaoxatridecane as a supramolecular ionophore. *Materials Science and Engineering: C*. 2014 May;38:186–91.
9. Rezvani Ivani SA, Darroudi A, Arbab Zavar MH, Zohuri G, Ashraf N. Ion imprinted polymer based potentiometric sensor for the trace determination of Cadmium (II) ions. *Arabian Journal of Chemistry*. 2017 Feb;10:S864–9.

10. Khani R, Ghiamati E, Boroujerdi R, Rezaeifard A, Zaryabi MH. A new and highly selective turn-on fluorescent sensor with fast response time for the monitoring of cadmium ions in cosmetic, and health product samples. *Spectrochimica Acta Part A: Molecular and Biomolecular Spectroscopy*. 2016 Jun;163:120–6.
11. Dong Y, Gai K. The application of glyoxal-bis-(2-hydroxyanil) to the determination of trace amounts of cadmium by spectrofluorimetry. *Journal of the Brazilian Chemical Society*. 2006 Feb;17(1):135–8.
12. Ullah M, Haque ME. Spectrophotometric Determination of Toxic Elements (Cadmium) in Aqueous Media. *Journal of Chemical Engineering [Internet]*. 2011 Mar 10 [cited 2017 Apr 11];25(0). Available from: <http://www.banglajol.info/index.php/JCE/article/view/7233>
13. Bulgariu L, Bulgariu D, Sârghie I. Spectrophotometric Determination of Cadmium(II) Using p,p'-Dinitro-SYM-Diphenylcarbrazid in Aqueous Solutions. *Analytical Letters*. 2005 Nov;38(14):2365–75.
14. Zougagh M. Determination of cadmium in water by ICP-AES with on-line adsorption preconcentration using DPTH-gel and TS-gel microcolumns. *Talanta*. 2002 Mar 11;56(4):753–61.
15. Constantin M, Bucatariu S, Ascenzi P, Simionescu BC, Fundueanu G. Poly (NIPAAm-co- β -cyclodextrin) microgels with drug hosting and temperature-dependent delivery properties. *Reactive and Functional Polymers*. 2014;84:1–9.
16. Li L, ErLong L, JiangHui L, JinHua W, XiaoLin L, Feng L, et al. Foodstuffs-determination of elements and their chemical species-general considerations and specific requirements-an translation from EN 13804: 2013. *Journal of Food Safety and Quality*. 2014;5(10):3349–3355.
17. Demir S, Kahraman MV, Bora N, Kayaman Apohan N, Ogan A. Preparation, characterization, and drug release properties of poly(2-hydroxyethyl methacrylate) hydrogels having β -cyclodextrin functionality. *Journal of Applied Polymer Science*. 2008 Jul 15;109(2):1360–8.



Development of UV-cured Polymeric Fluorescence Sensor for Boron Determination

Soner Çubuk*, Mirgül Kosif, Ece Kök Yetimoğlu, Memet Vezir Kahraman

Marmara University, Faculty of Arts and Sciences, Chemistry Department, 34722
Istanbul, Turkey

Abstract: This study reports the preparation and characterization of a new polymeric fluorescence sensor for the determination of boron. The sensor was prepared by the UV-curing of glycosyloxyethyl methacrylate (GOEM), 1,6-hexanediol diacrylate (HDDA), 2-hydroxyethylmethacrylate (HEMA), and 2,2'-dimethoxy-2-phenylacetophenone (DMPA) was used as the photoinitiator. The characteristics of the sensor performance including sensitivity, response time, pH effect, stability, and matrix interferences were studied. The excitation and emission wavelengths of the fluorescence sensor were 378 and 423 nm, respectively. With the presented sensor, the optimum pH value for the boron solution was determined as pH 6.0, and the optimum analysis time was selected as 45 seconds. Under the optimized conditions, the linear response range was found to be $9.25 \times 10^{-7} \text{ mol L}^{-1}$ and $9.25 \times 10^{-6} \text{ mol L}^{-1}$. The limit of detection (LOD) was $2.90 \times 10^{-8} \text{ mol L}^{-1}$ and the limit of quantification (LOQ) was $9.66 \times 10^{-8} \text{ mol L}^{-1}$ ($n=7$) with 1.2% relative standard deviation. In addition, boron could be selectively detected by the proposed sensor even in the presence of possible interfering substances. The fluorometric sensor was also successfully applied to real environmental water samples.

Keywords: Boron; fluorescence; UV-curing; sensor.

Cite this: Cubuk S, Kosif M, Kok Yetimoglu E, Kahraman MV. Development of UV-cured Polymeric Fluorescence Sensor for Boron Determination. JOTCSA. 2017; 4(2): 73-86.

Submitted: March 03, 2017. **Revised:** March 10, 2017. **Accepted:** April 10, 2017.

DOI: 10.18596/jotcsa.296243.

*Corresponding author: Soner Çubuk. E-mail: sonercubuk@marmara.edu.tr.

INTRODUCTION

Boron is used in many areas such as defense industry, jet and rocket fuel, soap, detergent, solder, photography, textile dyes, nuclear field, glass fiber, and paper industry. Boron is also necessary for humans and animals as well as being used for different purposes in various industries. This element has a supportive effect on the metabolism such as calcium, magnesium, and vitamin D. However, excessive use for humans can result in eczema, abdominal pain, and nausea (1, 2). In addition, boron is an essential element for plants and its deficiency affects crop productivity and plant growth. The boron content of irrigation waters is very important because it can cause serious damage to some plants when the boron concentration exceeds 1.0 mg L^{-1} . According to the World Health Organization (WHO) guidelines for Drinking Water Quality, the amount of boron contained in safe drinking water should not exceed 2.4 mg L^{-1} (3, 4).

The development of methods for the determining of low levels of boron used in various fields is an important issue. For this purpose, numerous methods have been reported such as spectrophotometry (5-8), spectrofluorimetry (9,10), flame atomic emission spectrophotometry (FAES) (11), voltammetry (12, 13), potentiometry (14), ion chromatography (IC) (15) and direct current plasma optical emission spectrometry (DCP-OES) (16). Some of these methods have been described in concentrated sulfuric acid and others have included the solvent extraction procedure. The necessity of carrying out experiments in the concentrated sulfuric acid medium is an important problem. In addition, some of these methods require a long period of time to complete the reaction, or preheating. There is also the interferences of foreign ions among the handicaps of these methods. Another problem is that these methods involve sophisticated instrumentation and complex data collection and processing procedures that require trained personnel. Therefore they are expensive methods and their application areas are limited.

In our study, GOEM-based polymeric fluorescent sensor has been prepared and applied for the detection of trace amounts of boron in environmental water samples. The performance parameters such as response time, pH effect, reproducibility, working linear range, LOD and LOQ were also investigated. The determination of the boron concentration in the real water samples was successfully conducted using the developed sensor.

MATERIALS AND METHODS

Reagents and instruments

Glycosyloxyethyl methacrylate (GOEM), 1,6-hexanediol diacrylate (HDDA), 2-hydroxyethylmethacrylate (HEMA) and a photo initiator, namely 2,2'-dimethoxy-2-phenylacetophenone (DMPA) and all other chemicals were supplied from Sigma and used without pretreatment. All experiments performed at room temperature 25 °C with a totally purified water source produced by using a Milli Q-water purification system (Millipore, Labor Teknik-Turkey). The specific resistivity of obtained pure water was recorded as 18.2 MΩcm. A digital pH meter (WTW pH7110) which was continuously calibrated with standard Merck buffer solutions was used to measure pH values of standard solutions. The functional groups in the prepared polymeric membrane were determined by Perkin-Elmer Spectrum 100 attenuated total reflectance-fourier transform infrared spectrophotometer (ATR-FTIR) at 4000-400 cm^{-1} . In addition, a Philips XL30 ESEM-FEG / EDAX scanning electron microscope (SEM) was used to investigate the surface morphology of the membrane. Fluorescence measurements were conducted by using a Varian Cary Eclipse spectrofluorometer fitted with a Xenon light source. The slit widths of both excitation and emission bands were set at 5 nm. Perkin Elmer Optima 8300 inductively coupled plasma optical emission spectrometry (ICP-OES) was used to compare the boron concentrations of the real samples with those acquired with the prepared sensor.

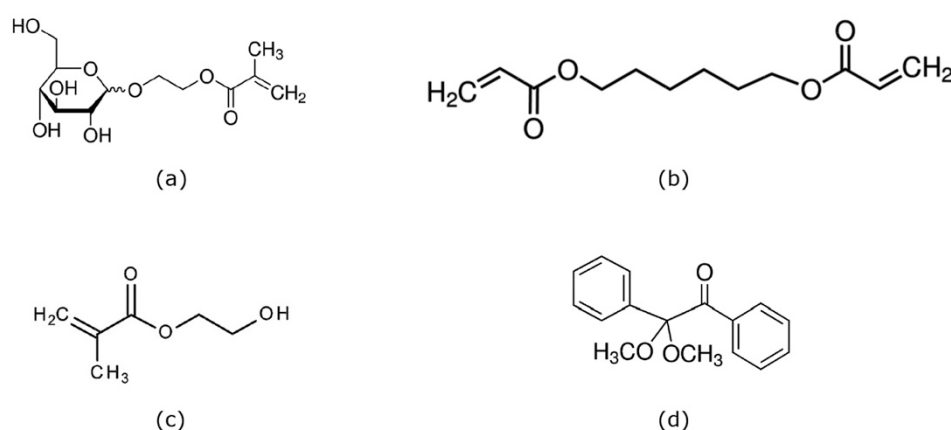


Figure 1: Representation of monomers and cross-linker structures of polymeric membrane. a) GOEM, b) HDDA, c) HEMA, d) DMPA.

Preparation method of fluorescent sensor

The polymeric sensor was prepared by the free radical polymerization of GOEM, HEMA, and HDDA where the latter was used as a crosslinker. Membrane films obtained after the

preparation process can exhibit a number of undesirable conditions such as not uniformly drying, twisting, very rapid swelling in aqueous media or late interaction with aqueous solution as it is excessively hydrophilic, dispersion in water or at different pH. In such cases, reactive monomer, cross-linking monomers and photoinitiator ratios, and curing time under UV light are changed to produce polymeric membranes at desired properties. The optimum monomer and photoinitiator quantities were decided by considering these criteria. A liquid mixture consisting of 63% HDDA, 32% HEMA, 5% GOEM and 3% of total formulation DMPA was stirred well and then poured into specially designed mold (W(cm) x L(cm) x D(cm) =1.2x4.0x2.0). Finally, the formulations were irradiated for 200 s under high-pressure UV lamp (OSRAM 300 W, $\lambda_{\max} = 365$ nm). Then, the membranes were soaked into plenty of deionized water for 12 hours to remove any unreacted residues. At the final step, the membranes were let dry in a vacuum oven at 30 °C to reach a constant weight.

RESULTS AND DISCUSSION

As it can be seen from the FTIR spectrum (Figure 2), the peak at 3440 cm^{-1} indicates the hydroxyl group of HEMA and GOEM, the strong peak at 1720 cm^{-1} shows the C=O stretching vibration of HEMA. Asymmetric $-\text{CH}_2-$ stretching was observed at 2936 cm^{-1} . The symmetric C-H vibration was found at 2865 cm^{-1} and the asymmetric C-O-C stretching was at 1157 cm^{-1} . The peaks at 1407 cm^{-1} and 1071 cm^{-1} were represented CHOO- and C-O vibrations, respectively (12).

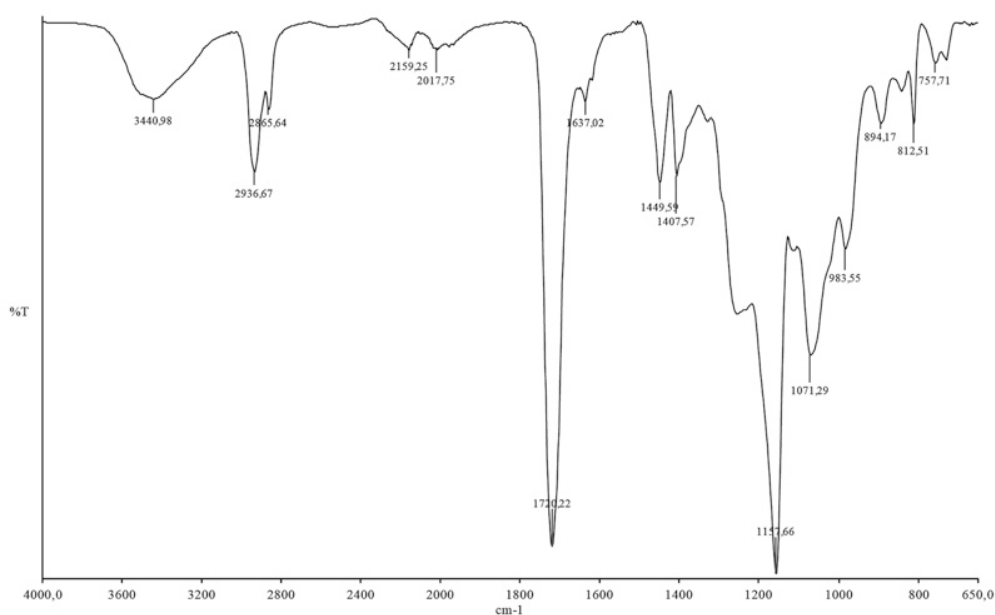


Figure 2: FTIR spectrum of boron-sensing polymeric membrane.

The surface area should be homogeneous and non-porous in order that a polymeric film can be useful as a fluorescent sensor. The Figure 3 shows the SEM image results of the boron sensing membrane. The surface of the membrane was scanned at 2500x and 10000x magnification factors for its morphological features. As seen from the SEM images, the membrane surface stands crack-free and expectedly displays a satisfactory homogenous and non-porous surface.

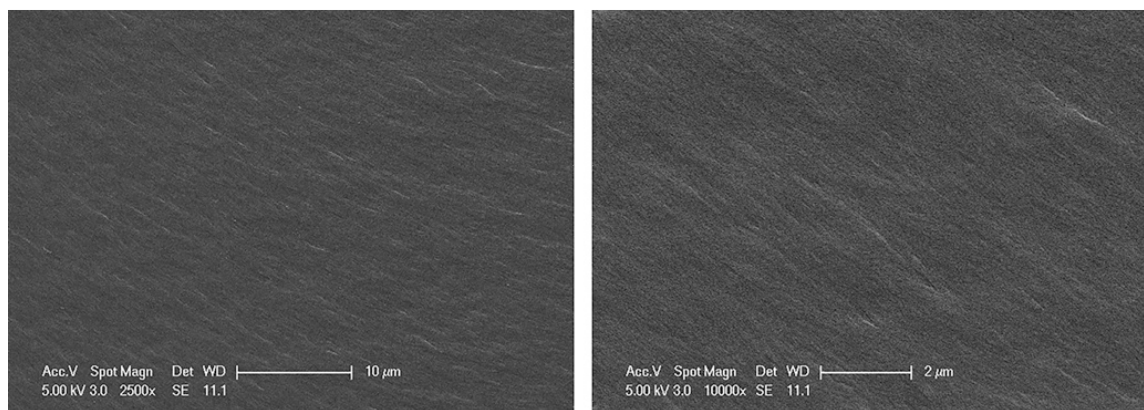


Figure 3: SEM images of polymeric membrane at different magnification levels (left: 2500x, right: 10000x).

Spectral characterization results

The changes in the fluorescence intensity in the presence and absence of boron were measured by wavelength scanning. The excitation and emission wavelength maxima were recorded 378 nm and 423 nm, respectively (Figure 4).

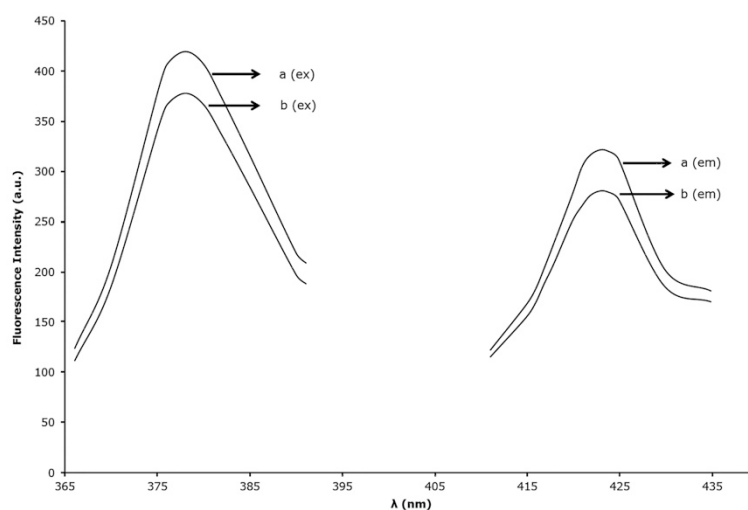


Figure 4: The excitation and emission spectra including changes in the fluorescence intensity of the membrane in the absence (a) and presence (b) of $2.31 \times 10^{-6} \text{ mol L}^{-1}$ boron ($\lambda_{\text{ex}} = 378 \text{ nm}$, $\lambda_{\text{em}} = 423 \text{ nm}$).

The study of optimal pH value

The measurements of fluorescence intensity of the developed sensor were made between the pH range of 1.0–8.0 and within the presence of 2.31×10^{-6} mol L⁻¹ boron solution. Buffer solutions were used to adjust the pH value of the medium. In solutions with a pH greater than 8, studies were not conducted because the membrane swelled rapidly and degraded. The membrane was designed to contain GOEM reactive monomer so that it could form a chelate with the boron. Hydroxyl groups and carbonyl groups in the polymeric structure are expected to chelate to boron. Boron complexes are stable in neutral and slightly basic solutions. In this work, as the hydroxyl groups in the polymeric structure are in the *trans* configuration, the formation of the neutral boron ester seems to be favorable, which can also be seen in the literature. Furthermore, tetra-coordinated anionic chelate formation might also be possible by incorporation by hydroxyl and carbonyl groups in the polymeric structure at pH: 6. In addition, it is considered that the fluorescence intensity decreases due to the borate complex in anionic form, which is present at a pH greater than pH 6. The results were shown in Figure 5. It can be seen that the fluorescence intensity notably increased in the range of pH 1.0 to 6.0 by giving the maximum intensity peak at pH 6.0. When the pH is higher than 6.0, it started to decrease. Therefore, pH 6.0 was selected as the optimum pH and this value was used in further experiments.

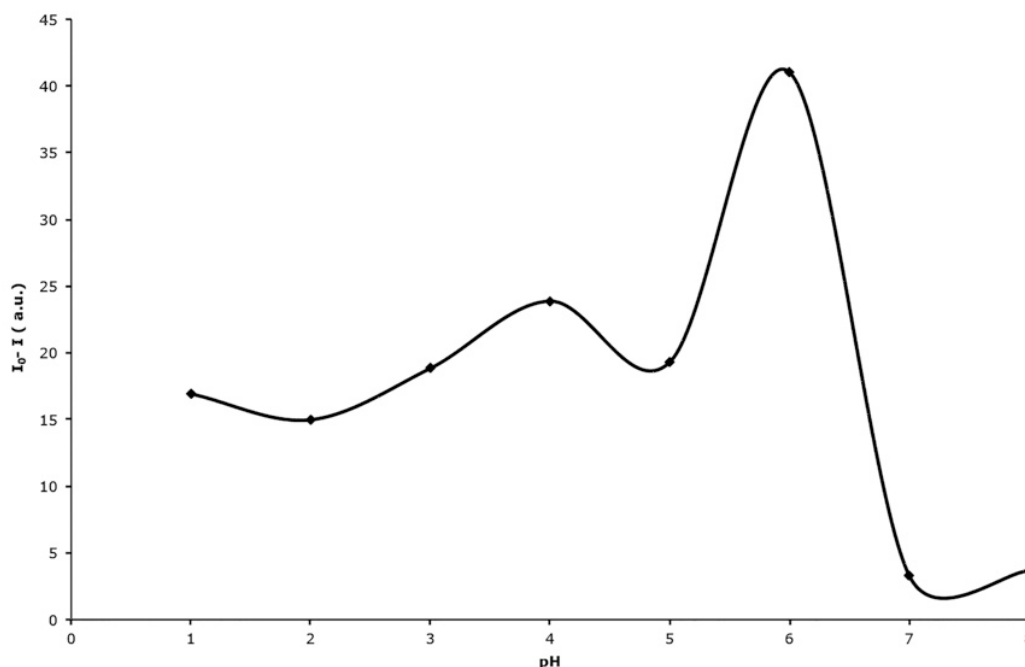


Figure 5: Changes in fluorescence intensity with increasing pH values (I_0 and I show fluorescence intensities before and after 2.31×10^{-6} mol L⁻¹ boron addition, respectively).

Effect of response time on the fluorescence intensity

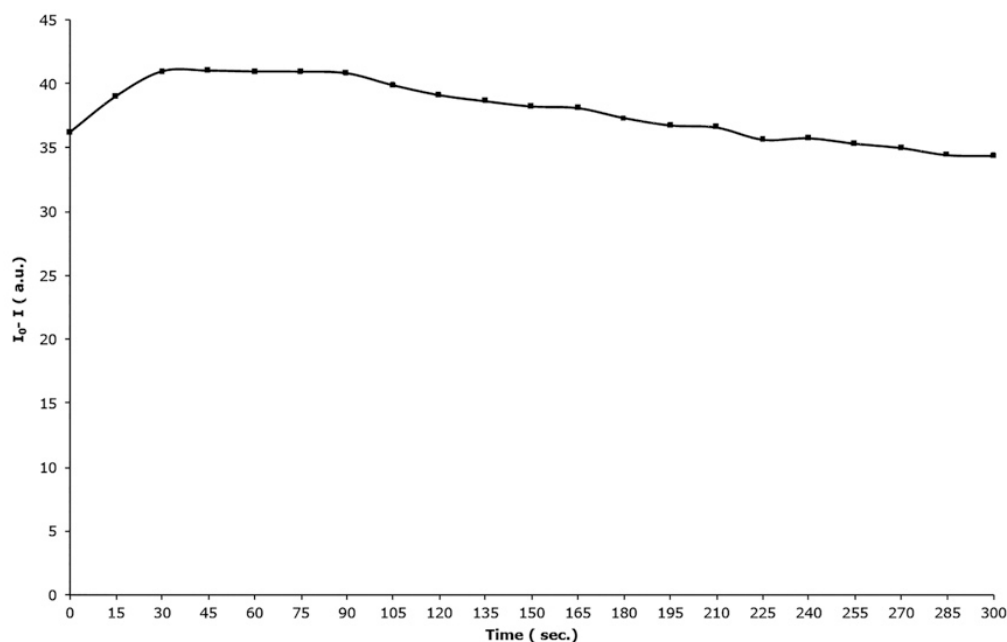


Figure 6: Changes of fluorescence intensity of the sensor as a function of time ($C = 2.31 \times 10^{-6} \text{ mol L}^{-1}$ boron; $(I_0 - I)$ is found by subtracting the fluorescence intensities measured in the absence of boron (I) from those obtained in the presence of boron (I_0)).

Figure 6 indicates the time-dependent changes in the fluorescence intensity of the membrane at pH 6.0. The measurements were carried out for 300 seconds at a time interval of 15 seconds in the presence of $2.31 \times 10^{-6} \text{ mol L}^{-1}$ boron. As a result, it was observed that the fluorescence intensity of the membrane increased for 30 seconds, remained constant for 60 seconds and then tended to decrease. For this reason, the optimal response time was chosen to be 45 seconds and this value was used in all other experiments.

Measurement range, LOD and LOQ

The calibration graph is plotted as a function of the logarithm of the boron concentration versus the fluorescence intensities under optimum conditions (Figure 7). The fluorescence intensities of boron solutions at different concentrations were measured and the linear relationship between concentration and fluorescence intensity was found between $9.25 \times 10^{-7} \text{ mol L}^{-1}$ and $9.25 \times 10^{-6} \text{ mol L}^{-1}$. Fluorescence intensities in the absence and presence of boron are indicated by the symbols I_0 and I , respectively. LOD and LOQ were calculated as $2.90 \times 10^{-8} \text{ mol L}^{-1}$ and $9.66 \times 10^{-8} \text{ mol L}^{-1}$ respectively ($n=7$).

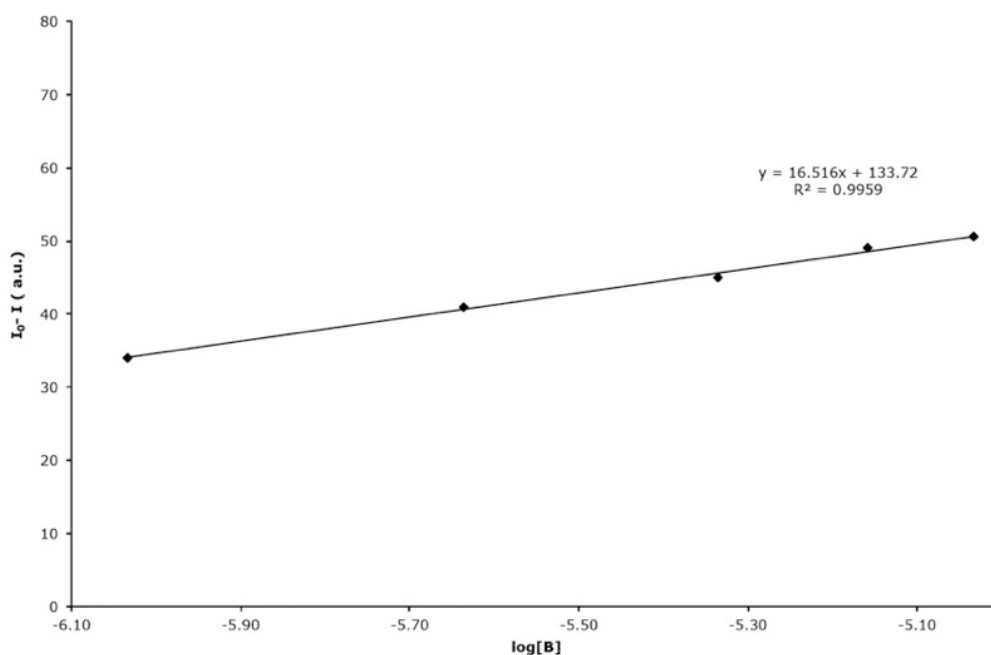


Figure 7: Calibration curve obtained under optimal experimental conditions.

Reproducibility, reversibility, and stability of the sensor

In the regeneration process, it was observed that the sensor in contact with 2.31×10^{-6} mol L⁻¹ of boron solution was able to give initial fluorescence intensities after a wash of only about 40 seconds with distilled water. Thus, the prepared sensor was found to be fully reversible. Reuse of the reagent is not possible, because some of the methods given in the literature are based on the formation of a colored product by complex formation. In addition, disposable electrodes are also used in some of these methods, so it is not possible to reuse the same electrode. However, it was also found that the same sensor can be used 565 times by using the regeneration method proposed in this work. Moreover, the same sensor remained stable for 720 days without any change in structure and its fluorescence intensity.

Analyses of boron in natural water samples

The boron contents in drinking water, natural ground water, and standard irrigation were determined by the proposed method. All samples were used directly without any pretreatment. The comparison of the boron concentrations of the samples obtained by ICP-OES and developed method is given in Table 1. The results of developed method and ICP-OES were checked by t-test for accuracy of the presented method. For comparison the t-test (at 95% confidence level) was used but no significant difference between both developed method and ICP-OES was found. According to the results, the proposed sensor could be used safely in determining the boron content in the environmental water samples.

Table 1: Results of analysis of boron concentrations in real water samples by the developed method and ICP-OES (95% confidence levels, n=6).

Samples	*This work (mol L ⁻¹)	*ICP-OES (mol L ⁻¹)	RSD (%)	Recovery (%)
Drinking water	(3.38±0.04) ×10 ⁻⁶	(3.35±0.02) ×10 ⁻⁶	1.16	100.24
Irrigation water	(1.91±0.06) ×10 ⁻⁶	(1.89±0.04) ×10 ⁻⁶	1.13	101.12
Ground water	(2.02±0.03) ×10 ⁻⁶	(2.00±0.02) ×10 ⁻⁶	1.17	101.18

*: The obtained values were expressed as $\bar{x} \pm \frac{t.s}{\sqrt{N}}$

The influence of some common coexisting ions

The boron solution at a concentration of 2.31×10⁻⁶ mol L⁻¹ was used to demonstrate the selectivity of the sensor to boron. The foreign ion solutions in different concentrations were added to this solution to monitor how much the fluorescence intensity changed. Table 2 contains the tolerable limit concentrations of the foreign ions. As it can be seen from the table, it is obvious that the developed sensor is highly selective. The potential foreign ions including the strongly interfering ions such as Fe³⁺, Zn²⁺ and Cu²⁺ had no significant effect on the fluorescence intensity of the sensor.

Table 2: Tolerance limit concentration of foreign ions (C=2.31×10⁻⁶ mol L⁻¹).

Foreign ions	Tolerance levels (mol L ⁻¹) *
Pb ²⁺	3.62 10 ⁻⁴
Ni ²⁺	8.52 10 ⁻⁴
Ag ⁺	4.63 10 ⁻⁴
Fe ³⁺	1.79 10 ⁻³
Cr ³⁺	2.40 10 ⁻³
Mn ²⁺	9.09 10 ⁻⁴
Cu ²⁺	1.57 10 ⁻³
Co ²⁺	8.49 10 ⁻⁴
Ca ²⁺	2.50 10 ⁻³
Mg ²⁺	5.21 10 ⁻³
Cd ²⁺	4.45 10 ⁻⁴
Sb ³⁺	3.08 10 ⁻⁴
Hg ²⁺	1.25 10 ⁻⁴
Zn ²⁺	1.34 10 ⁻³
Al ³⁺	2.78 10 ⁻³
Na ⁺	2.17 10 ⁻³

* Less than ±5% relative error.

Comparison of some analytical methods with the proposed sensor method

The comparison of the developed method with several methods and some important parameters are summarized in Table 3. Some of these methods are either performed using a concentrated acid solution or involve an extraction process or require a long analysis time. They are also influenced by the interference of many foreign ions. The developed method is carried out with pH 6 acetate buffer instead of a corrosive medium such as sulfuric acid. Moreover, it did not involve any extraction step and did not cause loss of the analyte.

It is obvious from Table 3, the new polymeric sensor, when compared to the previous techniques, has the lowest detection limit, 2.87×10^{-8} mol L⁻¹. In addition, the prepared sensor exhibits a high selectivity even in the presence of many foreign ions without the need to use a masking solution. Furthermore, the new polymeric sensor has a minimum response time (45 seconds) and stability up to 720 days compared to the methods in Table 3.

Table 3: Comparison with some methods for boron determination.

Reference	Reagent	Method	Linear range (mol L ⁻¹)	pH or Medium	Response time	LOD (mol L ⁻¹)
5	4-methoxy-azomethine-H	Spectrophotometry	0- 1.3x10 ⁻⁴	pH: 5.7	NM	4.90x10 ⁻⁷
6	2,2,4-Trimethyl-1,3-Pentenediol+Carminic Acid	Spectrophotometry	7.40x10 ⁻⁷ - 1.85x10 ⁻⁶	Chloroform	3 hour	2.76x10 ⁻⁷
7	Victoria Blue 4R	Spectrophotometry	2.78x10 ⁻⁶ -5.09x10 ⁻⁵	pH: 2-5	30 min.	1.85x10 ⁻⁶
8	Curcumine- oxalic acid	Spectrophotometry	0-3.7x10 ⁻⁵	HCl/ ethanol	1 hour	7.40x10 ⁻⁷
8	Carminic acid	Spectrophotometry	6.17x10 ⁻⁶ - 6.17x10 ⁻⁵	H ₂ SO ₄	1 hour	6.17x10 ⁻⁶
9	Dibenzoylmethane	Spectrofluorimetry	5x10 ⁻⁸ - 6x10 ⁻⁷	Ether-Conc. H ₂ SO ₄	60 min.	4.62x10 ⁻⁸
10	Alizarin Red-S	Spectrofluorimetry	2.31x10 ⁻⁶ - 9.25x10 ⁻⁵	pH 7.4	NM	6.66x10 ⁻⁷
11	Methanol	FAES	9.25x10 ⁻⁴ - 1.85x10 ⁻²	60% H ₂ SO ₄	60 sec.	2.74x10 ⁻⁴
12	Alizarin Red S	Voltammetry	0- 1.48x10 ⁻⁵	7.5	5 min.	1.48x10 ⁻⁶
13	Tiron	Voltammetry	2.59x10 ⁻⁵ - 1.11x10 ⁻³	7.5	NM	7.77x10 ⁻⁶
14	NaF	Potentiometry	9.25x10 ⁻⁵ -4.63x10 ⁻²	pH:1	20 min.	NM
15	%10 HF	IC	4.63x10 ⁻⁶ -4.63x10 ⁻²	1 M NaOH	10 min.	4.63x10 ⁻⁶
16	NM	DCP-OES	0-4.62x10 ⁻⁵	MIBK/ glacial CH ₃ COOH	NM	1.94x10 ⁻⁶
This work	GOEM	Spectrofluorimetry	9.25x 10 ⁻⁷ - 9.25x10 ⁻⁶	pH:6	45 sec.	2.87x10 ⁻⁸

NM: Not mentioned

CONCLUSION

In this study, a rapid and selective fluorescence polymeric sensor was developed for boron determination in environmental water samples. The developed sensor does not include the disadvantages of conventional methods such as extraction process, prolonged color development, and use of concentrated acids. The boron concentration was measured spectrofluorimetrically with the prepared sensor. It is also a great advantage that the fluorescence sensor can be regenerated in a short time using distilled water. Moreover, the same sensor could be used 565 times for boron determination. The values of LOD and LOQ were 2.9×10^{-8} mol L⁻¹ and 9.66×10^{-8} mol L⁻¹, respectively. Another advantage is that the sensor allows the determination of boron even in the presence of many foreign ions. It was found that the results were satisfactory when the boron concentration in the environmental water samples was analyzed by the developed sensor and ICP-OES method.

REFERENCES

1. Garrett DE. Borates: handbook of deposits, processing, properties, and use. San Diego: Academic Press; 1998. 483 p.
2. Stellman JM, International Labour Organisation, editors. Encyclopaedia of occupational health and safety. 4th ed. Geneva: International Labour Office; 1998. 2 p.
3. Edition F. Guidelines for drinking-water quality. WHO chronicle. 2011;38:104–108.
4. Organization WH, others. Boron (Environmental health criteria monograph 204). World Health Organization, IPCS, Geneva, Switzerland. 1998;
5. Zaijun L, Zhu Z, Jan T, Hsu C-G, Jiaomai P. 4-Methoxy-azomethine-H as a reagent for the spectrophotometric determination of boron in plants and soils. *Analytica Chimica Acta*. 1999 Dec;402(1-2):253–7.
6. Aznarez J, Ferrer A, Rabadan J, Marco L. Extractive spectrophotometric and fluorimetric determination of boron with 2, 2, 4-trimethyl-1, 3-pentanedial and carminic acid. *Talanta*. 1985;32(12):1156–1158.
7. Balogh IS, Andruch V, Kádár M, Billes F, Posta J, Szabová E. A simple method of boron determination in mineral waters using Victoria blue 4R. *International Journal of Environmental Analytical Chemistry*. 2009 May 15;89(6):449–59.

8. Rice EW, American Public Health Association, editors. Standard methods for the examination of water and wastewater. 22. ed. Washington, DC: American Public Health Association; 2012. 1120 p.
9. Marcantonatos M, Gamba G, Monnier D. Contribution à l'étude du dosage de traces d'acide borique par luminescence. *Helvetica Chimica Acta*. 1969;52(2):538-43.
10. Campaña AMG, Barrero FA, Ceba MR. Spectrofluorimetric determination of boron in soils, plants and natural waters with Alizarin Red S. *The Analyst*. 1992;117(7):1189-91.
11. SARICA DY, ERTAŞ N. Flow injection analysis for boron determination by using methyl borate generation and flame atomic emission spectrometry. *Turkish Journal of Chemistry*. 2001;25(3):305-310.
12. Çetinkaya E, Dönmez KB, Deveci S, Doğu M, Şahin Y. Determination of plant available boron in agricultural soil by using voltammetric method. *EURASIAN JOURNAL OF SOIL SCIENCE (EJSS)*. 2014 Sep 1;3(3):182.
13. Liv L, NAKİBOĞLU N. Simple and rapid voltammetric determination of boron in water and steel samples using a pencil graphite electrode. *Turkish Journal of Chemistry*. 2016;40(3):412-421.
14. Ohyama S, Abe K, Ohsumi H, Kobayashi H, Miyazaki N, Miyadera K, et al. Fully Automated Measuring Equipment for Aqueous Boron and Its Application to Online Monitoring of Industrial Process Effluents. *Environmental Science & Technology*. 2009 Jun;43(11):4119-23.
15. Hill CJ, Lash RP. Ion chromatographic determination of boron as tetrafluoroborate. *Analytical Chemistry*. 1980 Oct;52(1):24-7.
16. Brennan MC, Svehla G. Flow injection determination of boron, copper, molybdenum, tungsten and zinc in organic matrices with direct current plasma optical emission spectrometry. *Fresenius' Zeitschrift für Analytische Chemie*. 1989;335(8):893-9.



Chemical investigation and antioxidant activity of fractions of *Lannea humilis* (Oliv.) Engl.

Achika Jonathan Ilemona, Ayo Racheal Gbekele-Oluwa, Oyewale Adebayo Ojo, and James Dama Habila

Department of Chemistry, Ahmadu Bello University, Zaria. Kaduna State, Nigeria.

Abstract: The aim of this experiment was to establish the phytochemical constitution and antioxidant activity of the fractions of *Lannea humilis*. Chemical investigation and antioxidant activity of the fractions were carried out using standard methods. Steroids and terpenes were available in the hexane, ethyl acetate, and methanol fractions, while tannins, flavonoids and alkaloids were available in the ethyl acetate and methanol extracts. Carbohydrate and saponins were available in the methanol fraction. The antioxidant activity of this plant extracts demonstrated a dose-dependent increment. The ethyl acetate extract displayed most noteworthy antioxidant activity of 98% at 240 $\mu\text{g.mL}^{-1}$, followed by the hexane extract which had a percentage antioxidant activity of 92 % at 240 $\mu\text{g.mL}^{-1}$. The methanol extract demonstrated percentage antioxidant activity of 71 % at 240 $\mu\text{g.mL}^{-1}$. This result shows that this plant can be used as a good antioxidant. These observations demonstrated that this plant has antioxidant activity and consequently can be used as an antioxidant agent.

Keywords: Antioxidant activity; 2,2-diphenyl-1-picrylhydrazyl; phenolic compounds; antioxidant activity; *Lannea humilis*.

Cite this: Ilemona AJ, Gbekele-Oluwa AR, Ojo OA, and Habila JD. Chemical investigation and antioxidant activity of fractions of *Lannea humilis* (Oliv.) Engl. JOTCSA. 2017; 4(2): 87-96.

Submitted: January 27, 2017. **Revised:** March 10, 2017. **Accepted:** March 27, 2017.

DOI: 10.18596/jotcsa.288249.

***Corresponding author.** E-mail: adajiileileile@gmail.com

INTRODUCTION

Antioxidants have various applications because of their different parts in reducing destructive impacts of oxidative stress (1). Antioxidant agents respond by free radical or molecular oxygen extinguishing, being able to either postpone or restrain oxidation which happens under the influence of molecular oxygen species. Antioxidants are in charge of the shielding mechanism of the living being against the pathologies connected with the assault of free radicals, in this manner the consumption of plant related antioxidants is responsible for the avoidance of degenerative ailments brought about by oxidative anxiety, for example, Cancer, Parkinson, Alzheimer, or Atherosclerosis [2]. Free radicals are broadly accepted to facilitate the development of a few ailments by bringing about oxidative anxiety and eventually oxidative harm which are reasons for some pathological diseases (3-6). Researchers recommend that if oxidative harm could be observed to be in charge of the continually increasing occurrence of different neurotic conditions, then quest for normal cancer prevention agents that could prevent the oxidation of free radicals would be scientifically valuable (7, 8). The phytochemicals in plants, green tea for example, have antioxidants properties used to enhance and give security against numerous ailments connected with reactive oxygen species (ROS, for instance, tumor and neurodegenerative diseases) (9, 10). It belongs to the family *Anacardiaceae*, it a deciduous bush growing up to 3 meters tall, at times turning into a tree with a level or spreading crown. A decoction of the stem bark of this plant is utilized in the treatment of sickness, hack, bodily torments intense looseness of the bowels, cholera, and asthma (11).

MATERIALS AND METHODS

Collection and identification of plant

The fresh stem bark of *L. humilis* was collected from Otukpo, Benue state, Nigeria in January 2015. The plant was identified with a voucher specimen number 3231 by Mal. S. Namadi at the Herbarium section, Department of Botany, Faculty of Life Science, Ahmadu Bello University, Samaru, Kaduna State, Nigeria.

Extraction of plant materials

The stem bark of *L. humilis* were air-dried at room temperature (27 °C) for 2 weeks, after which it was grinded to a uniform powder. The crude methanol extract was prepared by soaking 100 g of the dry powdered plant materials in 1 L of methanol at ambient temperature for 48 h. The extract was filtered after 48 hrs and was concentrated using a rotary evaporator with the water bath set at 40 °C. A portion of this extract was reconstituted in water to yield a water-soluble fraction and water-insoluble fraction. The two fractions were subsequently partitioned successively and exhaustively using hexane and ethyl acetate, which were then concentrated using a rotary evaporator.

Phytochemical screening

The extract and the fractions were qualitatively examined for phytochemicals following standard procedures (12, 13).

Determination of antioxidant activity

The radical scavenging activities of the extract against 2,2-diphenyl-1-picrylhydrazyl (DDPH) radical were determined using UV spectrophotometer at 515 nm. Radical scavenging activity was measured by a slightly modified method previously described (14). The following concentrations of the extracts were prepared, 15, 30, 60, 120, 240 µg.mL⁻¹ in methanol.

Vitamin C was used as the antioxidant standard at concentrations of 15, 30, 60, 120, 240 $\mu\text{g}\cdot\text{mL}^{-1}$. 1 mL of the extract was placed in a test tube, and 1 mL of 0.3 mM methanolic solution of DPPH added. A blank solution was prepared containing the same amount of methanol and DPPH. The radical scavenging activity was calculated using the following formula:

$$\% \text{radical scavenging activity} = \frac{\text{Absorbance of control} - \text{Absorbance of sample}}{\text{Absorbance of control}} \times 100$$

RESULTS AND DISCUSSION

Table 1: Phytochemical Screening of the Extracts of the Stem Bark of *L. humilis*

Metabolites	LHH	LHE	EHM
Terpenes	+	+	+
Sterols	+	+	+
Carbohydrates	-	-	+
Glycosides	-	-	+
Tannins	-	+	+
Flavonoids	-	+	+
Anthraquinones	-	-	+
Alkaloids	-	+	+

Key: + =present, - = absent, LHH: hexane fraction, LHE: ethyl acetate fraction, LHM: methanol fraction.

The result of the phytochemical screening of the fractions of the stem bark of *L. humilis* is reported in Table 1. The phytochemical examination of the hexane, ethyl acetate and methanol extracts of the stem bark extract of *L. humilis* has uncovered the availability of some bioactive principles. Steroids and terpenes were available in the hexane, ethyl acetate, and methanol fractions, while tannins, flavonoids, and alkaloids were available in the ethyl acetate and methanol fractions. Carbohydrate and saponins were available in the methanol fraction. Anthraquinones were absent in all the fractions. The availability of these metabolites

has proven earlier report that various plants in same family with *L. humilis* likewise have a large portion of the phytochemicals as observed in this plant (11). The presence of flavonoids, carbohydrate and cardiac glycosides in the ethyl acetate and methanol extract is not unexpected as the majority of these constituents are basically polar in nature. Flavonoids which are normal cancer prevention agent are acquired chiefly from plants, and are utilized for the treatment of degenerative infections (15). The inconceivable number of these chemical constituents in the stem bark of *L. humilis*, some of which are be bioactive legitimizes the ethnomedicinal uses of this plant in the treatment of diseases.

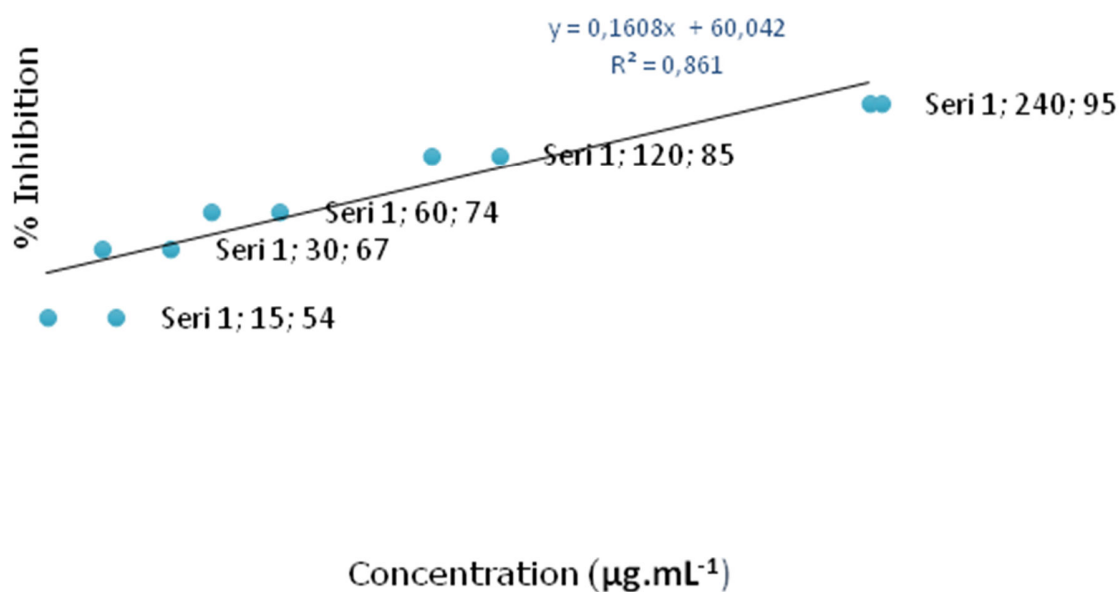


Figure 1: DDPH Scavenging Activity of the Hexane Extract of *Lannea humilis*.

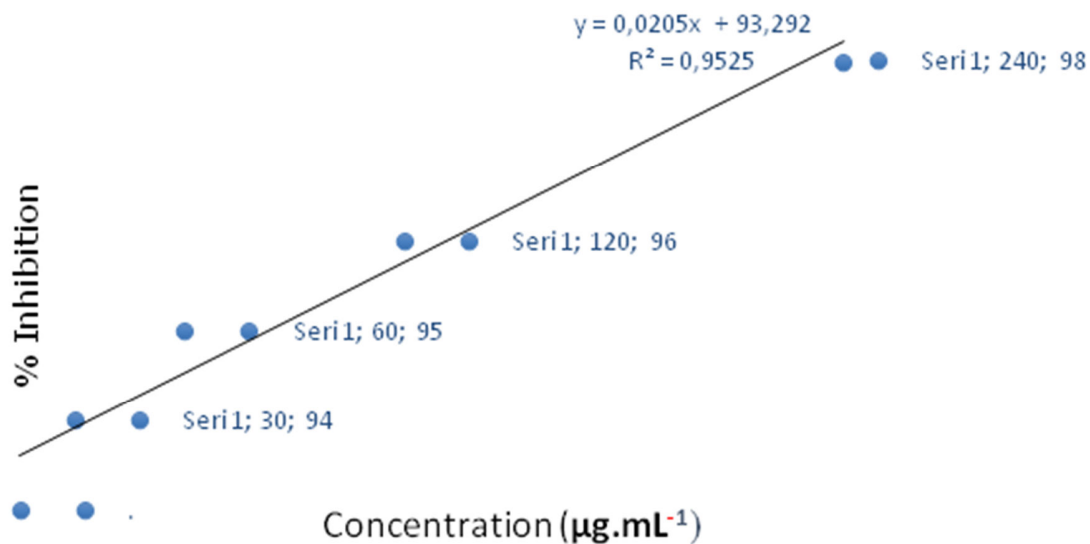


Figure 2: DDPH Scavenging Activity of the Ethyl acetate Extract of *Lannea humilis*.

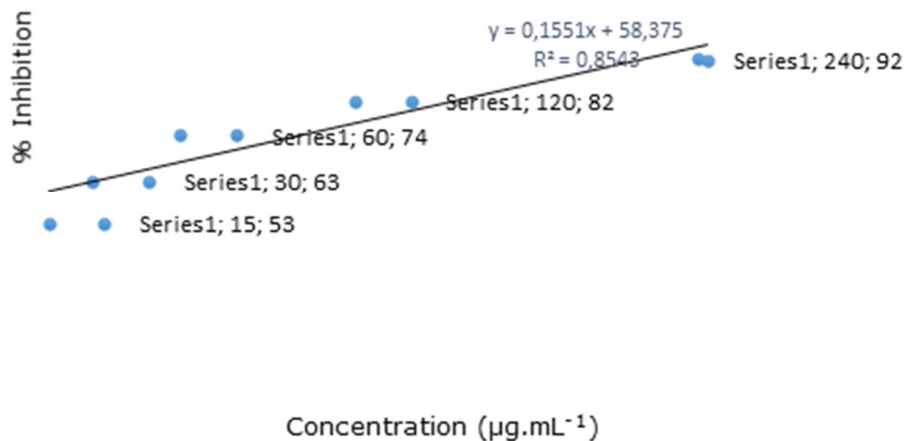


Figure 3: DDPH Scavenging Activity of the Methanol Extract of *Lannea humilis*.

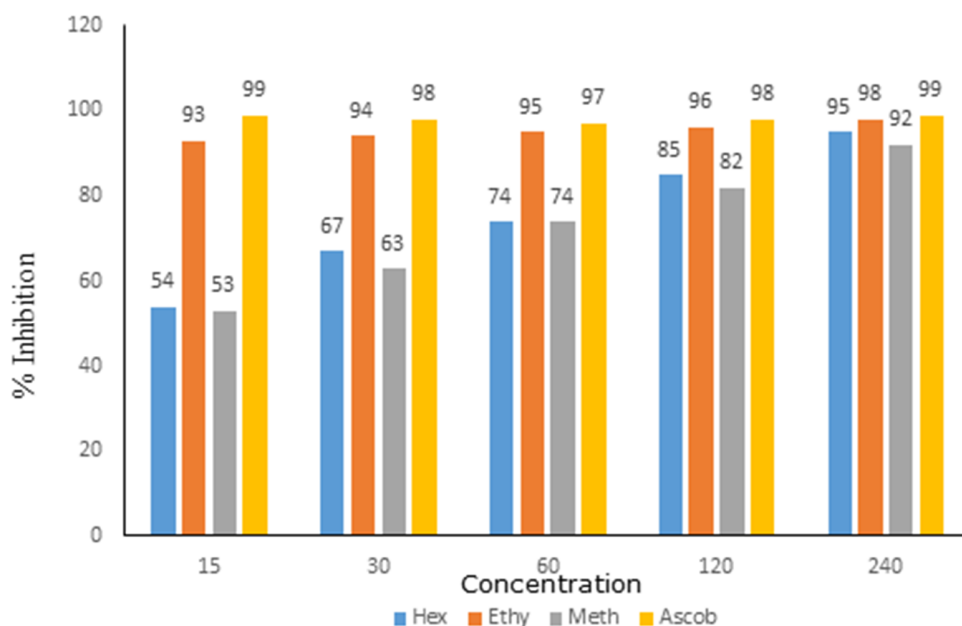


Figure 4: Inhibition of DPPH by the Hexane, Ethyl acetate and Methanol Extracts of *Lannea humilis* in Comparison with Ascorbic acid ($\mu\text{g.mL}^{-1}$).

The antioxidant capacity of the hexane, ethyl acetate and methanol fraction of *L. humilis* to repress and extinguish free radicals and responsive oxygen species was analyzed in this study. DPPH radical has been utilized widely as a free radical to test the reductive capacity of fractions or chemicals as free radical scavengers or hydrogen contributors and to assess the antioxidant activity of plant fractions (16, 17). Antioxidants respond to DPPH• by giving electron or hydrogen particle, in this way reducing it to 1,1-diphenyl-2-hydrazine (DPPH-H) or a substitute practically equivalent to hydrazine. The profound violet shade of DPPH at most extreme absorption of 515 nm is changed to light yellow, colorless or bleached product, resulting in decrease in absorption (18, 19). The hexane extract of *L. humilis* displayed noteworthy antioxidant activity of 95% at 240 $\mu\text{g.mL}^{-1}$ (Figure. 1) and compared well with the standard ascorbic acid. In like manner, the test technique for DPPH scavenging action connects amazingly with the adjustments in the different concentration of the hexane utilized, with relationship coefficients (r^2) of 0.861. This infers that the DPPH scavenging activity of

the extracts of this plant is concentration dependent as highest percentage inhibitions were observed at a corresponding highest concentration for all the extracts. The percentage inhibition created by the ethyl acetate extract was 98 % at a concentration of 240 $\mu\text{g}\cdot\text{mL}^{-1}$, while that of the methanol fraction of *L. humilis* was 92 % at the same concentration as shown in Figure 2 and 3. The three fractions of this plant showed comparable antioxidant activity with the positive standard antioxidant agent, ascorbic acid (Figure 4). These results show that the fractions of this plant can scavenge free radicals. The scavenging activity of the plant fractions on DPPH has been shown to be related to the phenolic concentration of the fractions (20, 21, 22), which is accepted to add to their electron exchange/hydrogen giving capacity. It could hence be inferred that flavonoids contents of the fractions of this plant as revealed in the phytochemical screening results is responsible for stabilizing radicals or scavenge their activities.

In conclusion, this result suggests that the phenolic compounds might be major contributors to the antioxidative activities of the stem bark *L. humilis*. Further efforts are underway to isolate and identify the active phenolic compounds from the plant.

REFERENCES

1. Omar UM, Shorbaji AM, Arrait EM, Al Agha TD, Al-Marzouki HF, Al Doghaither HA, et al. Comparative Study of the Antioxidant Activity of Two Popular Green Tea Beverages Available in the Local Market of Saudi Arabia. *Natural Science*. 2016;8(06):227.
2. Pisoschi AM, Negulescu GP. Methods for total antioxidant activity determination: a review. *Biochemistry and Analytical Biochemistry*. 2011;1(1):1-10.
3. El-Bahr SM. Biochemistry of free radicals and oxidative stress. *Science international*. 2013;1(5):111-117.
4. Gan L, Johnson JA. Oxidative damage and the Nrf2-ARE pathway in neurodegenerative diseases. *Biochimica et Biophysica Acta (BBA)-Molecular Basis of Disease*. 2014;1842(8):1208-1218.
5. Somanah J, Bourdon E, Rondeau P, Bahorun T, Aruoma OI. Relationship between fermented papaya preparation supplementation, erythrocyte integrity and antioxidant status in pre-diabetics. *Food and Chemical Toxicology*. 2014;65:12-17.

6. Wong BX, Duce JA. The iron regulatory capability of the major protein participants in prevalent neurodegenerative disorders. *The Importance Of Iron In Pathophysiologic Conditions*. 2015;368.
7. Halliwell B. Role of free radicals in the neurodegenerative diseases. *Drugs & aging*. 2001;18(9):685–716.
8. Liu Q, Raina AK, Smith MA, Sayre LM, Perry G. Hydroxynonenal, toxic carbonyls, and Alzheimer disease. *Molecular aspects of medicine*. 2003;24(4):305–313.
9. Tran J, others. Green tea: a potential alternative anti-infectious agent catechins and viral infections. *Advances in Anthropology*. 2013;3(04):198.
10. Lobo V, Patil A, Phatak A, Chandra N, others. Free radicals, antioxidants and functional foods: Impact on human health. *Pharmacognosy reviews*. 2010;4(8):118.
11. Burkill H. *The useful plants of West Africa (tropical)*. Royal Botanic Gardens, Kew. 1985;319.
12. Sofowora A. *Medicinal plants and traditional medicine in Africa*. 1982;
13. Trease GE, Evans WC. *Pharmacognosy*. 1989. Bailliere Tindall, London. :45–50.
14. Mensor LL, Menezes FS, Leitão GG, Reis AS, Santos TC dos, Coube CS, et al. Screening of Brazilian plant extracts for antioxidant activity by the use of DPPH free radical method. *Phytotherapy research*. 2001;15(2):127–130.
15. Ali SS, Kasoju N, Luthra A, Singh A, Sharanabasava H, Sahu A, et al. Indian medicinal herbs as sources of antioxidants. *Food Research International*. 2008;41(1):1–15.
16. Da Porto C, Calligaris S, Celotti E, Nicoli MC. Antiradical properties of commercial cognacs assessed by the DPPH• test. *Journal of Agricultural and Food Chemistry*. 2000;48(9):4241–4245.
17. Manian R, Anusuya N, Siddhuraju P, Manian S. The antioxidant activity and free radical scavenging potential of two different solvent extracts of *Camellia sinensis* (L.) O. Kuntz, *Ficus bengalensis* L. and *Ficus racemosa* L. *Food Chemistry*. 2008;107(3):1000–1007.
18. Miliauskas G, Venskutonis P, Van Beek T. Screening of radical scavenging activity of some medicinal and aromatic plant extracts. *Food chemistry*. 2004;85(2):231–237.
19. Köksal E, Gülçin İ, Beyza S, Sarikaya Ö, Bursal E. In vitro antioxidant activity of silymarin. *Journal of enzyme inhibition and medicinal chemistry*. 2009;24(2):395–405.
20. Akinmoladun AC, Obuotor EM, Farombi EO. Evaluation of antioxidant and free radical scavenging capacities of some Nigerian indigenous medicinal plants. *Journal of Medicinal Food*. 2010;13(2):444–451.
21. Sen S, De B, Devanna N, Chakraborty R. Total phenolic, total flavonoid content, and antioxidant capacity of the leaves of *Meyna spinosa* Roxb., an Indian medicinal plant. *Chinese journal of natural medicines*. 2013;11(2):149–157.
22. Das N, Islam ME, Jahan N, Islam MS, Khan A, Islam MR, et al. Antioxidant activities of ethanol extracts and fractions of *Crescentia cujete* leaves and stem bark and the involvement of phenolic compounds. *BMC complementary and alternative medicine*. 2014;14(1):45.



Theoretical Investigation of Corrosion Inhibition of Iron Metal by Some Benzothiazole Derivatives: A Monte Carlo Study

Savaş KAYA¹, Nail ALTUNAY^{1,*}

¹Cumhuriyet University, Faculty of Science, Department of Chemistry, 58140, Sivas/TURKEY

Abstract: It is important to note that atomistic modeling and simulations are becoming increasingly popular in the field of corrosion inhibition of metal surfaces. In this work, we investigated the adsorption properties and corrosion inhibition efficiencies of some benzothiazole derivatives (ABT, TCHBT, TSCBT) against the corrosion of iron metal using molecular dynamics simulation approach. It is important to note that adsorption and binding energies calculated considering adsorption processes on Fe metal surface of aforementioned inhibitory molecules are in good agreement with experimental data reported earlier.

Keywords: Molecular Modeling; Monte Carlo; Benzothiazole; Metal Protection; Corrosion Inhibitors.

Cite this: Kaya S, Altunay N. Theoretical investigation of corrosion inhibition of iron metal by some benzothiazole derivatives: A Monte Carlo study. JOTCSA. 2017; 4(2): 97-102.

Submitted: January 26, 2017. **Revised:** April 17, 2017. **Accepted:** April 18, 2017.

DOI: 10.18596/jotcsa.288244.

***Corresponding author.** E-mail: naltunay@cumhuriyet.edu.tr

INTRODUCTION

Corrosion can be defined as an undesirable process that causes destruction of the metal surfaces (1). Nowadays, corrosion inhibition study is a very active field of research. It is important to note that iron and copper metals are widely used in industry and the corrosion of such metals is one of the reasons of great economic losses worldwide (2). One of the most common approaches considered to protect the metal surfaces from corrosion is to use corrosion inhibitor. A corrosion inhibitor is a chemical compound which, when added in small concentrations to an environment, minimizes or prevents corrosion (3).

Many researchers noted that most effective corrosion inhibitors are n -systems and heterocyclic compounds (4, 5). For that reason, organic inhibitors containing heteroatoms like nitrogen, oxygen, sulfur, and aromatic ring in their molecular structure are very effective in terms of the prevention of the corrosion of metal surfaces. Experimental corrosion analysis techniques are widely considered to elucidate the corrosion inhibition mechanisms and to analyze the corrosion inhibition efficiencies of new synthesized compounds, but they are generally expensive and time-consuming. Recently, to predict the corrosion inhibition efficiencies of molecules, quantum chemical and molecular dynamics simulation approaches are preferred by theoretical chemists because of their speed and usability (6).

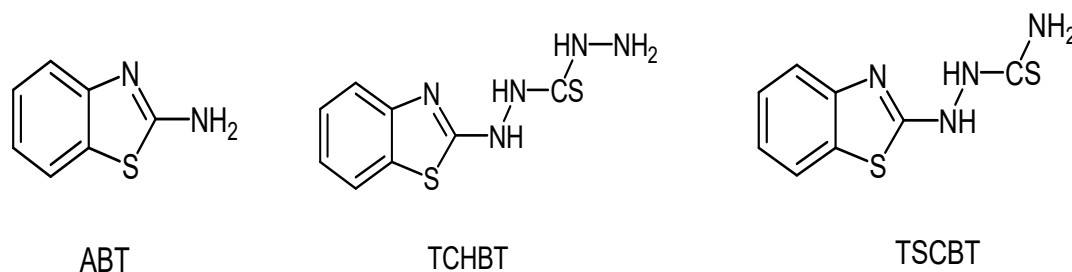


Figure 1: Molecular structures of studied benzothiazole derivatives.

In Figure 1, the molecular structures of considered molecules in this study are given. In the current literature, many benzothiazole derivatives reported as photostabilizers, metal complexing agents and non-toxic compounds. In 2012, Parameswari (7) and coworkers synthesized some benzothiazole derivatives, namely (benzothiazole-2-amine (ABT), benzothiazole-2-yl-thiocarbohydrazide (TCHBT) and benzothiazole-2-yl-thiosemicarbazide (TSCBT) and investigated their anticorrosive performances for mild steel in acidic medium by weight loss, potentiodynamic polarization and AC-impedance techniques. As a result of these studies, the authors obtained the experimental inhibition efficiency order for mentioned molecules as: TCHBT > TSCBT > ABT.

The objective of this work is to study the influence of the molecular structure on the inhibition of iron corrosion with the help of molecular dynamics simulations approach and to make a comparison with experimental data and theoretical data obtained in this study.

COMPUTATIONAL DETAILS

The interaction analysis between studied benzothiazole derivatives and Fe (110) surface were made with the help of molecular dynamics simulation approach and utilizing Forcite module from Accelrys, Inc (8). As model metal surface, Fe (110) surface was considered because in general this surface is preferred in the Monte Carlo studies including theoretical investigations about the adsorption on Fe metal of various organic molecules. Adopting the adsorption locator code applied in the Material Studio 8.0 software from Biovia-Accelrys Inc. USA, simulations were performed. To simulate the all molecules and metal-inhibitor systems, COMPASS (condensed phase optimized molecular potentials for atomistic simulation studies) force field was used. The simulations of the benzothiazole derivative labeled as ABT, TSCBT and TCHBT on iron surface were carried out to determine the low energy adsorption sites of these molecules. All simulations made in the study were performed in an NVT canonical ensemble at 298 K with a time step of 1.0 fs and a total simulation time of 1000 ps by providing via the Andersen thermostat the temperature control. In the calculations, vacuum media was preferred and five layers of Fe atoms were used.

Adsorption energy provides important clues about the power of the interaction between inhibitor molecule and metal surface. To calculate the adsorption energies between inhibitor molecules and Fe (110) metal surface, corrosion scientists use the following equation (9).

$$E_{\text{ads}} = E_{\text{complex}} - (E_{\text{Fe}} + E_{\text{inh}}) \quad (1)$$

In Eq. 1, E_{complex} is the total energy of an inhibitor molecule and the metal surface system. E_{Fe} is described as the energy of Fe surface without adsorption of any inhibitor molecule and E_{inh} represents the energy of isolated inhibitor molecules. As is known, the binding energy (E_{binding}) is considered as the negative value of the adsorption energy and is calculated via following equation (10, 11).

$$E_{\text{binding}} = -E_{\text{ads}} \quad (2)$$

RESULTS AND DISCUSSION

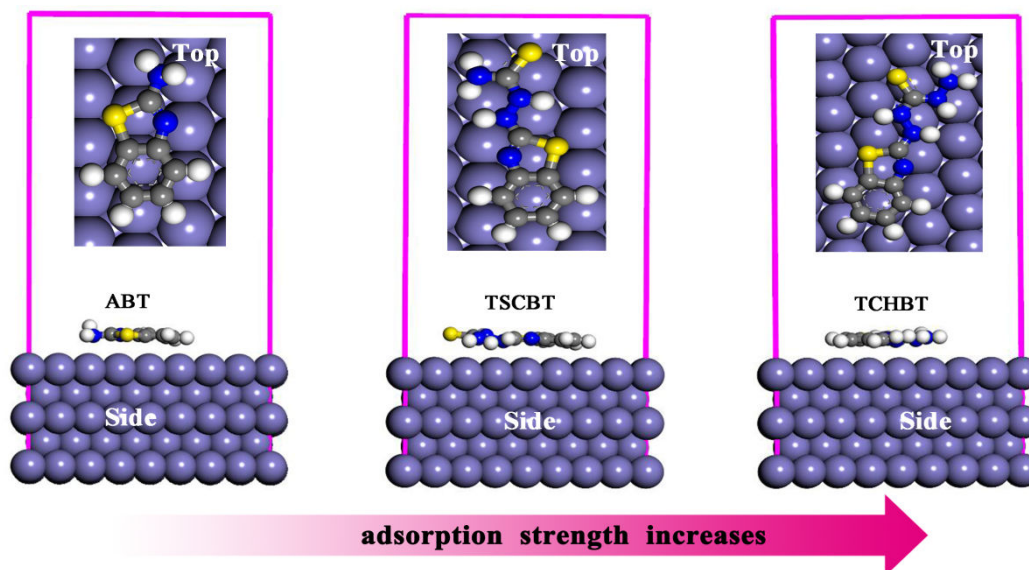


Figure 2. Representative snapshots of ABT, TSCBT, and TCHBT on Fe(110) surface (inset images show the on-top views).

Table 1. Adsorption and binding energies of three inhibitors adsorbed on Fe(110) surface.

Systems	E_{ads} (kJ mol ⁻¹)	E_{binding} (kJ mol ⁻¹)
Fe(110) + ABT	-352.9	352.9
Fe(110) + TSCBT	-482.9	482.9
Fe(110) + TCHBT	-494.0	494.0

In Table 1, adsorption and binding energies calculated between Fe (110) surface and three benzothiazole derivatives using Molecular dynamics simulations approach are given. Adsorption energy is defined as the energy released when inhibitor molecule was adsorbed on metal surface. As mentioned above, the binding energy is the negative value of the adsorption energy. The most stable low energy configurations for the adsorption of ABT, TSCBT and TCHBT molecules on Fe (110) in vacuum obtained are presented in Fig. 2. It is apparent from the molecular structures of studied benzothiazole derivatives; these molecules contain a number of lone pair electrons on N and S atoms as well as π -aromatic systems. For that reason, giving the lone pair electrons on heteroatoms to the unoccupied d orbitals of iron metal, mentioned molecules can form a stable coordination bonding. It can be noticed from Fig. 2, all of the benzothiazole derivatives are adsorbed nearly parallel to the Fe (110) surface with the help of the donation of π electrons of the rings appearing in the structures of the molecules and the lone pair of the heteroatoms.

It was reported in many studies that the primary mechanism of the interaction between corrosion inhibitors and metallic iron is by adsorption. Therefore, the adsorption energies calculated via molecular dynamics simulations approach can provide us a direct tool to compare the anticorrosive performances of inhibitor molecules. It is seen from the Table 1 that the calculated adsorption energies of the studied inhibitors on iron surface are -352.9, -482.9 and -494.0 for ABT, TSCBT and TCHBT molecules, respectively. All adsorption energies are negative and these negative values which denote that the adsorption happening between metal and inhibitors could occur spontaneously. The largest negative adsorption energy represents that the system is most stable and adsorption is very strong. On the other hand, positive and larger value of the binding energy implies the corrosion inhibitor combines with Fe (110) surface more easily and tightly (10). According to calculated adsorption and binding energies for studied benzothiazole derivative, corrosion inhibition efficiencies of mentioned molecules against the corrosion of iron metal follow the order: TCHBT > TSCBT > ABT. This ranking obtained via molecular dynamic simulation approach is same with experimentally observed result. This ranking obtained can be explained in terms of the molecular structures of studied benzothiazole derivatives. π -conjugated systems and molecules having many heteroatoms in their structures are more easily adsorbed on metal surfaces and exhibit higher inhibition efficiency. It is clear from the molecular structures given via Fig. 1 that TCHBT contains good number of heteroatoms with conjugated aromatic rings in its structures compared to others. For that reason, this molecule is the best corrosion inhibitor among studied benzothiazole derivatives.

CONCLUSION

In the present study, molecular simulation approach was employed to evaluate the corrosion inhibition performances against the corrosion of iron metal with some benzothiazole derivatives. The calculated adsorption and binding energies showed that ABT, TCHBT, TSCBT molecules are good corrosion inhibitors against the corrosion of iron. All the values of the adsorption energies are negative and these negative values are evidences of a spontaneous and strong adsorption process. Side chains appearing in the molecular structures of studied benzothiazole derivatives are very important the adsorption on Fe surface of these molecules. As results, the results obtained theoretically in this study are in good agreement with experimental data reported earlier.

REFERENCES

1. Kaya S, Tüzün B, Kaya C, Obot IB. Determination of corrosion inhibition effects of amino acids: Quantum chemical and molecular dynamic simulation study. *Journal of the Taiwan Institute of Chemical Engineers*. 2016 Jan;58:528–35.
2. Obot IB, Obi-Egbedi NO. Adsorption properties and inhibition of mild steel corrosion in sulphuric acid solution by ketoconazole: Experimental and theoretical investigation. *Corrosion Science*. 2010 Jan;52(1):198–204.

3. Wazzan NA, Obot IB, Kaya S. Theoretical modeling and molecular level insights into the corrosion inhibition activity of 2-amino-1,3,4-thiadiazole and its 5-alkyl derivatives. *Journal of Molecular Liquids*. 2016 Sep;221:579–602.
4. Umoren SA, Obot IB. POLYVINYLPIRROLIDONE AND POLYACRYLAMIDE AS CORROSION INHIBITORS FOR MILD STEEL IN ACIDIC MEDIUM. *Surface Review and Letters*. 2008 Jun;15(03):277–86.
5. Issa RM, Awad MK, Atlam FM. Quantum chemical studies on the inhibition of corrosion of copper surface by substituted uracils. *Applied Surface Science*. 2008 Dec;255(5):2433–41.
6. Khaled KF. The inhibition of benzimidazole derivatives on corrosion of iron in 1 M HCl solutions. *Electrochimica Acta*. 2003 Jul;48(17):2493–503.
7. Parameswari K, Chitra S, Selvaraj A, Brindha S, Menaga M. Investigation of Benzothiazole Derivatives as Corrosion Inhibitors for Mild Steel: *Portugaliae Electrochimica Acta*. 2012;30(2):89–98.
8. Frenkel D, Smit B. *Understanding molecular simulation: from algorithms to applications*. 2nd ed. San Diego: Academic Press; 2002. 638 p. (Computational science series).
9. Kaya S, Banerjee P, Saha SK, Tüzün B, Kaya C. Theoretical evaluation of some benzotriazole and phospono derivatives as aluminum corrosion inhibitors: DFT and molecular dynamics simulation approaches. *RSC Adv*. 2016;6(78):74550–9.
10. Obot IB, Kaya S, Kaya C, Tüzün B. Density Functional Theory (DFT) modeling and Monte Carlo simulation assessment of inhibition performance of some carbohydrazide Schiff bases for steel corrosion. *Physica E: Low-dimensional Systems and Nanostructures*. 2016 Jun;80:82–90.
11. Umoren SA, Obot IB, Gasem ZM. Adsorption and corrosion inhibition characteristics of strawberry fruit extract at steel/acids interfaces: experimental and theoretical approaches. *Ionics*. 2015 Apr;21(4):1171–86.



A Versatile Water-Soluble Ball-Type Phthalocyanine as Potential Antiproliferative Drug: The Interaction with G-Quadruplex Formed From Tel 21 and cMYC

Efkan BAĞDA¹, Esra BAĞDA², Ebru YABAŞ^{3*}

¹Department of Molecular Biology and Genetics, Cumhuriyet University Faculty of Science, 58140, Sivas, Turkey.

²Department of Analytical Chemistry, Cumhuriyet University Faculty of Pharmacy, 58140, Sivas, Turkey.

³Department of Chemistry and Chemical Processing Technologies, Cumhuriyet University Imranlı Vocational School, 58980, Sivas, Turkey.

Abstract: G-quadruplexes are biologically important DNA conformations exist generally in guanine-rich segments of DNA, such as telomere and proto-oncogene. The formation of these secondary structures is thought to inhibit the expression of certain genes, such as the inhibition of telomerase. The inhibition of telomerase and suppression of a specific gene expression are important approaches for interruption of cancer cell's proliferation. In the present study, the effect of a versatile water soluble ball-type phthalocyanine (BtPc) on G-quadruplex formation and stabilization was investigated to demonstrate its potential usage in cancer chemotherapy. Two important guanine rich oligomers, cMYC and Tel 21 were used as G-quadruplex former sequence. To the best of our knowledge, this is the first study about the interaction of a BtPc with G-quadruplex structures. The interactions of the compound with G-quadruplex molecules were monitored spectrophotometrically. The binding constants were calculated from Benesi-Hildebrand equation and the highest binding constant ($0.1114 \mu\text{M}^{-1}$) was found for Tel 21 in the presence of KCl. The structural differentiations of G-quadruplex after binding were investigated with circular dichroism spectrophotometry. The CD spectra were demonstrated the stabilization of both parallel and anti-parallel Tel 21 G-quadruplex in the presence of KCl and stabilization of anti-parallel form in the absence of KCl. The stability of the parallel structure was achieved for cMYC in the absence of KCl up to $4.10 \mu\text{M}$ of Pc. The disruption of staking of parallel form was achieved for cMYC in the presence of KCl. The replacement ability of the molecule with a known DNA binding molecule, ethidium bromide, was clarified fluorometrically. The Stern-Volmer studies were conducted for determination of the quenching mechanism. The strong interaction of the molecules (BtPc with oligomer) showed us the potential usage of these drug conjugates for targeted photodynamic therapy in the future.

Keywords: G-quadruplex, CD spectroscopic titration, telomere, oncogene.

Cite this: 1. Bağda E, Bağda E, Yabaş E. A versatile water soluble ball-type phthalocyanine as potential antiproliferative drug: the interaction with G-quadruplex formed from Tel 21 and cMYC. JOTCSA. 2017;4(2):103–20.

Submitted: January 27, 2017. **Revised:** March 23, 2017. **Accepted:** April 25, 2017.

DOI: 10.18596/jotcsa.288284

*Corresponding author. E-mail: yabasebru@gmail.com, eyabas@cumhuriyet.edu.tr

INTRODUCTION

Guanine-rich segments of DNA can fold into four stranded structures which are named G-quadruplexes [1-3]. The formation of G-quadruplexes was known for more than 40 years, but their existence *in vivo* has been discovered recently [4,5]. According to Bhattacharjee *et al.*, DNA can fold into a G-quadruplex structure, formed by $\pi \rightarrow \pi$ stacking of G-quartets [4]. G-quartets are composed of cyclic arrangement of four guanine molecules connected via Hoogsteen hydrogen bonds and they are stabilized by a central monovalent cation, such as K^+ or Na^+ [4].

G-quadruplexes can exist in telomeric and promotor region of oncogenes [6,7]. The presence of these highly ordered structures in telomeric end of DNA and oncogene regulatory regions are evident [7,8] and they have biologically important roles. The guanine rich DNA sequences exist in different sequence of chromosome [9,10]. The telomeric region of DNA is one of most known sequence of them. According to Gao *et al.* [11], telomerase is responsible for adding telomere repeats to telomeric DNA to maintain the integrity and stability of chromosome.

In normal somatic cells, the length of telomere sequence shortens at every cell division until they enter replicative senescence [12]. The telomerase activities in normal cell are highly lower compared to cancer cells, so the inhibition of telomerase is an important target for cancer chemotherapy. According to Gao *et al.*, it is very important that, telomerase binds to linear telomere DNA, not folded, like quadruplex structure [11]. The recognition of the structure by the enzyme cannot be achieved when the sequence forms secondary structures like G-quadruplexes. So, the formation of G-quadruplex structures results in inhibition of telomerase and interruption of replication of DNA [13]. Considering this point, the effective G-quadruplex stabilizing agents are promising alternative in cancer therapeutics. Besides, G-quadruplexes are thought to be useful drug delivery vehicles for especially cancer therapy [14]. Their thermal stability and easy/ low cost production make them alternative targetable drug carriers. The delivering the drug to a target cell or tissue via conjugation with a specific G-quadruplex structure seems highly feasible. So, the binding a potential drug with a suitable G-quadruplex structure is important for its potential therapeutic usage.

Phthalocyanines are attractive molecules due to their interesting biological applications [15]. With differentiation of the peripheral side groups and central metal

ions, various different types of new phthalocyanines can be synthesized. The important biological characteristics of phthalocyanines such as antibacterial, antifungal, antioxidant activity made scientists focus on the applicability of these molecules in different medical areas.

The interesting studies related with the interaction of G-quadruplexes with different phthalocyanines have been reported in the literature. Among them, generally mono type phthalocyanines were employed. Synthesis of different types of phthalocyanines (double-decker, clamshell, etc.) have been also accomplished by different research groups [16]. The first studies about synthesis of BtPc were conducted by Tolbin *et al* [17,18] but biological applications of BtPcs are rare in the literature.

Literature survey

The G-quadruplex stabilization effect of special molecules has attracted attention due to their potential usages in cancer therapy. There are interesting examples of G-quadruplex interactive molecules in the literature: Bhattacharjee *et al.* found that Zn(II) 5,10,15,20-tetrakis(N-methyl-4-pyridyl)porphyrin was a G-quadruplex interactive molecule [4]. They showed unambiguously, and for the first time, that ZnTMPyP4 greatly facilitated the folding of d(TAGGG)₂ into parallel G-quadruplex, probably by driving the equilibrium between unfolded and folded G-quadruplex toward the latter under otherwise unfavorable conditions (low amount of potassium ions). Chan *et al.* studied with methylene blue derivatives as a promising scaffolds for binding the cMYC oncogene G-quadruplex DNA [6]. They used a structure-based lead optimization approach to generate MB derivatives that displayed superior binding affinity and selectivity for the cMYC G-quadruplex over double-stranded DNA or other G-quadruplex structures. Gao *et al.* worked with 2,7-diamino-10-(3,5-dimethoxy)benzyl-9(10H)-acridone derivatives as potent telomeric G-quadruplex DNA ligands [11]. They showed that some of the compounds displayed good antiproliferative activity against leukemia CCRF-CEM cells, among which compound 6a containing dimethylamine substituents at the terminal C2 and C7 positions exhibited the highest cytotoxicity with IC₅₀ at 0.3 μM. In addition, compound 6a showed little toxicity against normal 293T cells proliferation with IC₅₀ more than 100 μM. The study conducted by Hassani *et al.* was about the interaction of copper porphyrazines and phthalocyanines with human telomeric G-quadruplex DNA. They found that interaction of the cationic porphyrazines was remarkably stronger than the anionic phthalocyanines [25]. Another study concerning the interaction of thymoquinone with G-quadruplex DNA was conducted by Salem *et al.* [26]. They

concluded that interaction of thymoquinone with G-quadruplex will contribute to the inhibition of telomerase enzyme and cancer's proliferation. Yaku *et al.* studied the telomere G-quadruplex-binding and telomerase-inhibiting capacity of two cationic and two anionic G-quadruplex ligands [27]. They concluded that ligands that bind to G-quadruplex via interactions such π - π stacking and hydrogen bonding may represent superior telomerase inhibitors in living cell media.

Phthalocyanines are highly interesting molecules and different types of phthalocyanines (mono, ball-type, double-decker, *etc.*) and similar molecules have been synthesized due to their usages in medicinal area. In the present study, water soluble BtPc molecule was employed as G-quadruplex interactive molecule.

In our previous study, we have synthesized a new water-soluble, BtPc, and reported the ct- DNA binding ability [15]. As mentioned in many study existing in the literature [19-21], G-quadruplexes are important therapeutic targets. In the present study, in order to clarify the usage of synthesized compound in cancer therapy, the interaction of BtPc molecule with G-quadruplex former oligonucleotides (Tel 21 and cMYC) were investigated in detailed. The interactions were clarified with ultraviolet visible (UV-Vis.) and circular dichroism (CD) spectrophotometric methods. An ethidium bromide (EtBr) replacement assay was conducted to understand the interaction closely. The experiments were done in the presence and absence of potassium chloride (KCl) because monovalent cations are known as G-quadruplex stabilization agents [22]. In the first part of our experiments, with the presence of KCl, the interaction of BtPc with pre-formed G-quadruplex was studied. In the absence of KCl, the G-quadruplex forming or stabilizing ability of BtPc was investigated.

EXPERIMENTAL

Reagents and instruments

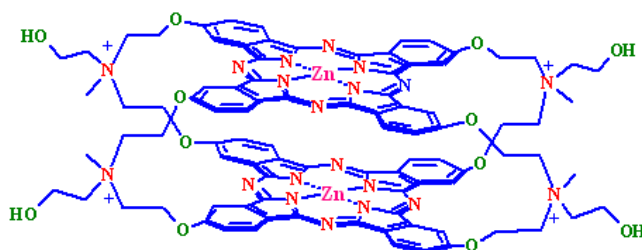
All chemicals were of analytical and molecular biology grade. The oligomers (cMYC and Tel 21) were purchased from Alpha DNA and used without further purification. The sequence of cMYC was TGAGGGTGGGAGGGTGGGAA and Tel 21 was GGGTTAGGGTTAGGGTTAGGGG (5' to 3'). The stock (100 μ M) oligomer solutions were prepared in pH 7.4 TE (Tris-EDTA, 10 mM Tris HCl, 1 mM EDTA) buffer in the presence and absence of 150 mM KCl. After dissolution of oligomers, the solutions were annealed at 95 °C for five minutes and cooled to room temperature slowly. The

solutions were incubated at +4 °C at least overnight. The double distilled water (after autoclaving) was used all throughout the experiments. The BtPc solution was prepared in both salty (150 mM KCl) and salt-free pH 7.4 TE buffer. BtPc solution was magnetically stirred at least four hours for complete dissolution.

All spectrophotometric measurements were conducted with a MAPADA series 6-spectrophotometer with using a 1 cm pathway quartz cell. A Shimadzu RF 5301 fluorescence spectrophotometer was used for spectrofluorometric measurements. pH measurements were conducted with Sartorius basic pH meter with a glass electrode. The pH meter was calibrated with using standard buffer solutions (pH= 4.0, 7.0, 10) purchased from Reagecon (Sahnon Free zone, Ireland). A Shimadzu analytical balance was used for weighing the chemicals. CD spectra were collected with a Jasco J-815 CD spectrophotometer.

Synthesis of BtPc

The detailed synthesis route was given in our previous study [15]. The synthesis steps were as follows: BtPc was synthesized by the cyclotetramerization of synthesized triethanolamine-substituted phthalonitrile derivative and water solubility of the compound was achieved after quaternization.



Water Soluble Ball Type Phthalocyanine.

Analysis by UV-Vis. and CD Spectroscopy

UV-Vis spectrophotometric experiments were performed with gradual addition of aliquots of Tel 21 and cMYC to BtPc solution (final oligomer concentrations were between 3.23-8.54 μM). The experiments were conducted with and without 150 mM KCl. The absorbance values were recorded against buffer solution with or without KCl. In order to evaluate the binding constant, spectrophotometric data were further processed with the Benesi-Hildebrand equation given below [8,23]:

$$\frac{1}{\Delta A_{\lambda}} = -\frac{1}{(\varepsilon_b - \varepsilon_f)[L_t]} + \frac{1}{(\varepsilon_b - \varepsilon_f)[L_t]K_{BH}[DNA]}$$

Where the ΔA is the absorbance change for corresponding λ_{\max} of BtPc (λ_{\max} is 602 nm in the presence of KCl and 611 nm in the absence of KCl), ε_b and ε_f stands for the molar extinction coefficients of bound and free ligand, $[L_t]$ is the total concentration of BtPc. The binding constant of DNA to Pc was evaluated with using slope and intercept values of Benesi-Hildebrand plot.

CD spectrophotometric titrations were conducted with gradual addition of BtPc (21 μM) to constant concentrations of Tel 21 (7.0 μM) and cMYC (2.4 μM) solutions. After addition of Pc solution, the solution was incubated for 5 minutes. The CD spectra were collected with the average of three scans. The spectra were taken against reagent blank.

Determination of quenching effect of BtPc molecule

Fluorometric experiments were done to evaluate the replacement ability of BtPc molecule with EtBr molecule. For the replacement assay, 5 μL of 10 mg/mL EtBr was introduced to the oligomeric solution (33 μM). After incubation for ten minutes, predetermined aliquots of BtPc (21 μM) solution was added to the mixture and the fluorometric intensity was monitored. The quenching effect of BtPc molecule was determined via Stern-Volmer equation given below [24]:

$$\frac{F_0}{F} = 1 + K_{SV}[BtPc]$$

Where F_0 was the fluorescence intensity of EtBr-oligomer complex and F was the fluorescence intensity of EtBr-oligomer complex after addition of BtPc. $[BtPc]$ was the concentration of the BtPc, and K_{SV} was the Stern-Volmer constant which could be used for the deduction of the binding/replacement ability of BtPc molecule. The slope of F_0/F versus $[BtPc]$ plot gave the K_{SV} value.

RESULTS AND DISCUSSION

Evaluation of UV-Vis. spectral data

UV-Vis spectrophotometry is the simplest, economic and commonly used method for studying both the stability of DNA secondary structures like G-quadruplexes and their interactions with different ligands [28].

As stated in our previous study [15] the UV-Vis. spectrum of BtPc molecule showing strong absorption band between 600-700 nm. In the present study, the absorption spectra of BtPc in pH 7.4 buffer with and without KCl were recorded. The presence of KCl resulted in hypochromism along with blue shift (9 nm) in Q-band region. These results represented the formation of aggregates in the presence of strong electrolyte [24].

The spectrophotometric analysis gives some information about the binding of two molecules. In generally, ligands show an absorption band in visible region and the interaction can be easily examined by the shifting of the λ_{\max} [29]. For DNA - small molecule interaction, the differentiation in absorbance and wavelength shift are useful data for prediction of strength of the interaction. The strong interactions generally result in significant differentiation in absorbance (hyper- or hypochromism) and sometimes in wavelength (bathochromic or hypsochromic shifts).

In the present study, as can be seen from Figure 1, the absorbance value of BtPc molecule has fallen from about 1.56 to 1.05 when the concentration of cMYC increased from 0-6.25 μM and a red shift about 21 nm occurred in the absence of KCl. On the other hand, for the same oncogene and for the same concentrations, the absorbance value of the BtPc molecule decreased from about 1.26 to 0.90 (for 0-6.25 μM) in the presence of KCl. The wavelength shift was also 21 nm.

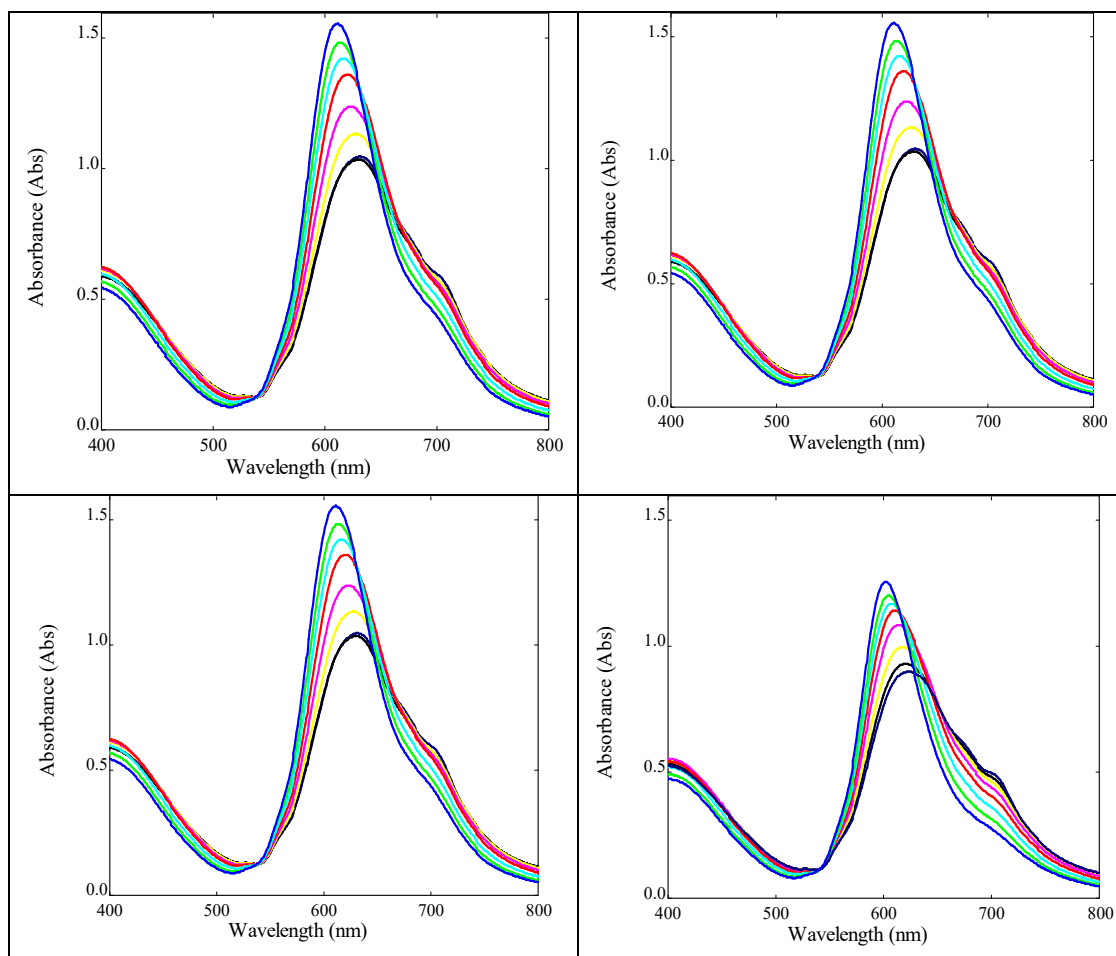


Figure 1: Change in molecular absorbance spectra of BtPc in Q band region with addition of cMYC in the absence (upper left) and presence (upper right) of 150 mM KCl, with addition of Tel 21 in the absence (lower left) and presence (lower right) of 150 mM KCl.

In the spectrophotometric titration of BtPc with Tel 21, the concentration of BtPc and Tel 21 was adjusted the same values of cMYC (0-6.25 μM). In the titration of BtPc with Tel 21, the absorbance value fallen from 1.56 to 1.16 with a red shift of 22 nm in the KCl free medium. The absorbance decreased from 1.28 to 1.02 accompanied with a red shift of 15 nm in the presence of KCl. The absorbance decreases were the obvious indicators of the BtPc oncogene/G-quadruplex interactions. The spectral data were treated with Benesi-Hildebrand equation. As shown in Table 1, the binding constant of Tel 21 had the highest value (about 0.1114 μM^{-1}) in the presence of KCl (as can be seen in section CD spectroscopic analysis, the ellipticity values of Tel 21 at 265 and 290 nm increased in the presence of KCl, which confirmed stabilization of both parallel and anti-parallel structures with BtPc molecule).

As can be seen in Table 1, for all spectral analyses, bathochromic shifts were observed for all circumstances. This was due to combination of BtPc's π electrons and n electrons of bases. The energy level of $n - n^*$ transition decreases [29].

Table 1: Spectrophotometric titration data and Benesi-Hildebrand binding constants.

		K binding constant, μM^{-1}	λ shift, nm
Without KCl	cMYC	0.0743 \pm 0.0023	21
	Tel 21	0.0654 \pm 0.0067	22
With KCl	cMYC	0.0718 \pm 0.0042	21
	Tel 21	0.1114 \pm 0.010	15

CD spectroscopic analysis

DNA segments can adopt various structures that are dependent on their environment. CD is a powerful tool for clarifying the secondary structure of biomolecules and binding characteristics of small molecules [29]. The CD spectrum of parallel G-quadruplex generally displays two major peaks with a positive ellipticity at about 260 nm and a negative at about 240 nm. For anti-parallel structure, a positive at about 290 nm and a negative at about 240 nm are characteristics of the spectrum [29].

In the present study, as can be seen from Figure 2, a strong positive peak at about 260 nm, and a negative peak around 240 nm was due to formation of parallel structure of G-quadruplex for cMYC. The CD spectrum of Tel 21 showed a negative band around 240 nm and, two positive peaks around 260 and 295 nm. The presence of these two characteristic peaks for Tel 21 was an obvious indicator of presence of two types of the structure in the solution. The titration of cMYC with BtPc caused no significant change in CD spectrum, *e.g.*, significant change in wavelength, or appearance or fully disappearance of a band. The decrease in ellipticity at 260 nm during titration of cMYC with BtPc in the presence of 150 mM of KCl indicated disruption of stacking of parallel form of G-quadruplex. [30]. Controversially, in KCl free medium, an increase in the parallel conformation of cMYC with addition of BtPc was observed. According to Saleem *et al.* [26], a decrease in CD intensity implies the intercalation type binding, and an increase shows the groove binding. From the results, it was estimated that the binding of BtPc to cMYC was intercalative in the presence of KCl and groove binding in the absence of KCl.

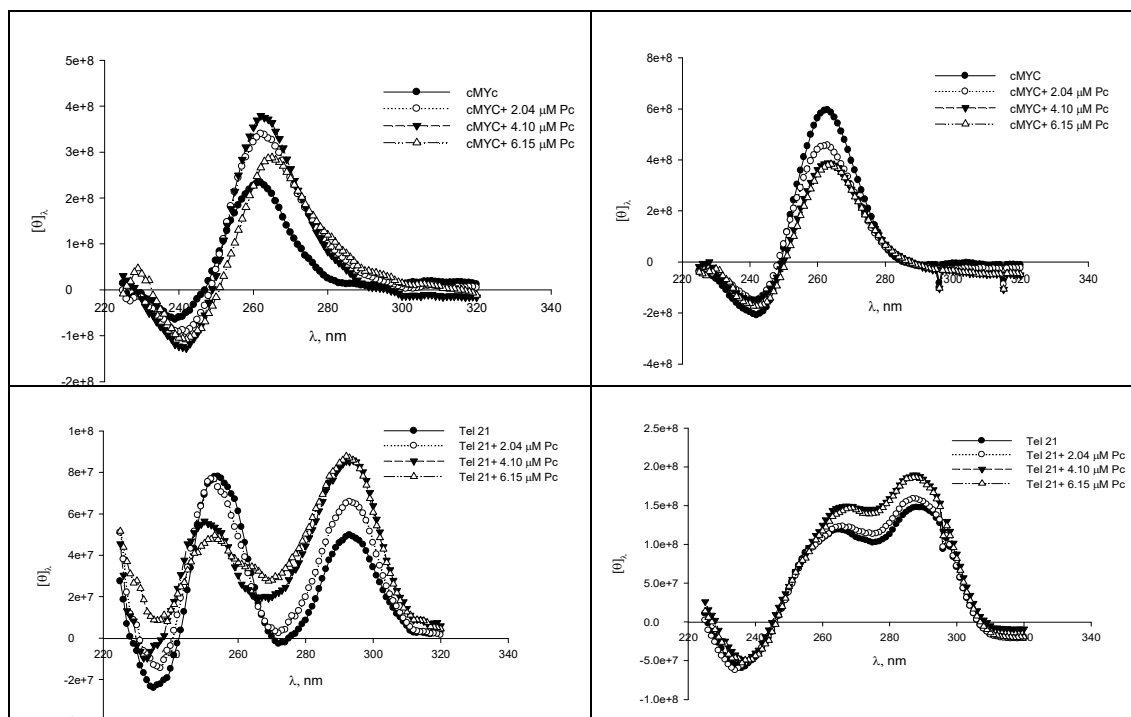


Figure 2: Change in CD spectrum of cMYC with addition of BtPc in the absence (upper left) and presence (upper right) of 150 mM KCl, spectrum of Tel 21 with addition of BtPc in the absence (lower left) and presence (lower right) of 150 mM KCl.

The titration of Tel 21 with BtPc in the presence of KCl caused the stabilization of hybrid type of structure, e.g. the ellipticity of both bands at 260 and 290 nm increased with increasing the concentration of BtPc. As stated above, an increase in ellipticity both at 260 and 290 nm might be an evidence of binding as groove type in the presence of KCl. In contrast, as shown in Figure 2, in KCl free medium, when the ellipticity of 260 nm decreased, the ellipticity of 290 nm increased with an increase in concentration of BtPc. These results implied the conversion of parallel structure of Tel 21 to anti-parallel structure favorably with addition of BtPc.

Briefly, addition of BtPc to cMYC resulted in a distortion of parallel structures in the presence of KCl, conversion of irregular oligomers to parallel type G-quadruplex structure in the absence of KCl. Secondly, addition of BtPc to Tel 21 favored the formation of both parallel and anti-parallel structures from irregular form in the presence of KCl and resulted in conversion to anti-parallel structure from parallel structure in the absence of KCl. As a whole, as can be seen from CD spectra, binding of BtPc molecule to G-quadruplex structure induced structural deviations. As stated by Vivec *et al*, this type of structural switch has been found for other studies [19].

Fluorescence replacement assay

EtBr is a well-known dsDNA intercalator reagent that used for much biological and molecular biological application. It also shows affinity towards G-quadruplex molecules [31,32]. Koeppel *et al.* showed the affinity of EtBr derivatives to G-quadruplex structures [32]. Fluorescence intensity of EtBr greatly increases in the presence of G-quadruplex. In the present study the fluorescence intensity of cMYC increased about 80 times and 100 times in the presence and absence of KCl. The fluorescence intensity of Tel 21 also increased in the presence of EtBr. From the point of view, we done replacement assay with EtBr. The fluorescence intensities of G-quadruplex DNA-EtBr system decreased with the addition of quencher molecule, *e.g.* BtPc molecule (from 0.0 to 5.2 μM) (Figures 3a and 3b). As shown in Figure 4, Stern-Volmer plots were deviated from linearity, which implied that the quenching mechanisms were consisting of both static and dynamic quenching. The regression coefficient of Stern-Volmer had the lowest value for cMYC-EtBr replacing with BtPc in the presence of KCl ($r^2= 0.92$) (Figure 4). The regression coefficient of Stern-Volmer plots for Tel 21 in the presence and absence of KCl and cMYC in the absence of KCl were equal or higher than 0.97.

For the linear part of Stern-Volmer plot, *e.g.* for the 5.56×10^{-7} - 3.76×10^{-6} M of BtPc of which the regression coefficient higher than 0.98, the Stern-Volmer constants were calculated (they can be seen in Table 2). In the presence of KCl, cMYC had the highest K_{sv} constant. This might be an evidence of easiness of EtBr replacement. With taking account CD spectrophotometric results, addition of BtPc to cMYC resulted in decrease in parallel structure and increase in perturbation because of intercalation of BtPc.

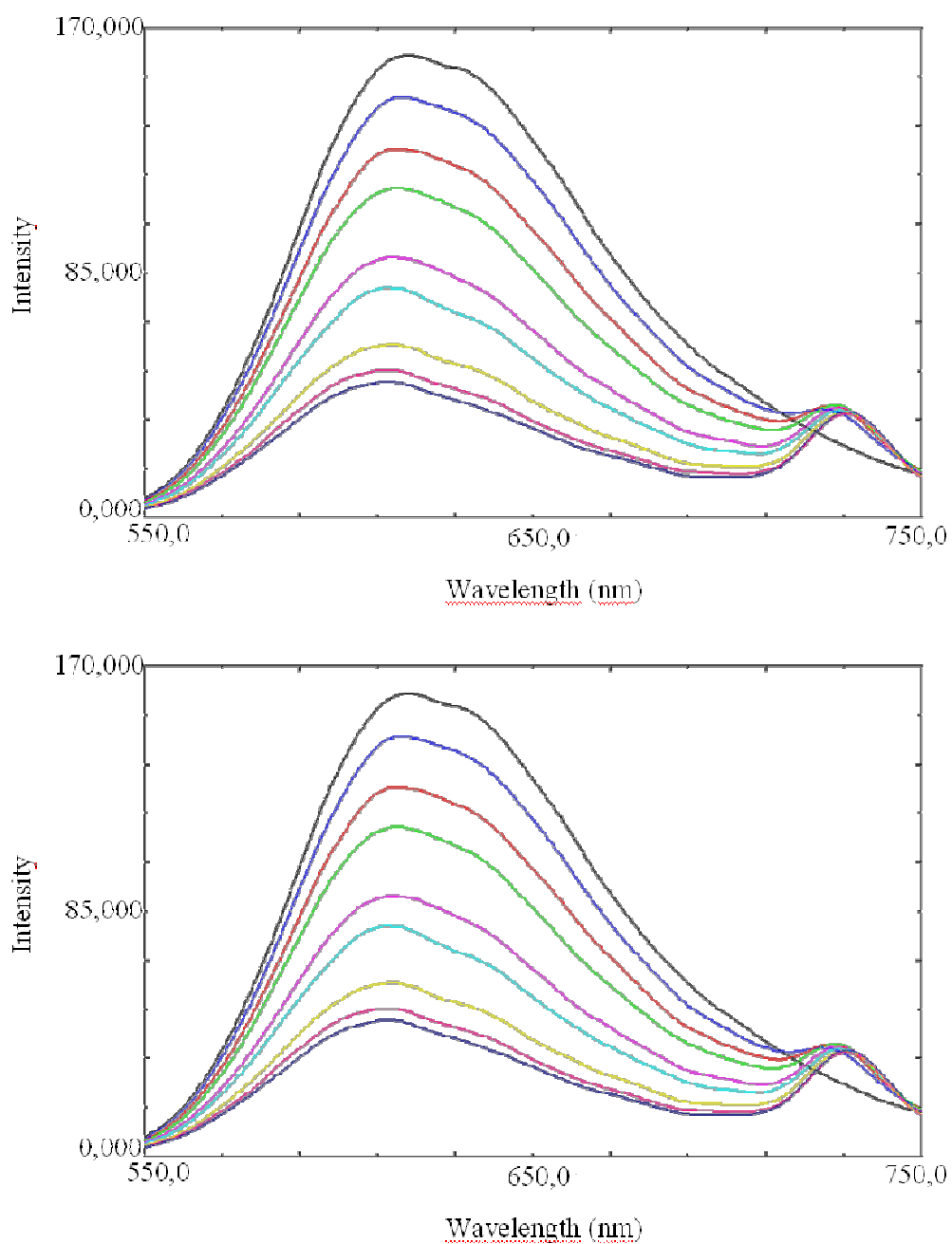


Figure 3a: Change in fluorometric intensity of EtBr- cMYC with addition of BtPc in the absence (up) and presence (down) of 150 mM KCl.

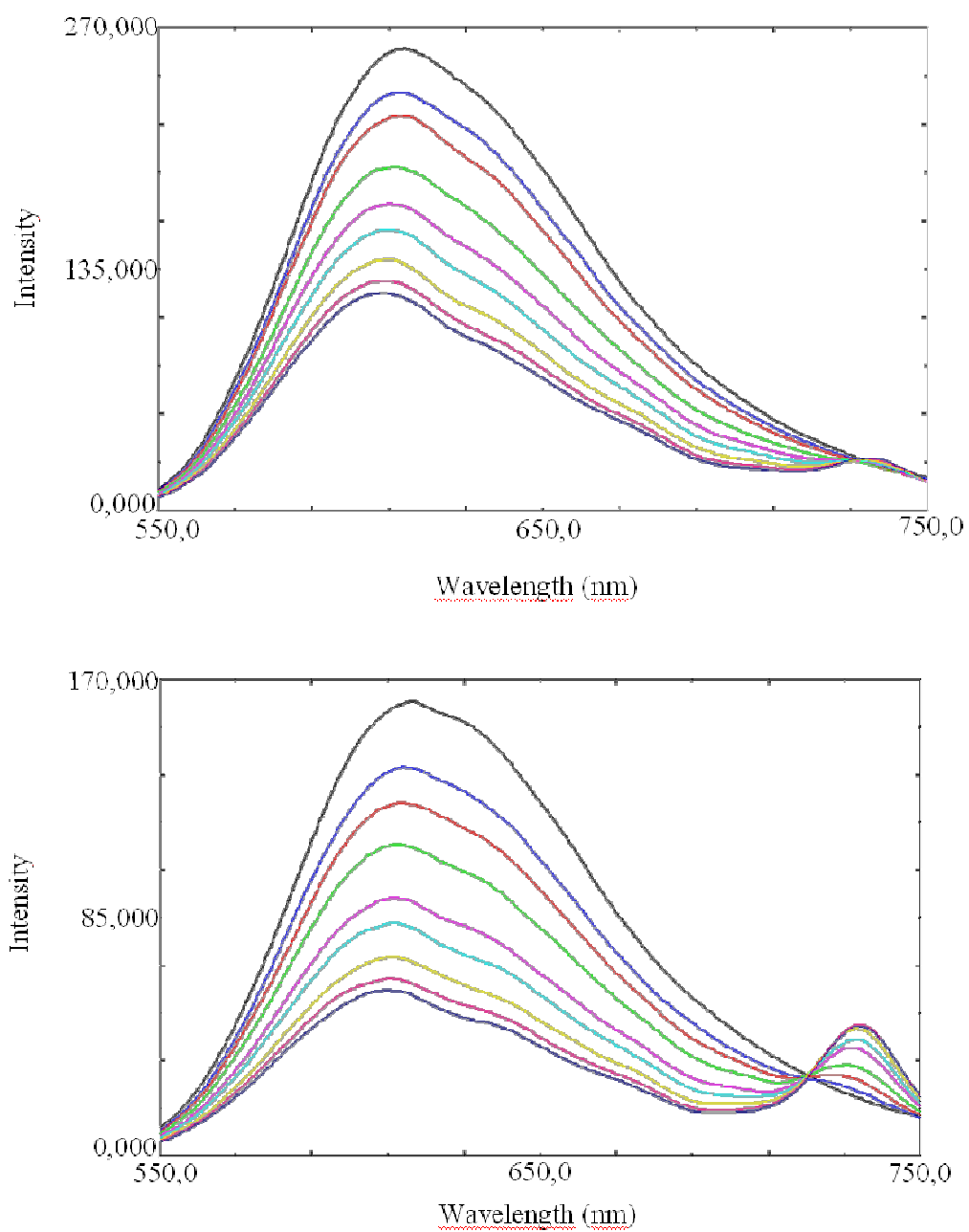


Figure 3b: Change in fluorometric intensity of EtBr- Tel 21 with addition of BtPc in the absence (up) and presence (down) of 150 mM KCl.

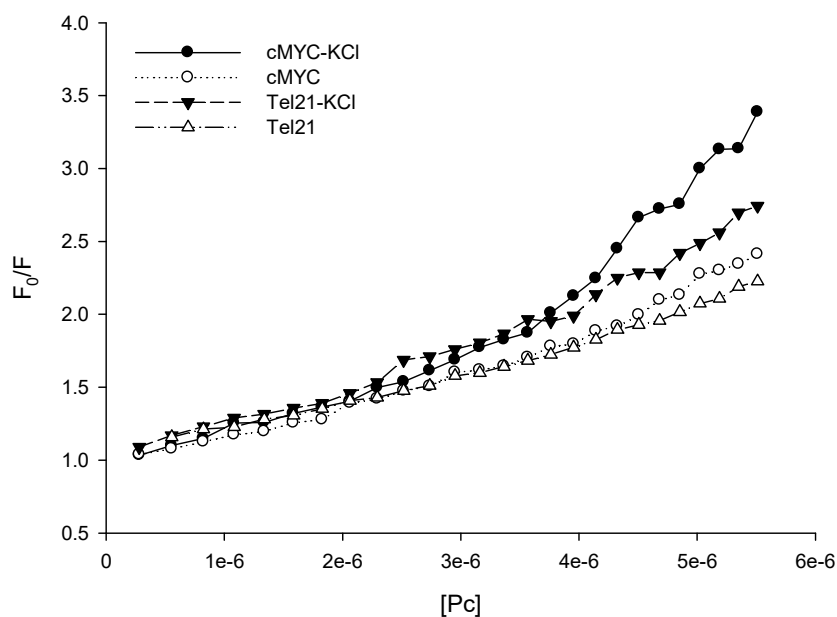


Figure 4: Stern-Volmer plots for quenching of EtBr-oligomer with addition of BtPc, regression coefficients (r^2) are higher than 0.97 except cMYC in the presence of KCl (0.92).

Table 2: Stern-Volmer equations for 5.56×10^{-7} - 3.76×10^{-6} M of BtPc.

		Stern-Volmer plot, M^{-1}	r^2
Without KCl	cMYC	$y = 2.2 \times 10^5 x + 0.93$	0.99
	Tel 21	$y = 1.8 \times 10^5 x + 1.0$	0.99
With KCl	cMYC	$y = 2.7 \times 10^5 x + 0.91$	0.98
	Tel 21	$y = 2.6 \times 10^5 x + 0.98$	0.98

CONCLUSION

In our previous study, it was documented that BtPc has a potential usage for anticancer treatment due to its affinity to dsDNA. The certain sequences, like guanine rich segment of DNA, have the ability to form G-quadruplex structures. As the stabilization of G-quadruplex structure thought to be a promising target for cancer treatment, the binding and stabilization effect of BtPc was investigated in the present study. A telomeric and a proto-oncogenic sequence were investigated for the mentioned purposes.

The highest binding constant was found for Tel 21 in the presence of KCl, which indicated the stabilization effects of BtPc to mentioned G-quadruplex. The CD

spectrums were also demonstrated the stabilization of both parallel and anti-parallel Tel 21 G-quadruplex in the presence of KCl. Besides, the stabilization of anti-parallel form of G-quadruplex was achieved for Tel 21 in the absence of KCl. The stability of the parallel structure was achieved for cMYC in the absence of KCl up to 4.10 μM of Pc. The disruption of staking of parallel form was achieved for cMYC in the presence of KCl. According to fluorometric data, in the presence of KCl, the Stern-Volmer constants have the higher values for both Tel 21 and cMYC compared to values obtained in the absence of KCl.

With the results achieved in the present study, binding of BtPc with G-quadruplex can be employed as a guide for new studies in the following ways: (i) As the G-quadruplexes are generally over expressed in cancer cells, BtPc molecules have the accumulation potential within cancer cells. (ii) G-quadruplexes are used as drug delivery vehicles; targeted delivery of BtPc to a certain cell/tumor is possible via conjugation with a specific G-quadruplex.

Conflict of interest: The authors declare that they have no conflict of interest.

REFERENCES

- 1 A. Ali, S. Bhattacharya, DNA binders in clinical trials and chemotherapy, *Bioorganic Med. Chem.* 22 (2014) 4506–4521.
- 2 M. Di Antonio, R. Rodriguez, S. Balasubramanian, Experimental approaches to identify cellular G-quadruplex structures and functions, *Methods.* 57 (2012) 84–92.
- 3 H. Han, L.H. Hurley, G-quadruplex DNA: A potential target for anti-cancer drug design, *Trends Pharmacol. Sci.* 21 (2000) 136–142.
- 4 A.J. Bhattacharjee, K. Ahluwalia, S. Taylor, O. Jin, J.M. Nicoludis, R. Buscaglia, et al., Induction of G-quadruplex DNA structure by Zn(II) 5,10,15,20-tetrakis(N-methyl-4-pyridyl)porphyrin, *Biochimie.* 93 (2011) 1297–1309.
- 5 T.A. Brooks, L.H. Hurley, Targeting MYC Expression through G-Quadruplexes, *Genes Cancer.* 1 (2010) 641–649.
- 6 D.S.H. Chan, H. Yang, M.H.T. Kwan, Z. Cheng, P. Lee, L.P. Bai, et al., Structure-based optimization of FDA-approved drug methylene blue as a c-myc G-quadruplex DNA stabilizer, *Biochimie.* 93 (2011) 1055–1064.
- 7 V. Dapic, Biophysical and biological properties of quadruplex oligodeoxyribonucleotides, *Nucleic Acids Res.* 31 (2003) 2097–2107.
- 8 J. Moon, J.H. Han, D.Y. Kim, M. Jung, S.K. Kim, Effects of deficient of the Hoogsteen base-pairs on the G-quadruplex stabilization and binding mode of a cationic porphyrin, *Biochem. Biophys. Reports.* 2 (2015) 1–7.
- 9 E.W. White, Selective Recognition of Quadruplex DNA by Small Molecules by, (2006).

- 10 T. Simonsson, G-quadruplex DNA structures - Variations on a theme, *Biol. Chem.* 382 (2001) 621–628.
- 11 C. Gao, W. Zhang, S. He, S. Li, F. Liu, Y. Jiang, Synthesis and antiproliferative activity of 2,7-diamino 10-(3,5-dimethoxy)benzyl-9(10H)-acridone derivatives as potent telomeric G-quadruplex DNA ligands, *Bioorg. Chem.* 60 (2015) 30–36.
- 12 A. De Cian, L. Lacroix, C. Douarre, N. Temime-Smaali, C. Trentesaux, J.-F. Riou, et al., Targeting telomeres and telomerase, *Biochimie.* 90 (2008) 131–155.
- 13 L. Zhang, J. Huang, L. Ren, M. Bai, L. Wu, B. Zhai, et al., Synthesis and evaluation of cationic phthalocyanine derivatives as potential inhibitors of telomerase, *Bioorganic Med. Chem.* 16 (2008) 303–312.
- 14 P. Charoenphol, H. Bermudez, Design and application of multifunctional DNA nanocarriers for therapeutic delivery, *Acta Biomater.* 10 (2014) 1683–1691.
- 15 E. Yabaş, E. Bağda, E. Bağda, The water soluble ball-type phthalocyanine as new potential anticancer drugs, *Dye. Pigment.* 120 (2015) 220–227.
- 16 G. De Torre, G. Bottari, U. Hahn, T. Torres, *Functional Phthalocyanine Molecular Materials*, 2010.
- 17 A.Y. Tolbin, A. V. Ivanov, L.G. Tomilova, N.S. Zefirov, Preparation of 1,2-bis(3,4-dicyanophenoxymethyl)benzene and the binuclear zinc phthalocyanine derived from it, *Mendeleev Commun.* 12 (2002) 96–97.
- 18 L. Hassani, F. Hakimian, E. Safaei, Spectroscopic investigation on the interaction of copper porphyrazines and phthalocyanine with human telomeric G-quadruplex DNA, *Biophys. Chem.* 187–188 (2014) 7–13.
- 19 A.A. Salem, I.A. El Haty, I.M. Abdou, Y. Mu, Interaction of human telomeric G-quadruplex DNA with thymoquinone: A possible mechanism for thymoquinone anticancer effect., *Biochim. Biophys. Acta.* 1850 (2015) 329–42.
- 20 H. Yaku, T. Murashima, H. Tateishi-Karimata, S.I. Nakano, D. Miyoshi, N. Sugimoto, Study on effects of molecular crowding on G-quadruplex-ligand binding and ligand-mediated telomerase inhibition, *Methods.* 64 (2013) 19–27.
- 21 V. Kumar, A. Sengupta, K. Gavvala, R.K. Koninti, P. Hazra, Spectroscopic and thermodynamic insights into the interaction between proflavine and human telomeric G-quadruplex DNA., *J. Phys. Chem. B.* 118 (2014) 11090–9.
- 22 S. Neidle, M. a Read, G-quadruplexes as therapeutic targets., *Biopolymers.* 56 (2001) 195–208.
- 23 S. Neidle, *Genomic Quadruplexes as Therapeutic Targets*, *Ther. Appl. Quadruplex Nucleic Acids.* (2012) 119–138.
- 24 D. Ren iuk, I. Kejnovska, P. kolakova, K. Bedna ova, J. Motlova, M. Vorli kova, Arrangements of human telomere DNA quadruplex in physiologically relevant K⁺ solutions, *Nucleic Acids Res.* 37 (2009) 6625–6634.
- 25 H. a Benesi, J.H. Hildebrand, A spectrophotometric investigation of the interaction of iodine with aromatic hydrocarbons, *J. Am. Chem. Soc.* 71 (1949) 2703–2707.
- 26 H. Dezhampannah, T. Darvishzad, M. Aghazadeh, Thermodynamic and spectroscopic study on the binding of interaction anionic phthalocyanine with calf thymus DNA, *Spectrosc. An Int. J.* 26 (2011) 357–365.

27 J. Jaumot, R. Gargallo, Experimental Methods for Studying the Interactions between G-Quadruplex Structures and Ligands, *Curr. Pharm. Des.* 18 (2012) 1900–1916.

28 M. Sirajuddin, S. Ali, A. Badshah, *Journal of Photochemistry and Photobiology B : Biology Drug – DNA interactions and their study by UV – Visible , fluorescence spectroscopies and cyclic voltametry*, *J. Photochem. Photobiol. B Biol.* 124 (2013) 1–19.

29 S. Paramasivan, I. Rujan, P.H. Bolton, Circular dichroism of quadruplex DNAs: Applications to structure, cation effects and ligand binding, *Methods.* 43 (2007) 324–331.

30 M. Islam, S. Fujii, S. Sato, T. Okauchi, S. Takenaka, A Selective G-Quadruplex DNA-Stabilizing Ligand Based on a Cyclic Naphthalene Diimide Derivative, *Molecules.* 20 (2015) 10963–10979.

31 Q. Guo, M. Lu, L. a Marky, N.R. Kallenbach, Interaction of the dye ethidium bromide with DNA containing guanine repeats., *Biochemistry.* 31 (1992) 2451–2455.

32 F. Koeppel, J.F. Riou, a Laoui, P. Mailliet, P.B. Arimondo, D. Labit, et al., Ethidium derivatives bind to G-quartets, inhibit telomerase and act as fluorescent probes for quadruplexes., *Nucleic Acids Res.* 29 (2001) 1087–1096.



Novel Straight-Chained Sulfanyl Members of Arylamino-1,4-naphthoquinones: Synthesis and Characterization

Nilufer Bayrak^{1, *}

¹Istanbul University, Department of Chemistry, Faculty of Engineering, 34320 Avcilar, Istanbul, Turkey

Abstract: The aim of this paper is to describe the synthesis and characterization of new members of straight-chained sulfanyl derivatives of arylamino-1,4-naphthoquinones. 2-(4-(trifluoromethyl)phenylamino)-3-chloronaphthalene-1,4-dione (**3a**) and 2-(3-(trifluoromethyl)phenylamino)-3-chloronaphthalene-1,4-dione (**3b**) prepared by a nucleophilic substitution reaction between 2,3-dichloronaphthalene-1,4-dione' (**1**) and arylamines containing a trifluoro group at the meta or para positions (**2a, 2b**) were used as building blocks for straight-chained sulfanyl arylamino-1,4-naphthoquinones. The structures of all the novel compounds (**5a-f**) were established by spectroscopic evidence including FTIR, ¹H NMR, ¹³C NMR, and MS data.

Keywords: Sulfanyl 1,4-naphthoquinone; arylamine; trifluoromethyl group.

Cite this: Bayrak N. Novel Straight-chained Sulfanyl Members of Arylamino-1,4-naphthoquinones: Synthesis and Characterization. JOTCSA. 2017;4(2):121-30.

Submitted: March 28, 2017. **Revised:** April 24, 2017. **Accepted:** April 25, 2017.

DOI: 10.18596/jotcsa.301558.

***Corresponding author.** E-mail: nbayrak@istanbul.edu.tr, (Tel:+90-212-4737070)

INTRODUCTION

Intense efforts are being made to synthesize good candidates for both further studies of chemical and structural modifications as well as biological applications (1-3). The naphthoquinone moiety, a common element in a number of different natural and synthetic structures such as menadione, lapachol and NQ304 (2-chloro-3-(4-hexylphenyl)-amino-1,4-naphthoquinone), is an important factor in the discovery of active substances. It is understood from the literature that the biological activity may be effected by the number and position of the substituents in the naphthoquinone moiety (4-8). It is no surprise that an impressive number of antibiotics like pyrano naphthoquinones involving eleutherin, nanaomycin, and kalafungin contains a naphthoquinone core (9-11). The biological potential of a derivative of naphthoquinone can be altered by the addition of a substituted aniline to the structure (12, 13). The electron donating or withdrawing features of the substituents on the aniline influence their redox functions (12). As the small and electron withdrawing group, trifluoromethyl (CF₃) has unique chemical properties due to its stereoelectronic and physiological profile that is relevant to the position of -CF₃ on aniline ring (13, 14). In addition to their marked antimicrobial, antifungal, antimalarial, antileishmanial, antiviral, anti-oxidant properties, sulfanyl amino derivatives of 1,4-naphthoquinones have also been found to be effective in inhibiting the proliferation of cancer cells (15-17). There are many reports on anticancer screening of 1,4-naphthoquinones containing an amino, a substituted amino or sulfanyl substituents in the 2-position that proves the biological convenience of this structures (18). In the frame of our studies on the synthesis of new naphthoquinone derivatives with antimicrobial, antibiofilm, and anticancer activities, we have recently reported the effect of a number of sulfanyl arylamino-1,4-naphthoquinones on Gram positive/negative bacteria and human tumor cell lines (19).

From the previous studies of structural modifications including changes of substituents in the side chain of the naphthoquinone ring, it can be deduced that the presence of an arylamine containing trifluoromethyl group and straight-chained sulfanyl compounds attached to the quinone ring can contribute to improve the bioactivity of these compounds. Thus, it is planned to synthesize and characterize several new straight-chained sulfanyl 1,4-naphthoquinones bearing arylamine rings with trifluoromethyl group so prevalent in drug molecules.

MATERIALS AND METHODS

All chemicals were commercially purchased from various suppliers and were used directly without further purification. The purity of the reaction products was monitored by thin-layer chromatography on analytical thin layer chromatography (TLC), purchased from Merck - KGaA (silica gel 60 F₂₅₄) based on Merck DC-plates (aluminum based). Visualization of the chromatogram was performed by UV light (254 nm). Column chromatographic separations were carried out using silica gel 60 (Merck, 63–200 μm particle size, 60–230 mesh). NMR spectra were recorded with a Varian UNITY INOVA instrument (500 MHz frequency for ¹H and 125 MHz frequency for ¹³C NMR) with CDCl₃ as solvent referring to signal center at δ 7.19 td (triplet of doublet), h (hextet) and δ 76.0 ppm, respectively. The peak multiplicities are abbreviated as follows: s (singlet), br s (broad singlet), d (doublet), t (triplet), p (pentet), dd (doublet of doublets) and m (multiplet). Chemical shifts were given in ppm (δ) relative to TMS, and coupling constants (J) were expressed in hertz (Hz). FTIR spectra were recorded as ATR on an Agilent Cary 630 FT-IR spectrometer. Mass spectra were obtained on a ThermoFinnigan LCQ Advantage MAX MS/MS spectrometer equipped with an ESI (Electrospray ionization) sources. Melting points (mp) were determined with a Buchi B-540 melting point apparatus and were uncorrected.

General Procedure for Synthesis of the Arylamino Chloro 1,4-Naphthoquinone Derivatives (3a-b)

2-Arylamino-3-chloro-1,4-naphthoquinone derivatives (**3a-b**) were prepared from the reaction between 2,3-dichloronaphthalene-1,4-dione (**1**) with trifluoromethyl-substituted arylamines (**2a-b**) according to methods reported in the literature and references cited therein (20-22).

General Procedure for Synthesis of the Straight-chained Sulfanyl Arylamino-1,4-naphthoquinone Derivatives (5a-f)

2-Arylamino-3-chloro-1,4-naphthoquinone derivatives (**3a-b**) and straight-chained sulfanyl compounds (**4a, 4b, 4c**) in CH₂Cl₂ were stirred at room temperature by using Et₃N as stated in the literature (2). The resulting solution was extracted with 100 mL chloroform then washed with water (4x100 mL) and dried over calcium chloride. The solvent was removed *in vacuo*. The residue was subjected to column chromatography on silica gel using suitable solvents to give the products.

2-(4-(trifluoromethyl)phenylamino)-3-(propylthio)naphthalene-1,4-dione (**5a**). It was synthesized from 2-(4-(trifluoromethyl)phenylamino)-3-chloronaphthalene-1,4-dione (**3a**) and propane-1-thiol (**4a**) as red oil by using the general procedure. Yield: 0.079 g, 71%. FTIR (ATR) $\nu(\text{cm}^{-1})$: 3324 (-NH), 3065 ($\text{CH}_{\text{arom.}}$), 2921, 2846 ($\text{CH}_{\text{aliph.}}$), 1681, 1652 (C=O), 1600, 1569 (C=C). ^1H NMR (500 MHz, CDCl_3) δ (ppm): 8.20-8.17 dd, J : 7.79, 1.19 Hz, 1H (- $\text{CH}_{\text{arom.}}$); 8.14-8.12 dd, J : 7.53, 1.03 Hz, 1H (- $\text{CH}_{\text{arom.}}$); 7.83 br s, 1H (-NH); 7.80-7.76 td, J : 7.53, 1.47 Hz, 1H (- $\text{CH}_{\text{arom.}}$); 7.74-7.70 td, J : 7.49, 1.42 Hz, 1H (- $\text{CH}_{\text{arom.}}$); 7.62-7.60 d, J : 8.44 Hz, 2H (- $\text{CH}_{\text{arom.}}$); 7.09-7.07 d, J : 8.69 Hz, 2H (- $\text{CH}_{\text{arom.}}$); 2.64-2.61 t, J : 7.39 Hz, 2H (- SCH_2); 1.47-1.42 m, 2H (- CH_2 -); 0.87-0.83 t, J : 7.31 Hz, 3H (- CH_3). ^{13}C NMR (125 MHz, CDCl_3) δ (ppm): 181.2, 180.1, 143.7, 141.5, 134.6, 133.3, 133.2, 130.6, 127.0, 126.8, 125.8, 121.9, 121.2, 35.7, 22.9, 13.2. MS (ESI+) m/z (%): 391 (100, $[\text{M}]^+$). Anal. Calcd. for $\text{C}_{20}\text{H}_{16}\text{F}_3\text{NO}_2\text{S}$ (391.41).

2-(4-(Trifluoromethyl)phenylamino)-3-(pentylthio)naphthalene-1,4-dione (**5b**). It was synthesized from 2-(4-(trifluoromethyl)phenylamino)-3-chloronaphthalene-1,4-dione (**3a**) and pentane-1-thiol (**4b**) as a red powder by using the general procedure. Yield: 0.046 g, 39%; mp 93-94 °C. FTIR (ATR) $\nu(\text{cm}^{-1})$: 3305 (-NH), 3061 ($\text{CH}_{\text{arom.}}$), 2928, 2846, 2878 ($\text{CH}_{\text{aliph.}}$), 1669, 1656 (C=O), 1602, 1554 (C=C). ^1H NMR (500 MHz, CDCl_3) δ (ppm): 8.19-8.15 dd, J : 7.81, 0.97 Hz, 1H (- $\text{CH}_{\text{arom.}}$); 8.13-8.08 d, J : 7.32, 0.98 Hz, 1H (- $\text{CH}_{\text{arom.}}$); 7.82 br s, 1H (-NH); 7.78-7.75 td, J : 7.32, 1.46 Hz, 1H (- $\text{CH}_{\text{arom.}}$); 7.73-7.67 td, J : 7.81, 1.46 Hz, 1H (- $\text{CH}_{\text{arom.}}$); 7.63-7.56 d, J : 8.29 Hz, 2H (- $\text{CH}_{\text{arom.}}$); 7.10-7.02 d, J : 8.29 Hz, 2H (- $\text{CH}_{\text{arom.}}$); 2.56-2.64 t, J : 7.8 Hz, 2H (S- CH_2 -); 1.34-1.44 m, 2H (- CH_2 -); 1.24-1.14 m, 4H (- CH_2); 0.86- 0.76 t, J : 7.33 Hz, 3H (- CH_3). ^{13}C NMR (125 MHz, CDCl_3) δ (ppm): 181.2, 180.1, 143.4, 141.3, 134.6, 133.3, 133.1, 130.6, 127.0, 126.8, 125.7, 122.0, 121.1, 33.6; 30.7, 29.0, 22.1, 13.8. MS (ESI+) m/z (%): 418 (100, $[\text{M}-\text{H}]^+$). Anal. Calcd. for $\text{C}_{22}\text{H}_{20}\text{F}_3\text{NO}_2\text{S}$ (419.46).

2-(4-(trifluoromethyl)phenylamino)-3-(nonylthio)naphthalene-1,4-dione (**5c**). It was synthesized from 2-(4-(trifluoromethyl)phenylamino)-3-chloronaphthalene-1,4-dione (**3a**) and nonane-1-thiol (**4c**) as an orange powder by using the general procedure. Yield: 0.047 g, 35%; mp 71-72 °C. FTIR (ATR) $\nu(\text{cm}^{-1})$: 3328 (-NH), 3074 ($\text{CH}_{\text{arom.}}$), 2926, 2857 ($\text{CH}_{\text{aliph.}}$), 1669, 1651 (C=O), 1604, 1556 (C=C). ^1H NMR (500 MHz, CDCl_3) δ (ppm): 8.18-8.16 dd, J : 7.81, 1.46 Hz, 1H (- $\text{CH}_{\text{arom.}}$); 8.12-8.07 dd, J : 7.81, 1.46 Hz, 1H (- $\text{CH}_{\text{arom.}}$); 7.82 br s, 1H (-NH); 7.78-7.75 td, J : 7.81, 1.46 Hz, 1H (- $\text{CH}_{\text{arom.}}$); 7.73-7.69 td, J : 7.81, 1.47 Hz, 1H (- $\text{CH}_{\text{arom.}}$); 7.63-7.56 d, J : 8.30 Hz, 2H (- $\text{CH}_{\text{arom.}}$); 7.09-7.03 d, J : 8.78 Hz, 2H (- $\text{CH}_{\text{arom.}}$); 2.65-2.57 t, J : 7.32 Hz, 2H (S- CH_2 -); 1.42-1.33 m, 2H (- CH_2 -); 1.31-1.12 m, 12H (- CH_2); 0.51-

0.30 t, J : 7.32 Hz, 3H (-CH₃). ¹³C NMR (125 MHz, CDCl₃) δ (ppm): 181.1, 180.1, 143.4, 141.4, 134.6, 133.3, 133.1, 130.6, 127.0, 126.7, 125.7, 125.6, 122.0, 121.1, 33.7, 31.8, 29.4, 29.3, 29.2; 29.0; 28.6, 22.6, 14.1. MS (ESI+) m/z (%): 476 (100, [M+H]⁺). Anal. Calcd. for C₂₆H₂₈F₃NO₂S (475.57).

2-(3-(trifluoromethyl)phenylamino)-3-(propylthio)naphthalene-1,4-dione (**5d**). It was synthesized from 2-(3-(trifluoromethyl)phenylamino)-3-chloronaphthalene-1,4-dione (**3b**) and propane-1-thiol (**4a**) as an orange powder by using the general procedure. Yield: 0.063 g, 56%, mp 100-101 °C. FTIR (ATR) ν (cm⁻¹): 3280 (-NH), 3081 (CH_{arom.}), 2933, 2833 (CH_{aliph.}), 1670, 1641 (C=O), 1599, 1524 (C=C). ¹H NMR (500 MHz, CDCl₃) δ (ppm): 8.18-8.16 dd, J : 7.32, 0.98 Hz, 1H (-CH_{arom.}); 8.12-8.07 dd, J : 7.32, 0.97 Hz, 1H (-CH_{arom.}); 7.86 s, 1H (-NH); 7.76-7.73 td, J : 7.32, 1.47 Hz, 1H (-CH_{arom.}); 7.72-7.65 td, J : 7.32, 0.97 Hz, 1H (-CH_{arom.}); 7.49-7.42 t, J : 7.81 Hz, 1H (-CH_{arom.}); 7.42-7.37 d, J : 7.81 Hz, 1H (-CH_{arom.}); 7.28 s, 1H (-CH_{arom.}); 7.20-7.15 d, J : 7.81 Hz, 1H (-CH_{arom.}); 2.63-2.55 t, J : 7.32 Hz, 2H (S-CH₂-); 1.45-1.35 h, J : 7.32 Hz, 2H (-CH₂-); 0.87-0.76 t, J : 7.32 Hz 3H (-CH₃). ¹³C NMR (125 MHz, CDCl₃) δ (ppm): 181.0, 180.2, 144.1, 138.9, 134.6, 133.4, 133.0, 130.5, 128.9, 127.0, 126.7, 125.1, 120.8, 120.2, 118.8, 35.7, 22.8, 13.2. MS (ESI+) m/z (%): 392 (100, [M+H]⁺). Anal. Calcd. for C₂₀H₁₆F₃NO₂S (391.41).

2-(3-(trifluoromethyl)phenylamino)-3-(pentylthio)naphthalene-1,4-dione (**5e**). It was synthesized from 2-(3-(trifluoromethyl)phenylamino)-3-chloronaphthalene-1,4-dione (**3b**) and pentane-1-thiol (**4b**) as red oil by using the general procedure. Yield: 0.078 g, 66%. FTIR (ATR) ν (cm⁻¹): 3286 (-NH), 3082 (CH_{arom.}), 2930, 2868 (CH_{aliph.}), 1686, 1650, (C=O), 1614, 1536 (C=C). ¹H NMR (500 MHz, CDCl₃) δ (ppm): 8.20-8.18 dd, J : 7.42, 1.23 Hz, 1H (-CH_{arom.}); 8.14-8.12 dd, J : 7.55, 1.11 Hz, 1H (-CH_{arom.}); 7.84 s, 1H (-NH); 7.80-7.76 td, J : 7.54, 1.44 Hz, 1H (-CH_{arom.}); 7.74-7.70 td, J : 7.51, 1.38 Hz, 1H (-CH_{arom.}); 7.50-7.46 t, J : 7.81 Hz, 1H (-CH_{arom.}); 7.43-7.41 d, J : 7.78 Hz, 1H (-CH_{arom.}); 7.29 s, 1H (-CH_{arom.}), 7.20-7.18 d, J : 7.90 Hz, 1H (-CH_{arom.}); 2.63-2.59 t, J : 7.35 Hz, 2H (-SCH₂); 1.42-1.20 m, 6H (-CH₂-); 0.84-0.81 t, J : 7.0 Hz, 3H (-CH₃). ¹³C NMR (125 MHz, CDCl₃) δ (ppm): 181.1, 180.2, 144.0, 138.8, 134.7, 133.4, 133.0, 130.6, 128.9, 127.0, 126.8, 125.0, 120.8, 120.4, 118.7, 33.8, 30.8; 29.0, 22.1, 13.8. MS (ESI+) m/z (%): 420 (100, [M+H]⁺). Anal. Calcd. for C₂₂H₂₀F₃NO₂S (419.46).

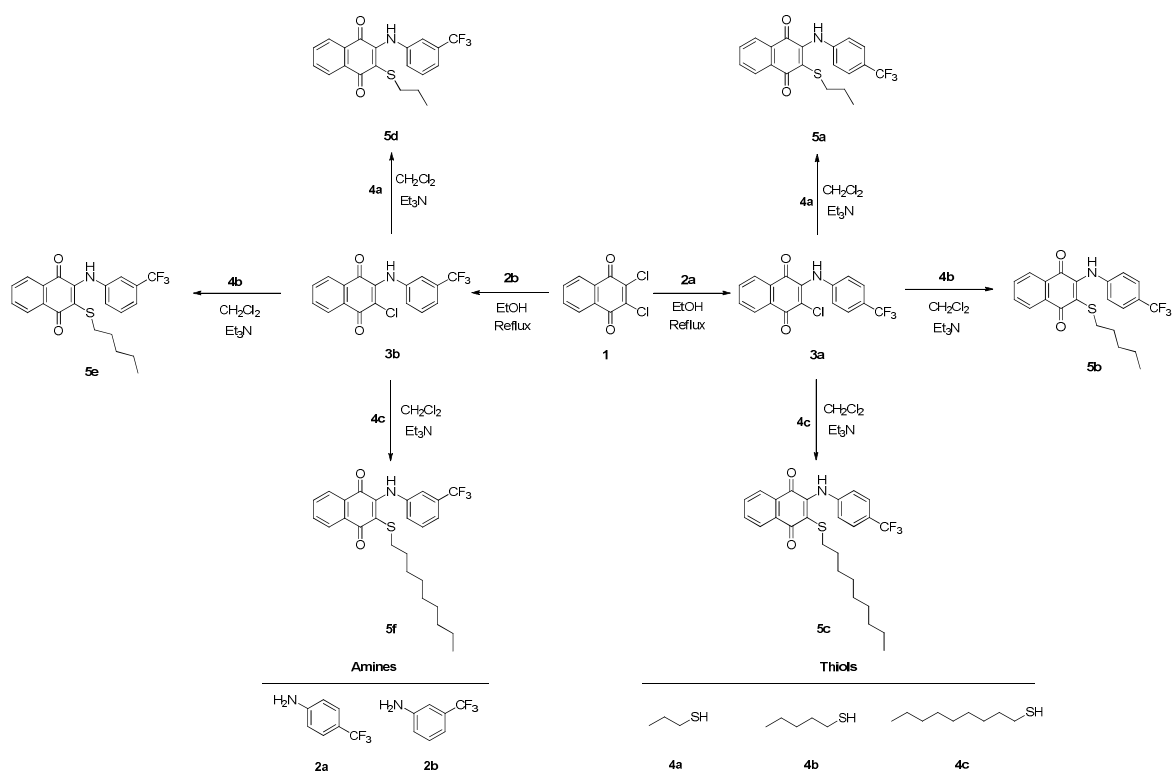
2-(3-(trifluoromethyl)phenylamino)-3-(nonylthio)naphthalene-1,4-dione (**5f**). It was synthesized from 2-(3-(trifluoromethyl)phenylamino)-3-chloronaphthalene-1,4-dione (**3b**) and nonane-1-thiol (**4c**) as red oil by using the general procedure. Yield: 0.096 g, 71 %. FTIR

(ATR) $\nu(\text{cm}^{-1})$: 3289 (-NH), 3086 ($\text{CH}_{\text{arom.}}$), 2928, 2861 ($\text{CH}_{\text{aliph.}}$), 1671, 1641 (C=O), 1604, 1514 (C=C). ^1H NMR (500 MHz, CDCl_3) δ (ppm): 8.20-8.18 dd, J : 7.59, 0.88 Hz, 1H (- $\text{CH}_{\text{arom.}}$); 8.14-8.12 dd, J : 7.56, 0.90 Hz, 1H (- $\text{CH}_{\text{arom.}}$); 7.84 s, 1H (-NH); 7.80-7.76 td, J : 7.54, 1.41 Hz, 1H (- $\text{CH}_{\text{arom.}}$); 7.74-7.70 td, J : 7.51, 1.35 Hz, 1H (- $\text{CH}_{\text{arom.}}$); 7.50-7.46 t, J : 7.85 Hz, 1H (- $\text{CH}_{\text{arom.}}$); 7.43-7.41 d, J : 7.80 Hz, 1H (- $\text{CH}_{\text{arom.}}$); 7.29 s, 1H (- $\text{CH}_{\text{arom.}}$); 7.19-7.17 d, J : 7.90 Hz, 1H (- $\text{CH}_{\text{arom.}}$); 2.63-2.59 t, J : 7.40 Hz, 2H (- SCH_2); 1.41-1.18 m, 14H (- CH_2 -); 0.91-0.87 t, J : 7.86 Hz, 3H (- CH_3). ^{13}C NMR (125 MHz, CDCl_3) δ (ppm): 181.1, 180.2, 144.0, 138.8, 134.6, 133.4, 133.0, 130.6, 128.9, 127.0, 126.7, 125.0, 120.8, 120.4, 118.8, 33.8, 31.8, 29.7, 29.4, 29.2, 29.0, 28.6, 22.6, 14.1. MS (ESI+) m/z (%): 474 (100, $[\text{M}-\text{H}]^+$). Anal. Calcd. for $\text{C}_{26}\text{H}_{28}\text{F}_3\text{NO}_2\text{S}$ (475.57).

RESULTS AND DISCUSSION

In order to prepare new straight-chained sulfanyl quinone precursors containing an aryl amine with electron donating group as trifluoromethyl at meta or para positions, 2-(4-(trifluoromethyl)phenylamino)-3-chloronaphthalene-1,4-dione (**3a**) and 2-(3-(trifluoromethyl)phenylamino)-3-chloronaphthalene-1,4-dione (**3b**) were obtained as starting compounds by means of nucleophilic substitution reactions of 2,3-dichloro-1,4-naphthoquinone (**1**) with arylamines containing trifluoromethyl group at meta and para positions (**2a**, **2b**) by the method previously reported (20-22). The reaction involves replacing the chlorine atom present at the 2-position of 2,3 dichloro 1,4 naphthoquinone with an amine functional group. Nucleophilic substitution reaction of 2,3-dichloronaphthalene-1,4-dione (**1**) with primary aryl amines (**2a**, **2b**) in ethanol resulted in the synthesis of 2-(arylamino)-3-chloro-naphthalene-1,4-diones (**3a**, **3b**). Trifluoromethyl substituted amino chloro quinone substrates proved to be compatible with further nucleophilic reaction protocols due to chlorine atom in the structure which is differentiable functional group to allow easy manipulations of the molecular architecture. Compounds **3a** and **3b** are efficient new sulfanyl quinone precursors and possible synthones for new quinone derivatives. Reactions of **3a** and **3b** with propane, pentane, and nonane derivatives of aliphatic sulphanyl compounds lead to the formation of novel straight-chained sulfanyl arylamino-1,4- naphthoquinones (**5a-f**) in good yields. The reactions were performed at room temperature using a base like previous studies (2) and the reaction products were separated by column chromatography using eluents of varying polarity chloroform with hexane. The structures of the new members were identified by using spectroscopic analyses. The FTIR spectra of **5a-f** showed two strong signals between 1681 and 1641 cm^{-1} for the carbonyl groups of the naphthoquinone moieties. The ^1H NMR

spectra of **5a-f** exhibited d, dd, t and td at 8.20 - 7.02 ppm for the aromatic groups, a singlet at around 7.82-7.86 ppm for the protons of the amine group, triplets at 2.55 - 2.65 ppm for methylene protons of SCH₂ groups, multiplet at 1.18-1.49 and hextet 1.35-1.45 for other methylene protons **5a-c**, **5e-f** and **5d**, respectively, triplets at 0.30 - 0.91 ppm for the methyl protons. In the ¹³C NMR spectrum we can easily note the presence of methyl carbons around 13.2-14.1, CH₂ carbons around 22.1-35.7 ppm, carbonyl carbons around 180.1-181.2 for quinone skeleton and C=C carbons around 118.7-143.7, as well as aromatic carbons from the naphthoquinone and aromatic amines introduced.



Scheme 1. Synthesized straight-chained sulfanyl 1,4-naphthoquinone derivatives substituted with aryl amines containing trifluoromethyl group.

CONCLUSION

The initial goal of our investigation was to synthesize the starting compounds 2-(4-(trifluoromethyl)phenylamino)-3-chloronaphthalene-1,4-dione (**3a**) and 2-(3-(trifluoromethyl)phenylamino)-3-chloronaphthalene-1,4-dione (**3b**) from the reactions of **1** with arylamines (**2a**, **2b**). After that, our attention was turned to preparing novel straight-chained sulfanyl arylamino-1,4-naphthoquinones (**5a-f**) by using **3a** and **3b** and aliphatic

sulfanyl compounds (**4a**, **4b**, **4c**). Based on what has been described about the importance of naphthoquinone derivatives, the main objective of this study was the development of new straight-chained sulfanyl amino naphthoquinones having an aryl amine with trifluoromethyl group at meta and para positions that may have potential pharmaceutical value.

ACKNOWLEDGMENTS

The author thanks to the Scientific Research Projects Coordination Unit of Istanbul University.

REFERENCES

1. Cole ST. Who will develop new antibacterial agents? *Philos T R Soc B*. 2014;369(1645).
2. Tandon VK, Maurya HK, Mishra NN, Shukia PK. Design, synthesis and biological evaluation of novel nitrogen and sulfur containing hetero-1,4-naphthoquinones as potent antifungal and antibacterial agents. *Eur J Med Chem*. 2009;44(8):3130-7.
3. Kumagai Y, Shinkai Y, Miura T, Cho AK. The Chemical Biology of Naphthoquinones and Its Environmental Implications. *Annu Rev Pharmacol*. 2012;52:221-47.
4. Salas CO, Faundez M, Morello A, Maya JD, Tapia RA. Natural and Synthetic Naphthoquinones Active Against *Trypanosoma Cruzi*: An Initial Step Towards New Drugs for Chagas Disease. *Curr Med Chem*. 2011;18(1):144-61.
5. Pinto AV, de Castro SL. The Trypanocidal Activity of Naphthoquinones: A Review. *Molecules*. 2009;14(11):4570-90.
6. Klaus V, Hartmann T, Gambini J, Graf P, Stahl W, Hartwig A, et al. 1,4-Naphthoquinones as inducers of oxidative damage and stress signaling in HaCaT human keratinocytes. *Arch Biochem Biophys*. 2010;496(2):93-100.
7. Kim TJ, Yun YP. Antiproliferative activity of NQ304, a synthetic 1,4-naphthoquinone, is mediated via the suppressions of the PI3K/Akt and ERK1/2 signaling pathways in PDGF-BB-stimulated vascular smooth muscle cells. *Vasc Pharmacol*. 2007;46(1):43-51.
8. Ryu CK, Shim JY, Chae MJ, Choi IH, Han JY, Jung OJ, et al. Synthesis and antifungal activity of 2/3-arylthio- and 2,3-bis(arylthio)-5-hydroxy-/5-methoxy-1,4-naphthoquinones. *Eur J Med Chem*. 2005;40(5):438-44.
9. Brimble MA, Duncalf LJ, Nairn MR. Pyranonaphthoquinone antibiotics - isolation, structure and biological activity. *Nat Prod Rep*. 1999;16(3):267-81.
10. Qabaja G, Jones GB. Annulation strategies for benzo[b]fluorene synthesis: Efficient routes to the kinafluorenone and WS-5995 antibiotics. *J Org Chem*. 2000;65(21):7187-94.
11. Uno H. Synthesis of Naturally-Occurring Quinones .17. Allylation of 2-Alkanoyl 1,4-Quinones with Allylsilanes and Allylstannanes - Efficient Synthesis of Pyranonaphthoquinone Antibiotics. *J Org Chem*. 1986;51(3):350-8.
12. Benites J, Valderrama JA, Bettega K, Pedrosa RC, Calderon PB, Verrax J. Biological evaluation of donor-acceptor aminonaphthoquinones as antitumor agents. *Eur J Med Chem*. 2010;45(12):6052-7.

13. Samant BS, Chakaingesu C. Novel naphthoquinone derivatives: Synthesis and activity against human African trypanosomiasis. *Bioorg Med Chem Lett*. 2013;23(5):1420-3.
14. Druzhinin SV, Balenkova ES, Nenajdenko VG. Recent advances in the chemistry of alpha,beta-unsaturated trifluoromethylketones. *Tetrahedron*. 2007;63(33):7753-808.
15. Tandon VK, Maurya HK, Yadav DB, Tripathi A, Kumar M, Shukla PK. Naphtho[2,3-b][1,4]-thiazine-5,10-diones and 3-substituted-1,4-dioxo-1,4-dihydronaphthalen-2-yl-thioalkanoate derivatives: Synthesis and biological evaluation as potential antibacterial and antifungal agents. *Bioorg Med Chem Lett*. 2006;16(22):5883-7.
16. Tandon VK, Maurya HK, Tripathi A, ShivaKeshava GB, Shukla PK, Srivastava P, et al. 2,3-Disubstituted-1,4-naphthoquinones, 12H-benzo[b]phenothiazine-6, 11-diones and related compounds: Synthesis and Biological evaluation as potential antiproliferative and antifungal agents. *Eur J Med Chem*. 2009;44(3):1086-92.
17. Bayrak N, Yildirim H, Tuyun AF, Kara EM, Celik BO, Gupta GK. Synthesis, Biological, and Computational Study of Naphthoquinone Derivatives Containing Heteroatoms. *J Chem Soc Pakistan*. 2016;38(6):1211-21.
18. Bhasin D, Chettiar SN, Etter JP, Mok M, Li PK. Anticancer activity and SAR studies of substituted 1,4-naphthoquinones. *Bioorg Med Chem*. 2013;21(15):4662-9.
19. Bayrak N, Yildirim H, Tuyun AF, Kara EM, Celik BO, Gupta G.K, Ciftci H, Fujita M, Otsuka M., Nasiri H.R. Synthesis, Computational Study, and Evaluation of in vitro Antimicrobial, Antibiofilm, and Anticancer Activities of New Sulfanyl Aminonaphthoquinone Derivatives. *Lett Drug Des Discov*. In press, DOI: 10.2174/1570180813666161020164931
20. Tuyun AF, Bayrak N, Yildirim H, Onul N, Kara EM, Celik BO. Synthesis and In Vitro Biological Evaluation of Aminonaphthoquinones and Benzo[b]phenazine-6,11-dione Derivatives as Potential Antibacterial and Antifungal Compounds. *J Chem*. 2015, 645902.
21. Buu-Hoi NPR, R.; Hubert-Habart, M., Empêchement stérique dans la réaction des amines sur les quinones halogénées. *Recl Trav Chim Pay B*. 1954;73:188-92.
22. Mital AS, M.; Bindal, S.; Mahlavat, S.; Negi, V., Substituted 1,4-naphthoquinones as a new class of antimycobacterial agents *Der Pharma Chem* 2010;2:63-73.



Determination of Bisphenol A in Beverage Samples Using Ultrasonic- Extraction and Atomic Absorption Spectrometry

Emre Yıldırım¹, Nail Altunay^{1,*}, and Ramazan Gürkan¹

¹Cumhuriyet University, Faculty of Sciences, Department of Chemistry, TR-58140, Sivas, Turkey

Abstract: In this work, a simple and versatile ultrasound-assisted extraction (UAE) procedure, which provides high separation efficiency for bisphenol A (BPA), was developed for its indirect determination in beverages in contact with plastic containers by flame atomic absorption spectrometry (FAAS). The method is based on charge transfer reaction, in which BPA reacts with Cu(II) in alkaline tartrate solutions of pH 8.0 to produce Cu(I), which reacts with ion-pairing reagent, Promethazine, being a phenothiazine derivative (PMZ), in the presence of cetyl trimethylammonium bromide (CTAB). For the indirect determination of BPA using FAAS, the change in signal of Cu(II) depending on BPA concentration was investigated in detail. At optimal conditions, the analytical features of the method were obtained as follows; linearity ranges of 1.5-100 $\mu\text{g L}^{-1}$ for direct aqueous calibration solutions and 3-125 $\mu\text{g L}^{-1}$ for matrix matched calibration solutions; the limits of detection and quantification of 0.47 and 1.56 $\mu\text{g L}^{-1}$; sensitivity enhancement and pre-concentration factors of 135 and 150, respectively. The method accuracy was validated by repeatability/reproducibility precision studies using standard addition method. As the last, the method was successfully applied for determination of BPA in selected samples. BPA as a food stimulant was detected in ranges of 2.70-3.80 $\mu\text{g L}^{-1}$ in waters and 3.10-5.40 $\mu\text{g L}^{-1}$ in milk products while its levels changed in ranges of 6.40-7.70 and 4.30-19.2 $\mu\text{g L}^{-1}$ in beverages with and without alcohol. These levels were highly lower than the specific migration limit set by European Union.

Keywords: Bisphenol A, beverage samples, ultrasonic extraction, atomic absorption spectrometry, Cu complex.

Submitted: January 28, 2017. **Revised:** April 22, 2017. **Accepted:** May 04, 2017.

Cite this: Yıldırım E, Altunay N, Gürkan R. Determination of Bisphenol A in Beverage Samples Using Ultrasonic- Extraction and Atomic Absorption Spectrometry. JOTCSA. 2017;4(2):607-30.

DOI: 10.18596/jotcsa.288389.

***Corresponding author.** E-mail: naltunay@cumhuriyet.edu.tr

INTRODUCTION

Over the past few decades, endocrine disruptors (EDCs) have become a central topic in the international discussion in environmental and food chemistry because of their potential negative effects on the endocrine systems (1). Among phenolic EDCs, 2,2-bis(4-hydroxyphenyl) propane (bisphenol A, BPA) is a principal component of both polycarbonate and epoxy resins, and is widely used in the manufacture of consumer goods and products, including food containers and utensils, baby bottles, and water supply pipes (2, 3). Thus, there is a major source of concern for regulatory agencies and scientists. Bisphenol A can easily migrate into the food samples from lacquer-coated cans and plastic products due to hydrolysis of the polymer during thermal treatment (4). Consequently, it can cause adverse health effects such as recurrent miscarriages, endometrial hyperplasia, and polycystic ovarian syndrome (5). The scientific panel on food additives, flavourings and processing aids in contact with food of the European Food Safety Authority (EFSA) reported its risk assessment for BPA in 2007 and calculated a total daily intake (TDI) for BPA of $0.05 \text{ mg (kg body weight)}^{-1} \text{ day}^{-1}$ with a specific migration limit (SML) of 0.6 mg kg^{-1} for foods and its use was prohibited in the manufacture of polycarbonate feeding bottles intended for babies younger than one year since the beginning of 2011 (6, 7). So, there is still a strong requirement for rapid, efficient and sensitive analytical methods for the assessment of low amount of BPA exposure to humans.

To date, a variety of detection techniques have been developed to determine BPA in various samples, including micellar liquid chromatography (MLC) (8), liquid chromatography–fluorescence detection (LC-FD) (9), liquid chromatography–tandem mass spectrometry (LC-MS/MS) [10], gas chromatography–mass spectrometry (GC-MS) (11), capillary electrophoresis (CE) (12) and capillary zone electrophoresis (CZE) (13) as well as enzyme-linked immunosorbent assay (ELISA) (14) and micellar sensitive electroanalytical techniques such as linear sweep voltammetry (LSW) (15), differential pulse polarography (DPP) (16) and square wave voltammetry (SWV) (17).

In addition, analysis of trace levels of BPA in water and beverage samples using flame atomic absorption spectrometry (FAAS) is limited not only due to insufficient sensitivity, but also by matrix interference. Thus, different extraction procedures, including electrophoretic methods, ultrasonic-assisted extraction (UAE) (18), soxhlet extraction (19), cloud point extraction (CPE) (20), dispersive liquid–liquid micro-extraction (DLLME) (21) and solid phase extraction (SPE) (22) are frequently necessary to improve the detection limit and the selectivity. Among these procedures, the UAE is a key-technology in achieving the objective of sustainable “green chemistry”. Using ultrasound energy, full

extractions can now be completed in minutes with good reproducibility, lower organic solvent requirement, simplifying manipulation and work-up, giving higher purity of the selected samples (23). Moreover, the UAE procedures, either off- or on-line, are considered superior to other procedures for their simple, good pre-concentration factor, little organic solvent requirement, versatile use and time effectively. The UAE is an extraction procedure based on the clouding phenomenon of surfactants, and often used to preconcentrate toxic and non-toxic metals and metalloids from various sample matrices (24). Biodegradable surfactants like Tergitol TMN-6, Tergitol 15-S-7 and Tergitol 15-S-9 are used in CPE for extracting some polycyclic aromatic hydrocarbons (PAH) from real samples (25). Therefore, Tergitol 15-S-7 is expected to have many advantages in CPE combined with ultrasound energy of bisphenol A as a contaminant migrated from PC and PVC plastics into the beverage and foodstuffs (26).

Our research group considers the possibility of implementation of the UAE in combination with flame atomic absorption spectrometry (FAAS) in trace BPA analysis, and develop a new method for the determination of trace BPA in plastic bottle packaging beverage samples. For this purpose, (RS)-N,N-dimethyl-1-(10H-phenothiazin-10-yl)propan-2-amine, (Promethazine, PMZ) was selected as chelating reagent in the presence of Cu(II), tergitol 15-S-7 (extracting agent) at pH 8.0. To the best of our knowledge, there are no applications in the literature of FAAS for BPA determination from the prepared samples by ultrasonic-assisted extraction. Especially, the use of ultrasonic effect in sample preparation has provided features like low organic solvent usage and less extraction duration. The experimental parameters affecting the efficiency of UAE procedure and FAAS determination were systematically investigated. The precision and accuracy were confirmed by repeatability/reproducibility and recovery tests, respectively, and the method was then applied to the determination of BPA in the selected samples with satisfactory results.

MATERIALS AND METHODS

Apparatus

All measurements for the indirect determination of BPA were carried out using an atomic absorption spectrometer (AAS-6300 model, Shimadzu, Kyoto, Japan) equipped with a deuterium background correction and hollow cathode lamp of copper as the radiation source. The sequential device was used with following parameters: wavelength, 324.8 nm; lamp current, 3.0 mA; spectral bandwidth, 0.5 nm; burner height, 6.0 mm; acetylene and air flow rates, 1.8 L min⁻¹ and 15.0 L min⁻¹, respectively. A centrifuge (model Universal Hettich model, London, England) was used for complete phase separation. An ultrasound assisted water bath (UCP-10 model, Seoul, Korea) was used to fasten the extraction

process and digestion of the samples. A pH-meter (Selecta 2001 model, North America) was used for pH adjustment.

Chemicals and reagents

In this study, all chemical reagents used are at least analytical grade. The water utilized in throughout the experiment was high purity deionized water (18.2 M Ω cm), which obtained from a Labconco (Kansas City, USA) water purification system. Unless otherwise stated, the chemicals were purchased from Sigma (St. Louis, MO. USA) and Merck (Darmstadt, Germany). A stock solution of bisphenol A of 1000 mg L⁻¹ (Sigma), was prepared in methanol and kept at 4 °C in the dark. A stock solution of Cu(II), 1000 mg L⁻¹, was prepared by dissolving appropriate amounts of Cu(NO₃)₂ (Merck) in water. Working solutions were prepared daily by serial dilution of the stock solutions. A 1×10⁻⁴ mol L⁻¹ solution of PMZ as ion-pairing reagent was prepared daily by dissolving an appropriate amount of solid in water. A 3×10⁻³ mol L⁻¹ of the cationic surfactant solution, cetyl trimethyl ammonium bromide (CTAB, Sigma-Aldrich), was prepared by dissolving its suitable amount with the water. The non-ionic surfactant, a 10.0% (w/v) Tergitol 15-S-7 solution (Sigma-Aldrich), was prepared by dissolving in a mixture of water and methanol (9:1, v/v, Merck). The phosphate buffer solution of pH 8.0 (KH₂PO₄/NaOH, 0.2 mol L⁻¹) containing 5 mmol L⁻¹ sodium potassium tartrate to prevent precipitation of Cu(II) ions and to improve signal reproducibility in alkaline conditions near to neutral was used to control the pH of the solutions. Because of the ubiquity of BPA, to avoid its contamination, no alkylphenol polyethoxylates detergents or plastics were used. Before starting the experiment, all the glassware was baked for 6 h at 400 °C and then washed five times with high purity deionized water and dried.

Sampling, sample pre-treatment

To demonstrate the applicability and reliability of the proposed method for beverages in contact with plastic containers, two groups, including alcoholic beverages (beer and wine) and non-alcoholic beverages (cherry juice, apricot juice, grape juice, water and milk samples) were bought from local supermarkets in Sivas, Turkey, and prepared for determination of BPA using the method. The selected samples, which last consumption date is less than one month, were purchased. The samples were stored as subsamples vacuum-packed in plastic bags at -10 °C until analysis.

Sample pre-treatment is very important step to separate the analyte from the matrix, because they may react with other chemical reagents with the analyte during the experimental process.

An aliquot (30 mL) of the water samples were firstly filtered through a cellulose membrane filter (Millipore) of pore size 0.45 μm . The samples were used without any pre-treatment before determination, and then the pH value was adjusted to 7.0 with 0.01– 0.1 mol L^{-1} HCl and/or NaOH, and subjected to the extraction process.

Beverage samples were subjected to UAE prior to analysis. The samples were sequentially pre-treated as follows: (Step 1) an aliquot (200 mL) of the samples were transferred into a beaker and degassed in an ultrasonic bath. (Step 2) 20 mL of dichloromethane was added to the samples. (Step 3) The mixture was then shaken vigorously for 5 min at 3200 rpm using vortex device. (Step 4) The dichloromethane layer was transferred to a flask, and the extractant was evaporated to dryness under reduced pressure at 40 °C. (Step 5) The residue was dissolved in 5 mL of ethanol and filtered. (Step 6) The final solution was completed to 100 mL with water (27).

The milk samples (5 g or 10 mL) were diluted with 30 mL of water/methanol (5:1, v/v) to destabilize milk's emulsion and to reduce viscosity of samples after efficiently shaking or vortexing for 2 min, and then sonicated in an ultrasonic bath for 10 min approximately at 30 °C until a homogeneous clear solution is obtained. The protein, casein, and fat were removed from the sample matrix by adding 5.0 mL of 2.5% (w/v) trichloroacetic acid (TCA) solution to the homogenized milk samples. After centrifugation for 10 min at 4000 rpm, the slurries were collected, and the precipitated protein and fat was rinsed five times by 3.0 mL of methanol to maximize extraction of bisphenol A. The eluate was then diluted to 100 mL with water and filtered using the membrane filters (28).

The same procedures were used for the blank solutions to determine the contamination of the reagents used. All experimental procedures were performed in triplicate.

Ultrasonic extraction procedure

The UAE procedure for separation and preconcentration of BPA was checked with model solutions. Firstly, 25.0 mL portion of a solutions containing of BPA in the range of 2–100 $\mu\text{g L}^{-1}$, 0.2 mol L^{-1} of phosphate buffer containing 5 mmol L^{-1} tartrate (pH, 8.0), 75 $\mu\text{mol L}^{-1}$ of PMZ, 125 $\mu\text{mol L}^{-1}$ of Cu(II), 200 $\mu\text{mol L}^{-1}$ of CTAB and 3.5 mmol L^{-1} of non-ionic surfactant, Tergitol 15-S-7 as extractant were added to 50 mL graduate tubes. To facilitate the charge transfer sensitized complex formation and mass transfer at micellar interface, the solution was shaken vigorously for one minute at 3200 rpm using vortex mixer, and were then filled with water up to the mark. After accomplishing the complexation, the mixture was left to stand in an ultrasonic bath at 55 °C for 5 min. in order to provide the cloud event of non-ionic surfactant. After the turbid solution is obtained, separation of the

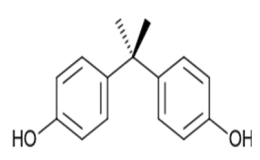
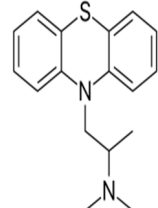
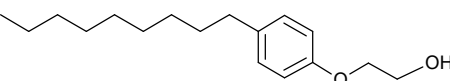
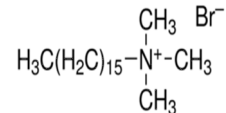
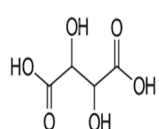
phases was provided by centrifugation for 10 min at 4000 rpm. The aqueous phase was carefully removed with a Pasteur pipette, and the surfactant-rich phase was diluted to 1.0 mL with methanol to reduce its viscosity. After UAE, the diluted phase was introduced into nebuliser of FAAS for indirect analysis of BPA.

RESULTS AND DISCUSSION

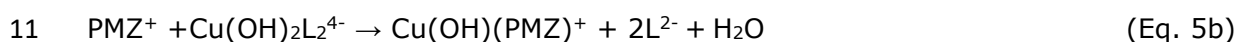
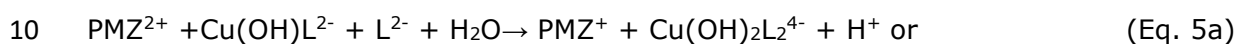
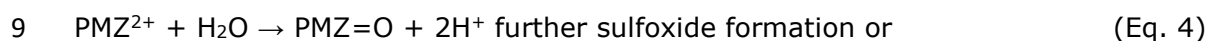
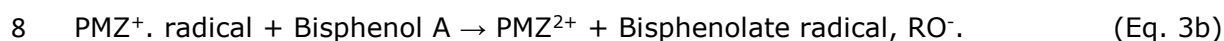
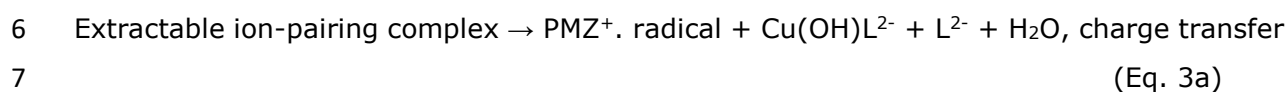
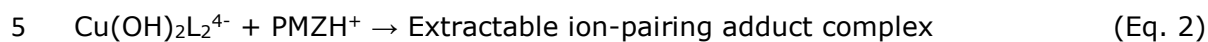
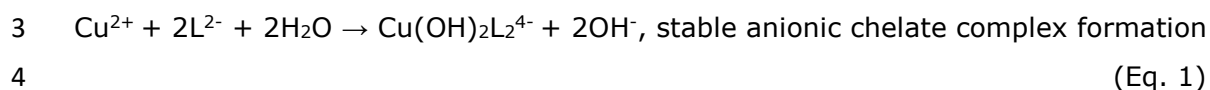
The various chemicals used in indirect determination of BPA in presence of Cu(II) by FAAS, and the possible chemical equations participated in pre-concentration procedure are as follows:

1

The chemicals used in preconcentration

Bisphenol A, BPA	Promethazine, PMZ	Tergitol 15-S-7	Cetyltrimethylammonium bromide, CTAB	Tartaric acid, H ₂ L	Copper(II) nitrate
					$\text{Cu}(\text{NO}_3)_2 \times 3\text{H}_2\text{O}$

2



12

13 Optimization of the UAE procedure

14 To demonstrate efficient extraction of BPA, the extraction system must be optimized. The
15 optimization involved testing different conditions such as pH, concentration of surfactant,
16 ion-pairing reagent concentration, metal concentration, sample volume, temperature, time
17 of ultrasonication, and interference effects from other matrix components. The variables
18 were optimized by setting all variables to be constant and optimizing one each time. The
19 BPA concentration was fixed at level of $25 \mu\text{g L}^{-1}$ during optimization studies.

20

21 Effect of pH

22 In the extraction procedure, pH of the aqueous solution one of the main factors for metal
23 chelates formation and the subsequent extraction. BPA is also a weakly acidic compound
24 (pK_a 9.7), and high pH can cause the ionization of compound(s) under test conditions (15).
25 The effect of sample pH on the analytical signal from 6.5 to 10.5 was studied for
26 measurement of Cu-complex, which is linearly related to bisphenol A concentration. The
27 results obtained are given in Fig. 1(a). As it can be observed, there was a significant
28 increase in analytical signal from pH 6.5 to pH 8.0, while the analytical signal decreased
29 when increasing the pH. The cause of decrease can greatly be dissociation of BPA to
30 phenolate anions with negative charge, due to have a pK_a value ranging from 9.6 to 11.3.
31 Another cause can be deprotonation of PMZ with a pK_a value of 9.1 (3). Therefore, the pH
32 of the solutions was adjusted to 8.0 using phosphate buffer solution (0.2 mol L^{-1}) containing
33 tartrate ions at level of 5 mmol L^{-1} , aiming the more efficient charge transfer complexation
34 between ion-pairing reagent, PMZH^+ and stable copper-tartrate complex, $[\text{Cu}(\text{OH})_2\text{L}_2]^{4-}$ in
35 presence of BPA in relation of the hydrolysis of the copper. Also, the effect of 0.2 mol L^{-1}
36 buffer volume at pH 8.0 was investigated in range of 0.5-5.0 mL, and a buffer volume of
37 2.5 mL was found to be enough, so as to give maximum, reproducible and stable analytical
38 signal.

39

40

41 *Effect of ion-pairing reagent concentration*

42 Among chemical variables, ion-pairing reagent concentration is a critical parameter for
43 formation of an ion-pairing complex also to compensate for any interactions with interfering
44 ions that may exist in the sample. Thus, the ion-pairing reagent must provide the following
45 features. (I) The ion-pair complex formed should be sufficiently hydrophobic, (II) have a
46 high partition coefficient, and (III) form the stable complex quickly and quantitatively with
47 minimum excess of reagent. As a result of the prior studies in literature, we selected PMZ,
48 a phenothiazine derivative as ion-pairing reagent in order to obtain efficient separation and
49 pre-concentration of BPA from sample matrix. Also, the pK_a value of this ion-pairing
50 reagent, which can easily be oxidized chemically or electrochemically, is 9.1 (29). It is a
51 versatile chelating ligand, which can be relatively able to form stable metal complexes (30)
52 and form aggregates in a micelle-like manner with the value of N_{agg} (aggregation number)
53 of the order of 6 to 15 depending on concentration, pH, and temperature (31).

54
55 The effect of PMZ concentration on the analytical signal is evaluated in the range of 10-
56 125 $\mu\text{mol L}^{-1}$. As it can be observed (Fig. 1(b)), the analytical signals are enhanced
57 remarkably depending on PMZ concentration. The analytical signal reaches to maximum
58 when the PMZ concentration is 75 $\mu\text{mol L}^{-1}$. When the concentration continues to increase
59 until 100 $\mu\text{mol L}^{-1}$, the analytic signal of BPA slightly decreased, later become flat. This is
60 the main reason; the excess of PMZ, which is in equilibrium of protonated and deprotonated
61 forms, PMZH^+ and PMZ , is presumably trapped in the micelles. A 75 $\mu\text{mol L}^{-1}$ of PMZ solution
62 was therefore selected for successful extraction in subsequent experiments.

63 64 *Effect of metal concentration*

65 In order to be able to perform an indirect analysis with FAAS, the amount of analyte must
66 be associated with a signal of metal. To accomplish this, preliminary study has been done
67 with different metal ions (iron, nickel, cobalt and copper) at equal amounts in the presence
68 of BPA and PMZ. The best sensitivity and stable signal is obtained when Cu(II) is used.
69 This state can be explained with the fact that Cu(II) ions form a stable anionic complex,
70 $[\text{Cu(OH)}_2\text{L}_2]^{4-}$ with tartrate ion in presence of BPA as a reducing species and PMZ, an ion-
71 pairing reagent, which can be easily oxidized in redox environment and form dimer and
72 further aggregates by pH dependent charge transfer. Also, it is implied in literature that
73 Cu^{2+} ions form a cationic complex with PMZ at pH 5.0, and anionic complex with tartrate
74 ions with stability constants of $\log \beta$: 20.7 and 17.3 in form of $\text{Cu(OH)}_2\text{L}_2^{4-}$ above pH 5.7
75 (30, 32). In this context, the effect of Cu(II) concentration was investigated in the range
76 of 25-300 $\mu\text{mol L}^{-1}$. The results obtained in triplicate (Fig. 1(c)) showed that the analytical
77 signal increases significantly with the Cu(II) concentration up to 125 $\mu\text{mol L}^{-1}$, at higher

78 concentrations there was no significant change. Therefore, a 125 $\mu\text{mol L}^{-1}$ Cu(II)
79 concentration was selected for successful extraction in subsequent experiments.

80

81 *Effect of auxiliary ligand concentration*

82 The UA-CPE efficiency depends on the formation of hydrophobic ion-pairing complex and
83 the mass transference between the phases. To create a stable ion-association between
84 cationic PMZH⁺ and anionic copper complex, Cu(OH)₂L₂⁴⁻ formed after pH sensitive charge
85 transfer process between BPA and Cu(II). Therefore, the cationic surfactant, CTAB, was
86 adopted and used as the sensitivity enhancer or counter ion in order to be able to detect
87 BPA at sub- $\mu\text{g kg}^{-1}$ or $\mu\text{g L}^{-1}$ levels. It is indicated that CTAB below and above its critical
88 micelle concentration (CMC) is used effectively to enhance the sensitivity and signal
89 reproducibility of the electroanalytical techniques such as differential pulse voltammetry,
90 linear sweep voltammetry and square wave voltammetry in determination of phenol and
91 BPA as contaminant in waters and foodstuffs stored in plastic container (33, 34). The effect
92 of CTAB concentration was investigated in the range 0.0–400 $\mu\text{mol L}^{-1}$. According to the
93 results shown in Fig. 1(d), the analytical signal increased by increasing CTAB concentration
94 up to 400 $\mu\text{mol L}^{-1}$ and decreased at higher concentrations. Excessive amount of CTAB is
95 passed to surfactant rich phase. Therefore, a 200 $\mu\text{mol L}^{-1}$ of CTAB concentration was
96 selected for successful extraction in subsequent experiments.

97

98 *Effect of extracting agent concentration*

99 In the extraction process, one of the most important parameters is the type and
100 concentration of the extracting agent. It is preferred that the extracting non-ionic
101 surfactants to be used in experiments have properties such as cheap, eco-friendly, effective
102 separation and commercial availability as well as being biodegradable and not absorbing
103 and fluorescing in the UV region, in which the BPA is generally detected by LC, CE and/or
104 CZE with detection of UV and fluorescence. Also, the surfactant concentration must be
105 sufficient above the CMC to guarantee a quantitative extraction. In addition to all these,
106 the volume ratio of the phases should be investigated, because an increase in surfactant
107 concentration can decrease the analytical signal depending on dilution of the extract in the
108 surfactant-rich phase volume. For all these reasons, the effect of type and concentration
109 of the extracting non-ionic surfactant was investigated.

110

111 As can be seen in Fig. 1(e), the best results were obtained when using Tergitol 15-S-7. At
112 lower concentrations, the phase separation was difficult due to the low-volume rich phase
113 and the inadequacy of the assemblies to entrap the hydrophobic complexes quantitatively.
114 Analytical signal was also increased in concentration range of 1.0-4.0 mmol L^{-1} , and the
115 highest signal was obtained at 3.5 mmol L^{-1} with a higher concentration of 40-fold, in which

116 its CMC value is 0.092 mmol L⁻¹. Therefore, it was selected for successful extraction in
117 subsequent experiments.

118

119 *Effect of sample volume*

120 Since amount of BPA is low into real samples, the effect of sample volume was also tested
121 in range of 10-250 mL with a constant amount of BPA. The results, as can be seen in Fig.
122 1(f), demonstrated that quantitative analytical signal for sample volumes was obtained in
123 range of 50-150 mL. Above 150 mL, the analytical signal decreased slightly. After UAE, the
124 surfactant-rich phase was completed to 1 mL with methanol, so the pre-concentration
125 factor was 150.

126

127 *Effects of equilibrium temperature and time*

128 Optimal equilibration temperature is necessary for the completion of the ion-pairing
129 complex formation and efficient phase separation. This hydrophobic complex, which is
130 bound to core and interface of the micelles by polar ethoxylate groups of micelles and
131 hydrophobic interactions, is extracted to the surfactant-rich phase, and this event can be
132 achieved when the equilibration temperature is above the cloud point temperature (CPT)
133 of a non-ionic surfactant. Therefore, the equilibration temperature was investigated in the
134 range of 25-70 °C. From studies, when the temperature increased in the range from 25 to
135 55 °C, the analytical signals increased correspondingly for BPA. At higher temperatures,
136 the analytical signal is decreased. This is because the resulting ion-pair complex is
137 reversibly dispersed to the solution depending on the temperature. Thus, 55 °C was chosen
138 as the optimal equilibration temperature for successful extraction in subsequent
139 experiments

140

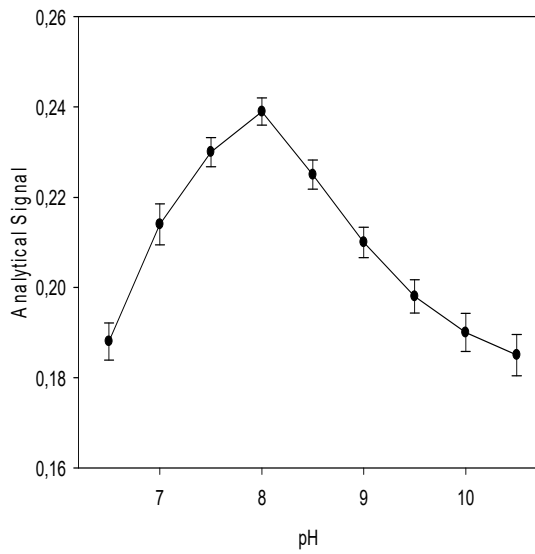
141 In the extraction process, the sonication time is one of the prime factors influencing the
142 BPA extraction and mass transfer into surfactant-rich phase. Sonication caused an increase
143 in the mass transfer, and a decrease in reaction time. To minimize the time required for
144 extraction, sonication time was investigated in range of 1-15 min and the results are shown
145 in Fig. 1(g). Based on the results, the best analytical signal was obtained at 10 min. Thus,
146 10 min was chosen as the optimal sonication time for successful extraction in subsequent
147 experiments.

148

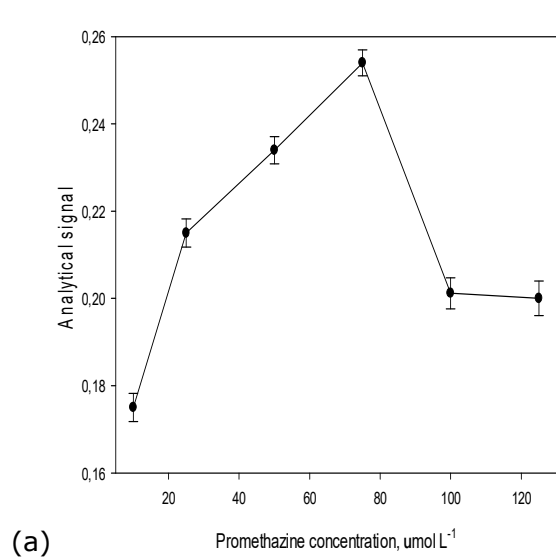
149 *Effect of solvent*

150 After centrifugation for 5 min at 4000 rpm, the obtained surfactant rich phase is low volume
151 and high viscous. Therefore, analysis with FAAS cannot be done. To overcome this problem,
152 this phase must be diluted with a suitable solvent. The results indicated that methanol was

153 a suitable diluting solvent and also a suitable matrix for indirect determination of BPA using
 154 FAAS.

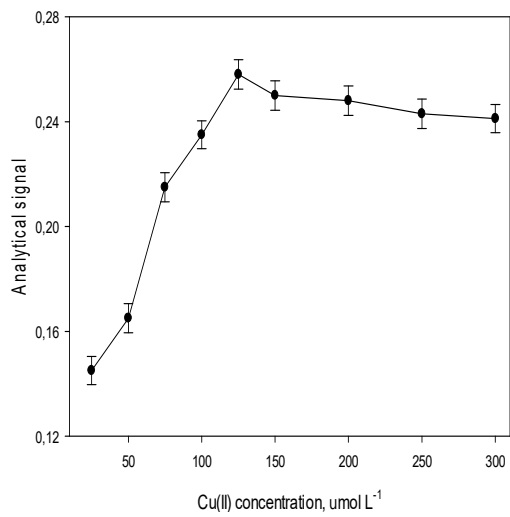


155

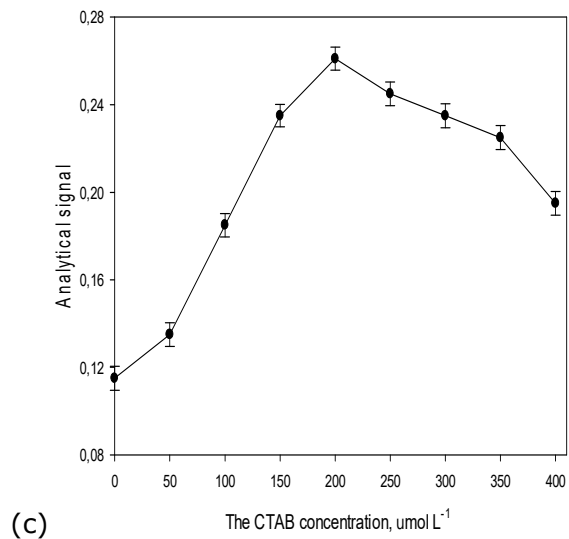


(a)

(b)

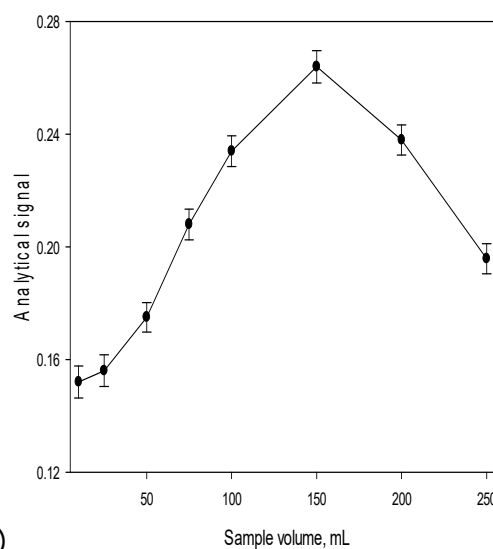
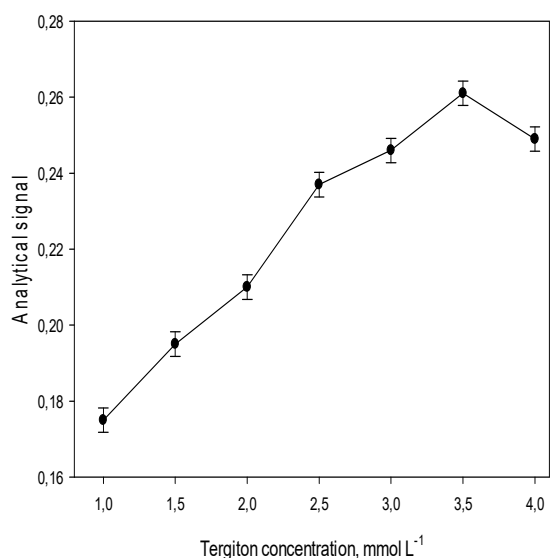


156



(c)

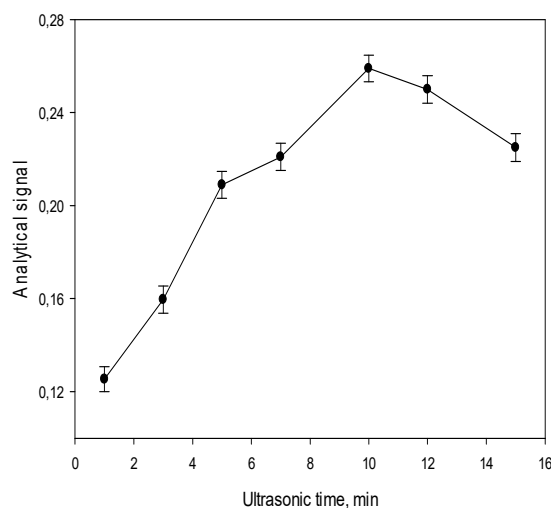
(d)



157

(e)

(f)



158

(g)

159 **Figure 1 (a-g).** Optimization of parameters affecting UAE for triplicate measurements of
 160 25 $\mu\text{g L}^{-1}$ BPA.

161 *The matrix effect*

162 The BPA exists along with different interfering species in selected samples. This event may
 163 be attributed to the extraction step, because high selectivity with careful utility of FAAS
 164 can be provided. Thus, the effects of some foreign ions were investigated by conducting
 165 UAE experiments using solutions containing 20 $\mu\text{g L}^{-1}$ of BPA in the presence of different
 166 mass ratios of foreign ions under the extraction conditions. Tolerable limit is considered as
 167 the interfering agent level that is not significantly affect the preconcentration via UAE and
 168 subsequent determination of BPA by FAAS as determinate error smaller than $\pm 5.0\%$. The
 169 results showed that at least 10000 $\mu\text{g L}^{-1}$ of Na^+ , Ca^{2+} , NH_4^+ , SO_4^{2-} , NO_3^- , Fe^{3+} , Al^{3+} , and
 170 Cl^- , 5000 $\mu\text{g L}^{-1}$ of Mg^{2+} and PO_4^{3-} , 1000 $\mu\text{g L}^{-1}$ of 2-chlorobenzaldehyde,
 171 bromobenzaldehyde, phenol, and 4-nitrophenol and 750 $\mu\text{g L}^{-1}$ of 2,4-dinitrophenol had no
 172 remarkable interferences with the determination of BPA. 2-aminophenol, acetaldehyde and

173 acetate could be tolerated up to 500 $\mu\text{g L}^{-1}$ and nonylphenol and octylphenol could be
174 tolerated up to 250 $\mu\text{g L}^{-1}$. As can be understood from the results, the tolerance limits of
175 the foreign ions have a good tolerance to matrix interference. Therefore, this method could
176 be applied to successfully for the extraction of BPA in selected sample matrices.

177

178 *Analytical figures of merit*

179 Under the optimal conditions, calibration graph was performed using standard addition
180 calibrations prepared following the UAE procedure. Table 1 shows the characteristic
181 performances of the proposed method. The calibration graph prepared from the aqueous
182 standards was linear in the range of 1.5-100 $\mu\text{g L}^{-1}$ with a good correlation coefficient (r)
183 of 0.9943. The limit of detection (LOD), defined as the concentration that gives a signal
184 equivalent to three times the standard deviation of 10 replicate measurements of the
185 procedural blank sample (blank digest preconcentrated by the UAE procedure), was 0.47
186 $\mu\text{g L}^{-1}$. For the precision of the method, the relative standard deviations (RSD) of the five
187 independent replicate measurements for 20 and 50 $\mu\text{g L}^{-1}$ of BPA are lower than 3.5%. The
188 percent recoveries obtained were in range of 95.8-103.9% for the spiked BPA
189 concentration of 20 and 50 $\mu\text{g L}^{-1}$ to the selected samples. As mentioned previously, the
190 amount of BPA in 150 mL of sample volume was determined after extraction process by
191 1.0 mL of surfactant-rich phase, therefore the pre-concentration factor for this method is
192 150. Sensitivity enhancement factor, which calculated from the ratio of the slopes of the
193 calibration curves obtained with and without pre-concentration, was 135.

194

195 Due to lack of a certified reference material (CRM), which is suitable to sample matrix for
196 evaluation of the accuracy, the matrix-matched solutions were also prepared by externally
197 adding eight pointed standard solutions of BPA ranging from 5 to 125 $\mu\text{g L}^{-1}$ to blank sample
198 matrix. The milk powder that does not contain the analyte was used as blank sample for
199 calibration of "matrix-matched". The further pre-treatment of the spiked samples was
200 carried out according to the two different extraction approaches described in sample
201 preparation section. After stepwise dilution from stock solution, the eight concentration
202 levels of concentrations for bisphenol A were 5, 10, 15, 25, 50, 75, 100 and 125 $\mu\text{g L}^{-1}$. In
203 a similar way, the externally spiked samples under optimal conditions were submitted to
204 UAE procedure, and then each point was detected three times by FAAS. From regression
205 analysis, the calibration data obtained for matrix-matched solutions and the analytical
206 features of the method based on these data are represented in Table 1. Additionally, the
207 recovery study for five replicate measurements of 20 and 50 $\mu\text{g L}^{-1}$ of the BPA was
208 conducted and found to be in range of 93.5-106.2% with lower RSD than 4.2%.

209

Table 1 The analytical features of the proposed method for BPA

Parameters	By direct calibration solutions	By matrix matched calibration solutions
Linear range ($\mu\text{g L}^{-1}$)	1.5-100	3-125
Regression equation	$A = 4.2 \times 10^{-3} [\text{BPA } \mu\text{g L}^{-1}] + 1.7 \times 10^{-4}$	$A = 3.7 \times 10^{-3} [\text{BPA, } \mu\text{g L}^{-1}] + 2.2 \times 10^{-4}$
Correlation coefficient, r	0.9943	0.9956
Limit of detection ($3\sigma_b/m$) ($\mu\text{g L}^{-1}$)	0.47	0.95
Limit of quantification ($10\sigma_b/m$) ($\mu\text{g L}^{-1}$)	1.56	3.20
Recovery (%)	95.8-103.9	93.5-106.2
Reproducibility (%)	3.4	4.1
Repeatability (%)	3.2	3.9
Sensitivity enhancement factor (EF)	135	115
Pre-concentration factor (PF)	150	150

210

The accuracy and precision

The accuracy was tested through the recovery tests from spiked samples. The work was carried out in the following way, analytical recovery was checked for 20 and 50 $\mu\text{g L}^{-1}$ of BPA, after spiking different aliquots of the selected samples. Each concentration level was repeated in five times by the UAE procedure, and each extract was determined through FAAS. The analytical recoveries obtained were in range of 95.0-103.8% for spiked concentrations. The more detailed results are given in Table 2 (a-c).

The precision was tested by studying the parameters of the repeatability and reproducibility. For the repeatability precision, using selected two of the beverages and milk samples fortified with BPA at the concentrations of 10, 25 and 50 $\mu\text{g L}^{-1}$ were calculated by analysing (five replicate). Then, the mean BPA concentrations were determined as 10.5, 24.3, 50.7 $\mu\text{g L}^{-1}$ and with associated RSD values of 3.4%, 3.1% and 2.9%, respectively. Regarding the reproducibility precision, the same three concentrations were calculated for five consecutive days, providing mean BPA concentrations of 10.2, 25.8, 51.1 $\mu\text{g L}^{-1}$ and associated RSD values of 3.2%, 2.8% and 2.7%, respectively. When looking at the results obtained, we can conclude that the method offers good precision.

Analytical applications

Different beverage samples in contact with plastic containers were analyzed using the proposed method in order to prove its suitability for the routine control and selective extraction of BPA. The results were given in Table 2(a-c) as well as the recoveries obtained after spiking the samples with 20 $\mu\text{g L}^{-1}$ and 50 $\mu\text{g L}^{-1}$ of BPA. The recovery% was calculated by using the equation: $\text{Recovery\%} = 100 (C_s - C_0)/m$ where C_s is the amount of total BPA in sample after spiking, C_0 is the amount of BPA in original sample and m is the amount of BPA spiked at known levels. The spiked recoveries of the method for analysis of BPA in water samples were found in range of 97.2-103.1%, with the RSD varying from 2.2 to 3.0%. For the beverage and milk samples, the spiked recoveries were found in range of 95.0-103.5% and 95.3-103.8%, respectively. The RSDs were lower than 3.9%. In the study, the lowest amount of BPA ($2.70 \pm 0.07 \mu\text{g L}^{-1}$) was found in water samples and the highest amount of BPA in grape juice ($19.2 \pm 0.5 \mu\text{g L}^{-1}$). This is the main reason; the acidic medium may accelerate the leaching of BPA into the sample. Thus, the method is capable of the determination of BPA in these sample matrices. In addition, BPA concentrations in range of 2.7 - 3.8 $\mu\text{g L}^{-1}$ (bottled drinking water), 3.1-5.4 $\mu\text{g L}^{-1}$ (milk samples) to 4.3-19.2 $\mu\text{g L}^{-1}$ (beverages with and without alcohol) were significantly lower than specific migration limit (SML) of 600 $\mu\text{g kg}^{-1}$ set by the EC Directive for BPA in foods or food simulants, so as not to lead any safety risk on humans consuming the samples.

Table 2(a) The analysis results of determination of BPA in spiked water samples using the proposed method (n: 5).

Added ($\mu\text{g L}^{-1}$)	Commercial drinking water ¹			Commercial drinking water ²			Commercial drinking water ³		
	Found ($\mu\text{g L}^{-1}$)	Recovery (%)	RSD (%)	Found ($\mu\text{g L}^{-1}$)	Recovery (%)	RSD (%)	Found ($\mu\text{g L}^{-1}$)	Recovery (%)	RSD (%)
-	2.70±0.07	-	2.5	3.80±0.1	-	3.0	3.10±0.08	-	2.7
20	22.1±0.5	97.2	2.4	24.4±0.7	103.1	2.7	22.8±0.6	98.5	2.5
50	51.7±1.2	98.1	2.2	54.7±1.4	101.8	2.6	52.6±1.3	99.0	2.4

^{1,2,3} Represents the waters in different brands.

Table 2(b) The analysis results of determination of BPA in spiked milk samples using the proposed method (n: 5).

Added ($\mu\text{g L}^{-1}$)	Whole milk			Semi-skimmed milk			Milkshake		
	Found ($\mu\text{g L}^{-1}$)	Recovery (%)	RSD (%)	Found ($\mu\text{g L}^{-1}$)	Recovery (%)	RSD (%)	Found ($\mu\text{g L}^{-1}$)	Recovery (%)	RSD (%)
-	4.8±0.1	-	2.9	3.1±0.1	-	3.3	5.4±0.2	-	3.5
20	24.1±0.6	96.3	2.7	22.2±0.7	95.3	3.1	26.2±0.8	103.8	3.2
50	53.6±1.3	97.5	2.5	51.3±1.4	96.4	2.8	56.6±1.7	102.3	3.0

1 **Table 2(c)** The analysis results of determination of BPA in spiked beverage samples
 2 using the proposed method (n: 5).

Sample group	Sample type	Added ($\mu\text{g L}^{-1}$)	Found ($\mu\text{g L}^{-1}$)	Recovery (%)	RSD (%)
Alcoholic beverages	Beer	-	6.4 \pm 0.2	-	3.5
		20	25.4 \pm 0.8	95.0	3.2
		50	54.8 \pm 1.5	96.7	2.8
	Wine	-	7.7 \pm 0.3	-	3.9
		20	28.4 \pm 1.1	103.5	3.7
		50	58.8 \pm 2.0	102.1	3.4
Non-alcoholic beverages	Cherry juice	-	8.5 \pm 0.3	-	3.2
		20	28.0 \pm 0.8	97.4	3.0
		50	57.8 \pm 1.7	98.6	2.9
	Apricot juice	-	4.3 \pm 0.1	-	2.5
		20	24.8 \pm 0.5	102.4	2.2
		50	54.9 \pm 1.2	101.2	2.1
	Grape juice	-	19.2 \pm 0.5	-	2.8
		20	38.6 \pm 0.9	96.9	2.5
		50	68.1 \pm 1.6	97.8	2.4

3

4 *Comparison with literature*

5 In order to indicate positive aspects of the proposed method, a comparison between the
 6 figures of merit of the proposed method and some of the recently published methods for
 7 extraction and determination of BPA is given in Table 3 in terms of some optimization
 8 parameters. As can be seen from the data, the pre-concentration factor of the proposed
 9 method is relatively higher and, consequently, its detection limit is either lower or
 10 comparable to the more sensitive method of chromatographic techniques except for LC-
 11 MS-MS and GC-MS with pre-concentration and *in situ* derivatization. However, these
 12 techniques have lower recovery and poor precision than those of our method especially at
 13 low concentrations. Additionally, they are complex and expensive, and needs expert user
 14 in his/her area and tedious and time consuming separation and/or pre-concentration steps
 15 before detection with UV, fluorescence and mass spectrometry. The combination of UAE
 16 with FAAS as element-selective detection tool enables accurate and reliable determination
 17 of BPA in ranges of 1.5-100 and 3-125 $\mu\text{g L}^{-1}$ by calibration curves prepared from aqueous
 18 standards and matrix-matched standards with detection limits of 0.47 and 0.95 $\mu\text{g L}^{-1}$,
 19 respectively. Also, the extraction time and the intra-day/inter-day precision of by the
 20 method as RSD% are far better than most of the other reported methods. In addition, the
 21 UAE procedure has some advantages including green chemistry solvents, simplicity,
 22 rapidity and low contamination risk for the analysis.

23

Table 3 Comparison of proposed method with those of other methods.

Sample matrix	Extraction process	Detection technique	^a LR ($\mu\text{g L}^{-1}$)	LOD ($\mu\text{g L}^{-1}$)	RSD (%)	Recovery (%)	^b EF or ^c PF	References
Waters and urine	¹ MISPE	² CE-UV	3-500	0.3	$\leq 7.2\%$	95.2-105.4%	50	(3)
Urine samples	³ CME	⁴ LC-FD	0.4-149	0.197	4.5%	88-95%	38	(8)
Soils	⁵ UAE	⁶ GC-MS	5-300	0.03 ng g ⁻¹	9.6%	88.1-107.7%	-	(18)
Waters	⁷ CPE	⁸ LC-UV	1-100	0.34	-	90-108.6%	50	(20)
Waters	⁹ SPE	¹⁰ LC-MS/MS	0.02-0.2	0.057	$\leq 13\%$	85-100%	-	(35)
Waters	¹¹ DLLME	¹² HPLC-UV	0.5-100	0.07	6.0%	93.4-98.2%	80	(36)
Serum	-	¹³ ELISA	0.3-100	0.3	13.6%	81.9-97.4%	-	(37)
Leachate	¹⁴ SPME	HPLC-UV	12.8-192	3.25	4.4%	94.5-103.3%	-	(38)
Soft drinks and powdered infant formula	¹⁵ LPME	GC-MS	1-1000	0.005	15%	82-111%, 68-114%	-	(39)
Water, urine, plasma and saliva samples	¹⁶ SBSE	GC-MS with and without derivatization	0.02-10, 2-100	0.005, 0.5	3.8-9.6%	95.2-104.6%	-	(40)
Beverages and Waters	UA-CPE	FAAS	1.5-100, 3-125	0.47, 0.95	$\leq 3.9\%$	95.8-103.9%	135, 150	Present method

24 ^aLinear range, ^bEnhancement factor, ^cPreconcentration factor ¹Molecularly imprinted solid-phase extraction; ²Capillary electrophoresis-UV
25 method; ³Coacervative microextraction; ⁴Liquid chromatography-fluorescence detection; ⁵Ultrasonic assisted extraction; ⁶Gas
26 chromatography-mass spectrometry; ⁷Cloud-point extraction; ⁸Liquid chromatography; ⁹Solid-phase extraction; ¹⁰Liquid chromatography-
27 tandem mass spectrometry; ¹¹Dispersive liquid-liquid microextraction; ¹²High-performance liquid chromatography; ¹³Enzyme-linked
28 immunosorbent assay; ¹⁴Solid phase microextraction; ¹⁵Liquid phase microextraction; ¹⁶Stir bar sorptive extraction.

29 CONCLUSIONS

30
31 In the present study, a simple, rapid, inexpensive, and sensitive analytical method, based
32 on highly effective coupling of UAE with highly selective FAAS was proposed to determine
33 BPA in different beverage samples. This study is the first method reported for indirect
34 determination of BPA using FAAS. Especially, the use of ultrasound energy in sample
35 preparation has provided features like low organic solvent usage, and less extraction
36 duration. Other advantages can be pointed out like the low limits of detection, good
37 precision and good selectivity, wide linear working range, high analytical signal, as well as
38 low reagent consumption, high pre-concentration and sensitivity enhancement factors. The
39 quantitation or determination limit of the proposed method is about $1.6 \mu\text{g L}^{-1}$, so it can
40 be used for the routine control of BPA in different beverage samples below the current
41 specific migration limit (SML) of $600 \mu\text{g L}^{-1}$ set by the EU Commission. As a result, the
42 effectiveness and efficiency of the proposed method was successfully demonstrated for
43 BPA determination and applied to different beverage samples.

44

45 ACKNOWLEDGMENTS

46

47 The current study was financially supported by Cumhuriyet University Scientific Research
48 Projects Commission as the research projects with the F-503 code.

49

50 REFERENCES

51

52 1. Braunrath, R, Podlipna, D, Padlesak, S, Cichna-Markl M. Determination of bisphenol A in canned
53 foods by immunoaffinity chromatography, HPLC, and fluorescence detection. *Journal of agricultural
54 and food chemistry*. 2005; 53(23): 8911-8917.

55

56 2. Calafat AM, Kuklennyik Z, Reidy JA, Caudill SP, Ekong J, Needham LL. Urinary concentrations of
57 bisphenol A and 4-nonylphenol in a human reference population. *Environmental health
58 perspectives*. 2005; 391-395.

59

60 3. Mei S, Wu D, Jiang M, Lu B, Lim JM, Zhou YK, Lee YI. Determination of trace bisphenol A in
61 complex samples using selective molecularly imprinted solid-phase extraction coupled with
62 capillary electrophoresis. *Microchemical Journal*. 2011; 98(1): 150-155.

63

64 4. Lang IA, Galloway TS, Scarlett A, Henley WE, Depledge M, Wallace RB, Melzer D. Association of
65 urinary bisphenol A concentration with medical disorders and laboratory abnormalities in adults.
66 *Jama*. 2008; 300(11): 1303-1310.

67

- 68 5. Najafi M, Khalilzadeh MA, Karimi-Maleh H. A new strategy for determination of bisphenol A in the
69 presence of Sudan I using a ZnO/CNTs/ionic liquid paste electrode in food samples. Food
70 chemistry. 2014; 158: 125-131.
71
- 72 6. Christian LJ, Mortensen A. European Food Safety Authority (EFSA), 2007.
73
- 74 7. Commission Directive 2011/8/EU of 28 January 2011 amending Directive 2002/72/EC as regards
75 the restriction of use of bisphenol A in plastic infant feeding bottles. Off J Eur Union. L26/11
76
- 77 8. García-Prieto A, Lunar ML, Rubio S, Pérez-Bendito D. Determination of urinary bisphenol A by
78 coacervativemicroextraction and liquid chromatography–fluorescence detection. Analytical
79 acta. 2008; 630(1): 19-27.
80
- 81 9. Alabi A, Caballero-Casero N, Rubio S. Quick and simple sample treatment for multiresidue
82 analysis of bisphenols, bisphenol diglycidyl ethers and their derivatives in canned food prior to
83 liquid chromatography and fluorescence detection. Journal of Chromatography A. 2014; 1336: 23-
84 33.
85
- 86 10. Wilczewska K, Namieśnik J, Wasik A. Troubleshooting of the determination of bisphenol A at
87 ultra-trace levels by liquid chromatography and tandem mass spectrometry. Analytical and
88 bioanalytical chemistry. 2016; 408(3): 1009-1013.
89
- 90 11. Deceuninck Y, Bichon E, Marchand P, Boquien CY, Legrand A, Boscher C, Le Bizec B.
91 Determination of bisphenol A and related substitutes/analogues in human breast milk using gas
92 chromatography-tandem mass spectrometry. Analytical and bioanalytical chemistry. 2015; 407(9):
93 2485-2497.
94
- 95 12. Zhang X, Zhu D, Huang C, Sun Y, Lee YI. Sensitive detection of bisphenol A in complex
96 samples by in-column molecularly imprinted solid-phase extraction coupled with capillary
97 electrophoresis. Microchemical Journal. 2015; 121: 1-5.
98
- 99 13. Zhong S, Tan SN, Ge L, Wang W, Chen, J. Determination of bisphenol A and naphthols in river
100 water samples by capillary zone electrophoresis after cloud point extraction. Talanta. 2011; 85(1):
101 488-492.
102
- 103 14. De Meulenaer B, Baert K, Lanckriet H, Van Hoed V, Huyghebaert A. Development of an
104 enzyme-linked immunosorbent assay for bisphenol A using chicken immunoglobulins. Journal of
105 agricultural and food chemistry. 2002; 50(19): 5273-5282.
106
- 107 15. Li J, Kuang D, Feng Y, Zhang F, Liu M. Voltammetric determination of bisphenol A in food
108 package by a glassy carbon electrode modified with carboxylated multi-walled carbon nanotubes.
109 Microchimica Acta. 2011; 172(3-4): 379-386.
110

- 111 16. Chen X, Ren T, Ma M, Wang Z, Zhan G, Li C. Voltammetric sensing of bisphenol A based on a
112 single-walled carbon nanotubes/poly {3-butyl-1-[3-(N-pyrrolyl) propyl] imidazolium ionic liquid}
113 composite film modified electrode. *Electrochimica Acta*. 2013; 111: 49-56.
114
- 115 17. Karimi-Maleh H, Sanati AL, Gupta VK, Yoosefian M, Asif M, Bahari A. A voltammetric biosensor
116 based on ionic liquid/NiO nanoparticle modified carbon paste electrode for the determination of
117 nicotinamide adenine dinucleotide (NADH). *Sensors and Actuators B: Chemical*. 2014; 204: 647-
118 654.
119
- 120 18. Sánchez-Brunete C, Miguel E, Tadeo JL. Determination of tetrabromobisphenol-A,
121 tetrachlorobisphenol-A and bisphenol-A in soil by ultrasonic assisted extraction and gas
122 chromatography–mass spectrometry. *Journal of Chromatography A*. 2009; 1216(29):5497-5503.
123
- 124 19. O’Mahony J, Moloney M, McCormack M, Nicholls IA, Mizaikoff B, Danaher M. Design and
125 implementation of an imprinted material for the extraction of the endocrine disruptor bisphenol A
126 from milk. *Journal of Chromatography B*. 2013; 931, 164-169.
127
- 128 20. Yi-Jun YU, Guan-Yong SU, Michael HW, Paul KS, Hong-Xia YU. Cloud point extraction of
129 bisphenol A from water utilizing cationic surfactant aliquat 336. *Chinese Journal of Analytical
130 Chemistry*. 2009; 37(12): 1717-1721.
131
- 132 21. Cunha SC, Cunha C, Ferreira AR, Fernandes JO. Determination of bisphenol A and bisphenol B
133 in canned seafood combining QuEChERS extraction with dispersive liquid–liquid
134 microextraction followed by gas chromatography–mass spectrometry. *Analytical and bioanalytical
135 chemistry*. 2012; 404(8): 2453-2463.
136
- 137 22. Hu X, Wu X, Yang F, Wang Q, He C, Liu S. Novel surface dummy molecularly imprinted silica as
138 sorbent for solid-phase extraction of bisphenol A from water samples. *Talanta*. 2016; 148: 29-36.
139
- 140 23. Chemat F, Rombaut N, Sicaire AG, Meullemiestre A, Fabiano-Tixier AS, Abert-Vian M.
141 Ultrasound assisted extraction of food and natural products. Mechanisms, techniques,
142 combinations, protocols and applications. A review. *Ultrasonics Sonochemistry*. 2017; 34:540-560.
143
- 144 24. Altunay N, Gürkan, R. An Inexpensive and Sensitive Method for Speciative Determination of
145 Sn (IV), Sn (II), and Total Sn as Sn (IV) in Selected Beverages by Micellar Improved
146 Spectrophotometry. *Food Analytical Methods*. 2015; 8(4): 994-1004.
147
- 148 25. Li JL, Chen BH. Equilibrium partition of polycyclic aromatic hydrocarbons in a cloud-point
149 extraction process. *Journal of colloid and interface science*. 2003; 263(2):625-632.
150
- 151 26. Bai D, Li J, Chen SB, Chen BH. A novel cloud-point extraction process for preconcentrating
152 selected polycyclic aromatic hydrocarbons in aqueous solution. *Environmental science &
153 technology*. 2001; 35(19): 3936-3940.

- 154
155 27. Deng P, Xu Z, Kuang Y. Electrochemical determination of bisphenol A in plastic bottled drinking
156 water and canned beverages using a molecularly imprinted chitosan-graphene composite film
157 modified electrode. *Food chemistry*. 2014; 157: 490-497.
158
- 159 28. Liu X, Ji Y, Zhang H, Liu M. Elimination of matrix effects in the determination of bisphenol A in
160 milk by solid-phase microextraction-high-performance liquid chromatography. *Food Additives and*
161 *Contaminants*. 2008; 25(6); 772-778.
162
- 163 29. Katzung, B. G., Masters, S. B., & Trevor, A. J. (Eds.). (2004). *Basic & clinical*
164 *pharmacology* (Vol. 8). New York, NY, USA:: Lange Medical Books/McGraw-Hill.
165
- 166 30. BagheriGhomi A, Mazinani F. Spectrophotometric Study of Stability Constants of Metal
167 Complexes of Promethazine at Different Temperatures. *Physical Chemistry & Electrochemistry*.
168 2013; 2(1): 13-19.
169
- 170 31. Kabir-ud-Din, Rub, MA, Alam MS. Micellization and Clouding Phenomenon of Phenothiazine
171 Drug Promethazine Hydrochloride: Effect of NaCl and Urea Addition. *Journal of Dispersion Science*
172 *and Technology*. 2010; 31(9): 1182-1187.
173
- 174 32. Ballesteros J C, Chainet E., Ozil, P., Meas, Y., & Trejo, G. (2011). Electrodeposition of Copper
175 from Non-Cyanide Alkaline Solution Containing Tartrate. *Int. J. Electrochem. Sci*, 6, 2632-2651.
176
- 177 33. Huang W, Zhou D, Liu X, Zheng X. Electrochemical determination of phenol using CTAB-
178 functionalized montmorillonite electrode. *Environmental technology*. 2009; 30(7):701-706.
179
- 180 34. Kim BK, Kim JY, Kim DH, Choi HN, Lee WY. Electrochemical determination of bisphenol A at
181 carbon nanotube-doped titania-nafion composite modified electrode. *Bulletin of the Korean*
182 *Chemical Society*. 2013; 34(4): 1065-1069.
183
- 184 35. Gallart-Ayala H, Moyano E, Galceran MT. On-line solid phase extraction fast liquid
185 chromatography-tandem mass spectrometry for the analysis of bisphenol A and its chlorinated
186 derivatives in water samples. *Journal of Chromatography A*. 2010; 1217(21):3511-3518.
187
- 188 36. Rezaee M, Yamini Y, Shariati S, Esrafil A, Shamsipur M. Dispersive liquid-liquid
189 microextraction combined with high-performance liquid chromatography-UV detection as a very
190 simple, rapid and sensitive method for the determination of bisphenol A in water samples. *Journal*
191 *of Chromatography A*. 2009; 1216(9): 1511-1514.
192
- 193 37. Ohkuma H, Abe K, Ito M, Kokado A, Kambegawa A, Maeda M. Development of a highly
194 sensitive enzyme-linked immunosorbent assay for bisphenol A in serum. *Analyst*. 2002; 127(1):
195 93-97.

196
197 38. Deng L, Liu Y X, Chen PY, Wang L, Deng NS. Determination of trace bisphenol A in leachate by
198 solid phase microextraction coupled with high performance liquid chromatography. Analytical
199 letters. 2006; 39(2): 395-404.
200
201 39. Cunha SC, Almeida C, Mendes E, Fernandes JO. Simultaneous determination of bisphenol A
202 and bisphenol B in beverages and powdered infant formula by dispersive liquid-liquid micro-
203 extraction and heart-cutting multidimensional gas chromatography-mass spectrometry. Food
204 Additives and Contaminants. 2011; 28(4): 513-526.
205
206 40. Kawaguchi M, Inoue K, Yoshimura M, Ito R, Sakui N, Okanouchi N, Nakazawa H. Determination
207 of bisphenol A in river water and body fluid samples by stir bar sorptive extraction with in situ
208 derivatization and thermal desorption-gas chromatography-mass spectrometry. Journal of
209 Chromatography B. 2004; 805(1): 41-48.
210



CSA-Catalyzed Three-component Synthesis of Fused Polycyclic Pyrazolo[4,3-e]pyridines Under Ultrasonic Irradiation and Their Antioxidant Activity

Emel Pelit^{1,*}

¹Kirklareli University, Faculty of Art and Sciences, Department of Chemistry, Kayali Campus, 39100, Kirklareli, Turkey

Abstract: New fused pyrazolo[4,3-e]pyridines were obtained by three-component reaction of 1,3-dimethyl-1*H*-pyrazol-5-amine or 3-phenyl-1*H*-pyrazol-5-amine, aromatic aldehydes and indan-1,3-dione in the presence of camphor-10-sulfonic acid (CSA) as an effective catalyst under ultrasound promoted conditions. The antioxidant activity of the pyrazolopyridine compounds **4b**, **5c**, **5e**, **7a**, **7b** and **7c** were determined.

Keywords: Pyrazolopyridines, three-component synthesis, ultrasonic irradiation, camphor-10-sulfonic acid (CSA), antioxidant activity.

Submitted: March 02, 2017. **Revised:** May 04, 2017. **Accepted:** May 08, 2017.

Cite this: Pelit E. CSA-Catalyzed Three-component Synthesis of Fused Polycyclic Pyrazolo[4,3-e]pyridines Under Ultrasonic Irradiation and Their Antioxidant Activity. JOTCSA. 2017;4(2):631-48.

DOI: 10.18596/jotcsa.295465.

***Corresponding author.** E-mail: epelit@klu.edu.tr.

INTRODUCTION

In the past few decades, multi-component reactions have increasing attention in synthetic organic chemistry due to the building of several new bonds can easily be achieved in a single step (1, 2). These synthetic methodologies have great utility, especially for the construction of heterocyclic compounds which exhibit biological activity (3). Multi-component reactions act in accordance with green chemistry principles in terms of a high degree of atomic economy, easier progress of reactions, decreased reaction times, lack of waste products, and low power consumption (4, 5).

Pyrazolopyridine compounds have shown many biological properties such as anti-viral agent (6, 7), (CDK1) inhibitor (8), HIV inhibitors (9), CCR1 antagonists (10), protein kinase inhibitors (11), and they also exhibit parasiticide properties and antimalarial activities (12-14). Many of them show fluorescence in the blue-green region and have been used in organic light emitting experimental diodes (15). Therefore many synthetic methods for the synthesis of pyrazolopyridines have been reported (16-19).

Along with other reaction parameters, the nature of the catalyst plays an important role in reaction's yield, selectivity, and general applicability. Thus, development of an inexpensive, reusable, and non-toxic catalyst for multi-component reactions continues to be a subject of interest. CSA has been demonstrated to be an efficient, non-toxic, and reusable organocatalyst for several reactions such as synthesis of β -amino carbonyl compounds (20), Friedel-Crafts reactions (21, 22), synthesis of spirocyclic compounds (23), rearrangement of 1,2-dialkynylallyl alcohols (24), and it is widely used in the optical resolution of amines (25).

Ultrasonic irradiation is widely used in synthetic organic chemistry as it is comply with the principles of green chemistry (26-28). Ultrasound irradiation is able to activate many organic reactions due to cavitation collapse (29, 30). Compared with traditional methods, many organic synthesis can be efficiently carry out in higher yields, higher selectivity, shorter reaction times, and milder reaction conditions under ultrasonic irradiation (31, 32).

This work aims to the preparation of pyrazolopyridines under ultrasonic irradiation in the presence of CSA as a catalyst. There is also a rising significance in antioxidants due to prevention of harmful effects of free radicals in human body (33, 34). Therefore in an attempt to extend biological interest to this new group of compounds most of the pyrazolopyridine compounds were tested for their free radical scavenging activity (determined for DPPH), reducing activity (reduction of the Fe^{3+} /ferricyanide complex to its

ferrous form), metal-chelating (chelating activity capacity of ferrous ions), superoxide scavenging activity, and total antioxidant activity.

MATERIALS AND METHODS

NMR spectra were determined on a Bruker Avance III-500 MHz NMR. Chemical shifts are given in ppm downfield from Me₄Si in DMSO-d₆ or CDCl₃ solution. Coupling constants are given in Hz. The FTIR spectra were recorded on a Perkin-Elmer FT-IR spectrometer (ATR) and absorption frequencies are reported in cm⁻¹. MS spectra were recorded on a Thermo Elemental X Series ICP-MS or AB Sciex 3200 QTRAP LC-MS/MS. Elemental analyses were measured with Flash EA 1112 Series or CHNS-932 LECO apparatus and were in good agreement ($\pm 0.2\%$) with the calculated values. Ultrasonication was performed in a Alex Ultrasonic Bath with a frequency of 32 kHz. The internal dimensions of the ultrasonic cleaner tank were 240x140x100 mm with liquid holding capacity of 3L. The reactor was a 100 mL pyrex round-bottom flask. The reaction flasks were suspended in the center of the bath, and the addition or removal of water controlled the temperature of the water bath. Melting points were measured on a Gallenkamp melting-point apparatus. TLC was conducted on standard conversion aluminum sheets pre-coated with a 0.2-mm layer of silica gel. All reagents were commercially available.

General Procedure for the Synthesis of Pyrazolopyridine Compounds (4a-b, 5c-e, 7a-d) Under Ultrasonic Irradiation

A mixture of CSA (7.3 mg, 0.03 mmol), 1,3-dimethyl-1*H*-pyrazol-5-amine or 3-phenyl-1*H*-pyrazol-5-amine, (1.00 mmol), indan-1,3-dione (1.00 mmol), and aromatic aldehyde (1.00 mmol) in 5 mL of EtOH was irradiated with ultrasound of low power (with a frequency of 32 kHz) at 40 °C for the period of time indicated in Table 3. The reaction flask was located at the maximum energy area in the cleaner and the surface of the reactants was placed slightly lower than the level of the water. The addition or removal of water controlled the temperature of the water bath. After completion of the reaction, as indicated by TLC monitoring, the resultant solid was washed with water and crystallized from ethanol to give products **4a-b**, **5c-e** and **7a-d**.

Antioxidant Activity

α,α -Diphenyl- β -picryl-hydrazyl (DPPH), butylated hydroxyanisole (BHA), butylated hydroxytoluene (BHT), trolox, resorcinol, gallic acid, linoleic acid, ethylenediaminetetraacetic acid (EDTA), 3-(2-pyridyl)-5,6-bis(4-phenyl-sulfonicacid)-1,2,4-triazine (Ferrozine), polyoxyethylenesorbitan monolaurate (Tween-20) and trichloroacetic acid (TCA), Ferrozine, Folin Ciocalteu solution, nicotinamide adenine

dinucleotide (NADH), phenazine methosulphate (PMS), nitroblue tetrazolium (NBT) were obtained from Sigma-Aldrich. Ammonium thiocyanate was purchased from Merck. All other chemicals used were in analytical grade and obtained from either Sigma–Aldrich or Merck.

Free Radical Scavenging Activity

The free radical scavenging activity was determined by the 1,1-diphenyl-2-picryl-hydrazyl (DPPH•). The activity was measured by following the methodology described by Brand-Williams et al (35). Briefly, 20 mg/L DPPH• in methanol was prepared and 1.5 mL of this solution was added to 0.75 mL of pyrazolopyrine compounds solution in water at different concentrations (25-400 µg/mL). After 30 minutes, the absorbance was measured at 517 nm. Water (0.75 mL) in place of the sample was used as control. Lower absorbance of the reaction mixture indicates higher free radical scavenging activity. The percent inhibition activity was calculated using the following equation:

$$\text{Free radical scavenging effect \%} = [(A_0 - A_1) / A_0] \cdot 100$$

(A_0 = the control absorbance and A_1 = the sample solution absorbance).

Reducing Power Assay

The reducing power of pyrazolopyridine compounds was determined by the method of Oyaizu (36). Different concentrations of pyrazolopyridine compounds (25-400 µg/mL) in 1 mL of water were mixed with phosphate buffer (2.5 mL, 0.2 M pH 6.6) and potassium ferricyanide [$K_3Fe(CN)_6$] (2.5 mL, 1%, w/v). The mixture was incubated at 50°C for 30 min. A portion of trichloroacetic acid (2.5 mL, 10%, w/v) was added to the mixture which was then centrifuged at 3000 rpm for 10 min. Finally, 2.5 mL of upper-layer solution was mixed with distilled water (2.5 mL) and $FeCl_3$ (0.5 mL, 0.1%, w/v), and the absorbance was measured at 700 nm. Increased absorbance of the reaction mixture indicates increased reducing power.

Metal Chelating Activity

The ferrous ions (Fe^{2+}) chelating activities of pyrazolopyridine compounds were measured according to the method of Decker and Welch (37). 1 mL of different concentrations of pyrazolopyrine compounds (25–400 µg/mL) were mixed with 3.7 mL of deionized water. The mixture was incubated with $FeCl_2$ (2 mM, 0.1 mL) for 30 min. After incubation, the reaction was initiated by addition of ferrozine (5 mM and 0.2 mL), and the mixture was shaken vigorously and left standing at room temperature for 10 min. Absorbance of the solution was then measured at 562 nm. A lower absorbance indicates a higher chelating

power. The Fe²⁺ chelating activity of the compounds was compared with EDTA at the same concentrations.

$$\text{Metal chelating activity (\%)} = [(A_0 - A_1)/A_0].100$$

Superoxide Scavenging Activity

Measurement of superoxide anion scavenging activity of pyrazolopyridine compounds was done based on the method described by Liu (38). Superoxide radicals are generated in PMS-NADH systems by oxidation of NADH and assayed by the reduction of nitroblue tetrazolium (NBT). In this experiments, the superoxide radicals were generated in 3 mL of *Tris*-HCl buffer (16 mM, pH 8.0) containing 1 mL of NBT (50 µM) solution, 1 mL of NADH (78 µM) solution and sample solution of pyrazolopyridine compounds (from 25-400 µg/mL) in water. The reaction started by adding 1 mL of phenazine methosulphate (PMS) solution (10 µM) to the mixture. The reaction mixture was incubated at 25 °C for 5 min and the absorbance at 560 nm was measured. Decreased absorbance of the reaction mixture indicates increased superoxide anion scavenging activity. The percentage inhibition of superoxide anion generation was calculated using the following formula:

$$\% \text{Inhibition} = [(A_0 - A_1)/A_0].100$$

Total Antioxidant Activity Assay

The total antioxidant activity of pyrazolopyridine compounds was measured according to the thiocyanate method described by Mitsuda et al (39). The solution of pyrazolopyridine compounds (150 µg/mL) in 2.5 mL of potassium phosphate buffer (0.04 M, pH 7.4) was added to 2.5 mL of linoleic acid emulsion in potassium phosphate buffer (0.04 M, pH 7.4). The mixed solution (5 mL) was incubated at 37 °C. During incubation at regular interval moments, a 0.1 mL of the mixture was diluted with 3.7 mL of methanol, followed by the addition of 0.1 mL of 30 % ammonium thiocyanate and 0.1 mL of 20 mM ferrous chloride in 3.5 % hydrochloric acid. The peroxide level was determined by measurement of the absorbance at 500 nm in. This step was repeated every 10 h until the control reached its maximum absorbance value. High absorbance indicates high linoleic acid oxidation. The per cent inhibition of lipid peroxidation in linoleic acid emulsion was calculated by the following equation:

$$\text{Inhibition of lipid peroxidation (\%)} = [(A_0 - A_1)/A_0].100$$

1,3-Dimethyl-4-phenylindeno[1,2-b]pyrazolo[4,3-e]pyridin-5(1H)-one (4a)

Red powder; m.p. 246-248 °C; FTIR (ATR, cm^{-1}): 3056, 3028, 2925, 2850, 1709, 1606, 1562, 1499, 1435, 1326, 1245, 1132, 1009, 776. ^1H NMR (500 MHz, CDCl_3 , delta, ppm): 7.85 (d, $J= 6.50$ Hz, 1H, Ar-H), 7.53-7.43 (m, 4H, Ar-H), 7.36-7.18 (m, 4H, Ar-H), 4.02 (s, 3H, N- CH_3), 1.90 (s, 3H, CH_3). ^{13}C NMR (125 MHz, CDCl_3): δ 190.05 (C=O), 164.77 (Ar-C), 153.28 (Ar-C), 145.92 (Ar-C), 144.36 (Ar-C), 142.38 (Ar-C), 137.54 (Ar-C), 134.57 (Ar-CH), 132.99 (Ar-C), 131.34 (Ar-CH), 129.08 (Ar-CH), 128.66 (Ar-CH), 127.91 (Ar-CH), 123.38 (Ar-CH), 121.13 (Ar-CH), 119.15 (Ar-C), 113.72 (Ar-C), 33.81 (N- CH_3), 14.62 (CH_3). MS: m/z (ESI) 326.2 [$\text{M}+\text{H}$] $^+$, 310.0, 297.0, 282.0, 252.8, 230.2, Anal. Calc. for $\text{C}_{21}\text{H}_{15}\text{N}_3\text{O}$: C, 77.52; H, 4.65; N, 12.91. Found: C, 77.38; H, 4.68; N, 12.86.

4-(1,3-dimethyl-5-oxo-1,4,5,10-tetrahydroindeno[1,2-b]pyrazolo[4,3-e]pyridin-4-yl)benzotrile (4b)

Red powder; m.p. 273-275 °C; FTIR (ATR, cm^{-1}): 3396, 3086, 3053, 2927, 2227, 1706, 1604, 1567, 1507, 1490, 1324, 1238, 1182, 1025, 857, 771. ^1H NMR (500 MHz, $\text{DMSO-}d_6$, delta, ppm): 8.03 (d, $J= 8.20$ Hz, 2H, Ar-H), 7.99 (d, $J= 7.50$ Hz, 1H, Ar-H), 7.78-7.73 (m, 3H, Ar-H), 7.63-7.57 (m, 2H, Ar-H), 4.07 (s, 3H, N- CH_3), 1.88 (s, 3H, CH_3). ^{13}C NMR (125 MHz, $\text{DMSO-}d_6$): δ 189.04 (C=O), 162.47 (Ar-C), 157.00 (Ar-C), 151.10 (Ar-C), 143.02 (Ar-C), 142.20 (Ar-C), 137.75 (Ar-C), 135.77 (Ar-C), 133.00 (Ar-CH), 131.74 (Ar-CH), 129.96 (Ar-CH), 129.04 (Ar-CH), 127.03 (Ar-CH), 124.72 (Ar-CH), 123.32 (Ar-CH), 121.13 (Ar-CH), 118.55 ($\text{C}\equiv\text{N}$), 111.74 (Ar-C), 106.65 (Ar-C), 33.82 (N- CH_3), 14.06 (CH_3). MS: m/z (ESI) 351.2 [M^+], 248.3, 233.0, 205.5, 102.1, Anal. Calc. for $\text{C}_{22}\text{H}_{14}\text{N}_4\text{O}$: C, 75.42; H, 4.03; N, 15.99. Found: C, 75.38; H, 4.15; N, 16.11.

4-(2,4-Difluorophenyl)1,3-dimethyl-4,10-dihydroindeno[1,2-b]pyrazolo[4,3-e]pyridin-5(1H)-one (5c)

Red powder; m.p. 274-276 °C; FTIR (ATR, cm^{-1}): 3630, 3138, 3070, 3028, 2937, 1689, 1655, 1600, 1542, 1497, 1450, 1350, 1287, 1197, 1134, 1088, 963, 866, 772. ^1H NMR (500 MHz, $\text{DMSO-}d_6$, delta, ppm): 10.76 (s, 1H, NH), 7.70 (d, $J = 7.20$ Hz, 1H, Ar-H), 7.46 (t, $J = 7.40$ Hz, 1H, Ar-H), 7.34 (t, $J = 7.40$ Hz, 1H, Ar-H), 7.27-7.17 (m, 2H, Ar-H), 7.15-7.07 (m, 1H, Ar-H), 6.95 (t, $J = 8.40$ Hz, 1H, Ar-H), 5.13 (s, 1H, C-H), 3.78 (s, 3H, N- CH_3), 1.73 (s, 3H, CH_3). ^{13}C NMR (125 MHz, $\text{DMSO-}d_6$): δ 189.85 (C=O), 161.56 (Ar-C), 160.27 (Ar-C), 159.62 (Ar-C), 158.30 (Ar-C), 155.90 (Ar-C), 143.81 (Ar-C), 137.75 (Ar-C), 136.40 (Ar-C), 134.10 (Ar-C), 131.35 (Ar-CH), 130.06 (Ar-CH), 119.98 (Ar-CH), 119.35 (Ar-CH), 111.40 (Ar-CH), 106.09 (Ar-C), 103.16 (Ar-CH), 102.18 (Ar-C), 35.16 (N- CH_3), 27.39 (C-H), 11.53 (CH_3). MS: m/z (ESI) 364.0 [$\text{M}+\text{H}$] $^+$, 344.2, 302.5, 268.2, 250.2, 236.0, 126.9, Anal. Calc. for $\text{C}_{21}\text{H}_{15}\text{F}_2\text{N}_3\text{O}$: C, 69.41; H, 4.16; N, 11.56. Found: C, 69.23; H, 4.14; N, 11.53.

1,3-Dimethyl-4-p-tolyl-4,10-dihydroindeno[1,2-b]pyrazolo[4,3-e]pyridin-5(1H)-one (5d)

Red powder; m.p. 251-253 °C; FTIR (ATR, cm^{-1}): 3242, 3173, 3144, 3043, 2921, 2849, 1739, 1653, 1599, 1536, 1499, 1349, 1196, 1108, 865, 761; ^1H NMR (500 MHz, CDCl_3 , delta, ppm): 10.90 (s, 1H, NH), 8.17-7.74 (m, 2H, Ar-H), 7.65-7.28 (m, 3H, Ar-H), 6.88 (d, $J= 6.50$ Hz, 1H, Ar-H), 6.80 (d, $J= 6.50$ Hz, 1H, Ar-H), 4.80 (s, 1H, C-H), 4.14 (s, 3H, N- CH_3), 2.49 (s, 3H, CH_3), 2.06 (s, 3H, Ph- CH_3). ^{13}C NMR (125 MHz, CDCl_3): δ 189.90 (C=O), 155.73 (Ar-C), 152.95 (Ar-C), 143.24 (Ar-C), 139.27 (Ar-C), 136.55, (Ar-C), 135.82 (Ar-C), 135.10 (Ar-C), 133.74 (Ar-CH), 129.09 (Ar-CH), 128.60 (Ar-CH), 126.38 (Ar-CH), 125.45 (Ar-CH), 123.18 (Ar-CH), 104.86 (Ar-C), 103.50 (Ar-C), 35.67 (N- CH_3), 33.30 (C-H), 21.16 (Ph- CH_3), 11.58 (CH_3). MS: m/z (ESI) 342.2 $[\text{M}+\text{H}]^+$, 298.0, 285.3, 250.1, 236.3, 180.1, Anal. Calc. for $\text{C}_{22}\text{H}_{19}\text{N}_3\text{O}$: C, 77.40; H, 5.61; N, 12.31. Found: C, 77.61; H, 5.49; N, 12.35.

1,3-Dimethyl-4-(5-nitrofuranyl)-4,10-dihydroindeno[1,2-b]pyrazolo[4,3-e]pyridin-5(1H)-one (5e)

Red powder; m.p. 300-302 °C; FTIR (ATR, cm^{-1}): 3371, 3156, 3117, 3068, 2975, 2936, 1702, 1683, 1602, 1590, 1497, 1479, 1353, 1232, 1188, 1091, 966, 813, 757. ^1H NMR (500 MHz, $\text{DMSO}-d_6$, delta, ppm): 10.97 (s, 1H, NH), 7.79 – 7.30 (m, 5H, Ar-H), 6.66 (br s, 1H, Ar-H), 5.25 (s, 1H, C-H), 3.79 (s, 3H, N- CH_3), 1.96 (s, 3H, CH_3). ^{13}C NMR (125 MHz, $\text{DMSO}-d_6$): δ 189.54 (C=O), 156.65 (Ar-C), 152.02 (Ar-C), 149.47 (Ar-C), 144.39 (Ar-C), 137.79 (Ar-C), 136.12 (Ar-C), 131.69 (Ar-C), 130.51 (Ar-C), 123.79 (Ar-CH), 120.41 (Ar-CH), 119.81 (Ar-CH), 114.50 (Ar-CH), 110.31 (Ar-CH), 108.15 (Ar-CH), 103.76 (Ar-C), 35.33 (N- CH_3), 29.00 (C-H), 11.83 (CH_3). MS: m/z (ESI) 363.3 $[\text{M}+\text{H}]^+$, 316.2, 272.0, 250.2, 192.0, Anal. Calc. for $\text{C}_{19}\text{H}_{14}\text{N}_4\text{O}_4$: C, 62.98; H, 3.89; N, 15.46. Found: C, 63.14; H, 4.08; N, 15.60.

3,4-Diphenyl-4,10-dihydroindeno[1,2-b]pyrazolo[4,3-e]pyridin-5(1H)-one (7a)

Red powder; m.p. 287-289 °C; FTIR (ATR, cm^{-1}): 3418, 3175, 3058, 3025, 2966, 2888, 1658, 1595, 1566, 1494, 1429, 1347, 1192, 1128, 1074, 970, 919, 760. ^1H NMR (500 MHz, $\text{DMSO}-d_6$, delta, ppm): 12.90 (s, 1H, NH), 11.41 (s, 1H, NH), 7.68-7.30 (m, 7H, Ar-H), 7.28-7.09 (m, 6H, Ar-H), 6.99 (d, $J= 6.50$ Hz, 1H, Ar-H), 5.34 (s, 1H, C-H). ^{13}C NMR (125 MHz, $\text{DMSO}-d_6$): δ 189.31 (C=O), 156.05 (Ar-C), 148.58 (Ar-C), 145.87 (Ar-C), 138.78 (Ar-C), 136.32 (Ar-C), 134.78 (Ar-C), 131.08 (Ar-CH), 130.07 (Ar-CH), 129.02 (Ar-C), 128.58 (Ar-CH), 128.06 (Ar-CH), 127.84 (Ar-CH), 127.57 (Ar-CH), 126.31 (Ar-CH), 125.78 (Ar-CH), 119.64 (Ar-CH), 119.01 (Ar-CH), 105.86 (Ar-C), 103.52 (Ar-C),

34.88 (C-H). MS: m/z (ESI) 376.3 $[M+H]^+$, 298.2, 268.8, 242.3, 227.2, 215.3, 180.1, Anal. Calc. for $C_{25}H_{17}N_3O$: C, 79.98; H, 4.56; N, 11.19. Found: C, 80.05; H, 4.52; N, 11.26.

4-(2,4-difluorophenyl)-3-phenyl-4,10-dihydroindeno[1,2-b]pyrazolo[4,3-e]pyridine-5(1H)-one (7b)

Red powder; m.p. 293-295 °C; FTIR (ATR, cm^{-1}): 3406, 3378, 3197, 3059, 3027, 2971, 2888, 1657, 1614, 1595, 1566, 1488, 1443, 1349, 1172, 1135, 1088, 972, 848, 770. 1H NMR (500 MHz, DMSO- d_6 , delta, ppm): 12.85 (s, 1H, NH), 11.44 (s, 1H, NH), 7.69 (d, $J=7.10$ Hz, 1H, Ar-H), 7.47 (d, $J=7.50$ Hz, 2H, Ar-H), 7.42 (t, $J=7.40$ Hz, 1H, Ar-H), 7.36-7.29 (m, 4H, Ar-H), 7.24-7.11 (m, 2H, Ar-H), 6.92 (t, $J=9.10$ Hz, 1H, Ar-H), 6.78 (t, $J=8.00$ Hz, 1H, Ar-H), 5.56 (s, 1H, C-H). ^{13}C NMR (125 MHz, DMSO- d_6): δ 189.06 (C=O), 161.38 (Ar-C), 160.25 (Ar-C), 159.34 (Ar-C), 158.38 (Ar-C), 156.46 (Ar-C), 148.33 (Ar-C), 139.06 (Ar-C), 136.28 (Ar-C), 134.74 (Ar-C), 131.48 (Ar-CH), 131.08 (Ar-CH), 130.16 (Ar-CH), 128.84 (Ar-CH), 128.45 (Ar-CH), 128.17 (Ar-CH), 126.38 (Ar-CH), 123.26 (Ar-CH), 119.63 (Ar-CH), 119.14 (Ar-CH), 111.08 (Ar-CH), 104.34 (Ar-C), 102.95 (Ar-CH), 102.77 (Ar-C), 28.17 (C-H). MS: m/z (ESI) 412.1 $[M+H]^+$, 298.2, 269.2, 241.1, 180.0, 168.0. Anal. Calc. for $C_{25}H_{15}F_2N_3O$: C, 72.99; H, 3.68; N, 10.21. Found: C, 73.06; H, 3.57; N, 10.32.

3-phenyl-4-(thiophen-2-yl)-4,10-dihydroindeno[1,2-b]pyrazolo[4,3-e]pyridine-5(1H)-one (7c)

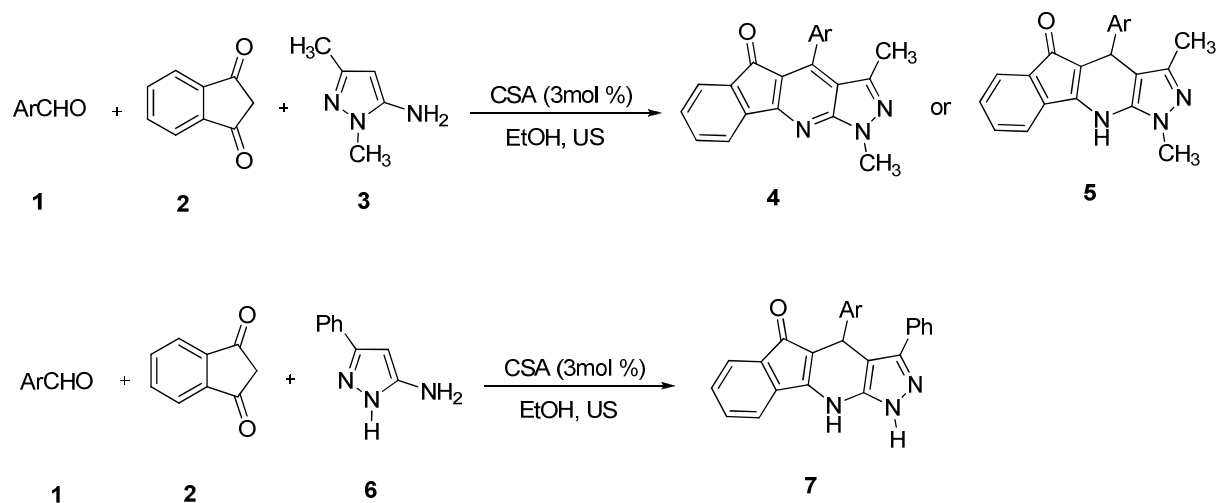
Red powder; m.p. 290-292 °C; FTIR (ATR, cm^{-1}): 3378, 3152, 3091, 3024, 2967, 2885, 1657, 1595, 1564, 1486, 1428, 1345, 1189, 1123, 1099, 1075, 1036, 966, 911, 756. 1H NMR δ_H (500 MHz, DMSO- d_6 , delta, ppm): 12.95 (s, 1H, NH), 11.45 (s, 1H, NH), 7.96-7.90 (m, 1H, Ar-H), 7.68 (d, $J=7.10$ Hz, 1H, Ar-H), 7.61 (d, $J=7.50$ Hz, 2H, Ar-H), 7.44-7.27 (m, 5H, Ar-H), 7.10 (d, $J=5.10$ Hz, 1H, Ar-H), 6.79 (d, $J=3.10$ Hz, 1H, Ar-H), 6.74 (dd, $J_1=4.90$ Hz, $J_2=3.60$ Hz, 1H, Ar-H), 5.70 (s, 1H, C-H). ^{13}C NMR (125 MHz, DMSO- d_6): δ 189.25 (C=O), 156.08 (Ar-C), 150.58 (Ar-C), 147.98 (Ar-C), 143.42 (Ar-CH), 141.38 (Ar-C), 139.20 (Ar-C), 136.16 (Ar-C), 135.64 (Ar-CH), 134.77 (Ar-C), 131.16 (Ar-CH), 130.20 (Ar-CH), 128.70 (Ar-CH), 128.23 (Ar-CH), 126.43 (Ar-CH), 123.74 (Ar-CH), 123.51 (Ar-CH), 122.80 (Ar-CH), 119.84 (Ar-CH), 119.19 (Ar-CH), 106.15 (Ar-C), 103.37 (Ar-C), 29.69 (C-H). MS: m/z (ESI) 382.3 $[M+H]^+$, 297.8. Anal. Calc. for $C_{23}H_{15}N_3OS$: C, 72.42; H, 3.96; N, 11.02. Found: C, 72.61; H, 3.90; N, 10.98.

4-(Furan-2-yl)-3-phenyl-4,10-dihydroindeno[1,2-b]pyrazolo[4,3-e]pyridine-5(1H)-one (7d)

Red powder; m.p. 294-296 °C; FTIR (ATR, cm^{-1}): 3376, 3188, 3139, 3096, 3062, 2945, 1727, 1691, 1606, 1589, 1467, 1351, 1220, 1161, 1017, 884, 774, 737. ^1H NMR δ_{H} (500 MHz, DMSO-d_6 , delta, ppm): 12.89 (s, 1H, NH), 11.42 (s, 1H, NH), 7.81-7.77 (m, 1H, Ar-H), 7.64-7.54 (m, 3H, Ar-H), 7.40-7.20 (m, 5H, Ar-H), 7.08 (d, $J = 5.30$ Hz, 1H, Ar-H), 6.75 (d, $J = 7.50$ Hz, 1H, Ar-H), 6.60 (d, $J = 7.40$ Hz, 1H, Ar-H), 5.60 (s, 1H, C-H). ^{13}C NMR (125 MHz, DMSO-d_6): δ 189.43 (C=O), 156.25 (Ar-C), 150.20 (Ar-C), 148.10 (Ar-C), 143.36 (Ar-C), 142.18 (Ar-CH), 136.50 (Ar-C), 135.76 (Ar-C), 134.60 (Ar-C), 133.12 (Ar-CH), 130.05 (Ar-CH), 128.60 (Ar-CH), 127.51 (Ar-CH), 127.02 (Ar-CH), 126.30 (Ar-CH), 123.45 (Ar-CH), 122.90 (Ar-CH), 119.10 (Ar-CH), 118.85 (Ar-CH), 107.70 (Ar-CH), 104.83 (Ar-C), 102.40 (Ar-C), 29.60 (C-H). MS: m/z (ESI) 366.2 $[\text{M}+\text{H}]^+$, 298.9. Anal. Calc. for $\text{C}_{23}\text{H}_{15}\text{N}_3\text{O}_2$: C, 75.60; H, 4.14; N, 11.50. Found: C, 75.54; H, 4.20; N, 11.55.

RESULTS AND DISCUSSION

Initially, the condensation reaction of benzaldehyde (1.00 mmol), indan-1,3-dione (1.00 mmol), and 1,3-dimethyl-1*H*-pyrazol-5-amine (1.00 mmol) was examined under ultrasonic irradiation without a catalyst at 60 °C in 5 mL of EtOH. The reaction was completed in 15 minutes with a yield of 80%. In order to observe the effect of CSA as a catalyst, the same reaction was examined under ultrasound irradiation (Table 1) in the presence of 3 mol % CSA at 40 °C. The reaction was completed in 7 minutes with a yield of 88%. Higher amount of catalyst or higher temperature did not lead to significant change in the reaction yields.



Scheme 1: Multi-component synthesis of pyrazolopyridine derivatives.

Table 1: Effect of amount of CSA on the synthesis of **4a**.

CSA (mol %)	Temperature (°C)	Time (min)	Yield (%) ^a
-	60	15	80
3	40	7	88
3	60	7	88
5	40	7	88
10	40	7	89

^aIsolated yield.

With the best optimized condition in hand, several pyrazolopyridines were synthesized at 40 °C using CSA catalyst in EtOH under ultrasonic irradiation (Scheme 1). The results are summarized in Table 2.

It is important to point out the fact that when 1,3-dimethyl-1*H*-pyrazol-5-amine, indan-1,3-dione and benzaldehyde or electron withdrawing 4-cyanobenzaldehyde were sonicated for required reaction time, the reaction leads to the formation of the aromatized pyrazolopyridine derivatives **4**, which were isolated and characterized, but in the case of using aromatic aldehydes containing electron releasing substituents, dihydropyrazolopyridine derivatives **5** were observed.

Then the same reaction was performed with 3-phenyl-1*H*-pyrazol-5-amine, indan-1,3-dione and aromatic aldehydes under the same conditions, this time only dihydropyrazolopyridine derivatives **7** were observed (Scheme 1, Table 2) as products.

Table 2: Synthesis of pyrazolopyridine using catalytic amount of CSA.

Product	Ar	Time (min)	Yield (%) ^a
4a	Phenyl	7	88
4b	4-Cyanophenyl	7	94
5c	2,4-Difluorophenyl	7	92
5d	4-Methylphenyl	7	90
5e	5-Nitrofuran-2-yl	7	96
7a	Phenyl	7	92
7b	2,4-Difluorophenyl	7	96
7c	Thiophen-2-yl	7	97
7d	Furan-2-yl	7	95

^aIsolated yield

The structure of the newly generated compounds have been confirmed by Fourier transform-infrared (FTIR), mass and NMR techniques. In the ¹H NMR spectra of dihydropyrazolopyridines **5c-e** and **7a-d**, benzylic C-H proton resonated at near δ 4.80-

5.70 and in their ^{13}C NMR spectra, the benzylic C—H carbon resonated at near δ 27-35. The mass spectra of all new compounds showed the expected molecular ion peak.

Mainly effective HAT agents are compounds with high hydrogen atom donating ability, which is compounds with low dissociation energies of heteroatom-H bond and/or compounds from which abstraction of hydrogen leads to C-centered radicals stabilized by resonance or compounds from which hydrogen abstraction leads to sterically hindered radicals (40). In this study, the antioxidant activity of compounds **4b**, **5c**, **5e**, **7a**, **7b** and **7c** were examined for free radical scavenging activity (determined for DPPH), reducing activity (reduction of the Fe^{3+} /ferricyanide complex to its ferrous form), metal chelating (chelating activity capacity of ferrous ions) capacity, superoxide scavenging activity, and total antioxidant activity.

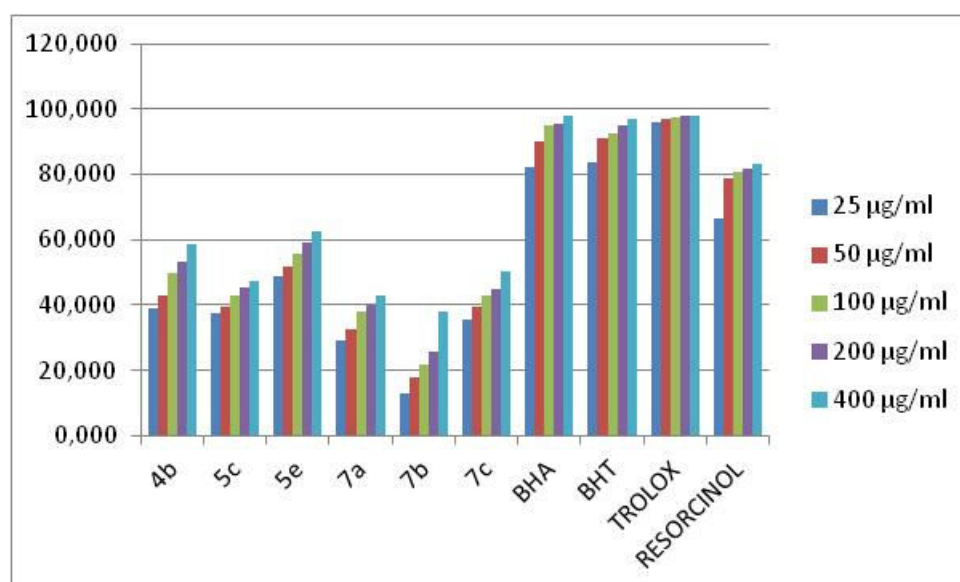


Figure 1: DPPH radical scavenging activity of pyrazolopyridine compounds. BHA, BHT, Trolox and Resorcinol were used as reference antioxidants.

DPPH• (1,1-diphenyl-2-picryl-hydrazyl) is a stable free radical and accepts an electron or hydrogen radical to become a stable diamagnetic molecule. The scavenging effect of pyrazolopyridine compounds (**4b**, **5c**, **5e**, **7a**, **7b** and **7c**) and standards (BHA, BHT, trolox, and resorcinol) on the DPPH• radical decreased in order of: BHA > trolox > BHT > resorcinol > **5e** > **4b** > **5c** > **7c** > **7a** > **7b** (Figure 1). These results indicate that pyrazolopyridine compounds had a moderate effect on scavenging free radical, and free radical scavenging activity was increased with increasing concentration. A higher DPPH radical scavenging activity is associated with a lower EC_{50} value.

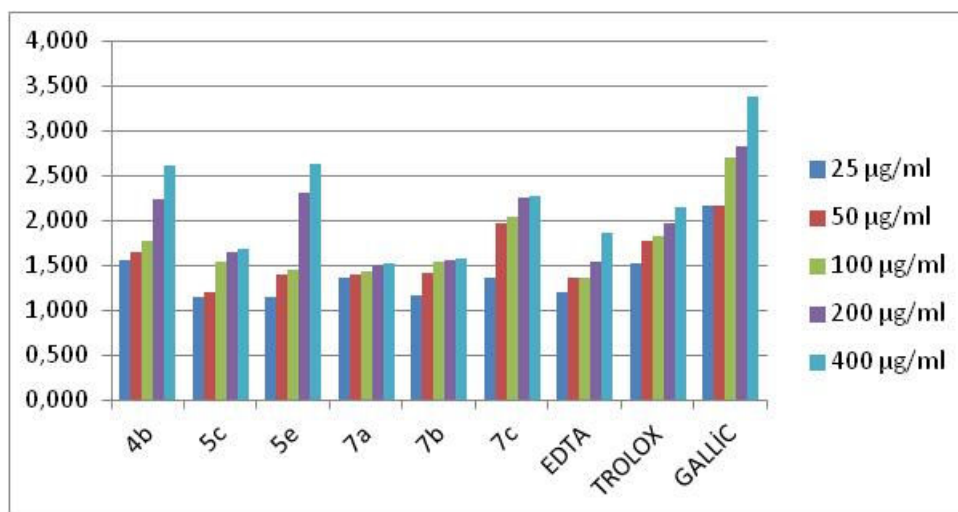


Figure 2: Reducing power of pyrazolopyridine compounds. EDTA, Trolox and Gallic acid were used as reference antioxidants.

In the reducing power assay, the presence of antioxidants in the sample would result in the reduction of ferric iron to ferrous iron by electron donation. Pyrazolopyridine compounds **4b**, **5e**, and **7c** showed higher reducing power than the other pyrazolopyridine compounds (Fig. 2), and reducing power was increased with increasing concentration.

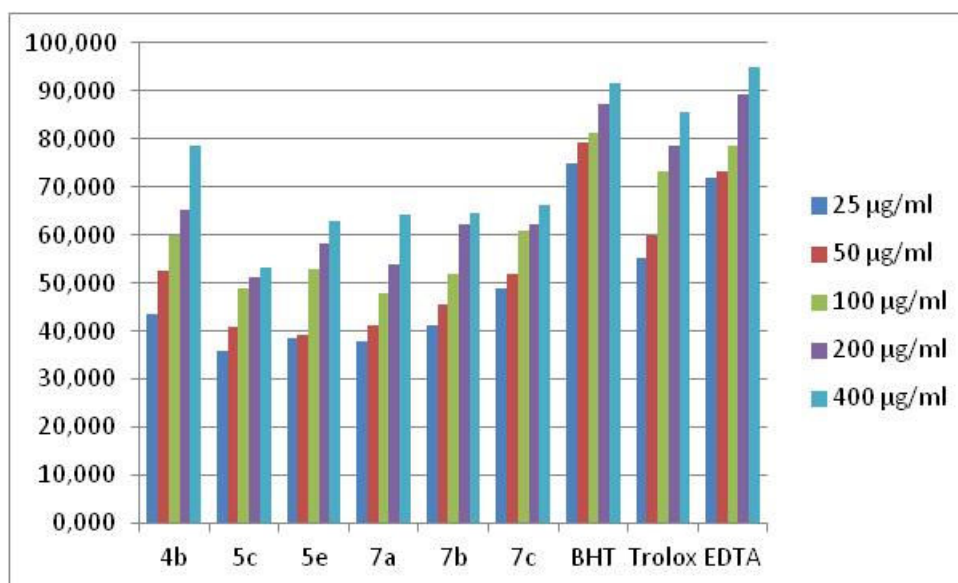


Figure 3: Metal chelating activity of pyrazolopyridine compounds. BHT, Trolox and EDTA were used as reference antioxidants.

The metal chelating activity for ferrous ion of the pyrazolopyridine compounds (**4b**, **5c**, **5e**, **7a**, **7b** and **7c**) was assayed by the inhibition of red-colored ferrozine/ FeCl_2 complex. EDTA, Trolox and BHT were used as standard compounds. The pyrazolopyridine compounds showed moderate metal chelating activity at 25, 50, 100, 200 and 400 $\mu\text{g/mL}$ (Fig. 3).

Nevertheless, compound **4b** exhibited the highest chelating activity among the tested pyrazolopyridine compounds at 400 $\mu\text{g}/\text{mL}$ (78.58 %).



Figure 4: Superoxide scavenging activity of pyrazolopyridine compounds. BHT, Trolox and BHA were used as reference antioxidants.

Fig. 4 shows the % inhibition of superoxide radical generation by 25, 50, 100, 200 and 400 $\mu\text{g}/\text{mL}$ of pyrazolopyridine compounds (**4b**, **5c**, **5e**, **7a**, **7b** and **7c**) and comparison with same concentrations of BHT, trolox and BHA. None of the compounds showed greater superoxide scavenging activity than the standards. The best inhibition (67.61%) was measured for the compound **4b** at 400 $\mu\text{g}/\text{mL}$.

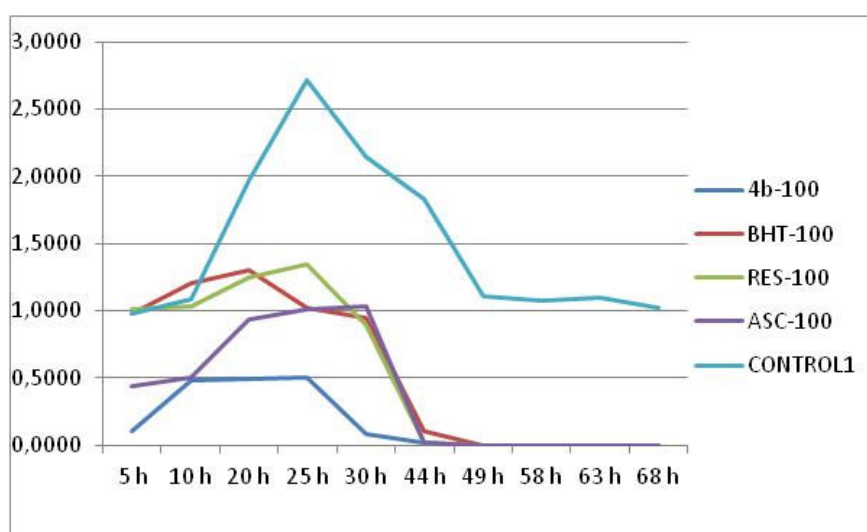


Figure 5: Total antioxidant activities of pyrazolopyridine compounds. BHT, Resorcinol and Ascorbic acid were used as reference antioxidants.

Total antioxidant activity of pyrazolopyridine compounds was determined by the thiocyanate method. Compound **4b** exhibited effective antioxidant activity. The effect of 100 µg/mL concentration of compound **4b** on lipid peroxidation of linoleic acid emulsion are shown in Figure 5. The results clearly showed that compound **4b** had stronger total antioxidant activity than BHT, resorcinol and ascorbic acid at the same concentration (100 µg/mL). The effects on lipid peroxidation of linoleic acid pyrazolopyridine compound **4b** and standards decreased in that order: compound **4b** > ascorbic acid > BHT > resorcinol.

In conclusion, this one-pot three component protocol using CSA as an organocatalyst in ethanol provides a practical method for the preparation of fused pyrazolo pyridines from 1,3-dimethyl-1*H*-pyrazol-5-amine or 3-phenyl-1*H*-pyrazol-5-amine, indan-1,3-dione and various aromatic aldehydes in short reaction times and excellent yields. The simplicity, high atom economy, easy execution, and work up are the notable features of this procedure. The antioxidant activity of compounds **4b**, **5c**, **5e**, **7a**, **7b** and **7c** were determinate. Most potent was found to be compound **4b** followed by **5e** and **7c**.

ACKNOWLEDGMENTS

This study was financially supported by Kirklareli University with the project number KLUBAP 015. I thank Assist. Prof. Dr. Melek Gül, Assoc. Prof. Dr. Emine Bağdatlı, and Assist. Prof. Dr. Aliye Gediz Ertürk for their guidance and helpful comments about antioxidant activity assays.

REFERENCES

1. Dömling A. Recent developments in isocyanide based multicomponent reactions in applied chemistry. *Chemical Reviews*. 2006; 106: 17-89. DOI: 10.1021/cr0505728.
2. Zhu J, Bienayme H. Eds. *Multicomponent Reactions*, Wiley-VCH: Weinheim, 2005, 484 p. ISBN: 978-3-527-30806-4.
3. Sunderhaus J.D, Martin S.F. Application of multicomponent reactions to the synthesis of diverse heterocyclic scaffolds. *Chemistry-A European Journal*. 2009; 15: 1300-08. DOI: 10.1002/chem.200802140.
4. Dömling A, Ugi I. Multicomponent reactions with isocyanides. *Angewandte Chemie International Edition*. 2000; 39: 3168-3210. DOI: 10.1002./1521-3773(20000915)39:18<3168AID-ANIE3168>3.0CO;2-U.
5. Zhu J, Wang Q, Wang M. X, Eds.; *Multicomponent Reactions in Organic Synthesis*, Wiley-VCH: Weinheim, 2015, 521 p. ISBN: 978-3-527-33237-3.
6. Crenshaw R. R, Luke G. M, Smirnoff P. Interferon inducing activities of derivatives of 1,3-dimethyl-4-(3-dimethylaminopropylamino)-1*H*-pyrazolo[3,4-*b*]quinoline and related compounds. *J. Med. Chem.* 1976; 19: 262-275. DOI: 10.1021/jm00224a013

7. Crenshaw R, Luke G. M, Smirnoff P. Canadian Patent 10, 32, 538; Chem. Abstr. 89 (1978) 179995r.
8. Huang S, Lin R, Yu Y, Lu Y, Connolly P.J, Chiu G, Li S, Emanuel S.L, Middleton S.A. Synthesis of 3-(1H-benzimidazol-2-yl)-5-isoquinolin-4-ylpyrazolo[1,2-b]pyridine, a potent cyclin dependent kinase 1 (CDK1) inhibitor. Bioorg. Med. Chem. Lett. 2007; 17: 1243-45. DOI: 10.1016/j.bmcl.2006.12.031.
9. Saggar S.A, Sisko J.T, Tucker T.J, Tynebor R.M, Su D.S, Antony N.J. US 2007021442, 2007.
10. Zhang P, Pennell A.M.K, Wright J.J.K, Chen W, Leleti M. R, Li Y, Li L, Xu Y. WO 2007002293, 2007 [Chem. Abstr. 2007, 146, 121980].
11. Chiu G, Li S, Connolly P.J, Middleton S.A, Emanuel S.L, Huang R, Lu Y. WO 2006130673, 2006 [Chem. Abstr. 2006, 146, 45513].
12. Feurer A, Luithle J, Wirtz S, Koenig G, Stasch J, Stahl E, Schreiber R, Wunder F, Lang D. WO 2004009589, 2004 [Chem. Abstr. 2004, 140, 146157].
13. Bristol-Meyers Co., French Demande 2, 149, 275; Chem. Abstr. 79 (1973) 78784n.
14. Stein R.G, Biel J.H, Singh T. Antimalarials. 4-Substituted 1H-pyrazolo[3,4-b]quinolines. J. Med. Chem. 1970; 13: 153-55. DOI: 10.1021/jm00295a049.
15. Kendre D.B, Toche R.B, Jachak M.N. Synthesis of novel dipyrazolo[3,4-b:3,4-d]pyridines and study of their fluorescence behavior. Tetrahedron. 2007; 63: 11000-04. DOI: 10.1016/j.tet.2007.08.052.
16. Diaz-Ortiz A, Dela Hoz A, Langa F. Microwave irradiation in solvent-free conditions: a eco-friendly methodology to prepare indazoles, pyrazolopyridines and bipyrazoles by cycloaddition reactions. Green Chem. 2000; 2: 165-72. DOI: 10.1039/B003752O.
17. Krygowski T.M, Anulewicz R, Cyranski M.K, Puchala A, Rasala D. Separation of the energetic and geometric contribution to the aromaticity. Part IX. Aromaticity of pyrazoles in dependence on the kind of substitution. Tetrahedron. 1998; 54: 12295-300. DOI: 10.1016/S0040-4020(98)00749-2.
18. Nikpassand M, Mamaghani M, Shirini F, Tabatabaeian K. A convenient ultrasound-promoted regioselective synthesis of fused polycyclic 4-aryl-3-methyl-4,7-dihydro-1H-pyrazolo[3,4-b]pyridines. Ultrasonics Sonochemistry. 2010; 17: 301-5. DOI:10.1016/j.ultsonch.2009.08.001.
19. Nikpassand M, Zare L, Shafaati T, Shariati S. Regioselective synthesis of fused azo-linked pyrazolo[4,3-e]pyridines using nano-Fe₃O₄. Chin. J. Chem. 2012; 30: 604-8. DOI: 10.1002/cjoc.201100181.
20. Kundu K, Nayak S.K. (±)-Camphor-10-sulfonic acid catalyzed direct one-pot three-component Mannich type reaction of alkyl (hetero)aryl ketones under solvent-free conditions: application to the synthesis of aminochromans. RSC Advances. 2012; 2012: 480-6. DOI: 10.1039/C1RA00652E.
21. Srivastava A, Singh S, Samanta S. (±)-CSA catalyzed Friedel-Crafts alkylation of indoles with 3-ethoxycarbonyl-3-hydroxyisoindolin-1-one: an easy access of 3-ethoxycarbonyl-3-indolyloisoindolin-1-ones bearing a quaternary α-amino acid moiety. Tetrahedron Letters. 2013; 54: 1444-8. DOI: 10.1016/j.tetlet.2013.01.010
22. Jiang X, Song Z, Xu C, Yao Q, Zhang A. (D,L)-10-Camphorsulfonic-acid-catalysed synthesis of diaryl-fused 2,8-dioxabicyclo[3.3.1]nonanes from 2-hydroxychalcones and naphthol derivatives. European Journal of Organic Chemistry. 2014; 418-25. DOI: 10.1002/ejoc.201301295.
23. Srivastava A, Mobin S.M, Samanta S. (±)-CSA catalyzed one-pot synthesis of 6,7-dihydrospiro[indole-3,10-isoindoline]-2,30,4(1H,5H)-trione derivatives: easy access of

- spirooxindoles and ibophyllidine-like alkaloids. *Tetrahedron Letters*. 2014; 55: 1863-7. DOI: 10.1016/j.tetlet.2014.01.154.
24. Dai W.M, Wu J, Fong K.C, Lee M.Y.H, Lau C.W. Regioselective synthesis of acyclic cis-enediynes via an acid-catalyzed rearrangement of 1,2-dialkynylallyl alcohols. *Syntheses, computational calculations, and mechanism*. *Journal of Organic Chemistry*. 1999; 64: 5062-82. DOI: 10.1021/jo982476v.
25. Kellogg R.M, Nieuwenhuijzen J.W, Pouwer K, Vries T.R, Broxterman Q.B, Grimbergen R.F.P, Kaptein B, La Crois R.M, De Wever E, Zwaagstra K, Van Der Laan A.C. Dutch resolution: Separation of enantiomers with families of resolving agents. A status report. *Synthesis*. 2003; 1626-38. DOI: 10.1055/s-2003-40508.
26. Vinatoru M, Bartha E, Badea F, Luche J.L. Sonochemical and thermal redox reactions of triphenylmethane and triphenylmethyl carbinol in nitrobenzene. *Ultrasonics Sonochemistry*. 1998; 5: 27-31. DOI: 10.1016/S1350-4177(98)00004-2.
27. Pelit E, Turgut Z. Three-component aza-Diels–Alder reactions using Yb(OTf)₃ catalyst under conventional/ultrasonic techniques. *Ultrasonics Sonochemistry*. 2014; 21: 1600-7. DOI: 10.1016/j.ultsonch.2014.01.009.
28. Dong C, Sanjay K, Ackmez M. Eds. *Handbook on Applications of Ultrasound Sonochemistry for Sustainability*. Boca Raton: CRC Press, Taylor & Francis Group; 2012, 793 p. ISBN: 9781439842065-CAT#K11960.
29. Mason T.J, Peters D. Eds. *Practical Sonochemistry, second ed., Power ultrasound uses and applications*. Woodhead Publishing, 2002, 166p. ISBN: 9781898563839.
30. Mason T.J. Sonochemistry and the environment – Providing a “green” link between chemistry, physics and engineering. *Ultrasonics Sonochemistry*. 2007; 14: 476-83. DOI: 10.1016/j.ultsonch.2006.10.008.
31. Luche J.L. Ed. *Synthetic Organic Sonochemistry*, Plenum Press, New York, 1998, 431 p. ISBN: 978-1-4899-1912-0.
32. Li J.T, Wang S.X, Chen G.F, Li T.S. Some applications of ultrasound irradiation in organic synthesis. *Current Organic Synthesis*. 2005; 2: 415-36. DOI: 10.2174/1570179054368509.
33. Sies H. Oxidative stress: oxidants and antioxidants. *Experimental Physiology* 1997; 82: 291-5. DOI: 10.1113/expphysiol.1997.sp004024.
34. Nakabeppu Y, Sakumi K, Sakamoto K, Tsuchimoto D, Tsuzuki T, Nakatsu Y. Mutagenesis and carcinogenesis caused by the oxidation of nucleic acids. *Biological Chemistry*. 2006; 387: 373-9. DOI: 10.1515/BC.2006.050.
35. Brand-Williams W, Cuvelier ME, Berset C. Use of a free radical method to evaluate antioxidant activity. *LWT—Food Science and Technology*. 1995; 28: 25–30. DOI: 10.1016/S0023-6438(95)80008-5.
36. Oyaizu M. Studies on product of browning reaction prepared from glucose amine. *Japanese Journal of Nutrition*. 1986; 44: 307–15. DOI: 10.5264/eiyogakuzashi.44.307.
37. Decker EA, Welch B. Role of ferritin as a lipid oxidation catalyst in muscle food. *Journal of Agricultural and Food Chemistry*. 1990; 38: 674–7. DOI: 10.1021/jf00093a019.
38. Liu F, Ooi VEC, Chang ST. Free radical scavenging activity of mushroom polysaccharide extracts. *Life Science*. 1997; 60: 763-71. DOI: 10.1016/S0024-3205(97)00004-0.
39. Mitsuda H, Yuasumoto K, Iwama K. Antioxidative action of indole compounds during the autooxidation of linoleic acid. *J.Japan Soc. Nutr. Food Sci*. 1996; 19: 210-14. DOI: 10.4327/jsnfs1949.19.210.

40. Huang D, Ou B, Prior RL. The chemistry behind antioxidant capacity assays. *J. Agric. Food Chem.* 2005; 53: 1841-56. DOI: 10.1021/jf030723c.



Synthesis and Characterization of Novel Aromatic Substituted γ - and δ -Ketoxime Esters

Belma Hasdemir

Department of Chemistry, Faculty of Engineering, Istanbul University, 34320 Avcılar, Istanbul, Turkey

Abstract: By starting their corresponding keto esters 1a-j, aryl-, substituted aryl- and heteroaryl-containing γ - and δ -oximes 2a-2j (ten in total) were obtained. Proton nuclear magnetic resonance spectroscopy, carbon nuclear magnetic resonance spectroscopy, fourier transform infrared spectroscopy, mass spectrometry and elemental analyses were applied to the synthesized compounds for elucidating their structures and to find the (*E*)-isomers.

Keywords: keto ester; γ -ketoxime ester; δ -ketoxime ester; hydroxylamine hydrochloride.

Submitted: February 07, 2017 . **Revised:** April 17, 2017. **Accepted:** May 29, 2017.

Cite this: Hasdemir B. Synthesis and Characterization of Novel Aromatic Substituted γ - and δ -Ketoxime Esters. JOTCSA. 2017 May;4(2):649-60.

DOI: <http://dx.doi.org/10.18596/jotcsa.290589>.

Corresponding author. E-mail: karaefe@istanbul.edu.tr

INTRODUCTION

Oximes are very important building blocks in synthetic organic chemistry because they are capable of undergoing numerous transformations. Oximes are widely used to protect, purify and characterize aldehydes and ketones. In addition, oximes can successfully be converted into amides (1), nitriles (2,3), amines (4,5), hydroxyamines (6), hydroxyamine *O*-ethers (7), nitroalkanes (8), 1,3-oxazoles, thiazoles and diazoles (9), *etc.* The products, as starting compounds, are proven to be biologically active amino acids (10), alkoxyimino esters and alkoxyamino amides (11) and derivatives of pyrrole skeleton (12). Moreover, oxime groups could be transferred into water-soluble compounds. Through its oxime and oxime ether, limonin is rendered water soluble as being an anti-inflammatory and analgesic agent (13).

Recently, oxime esters and related compounds are shown to possess bioactivities, thus being attractive to researchers, especially working with agrochemicals and medicinal compounds. Fungicidal (14), insecticidal (15,16), antitumor (17,18), herbicidal (19,20), antineoplastic (21) and antiviral (22,23) activities were introduced for oxime esters. It has been about fifty years since the synthesis and biological activities of oxime esters were shown in a large number of researches. In a previous study, the synthesis of biologically active hydroxyimino-, methoxyimino- and benzyloxyiminotetradecanoic acid methyl esters were reported and their DNA-binding, antimicrobial and antifungal activities were investigated (24).

Being capable of coordinating to metal ions, oxime ligands have been interesting due to their variable geometries (25-28) and fine tuning of their substituents (29,30). Oxime ligands are known to serve as analytical reagents (31,32) and also employed as models for Vitamin B₁₂ and dioxygen carrier systems (33), as well as catalysts in chemical processes (34-37).

In this study, it was aimed to obtain pure γ - and δ - oxime esters numbered as **2a-2j** as compounds for reference purposes. In the previous paper, Imoto et al. reported the 4-hydroxyimino-4-phenyl-butyric acid methyl ester **2a** and 5-hydroxyimino-5-phenyl-pentanoic acid methyl ester **2f** and they used these compounds as intermediates in the synthesis of oxyiminoalcanoic acids (38). Besides, **2a** was obtained as intermediates compound for use in the Beckmann rearrangement (39). In the another study, **2e** was used as starting materials for synthesis of aliphatic amino acids (40). In this work, seven novel compounds containing aryl, substituted aryl and heteroaryl groups (**2b-2d**, **2g-2j**) were synthesized. Their structures were elucidated with ¹H NMR, ¹³C NMR, elemental analysis and mass spectrometry.

MATERIALS AND METHODS

Unless otherwise stated, all reagents were obtained from commercial suppliers. Hydroxylamine hydrochloride (HONH₂.HCl) was purchased from Sigma Aldrich. γ - and δ -keto esters as starting materials were synthesized by Friedel-Crafts acylation (41,42). The reactions of **2** were checked for completion on silica gel on aluminum plates. They were purified by flash column chromatography on silica gel (Merck; 230-400 mesh) and ethyl acetate and hexane (7:3, v:v) was used as eluent.

Proton nuclear magnetic resonance spectroscopy was obtained at 500 MHz and carbon nuclear magnetic resonance spectroscopy was recorded at 125 MHz. As an internal standard, tetramethylsilane in deuteriochloroform (CDCl₃) was employed. A Shimadzu QP2010 Plus was used as the GC/MS spectrometer. Fourier transform infrared spectra were recorded on a Mattson 1000 spectrometer. A Büchi melting point B-540 apparatus was used for melting point determinations. The chemical yields are expressed with the pure isolated substances.

General procedure : preparation of oxime esters (43,44)

As a general procedure, the keto ester (1.0 eq) **1a-j** was dissolved in ethanol. Hydroxylamine hydrochloride (2.0 eq) was introduced into the reaction medium and the mixture was stirred overnight. Saturated ammonium chloride was used to dilute the mixture and it was extracted with ethyl acetate. Combined organic layers were washed with water and brine and dried over sodium sulfate. The solvent was evaporated and the crude product was subjected to column chromatography on silica gel and as eluent "(n-hexane:ethyl acetate 7:3)" to yield the oximes **2a-j**.

4-Hydroxyimino-4-phenyl-butyric acid methyl ester **2a**

Yield: 90%; colorless oil. **Anal. calcd.** for C₁₁H₁₃NO₃: C, 63.76; H, 6.32; N, 6.76 Found: C, 63.50; H, 6.42; N, 6.66. **IR** (neat, cm⁻¹) ν 3450 (OH stretching), 3030 (CH stretching of aromatic rings), 2953 (-CH₂- stretching), 1738 (C=O stretching of COOCH₃ group), 1680 (C=N stretching), 1500, 1453 (C=C- stretching of aromatic rings), 1261 (CH stretching in aliphatic plane), 1076 (C-O stretching), 769 (out-of-plane bending CH of aromatic ring). **¹H NMR** (500 MHz, CDCl₃) δ 7.51-7.49 (m, 2H), 7.28-7.27 (m, 3H), 3.55 (s, 3H, COOCH₃), 3.04 (t, *J* = 7.5 Hz, 2H), 2.53 (t, *J* = 7.5 Hz, 2H). **¹³C NMR** (150MHz, CDCl₃) δ 173.4 (C=O), 158.2 (C=N), 135.4 (C of aromatic ring), 129.6, 128.9, 126.5 (-

$\underline{\text{C}}\text{H}$ of aromatic ring), 52.0 ($\text{COO}\underline{\text{C}}\text{H}_3$), 30.6 ($\underline{\text{C}}\text{H}_2$), 22.3 ($\underline{\text{C}}\text{H}_2$). **MS** (m/z): 51, 77, 104, 117, 130, 158, 176, 206 ($\text{M}^+ -1$).

4-(4-Chloro-phenyl)-4-hydroxyimino-butyric acid methyl ester 2b

Yield: 88%; White crystal; mp:45-46°C. **Anal. Calcd.** for $\text{C}_{11}\text{H}_{12}\text{ClNO}_3$ C, 54.67; H, 5.00; Cl, 14.67; N, 5.80. Found: C, 54.73; H, 5.30; Cl, 14.55; N, 5.72. **IR** (neat, cm^{-1}) ν 3447 (OH stretching), 3099 (CH stretching of aromatic rings), 2961 ($-\text{CH}_2-$ stretching), 1734 ($\text{C}=\text{O}$ stretching of COOCH_3 group), 1680 ($\text{C}=\text{N}$ stretching), 1503, 1456 ($\text{C}=\text{C}$ - stretching of aromatic rings), 1263 (CH stretching in aliphatic plane), 1094 (C-O stretching), 939, 831 (out-of-plane bending CH of aromatic ring). **^1H NMR** (500 MHz, CDCl_3) δ 7.45 (d, $J = 10.0$ Hz, 2H), 7.24 (d, $J = 10.0$ Hz, 2H), 3.55 (s, 3H, COOCH_3), 3.04 (t, $J = 7.5$ Hz, 2H), 2.53 (t, $J = 7.5$ Hz, 2H). **^{13}C NMR** (150MHz, CDCl_3) δ 172.9 ($\text{C}=\text{O}$), 157.3 ($\text{C}=\text{N}$), 135.6 (C of aromatic ring), 139.0, 129.7, 127.8 ($-\underline{\text{C}}\text{H}$ of aromatic ring), 51.9 ($\text{COO}\underline{\text{C}}\text{H}_3$), 30.8 ($\underline{\text{C}}\text{H}_2$), 22.1 ($\underline{\text{C}}\text{H}_2$). **MS** (m/z): 55, 75, 111, 138, 153, 164, 182, 206, 240($\text{M}^+ -1$).

4-Hydroxyimino-4-(4-methoxy-phenyl)-butyric acid methyl ester 2c

Yield: 70%; colorless oil. **Anal. Calcd.** for $\text{C}_{12}\text{H}_{15}\text{NO}_4$ C, 60.75; H, 6.37; N, 5.90. Found: C, 60.90; H, 6.45; N, 5.80. **IR** (neat, cm^{-1}) ν 3470 (OH stretching), 3022 (CH stretching of aromatic rings), 2953 ($-\text{CH}_2-$ stretching), 1734 ($\text{C}=\text{O}$ stretching of COOCH_3 group), 1685 ($\text{C}=\text{N}$ stretching), 1526, 1456 ($\text{C}=\text{C}$ - stretching of aromatic rings), 1263 (CH stretching in aliphatic plane), 1032 (C-O stretching), 939, 847 (out-of-plane bending CH of aromatic ring). **^1H NMR** (500 MHz, CDCl_3) δ 7.48 (d, $J = 10.0$ Hz, 2H), 6.83 (d, $J = 10.0$ Hz, 2H), 3.75 (s, 3H, Ar- OCH_3), 3.58 (s, 3H, COOCH_3), 3.02 (t, $J = 7.5$ Hz, 2H), 2.54 (t, $J = 7.5$ Hz, 2H). **^{13}C NMR** (150MHz, CDCl_3) δ 173.3 ($\text{C}=\text{O}$), 160.9 ($\text{C}=\text{N}$), 157.7 (C of aromatic ring), 127.9, 127.6, 114.3 ($-\underline{\text{C}}\text{H}$ of aromatic ring), 55.5 (Ar- $\text{O}\underline{\text{C}}\text{H}_3$), 52.0 ($\text{COO}\underline{\text{C}}\text{H}_3$), 30.7 ($\underline{\text{C}}\text{H}_2$), 22.1 ($\underline{\text{C}}\text{H}_2$). **MS** (m/z): 55, 77, 91, 134, 149, 178, 207, 237(M^+).

4-Furan-2-yl-4-hydroxyimino-butyric acid methyl ester 2d

Yield: 60%; colorless oil. **Anal. Calcd.** for $\text{C}_9\text{H}_{11}\text{NO}_4$ C, 54.82; H, 5.62; N, 7.10. Found: C, 55.00; H, 5.40; N, 7.45. **IR** (neat, cm^{-1}) ν 3462 (OH stretching), 3138 (CH stretching of aromatic rings), 2953 ($-\text{CH}_2-$ stretching), 1780 ($\text{C}=\text{O}$ stretching of COOCH_3 group), 1680 ($\text{C}=\text{N}$ stretching), 1510, 1456 ($\text{C}=\text{C}$ - stretching of aromatic rings), 1248 (CH stretching in aliphatic plane), 1071 (C-O stretching), 824, 754 (out-of-plane bending CH of aromatic ring). **^1H NMR** (500 MHz, CDCl_3) δ 7.39-7.33 (m, 1H), 6.62 (d, $J = 5.0$ Hz, 1H), 6.36-6.35 (m, 1H), 3.61 (s, 3H, COOCH_3), 2.94 (t, $J = 7.5$ Hz, 2H), 2.59 (t, $J = 7.5$ Hz, 2H). **^{13}C NMR** (150MHz, CDCl_3) δ 172.0 ($\text{C}=\text{O}$), 154.6 ($\text{C}=\text{N}$), 148.4 (C of aromatic ring), 141.5, 111.1, 109.6 ($-\underline{\text{C}}\text{H}$ of aromatic ring), 50.7 ($\text{COO}\underline{\text{C}}\text{H}_3$), 30.4 ($\underline{\text{C}}\text{H}_2$), 20.5 ($\underline{\text{C}}\text{H}_2$). **MS** (m/z): 55, 79, 93, 107, 120, 138, 148, 166, 180, 197 (M^+).

4-Hydroxyimino-4-thiophen-2-yl-butyric acid methyl ester 2e

Yield: 65%; White crystal; mp:59.5-60.5°C. **Anal. Calcd.** for C₉H₁₁NO₃S C, 50.69; H, 5.20; N, 6.57; S, 15.04. Found: C, 50.96; H, 5.30; N, 6.15; S, 14.97. **IR (neat, cm⁻¹)** ν 3377 (OH stretching), 3115 (CH stretching of aromatic rings), 2953 (-CH₂- stretching), 1780 (C=O stretching of COOCH₃ group), 1675 (C=N stretching), 1549, 1456 (C=C- stretching of aromatic rings), 1186 (CH stretching in aliphatic plane), 1032 (C-O stretching), 855, 716 (out-of-plane bending CH of aromatic ring). **¹H NMR** (500 MHz, CDCl₃) δ 7.47-7.46 (m, 2H), 6.93 (t, *J* = 5.0 Hz, 1H), 3.59 (s, 3H, COOCH₃), 3.02 (t, *J* = 7.5 Hz, 2H), 2.61 (t, *J* = 7.5 Hz, 2H). **¹³C NMR** (150MHz, CDCl₃) δ 172.1 (C=O), 152.7 (C=N), 137.8 (C of aromatic ring), 129.9, 126.3, 124.6 (-CH of aromatic ring), 50.8 (COOCH₃), 29.5 (CH₂), 21.6 (CH₂). **MS** (m/z): 55, 65, 84, 97, 110, 123, 136, 154, 165, 196, 213(M⁺).

5-Hydroxyimino-5-phenyl-pentanoic acid methyl ester 2f

Yield: 85%; White crystal; mp:55.5-56.5°C. **Anal. Calcd.** for C₁₂H₁₅NO₃ C, 65.14; H, 6.83; N, 6.33. Found: C, 65.10; H, 6.90; N, 6.20. **IR** (neat, cm⁻¹) ν 3453 (OH stretching), 3023 (CH stretching of aromatic rings), 2946 (-CH₂- stretching), 1738 (C=O stretching of COOCH₃ group), 1682 (C=N stretching), 1500, 1453 (C=C- stretching of aromatic rings), 1246 (CH stretching in aliphatic plane), 1076 (C-O stretching), 769, 707 (out-of-plane bending CH of aromatic ring). **¹H NMR** (500 MHz, CDCl₃) δ 7.55-7.53 (m, 2H), 7.31-7.29 (m, 3H), 3.57 (s, 3H, COOCH₃), 2.79 (t, *J* = 7.5 Hz, 2H), 2.32 (t, *J* = 7.5 Hz, 2H), 1.84 (q, *J* = 7.5 Hz, 2H). **¹³C NMR** (150MHz, CDCl₃) δ 173.9 (C=O), 158.9 (C=N), 135.6 (C of aromatic ring), 129.5, 128.8, 126.5 (-CH of aromatic ring), 51.8 (COOCH₃), 33.8 (CH₂), 25.5 (CH₂), 21.8 (CH₂). **MS** (m/z): 51, 77, 104, 130, 144, 173, 204, 221(M⁺ +1).

5-(4-Chlorophenyl)-5-hydroxyimino-pentanoic acid methyl ester 2g

Yield: 80%; White crystal; mp:51.5-52.5°C. **Anal. Calcd.** for C₁₂H₁₄ClNO₃ C, 56.37; H, 5.52; Cl, 13.87; N, 5.48. Found: C, 56.20; H, 5.55; Cl, 13.80; N, 5.52. **IR** (neat, cm⁻¹) ν 3454 (OH stretching), 3038 (CH stretching of aromatic rings), 2953 (-CH₂- stretching), 1734 (C=O stretching of COOCH₃ group), 1680 (C=N stretching), 1503, 1456 (C=C- stretching of aromatic rings), 1263 (CH stretching in aliphatic plane), 1094 (C-O stretching), 847, 762 (out-of-plane bending CH of aromatic ring). **¹H NMR** (500 MHz, CDCl₃) δ 7.49 (d, *J* = 5.0 Hz, 2H), 7.27 (d, *J* = 10.0 Hz, 2H), 3.59 (s, 3H, COOCH₃), 2.76 (t, *J* = 7.5 Hz, 2H), 2.32 (t, *J* = 7.5 Hz, 2H), 1.81 (q, *J* = 7.5 Hz, 2H). **¹³C NMR** (150MHz, CDCl₃) δ 173.9 (C=O), 158.1 (C=N), 135.5 (C of aromatic ring), 134.0, 129.0, 127.7 (-CH of aromatic ring), 51.8 (COOCH₃), 33.7 (CH₂), 25.4 (CH₂), 21.6 (CH₂). **MS** (m/z): 55, 75, 88, 102, 138, 164, 192, 224, 256(M⁺).

5-Hydroxyimino-5-(4-methoxyphenyl)-pentanoic acid methyl ester 2h

Yield: 70%; White crystal; mp:102-103°C. **Anal. Calcd.** for C₁₃H₁₇NO₄ C, 62.14; H, 6.82; N, 5.57. Found: C, 62.04; H, 6.85; N, 5.50. **IR** (neat, cm⁻¹) ν 3470 (OH stretching), 3015 (CH stretching of aromatic rings), 2961 (-CH₂- stretching), 1753 (C=O stretching of COOCH₃ group), 1685 (C=N stretching), 1526, 1456 (C=C- stretching of aromatic rings), 1256 (CH stretching in aliphatic plane), 1040 (C-O stretching), 847, 747 (out-of-plane bending CH of aromatic ring). **¹H NMR** (500 MHz, CDCl₃) δ 7.50 (d, *J* = 5.0 Hz, 2H), 6.82 (d, *J* = 10.0 Hz, 2H), 3.73 (s, 3H, Ar-OCH₃), 3.58 (s, 3H, COOCH₃), 2.77 (t, *J* = 7.5 Hz, 2H), 2.32 (t, *J* = 7.5 Hz, 2H), 1.83 (q, *J* = 7.5 Hz, 2H). **¹³C NMR** (150MHz, CDCl₃) δ 173.9 (C=O), 160.7 (C=N), 158.4 (C of aromatic ring), 128.0, 127.8, 114.2 (-CH of aromatic ring), 55.5 (Ar-OCH₃), 51.7 (COOCH₃), 33.8 (CH₂), 25.4 (CH₂), 21.8 (CH₂). **MS** (m/z) : 55, 77, 90, 103, 133, 160, 188, 205, 251(M⁺).

5-Furan-2-yl-5-hydroxyimino-pentanoic acid methyl ester 2i

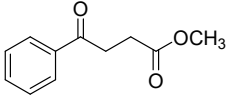
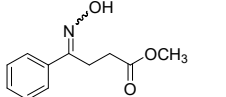
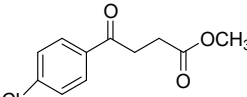
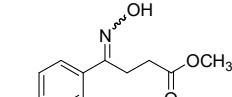
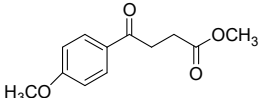
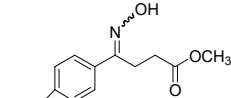
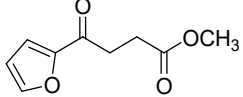
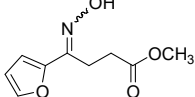
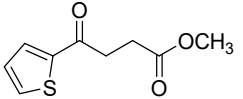
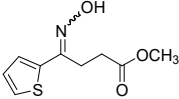
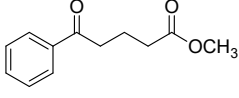
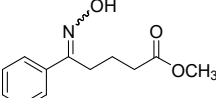
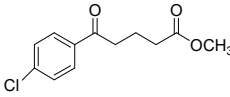
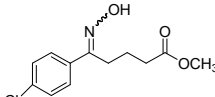
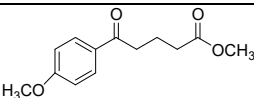
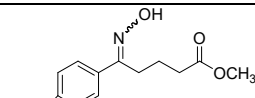
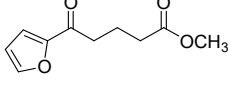
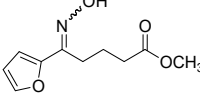
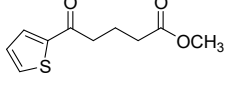
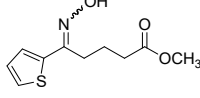
Yield: 65%; White crystal; mp:43.5-44.5°C. **Anal. Calcd.** for C₁₀H₁₃NO₄ C, 56.86; H, 6.20; N, 6.63. Found: C, 56.95; H, 6.10; N, 6.55. **IR** (neat, cm⁻¹) ν 3462 (OH stretching), 3138 (CH stretching of aromatic rings), 2953 (-CH₂- stretching), 1742 (C=O stretching of COOCH₃ group), 1682 (C=N stretching), 1456, 1387 (C=C- stretching of aromatic rings), 1256 (CH stretching in aliphatic plane), 1078 (C-O stretching), 932, 754 (out-of-plane bending CH of aromatic ring). **¹H NMR** (500 MHz, CDCl₃) δ 7.38-7.37 (m, 1H), 6.60 (d, 1H), 6.36-6.35 (m, 1H), 3.60 (s, 3H, COOCH₃), 2.68 (t, *J* = 7.5 Hz, 2H), 2.34 (t, *J* = 7.5 Hz, 2H), 1.91 (q, *J* = 7.5 Hz, 2H). **¹³C NMR** (150MHz, CDCl₃) δ 172.7 (C=O), 149.4 (C=N), 145.6 (C of aromatic ring), 142.6, 111.6, 109.2 (-CH of aromatic ring), 50.5 (COOCH₃), 32.4 (CH₂), 23.8 (CH₂), 20.8 (CH₂). **MS** (m/z) : 55, 85, 93, 107, 125, 138, 162, 160, 194, 205, 211(M⁺).

5-Hydroxyimino-5-thiophen-2-yl-pentanoic acid methyl ester 2j

Yield: 65%; White crystal; mp:55-56°C. **Anal. Calcd.** for C₁₀H₁₃NO₃S C, 52.85; H, 5.77; N, 6.16; S,14.11. Found: C, 52.95; H, 5.55; N, 6.20; S, 14.20. **IR** (neat, cm⁻¹) ν 3462 (OH stretching), 3115 (CH stretching of aromatic rings), 2953 (-CH₂- stretching), 1742 (C=O stretching of COOCH₃ group), 1682 (C=N stretching), 1456, 1387 (C=C- stretching of aromatic rings), 1256 (CH stretching in aliphatic plane), 1078 (C-O stretching), 847, 716 (out-of-plane bending CH of aromatic ring). **¹H NMR** (500 MHz, CDCl₃) δ 7.50-7.47 (m, 2H), 7.03 (t, *J* = 5.0 Hz, 1H), 3.59 (s, 3H, COOCH₃), 2.72 (t, *J* = 7.5 Hz, 2H), 2.37 (t, *J* = 7.5 Hz, 2H), 1.97 (q, *J* = 7.5 Hz, 2H). **¹³C NMR** (150MHz, CDCl₃) δ 172.1 (C=O), 152.7 (C=N), 137.8 (C of aromatic ring), 129.9, 126.3, 124.6 (-CH of aromatic ring), 50.8 (COOCH₃), 29.5 (CH₂), 21.6 (CH₂). **MS** (m/z) : 55, 84, 97, 110, 123, 136, 150, 178, 210, 227(M⁺).

The isomeric ratios of the compounds are shown in Table 1.

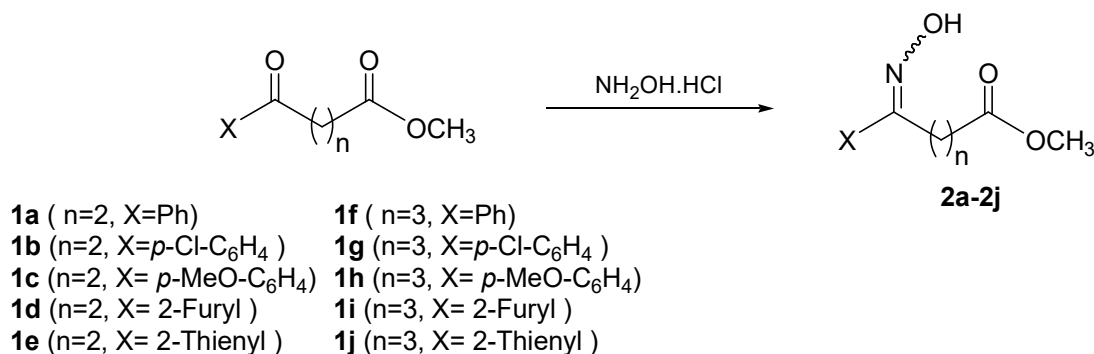
Table 1. Isomer ratios ((E)/(Z)) and yields of synthesized γ - and δ -ketoxime esters

Entry	Keto ester	Product	Yield ^a	(E)/(Z) Ratio ^b
1	 1a	 2a	90	<i>E</i>
2	 1b	 2b	88	<i>E</i>
3	 1c	 2c	70	<i>E</i>
4	 1d	 2d	60	<i>E</i>
5	 1e	 2e	65	<i>E</i>
6	 1f	 2f	85	<i>E</i>
7	 1g	 2g	80	<i>E</i>
8	 1h	 2h	70	<i>E</i>
9	 1i	 2i	65	<i>E</i>
10	 1j	 2j	65	<i>E</i>

^a Isolated yield. ^b (E)/(Z) ratio was determined by ¹H NMR.

RESULTS AND DISCUSSION

We have obtained oxime esters **2a-2j** with high yields and the products were synthesized with the reaction between aryl, substituted aryl and heteroaryl γ - and δ -keto esters **1a-1j** and hydroxyamine hydrochloride (see Scheme 1).



Scheme 1: Synthesis of γ - and δ -ketoxime esters

Hydroxyimino compounds are generally isolated as *E* isomer (45-47). In another work, hydroxyimino derivatives of keto esters were obtained also mainly as *E* isomer (24). According to these literatures (24, 45-48), the configuration of the synthesized compounds (**2a-2j**) in this work were determined by ¹H-NMR spectrum due to the splitting of the methoxy signal as studied in the previous study of our group (24). Two methoxy signals were seen for *E/Z* mixture. *E* signal resonated at lower field than *Z* signal (24, 48). ¹H-NMR spectras of the synthesized aryl-, substituted aryl- and heteroaryl containing γ - and δ -oxime esters **2a-2j** showed only one signal for methoxy peak as obtained in the previous study, therefore the configuration of these keto oxime esters were attributed to *E* structure. The position of phenyl grup let these keto oxime esters existing in *E* configuration because of the interaction between phenyl and hydroxy proton of the oxime groups and steric hinderance of the methylen protons.

As a conclusion, an extremely simple, suitable and efficient method was applied in this study for converting keto esters to their corresponding ketoxime esters of *E* configuration, which will be studied later for their biological activities.

REFERENCES

1. Bosch AI, Greez P, Diez-Barra E, Loupy A, Langa F. Microwave Assisted Beckmann Rearrangement of Ketoximes in Dry Media. *Synlett* 1995 1259-1260.
2. Kumar HMS, Reddy TP, Yadave JS. Efficient One-Pot Preparation of Nitriles from Aldehydes using N-Methyl-pyrrolidone. *Synthesis*, 1999 4: 586-587.
3. Biswanath Das, Madhusudhan P, Venkataiah B. An Efficient Microwave Assisted One-Pot Conversion of Aldehydes into Nitriles Using Silica Gel Supported NaHSO₄ Catalyst. *Synlett* 1999 10: 1569-1570.

4. Sasatani S, Miyazak T, Maruoka K, Yamamoto H. Diisobutylaluminum hydride a novel reagent for the reduction of oximes. *Tetrahedron Lett.* 1983 24: 4711-4112. DOI:10.1016/S0040-4039(00)86234-6.
5. Negi S, Matsukura M, Mizuno M, Miyake K. Synthesis of (2R)-1-(4-Chloro-2-pyridyl)-2-(2-pyridyl)ethylamine: A Selective Oxime Reduction and Crystallization-Induced Asymmetric Transformation. *Synthesis* 1996 8: 991-996.
6. Das MK, Bhaumik A. *Indian J Chem Sect B* 1997 36: 1020.
7. Miyabe H, Ushiro C, Naito T. Highly diastereoselective radical addition to glyoxylic oxime ether: asymmetric synthesis of α -amino acids. *Chem Commun.* 1997 1789-1790. DOI: 10.1039/A704562J.
8. Subhas Base D, Vanajatha G. A Versatile Method for the Conversion of Oximes to Nitroalkanes. *Synth Commun.* 1998 28:4531-453. DOI.org/10.1080/00397919808004517.
9. Bougrin K, Loupy A, Soufiaoui M. Trois nouvelles voies de synthèse des dérivés 1,3-azoliques sous micro-ondes. *Tetrahedron* 1998 54: 8055-8064.
10. Shouxin L, Debin J, Yihua Y, Xiaoli Z, Xia T, Jianrong H. Practical Procedure for Efficient Synthesis of α -Amino Acids. *Lett. Org. Chem.* 2009 6: 156-158.
11. Noverges B, Simón MM, Asensio G. Palladium-Catalyzed Alkoxy- and Aminocarbonylation of α -Halomethyl Oxime Ethers: Synthesis of 1,3-Alkoxyimino Esters and 1,3-Alkoxyimino Amides. *Adv. Synth. Catal.* 2015 357: 430-442. DOI:10.1002/adsc.201400710.
12. Lourdasamy E, Yao L, Park CM. Stereoselective Synthesis of α -Diazo Oxime Ethers and Their Application in the Synthesis of Highly Substituted Pyrroles through a [3+2] Cycloaddition. *Angew. Chem. Int. Ed.* 2010 49: 7963-7967. DOI: 10.1002/anie.201004073.
13. Yang Y, Wang X, Zhu Q, Gong G, Luo D, Jiang A, Yang L, Xu Y. Synthesis and pharmacological evaluation of novel limonin derivatives as anti-inflammatory and analgesic agents with high water solubility. *Bioorg. Med. Chem. Lett.* 2014 24: 1851-1855. DOI.org/10.1016/j.bmcl.2014.02.003.
- 14 a) Liu XH, Zhi LP, Song BA, Xu HL. Synthesis, characterization and antibacterial activity of 5-aryl pyrazole oxime esters derivatives. *Chemical Reserach in Chinese Universities.* 2008 24(4): 454-458. b) Tu S, Xie Y.Q, Gui SZ, Ye LY, Huang ZL, Huang YB, Che LM. Synthesis and fungicidal activities of novel benzothioephene-substituted oxime ether strobilurins. *Bioorg. Med. Chem. Lett.* 2014, 24: 2173-2176. DOI.org/10.1016/j.bmcl.2014.03.024
15. Ma JA, Huang RQ, Chai YX. Synthesis and insecticidal activities of new pyrethroid acid oxime ester derivatives. *Progress in Natural Science.* 2002 12(4): 271-277.
16. Jin GY, Li YC, Liu ZF, Zheng JY. Synthesis and biological activity of oximino-phosphorothioate containing 1,2,4-thiazole. *Chin.J.Appl.Chem.* 1997 14(6): 5-8.
17. Park HJ, Lee K, Park SJ, Ahn B, Lee JC, Cho HY, Lee KI. Identification of antitumor activity of pyrazole oxime ethers. *Bioorganic & Medicinal Chemistry Letters* 2005 15: 3307-3312. DOI.10.1016/j.bmcl.2005.03.082
18. Song BA, Liu XH, Yang S, Hu DY, Jin LH, Zhang H. Synthesis and Anticancer Activity of 2,3,4-Trimethoxyacetophenoxime ester Containing Benzothiazole Moiety. *Chinese Journal of Chemistry.* 2005 23: 1236-1240. DOI: 10.1002/cjoc.200591236
19. Li TG, Liu JP, Han JT, Fu B. Wang DQ, Wang MG. Synthesis and herbicidal activity of α -phenylsulfonyl-cyclododecanone oxime esters. *Chin. J.Org. Chem.* 2009 29(6): 898-903.
20. Whittingham WG, Mound WR, Russell SE, Pilkington BL, Kozakiewicz AM, Hunhes DJ, Turnbull MD, Whittle AJ. The synthesis of novelimidazolinones as potential fungicides. *Synthesis and Chemistry of Agrochemicals VI.* 2001 800(29): 314-326.

21. Jindal DP, Chattopadhyaya R, Guleria S, Gupta R. Synthesis and antineoplastic activity of 2-alkylaminoethyl derivatives of various steroidal oximes. *Eur. J. Med. Chem.* 2003 38: 1025-1034. DOI:10.1016/j.ejmech.2003.09.002
22. Ouyang G, Chen Z, Cai XJ, Song BA, Bhadury PS, Yang S, Jin LH, Xue W, Hu DY, Zeng S. Synthesis and antiviral activity of novel pyrazole derivatives containing oxime ester group. *Bioorganic & Medicinal Chemistry.* 2008 16(22): 9699-9707. DOI. 10.1016/j.bmc.2008.09.070
23. Ouyang G, Cai XJ, Chen Z, Song BA, Bhadury PS, Yang S, Jin LH, Xue W, Hu DY, Zeng S. Synthesis and antiviral activity of pyrazole derivatives containing an oxime moiety. *J.Agric.Food Chem.* 2008 50: 10160-10167. DOI. 10.1021/jf802489e
24. Başpınar Küçük H, Sergüzel Yusufoglu A, Açık L, Aydın B, Arslan L. Synthesis, (E)/(Z)-isomerization, and DNA binding, antibacterial, and antifungal activities of novel oximes and O-substituted oxime esters. *Turkish Journal of Chemistry.* 2016 40: 816-829. DOI.10.3906/kim-1604-2.
25. Chakravarty AR, Chakravorty A, Cotton FA, Falvello LR, Ghosh BK, Tomas M. cis-Dihalobis(aryloxo) ruthenium(II): synthesis, structure and reactions. *Inorg. Chem.* 1983 22: 1892-1896. DOI: 10.1021/ic00155a014.
26. Szczepura LF, Muller JG, Bessel CA, See RF, Janik TS, Churchill MR, Takeuchi KJ. Characterization of protonated trans bis(dioxime) ruthenium complexes: crystal structures of trans-Ru(DPGH)₂(NO)Cl, trans [Ru(DMGH)(DMGH₂)(NO)Cl]Cl, and trans-Ru(DMGH)₂(NO)Cl. *Inorg. Chem.* 1992 31: 859-869. DOI: 10.1021/ic00031a031.
27. Fukuchi T, Miki E, Mizumachi K, Ishimori T. Cis and Trans Isomers of Iodonitrosylbis(vicinal-dioximato)ruthenium(III). *Chem. Lett.* 1987 1133-1136. DOI.org/10.1246/cl.1987.1133.
28. Lianguri R, Morris JJ, Stanley WC, Bell-Loncella ET, Turner M, Boyko WJ, Bessel CA. Electrochemical and Spectroscopic Investigations of Oxime Complexes of bis(bipyridyl)ruthenium(II). *Inorganic Chimica Acta* 2000 315: 53-65. PII: S0020-1693(01)00315-2.
29. Muller JG, Takeuchi KJ. Preparation and characterization of trans-bis(.alpha.-dioximato)ruthenium complexes. *Inorg. Chem.* 1990 29: 2185-2188. DOI: 10.1021/ic00336a032.
30. Sharma VK, Pandey OP, Sengupta S.. Synthesis and Physicochemical Studies on Ruthenium(III) and Rhodium(III) Complexes with Chalcone Oximes. *Synth. React. Inorg. Met.-Org. Chem.* 1991 21: 1587. DOI.org/10.1080/15533179108020630.
31. Singh RB, Garg BS, Singh R. Oximes as spectrophotometric reagents—a review. *Talanta* 1979 26: 425-444. DOI:10.1016/0039-9140(79)80107-1.
32. Voiculescu N. Insertion of Chloroalumino-Organic Bridges in Coordinated Salicylaloxime. *Synth. React. Inorg. Met.-Org. Chem.* 2001 31(10): 1731-1742. DOI.org/10.1081/SIM-100108258.
33. Ramadan Abd El-MM, El-Mehasseb IM, Isssa RM. Synthesis, characterization and superoxide dismutase mimetic activity of ruthenium(III) oxime complexes. *Transition Met. Chem.* 1997 22: 529-534. DOI: 10.1023/A:1018588019441.
34. Alonso DA, Najera C, Pacheco MC. Oxime Palladacycles: Stable and Efficient Catalysts for Carbon-Carbon Coupling Reactions. *Org. Lett.* 2000 2(13): 1823-1826. DOI. 10.1021/ol0058644.
35. Baleizaño C, Corma A, Garcí'a H, Leyva A. Oxime Carbapalladacycle Covalently Anchored to High Surface Area Inorganic Supports or Polymers as Heterogeneous Green Catalysts for the Suzuki Reaction in Water. *J. Org. Chem.* 2004 69: 439-446. DOI. 10.1021/jo030302u
36. Zülfikaroğlu A, Taş M, Batı H, Batı B. The Synthesis and Characterization of Substituted Aminomethylglyoximes and Aminophenylglyoximes and Their Complexes with Some Transition Metals. *Synthesis and Reactivity in Inorganic and Metal-Organic Chemistry.* 2003 33(4): 625-638. DOI: 10.1081/SIM-120020328

37. Zhang P, Wang M, Dong J, Li X, Wang F, Wu L, Sun L. Photocatalytic Hydrogen Production from Water by Noble-Metal-Free Molecular Catalyst Systems Containing Rose Bengal and the Cobaloximes of BF_x-Bridged Oxime Ligands. *J. Phys. Chem. C.* 2010 *114*: 15868–15874. DOI. 10.1021/jp106512a.
38. Imoto H, Sugiyama Y, Kimura H, Momose Y. Studies on Non-Thiazolidinedione Antidiabetic Agents. 2.1) Novel Oxyiminoalkanoic Acid Derivatives as Potent Glucose and Lipid Lowering Agents. *Chem. Pharm. Bull.* 2003 *51*(2): 138-151.
39. Furuya Y, Ishihara K, Yamamoto H. Cyanuric Chloride as a Mild and Active Beckmann Rearrangement Catalyst. *J. Am. Chem. Soc.* 2005 *127*: 11240-11241. DOI.10.1021/ja053441x.
40. Fabrichnyi BP, Shalavina IF, Gol'dfarb Ya L. Synthesis of aliphatic amino acids from thiophene derivatives. VIII. The effect of certain factors on the yield of the product in the step of reductive desulfurization. *Zhurnal Obshchei Khimii* 1964 *34*(12): 3878-3887.
41. Maekawa T, Sakai N, Tawada H, Murase K, Hazama M, Sugiyama Y, Momose Y. Synthesis and Biological Activity of Novel 5-(w-Aryloxyalkyl)oxazole Derivatives as Brain-Derived Neurotrophic Factor Inducers. *Chem. Pharm. Bull.* 2003 *51*(5): 565–573.
42. Manuela M, Raposo M, Kirsch G. A Combination of Friedel-Crafts and Lawesson Reactions to 5-Substituted 2,2'-Bithiophenes. *Heterocycles* 2001 *55*(8): 1487–1498. DOI: 10.3987/COM-01-9249.
43. Schnermann MJ, Boger DL. Total Synthesis of Piericidin A1 and B1. *J. Am. Chem. Soc.* 2005 *127*: 15704-15705. DOI: 10.1021/ja055041f.
44. Gross PJ, Hartmann CE, Nieger M, Bräse S. Synthesis of Methoxyfumimycin with 1,2-Addition to Ketimines. *J. Org. Chem.* 2010 *75*: 229-232. DOI: 10.1021/jo902026s.
45. Demir AS. A novel synthesis of optically active α -amino acids. *Pure & Appl. Chem.* 1997 *69*: 105-108. DOI.org/10.1351/pac199769010105.
46. Demir AS, Cam HA, Camketen N, Hamamcı H, Doğanel F. An Efficient Synthesis of (1 S , 2 R)-1-Amino-2-Indanol, A Key Intermediate of HIV Protease Inhibitor, Indinavir. *Turk. J. Chem.* 2000 *24*: 141-146.
47. Demir AS, Sesenoglu Ö, Ülkü D, Arici C. Enantioselective Synthesis of 2-(2-Arylcyclopropyl)glycines: Conformationally Restricted Homophenylalanine Analogs. *Helv. Chim. Acta* 2004 *87*: 106-119. DOI: 10.1002/hlca.200490000.
48. Balsamo A, Bertini S, Gervasi G, Lapucci A, Nencetti S, Orlandini E, Rapposelli S, Rossello A, Soldani G. Enantiopure 3-(arylmethylidene)aminoxy-2-methylpropionic acids: synthesis and antiinflammatory properties. *Eur. J. Med. Chem.* 2001 *36*: 799-807. DOI.org/10.1016/S0223-5234(01)01275-2.

